# Using Salt Accumulations and Luminescence Dating to Study the Glacial History of Taylor Valley, Antarctica

Jonathan D. Toner

A dissertation
submitted in partial fulfillment of the
requirements for the degree of

Doctor of Philosophy

University of Washington
2012

Reading Committee:

Ronald S. Sletten, Chair

James K. Feathers

Darlene Zabowski

Program Authorized to Offer Degree:
Department of Earth and Space Sciences

University of Washington

## Abstract

Using Salt Accumulations and Optically Stimulated Luminescence Dating to Study the Glacial History of Taylor Valley, Antarctica

Jonathan D. Toner

Chair of the Supervisory Committee:
Associate Professor Ronald S. Sletten
Department of Earth and Space Sciences

Taylor Valley, Antarctica, preserves a record of late-Cenozoic Antarctic glaciations. The incursion of the Sea Ice Sheet (RSIS) into lower Taylor Valley during the Last Glacial Maximum is believed to have dammed large proglacial paleolakes. These inundation events are studied by analyzing soluble salt distributions along elevation transects. To better interpret the salt record, factors controlling salt composition and concentration are studied in detail in a soil sampled to 2.1 m depth. In addition, the deposition age of fluvial sediments and possible deltas are dated using luminescence of quartz and feldspar minerals.

Soluble salts in Taylor Valley vary with distance from McMurdo Sound. In western Taylor Valley, soluble salts are high and are similar to seawater. In eastern Taylor Valley, soluble salts are low and are comprised primarily of Na-$HCO_3$. Soluble salt distributions indicate that during the Last Glacial Maximum, the RSIS filled eastern Taylor Valley, thereby damming paleolakes in western Taylor Valley to approximately 300 m elevation. As the RSIS retreated, smaller paleolakes formed in eastern Taylor Valley up to about 120 m elevation. Na-$HCO_3$ salts in eastern Taylor Valley derive from calcite dissolution and cation exchange reactions as water percolates down soils. This mechanism of Na-$HCO_3$ formation predicts that Ca-Cl will evolve as a byproduct. Reactive transport at freezing temperatures was modeled using the modified versions of the geochemical speciation programs PHREEQC and FREZCHEM. This model reveals that cation exchange reactions may account for the Ca-Cl enrichment often found in Dry Valley groundwaters, including the enigmatic Don Juan Pond.

To complement the soluble salt record, fluvial terraces in Taylor Valley were dated using both quartz and feldspar luminescence. Quartz and feldspar luminescence results are consistent and indicate that terraces in eastern Taylor Valley are between 4 to 10 Ka old. These luminescence ages are 5 to 12 Ka younger than published $^{14}C$ dates. It is suggested that the $^{14}C$ ages date older glaciolacustrine sediments underlying fluvial terrace sediments and reflect a deglaciation record as the RSIS retreated from Taylor Valley. The luminescence ages indicate that terraces were deposited during warm climate conditions that followed deglaciation.

## TABLE OF CONTENTS

## LIST OF FIGURES

Figure Number Page

## LIST OF TABLES

## Acknowledgements

The following deserve thanks for having helped and supported me in the writing of this dissertation. I wish to thank my advisor, Ron Sletten, for his time, expertise, and guidance. Ron has spent many hours with me discussing this thesis, setting up experiments, and pushing me to reach higher. In addition, I would like to thank my dissertation committee for their time and support: Bernard Hallet, James Feathers, and Darlene Zabowski (graduate student representative).

Funding for this research was provided by: the National Science Foundation (Grant Nos. 0541054 and 0636998), the Department of Earth and Space Sciences and the Quaternary Research Center at the University of Washington, and the Kenneth C. Robbins & Peter Misch Fellowship. Logistics and field support provided by Raytheon at McMurdo Base Station.

Thanks to Dongsen Xue, Harvey Greenberg, Thomas Carpenter, Thomas Kennell, Andrew White, Ian Derrington, Lu Liu, Glen Berger, Michael Prentice, Robert Winglee, David Parkhurst, Bridget Hagedorn, and Scott Kuehner for their assistance in this research. Finally, I would like to give a special thanks to my family (Robert Toner, Barbara Toner, MaryEllen Bennett, Don Bennett, Michelle Toner, and Monica Toner), the University of Washington Climbing Club, and my wife, Lisa, for supporting me as I finished my graduate school career.

# Chapter 1 Introduction

## *1.1. Overview*

During the Last Glacial Maximum (LGM) an ice sheet from the Ross Sea, known as the Ross Sea Ice Sheet (RSIS), advanced into Taylor Valley and dammed the valley mouth (Denton et al., 1970; Stuiver et al., 1981). Behind this ice dam, the valley is thought to have filled with large proglacial lakes (Hall et al., 2010; Hall et al., 2000; Stuiver et al., 1981). The extent of the RSIS and proglacial paleolakes in Taylor Valley has been addressed by many authors (Barrett et al., 2010; Bockheim et al., 2008a; Hall et al., 2010; Hall et al., 2000; Prentice et al., 2009; Stuiver et al., 1981) and has implications for how ice sheets have responded to deglacial sea level rise and warming following the LGM (Hall et al., 2010; Stuiver et al., 1981). The timing of these glacial and lacustrine events are largely determined by $^{14}C$ dates of alluvial terrace deposits (Hall and Denton, 2000). Terraces have been interpreted as deltas deposited in paleolakes, so that $^{14}C$ dates record the timing of paleolake levels (Hall et al., 2010; Hall et al., 2000; Stuiver et al., 1981). However, $^{14}C$ dating in glacial environments, such as in Taylor Valley, can be complicated by reservoirs of old carbon (Bateman, 2008; Doran et al., 1999; Hall and Henderson, 2001; Hendy and Hall, 2006).

Soluble salts are useful indicators of paleolakes in the Dry Valleys (Barrett et al., 2010; Bockheim et al., 2008a; Field, 1975; Morikawa et al., 1975; Poage et al., 2008). To study the history of paleolakes in Taylor Valley, 89 soils along elevational transects were analyzed for soluble salts. In addition, a detailed analysis of stable isotopes, soluble ions, exchangeable cations, and texture was performed on a terrace sampled to 210 cm depth. To determine soil age and test $^{14}C$ dates of terraces against an independent dating method, luminescence dating was performed on terrace soils using both quartz and feldspar mineral grains.

## *1.2. Research Objectives*

The primary objectives of this research are to assess the distribution of soluble salt accumulations and soil ages in Taylor Valley, Antarctica, and to study how past lacustrine events and transport processes have influenced salt distributions. This research employs field and laboratory work, transport modeling, and dating techniques to address the following research goals:

- Measure the spatial distribution of soluble salts in Taylor Valley, Antarctica, both across the landscape and with soil depth. Investigate the role of past glacial history, salt accumulation, and salt leaching on the formation of these salt distributions.
- Determine transport processes in Taylor Valley, Antarctica, that control the vertical distribution of salts in soil profiles and develop a reactive-transport model to simulate these processes.
- Date terraces in Taylor Valley, Antarctica, using luminescence dating. Compare luminescence dates to radiocarbon dates and explore the implications of these dates for the glacial history of Taylor Valley.

### *1.3. Dissertation Outline*

This research is presented in three main chapters that will be submitted as papers for publication in refereed journals. Chapter 1, the introductory chapter, provides background information to familiarize the reader with the study location and past research. Chapter 2 explores the distribution of soluble salt accumulations in Taylor Valley and uses these salt distributions to delineate past glacial and lacustrine environments. Chapter 3 investigates the migration of soluble salts in a fluvial terrace soil that was sampled to 210 cm depth. The influence of cation exchange reactions on brine chemistry is explored through reactive transport modeling using the geochemical models PHREEQC and FREZCHEM. Chapter 4 investigates the age of terraces using luminescence dating of feldspar and quartz grains. The implications of these luminescence ages for existing $^{14}C$ dates and the history of Taylor Valley are explored.

Chapter 5, the concluding chapter, summarizes the main conclusions of chapters 2 through 4 and explores possible avenues for future research. At the end of the dissertation, appendices tabulate data not included in the main body of the dissertation. In addition, for each soil a picture is provided of the excavated soil and the overlying desert pavement surface.

*1.4. Background*

Antarctica contains two of the largest ice masses on earth: the East Antarctic Ice Sheet and the West Antarctic Ice Sheet. Were only the West Antarctic Ice Sheet to melt completely, sea levels would rise by 6 m (Church et al., 2001) and recent studies suggest that the West Antarctic Ice Sheet has been warming 0.1°C per decade since the 1950s (Steig et al., 2009). Many potential effects of climate change have already been observed in disintegrating Antarctic ice shelves (Cook et al., 2005), increased nutrient levels in sub-Antarctic lakes (Quayle, 2002), declining emperor penguin populations (Barbraud and Weimerskirch, 2001), and increasing vascular plant populations (Smith, 1994). To better understand how ice sheets in Antarctica will respond to rising temperatures and sea levels, it is important to research how Antarctic glaciers have responded to climate changes in the past.

Glacial scouring over the Cenozoic has eroded Antarctica's surface record, making much of it fragmented and difficult to access. This eroded and redeposited sediment is the focus of ANDRILL, a major offshore drilling project (Harwood et al., 2006). One of the few places where the surface record remains subaerial is the ice-free McMurdo Dry Valleys, comprising 0.048% or 6692 $km^2$ of the Antarctic Continent (Ugolini and Bockheim, 2008). Extremely low precipitation rates of less than 100 mm per year in the form of snow (Bromley, 1985; Fountain et al., 2010), mean annual temperatures of -14.8°C to -30°C (Clow et al., 1988; Doran et al., 2002a), and the absence of outlet glaciers from the East Antarctic Ice Sheet, have created a stable environment for soils to develop on bedrock and glacial deposits. These soils are preserved in persistent cold and dry conditions that are thought to have existed for the past 14 Ma (Denton et al., 1993;

Hall et al., 1997; Marchant and Denton, 1996; Marchant et al., 1994; Marchant et al., 1993; Marchant et al., 1996; Sugden et al., 2002a), although other studies propose that the landscape is younger (Krusic, 2009; Ng et al., 2005b; Sletten et al., 2003). Regardless, researchers agree that these surfaces are old and contain an extensive record of Antarctic glacial history.

An important component of the Dry Valley surface record is salt that accumulates in these soils over time. Dry Valley soils accumulate salt from marine sea-spray aerosols (Claridge and Campbell, 1968a, 1977; Keys and Williams, 1981), oxidized marine compounds precipitated onto the East Antarctic Ice Sheet (Bao et al., 2000; Claridge and Campbell, 1968a; Michalski et al., 2005), chemical weathering (Claridge and Campbell, 1977; Keys and Williams, 1981; Linkletter, 1972), and aeolian dust (Foley et al., 2006; Fortner et al., 2005; Witherow et al., 2006). Salts occur as chlorides, nitrates, sulfates, and carbonates, and virtually every crystalline phase of these salts in combination with calcium, magnesium, sodium, and potassium has been found (Keys and Williams, 1981; Nishiyama and Kurasawa, 1975). Some soils in the Dry Valleys can have extremely high concentrations of salt (Campbell and Claridge, 1975; Claridge and Campbell, 1968b). These soils can have visible accumulations of salt as encrustations under surface clasts, nodules, disseminated as salt flecks, or salt pans (Campbell and Claridge, 1982). The existence of high accumulations of soluble salts in older Dry Valley soils suggests that stable cold-dry conditions, capable of preserving salts, have prevailed for long periods of time (Bockheim, 1983; Hall et al., 1993; Marchant et al., 1994). The stability of salt accumulations in soils has been used to determine relative soil age since older soils typically contain more salt than younger soils (Bockheim, 1979, 1982, 1990; Everett, 1971; Graham, 2002; Pastor and Bockheim, 1980). Salt accumulations can also be indicative of past glacial or lacustrine events that redistribute salts (Barrett et al., 2010; Bockheim et al., 2008a; Field, 1975; Foley et al., 2006; Morikawa et al., 1975; Poage et al., 2008).

In Taylor Valley, sediments below approximately 350 m elevation were deposited by glacial and lacustrine systems that existed following the LGM (Denton et al., 1970; Hall et al., 2000; Stuiver et al., 1981). During the LGM, it is thought that an ice sheet from the Ross Sea expanded across McMurdo Sound and entered the mouth of Taylor Valley (Stuiver et al., 1981), filling the valley with proglacial paleolakes (Hall et al., 2000; Prentice et al., 2009; Stuiver et al., 1981). The formation of paleolakes in Taylor Valley would have redistributed soluble salt accumulations in soils (Barrett et al., 2010). This is because soils inundated by lake water are leached of salts (Bockheim et al., 2008a), while soils near lake margins accumulate salts from evaporating lake water (Barrett et al., 2009; Barrett et al., 2010). By studying salt distributions deposited in glacial and lacustrine paleoenvironments, the past extent and relative age of lacustrine events can be determined.

Salt accumulations deposited in paleoenvironments can be altered by salt leaching (Campbell and Claridge, 1982), especially in warmer and wetter coastal climates such as can be found in eastern Taylor Valley (Bao et al., 2008). To interpret relict soluble salt distributions deposited in paleoenvironments, it is important to understand how soluble salts are altered by leaching. Leaching may occur when melt water from summer snowfalls percolates down the soil (Dickinson and Rosen, 2003; Hagedorn et al., 2010) or from the influence of melt water from nearby snowdrifts (Gooseff et al., 2003). Even in the absence of direct melt water inputs from snow, ions have been observed migrating along thin brine films that remain liquid at extremely low temperatures (Ugolini and Anderson, 1973). In ice-cemented permafrost, which underlies many soils in the Dry Valleys (Bockheim et al., 2007), concentrated saline brine films form by freezing and evaporation (Dickinson and Rosen, 2003; Hagedorn et al., 2010), and remain liquid due to freezing point depression and unfrozen water associated with particle surfaces (Anderson, 1970). These brines have been shown to migrate at a rate of $10^{-11}$-$10^{-12}$ m $s^{-1}$ in a

Victoria Valley soil (Hagedorn et al., 2010) and about $10^{-11}$ m $s^{-1}$ in a Wright Valley soil (Ugolini and Anderson, 1973).

The mobility of salts in Dry Valley soils makes it difficult to determine absolute soil age based on total salt contents and salt accumulation rates. Soils in Taylor Valley have been extensively dated using $^{14}C$ dating techniques on fossil algae within glaciolacustrine sediments (Hall and Denton, 2000; Stuiver et al., 1981); however, the use of $^{14}C$ dating in periglacial environments is plagued by inherited reservoirs of carbon (Bateman, 2008). A dating technique that shows promise in regions where $^{14}C$ dating is problematic is luminescence dating (Bateman, 2008; Fuchs and Owen, 2008). Luminescence dating is a light sensitive dating technique that measures the time elapsed since mineral grains were last exposed to light (Aitken, 1998). By analyzing the luminescence age on a single-grain level, luminescence dating can be used to detect and correct for inherited age signals by looking at the distribution of single-grain ages (Duller, 2004, 2008; Olley et al., 1999).

### *1.5. Research Site Description*

#### *1.5.1. Location*

Field research was conducted in the Taylor Dry Valley, Antarctica (-77.6°S, 163.4°W) (Figure 1.1). The McMurdo Dry Valleys are cold-dry deserts that are generally ice-free, with the exception of local alpine glaciers and ice-covered lakes. This lack of ice cover is due to the Transantarctic Mountains, which block ice from the East Antarctic Ice Sheet from McMurdo Sound (Chinn, 1990). Taylor Valley is bounded by Taylor Glacier, an outlet of the East Antarctic Ice Sheet, on the west and opens out into McMurdo Sound to the east (Figure 1.2). The valley stretches about 30 km from the snout of the Taylor Glacier to McMurdo Sound and is comprised of two large closed drainage basins, Bonney Basin at the western end of the valley and Fryxell Basin to the east. Fryxell Basin and Bonney Basin are separated by a 116 m high threshold

near the terminus of the Suess Glacier in central Taylor Valley (Kellogg et al., 1980). Within these basins, cold-based alpine glaciers descend from the Asgard Range and Kukri Hills and spread out on the valley floor; the largest of these alpine glaciers are Canada and Commonwealth Glaciers in Fryxell Basin. During the summer, melt water from these alpine glaciers feeds numerous ephemeral streams that drain into closed-basin lakes (McKnight et al., 1999). The largest of these lakes are Lake Fryxell and Lake Hoare in Fryxell Basin, and Lake Bonney in Bonney Basin.

The two main basins in Taylor Valley, Fryxell Basin and Bonney Basin, have distinct characteristics (Figure 1.3). Bonney Basin is narrow, about 3 km wide, with steep valley walls. The valley bottom is occupied by the east and west lobes of Lake Bonney at 58 m elevation, which have a maximum depth of about 40 m and are separated by a sill at about 13 m depth below the lake surface (Spigel and Priscu, 1998). East of Lake Bonney, the valley floor rises to 116 m near the Suess Glacier in central Taylor Valley. Central Taylor Valley is occupied by a distinct transverse ridge of bedrock called the Nussbaum Riegel that reaches a height of about 700 m (Fountain et al., 1999). Here, the valley bottom becomes a narrow defile with steep walls. In Fryxell Basin, Taylor Valley abruptly broadens to a width of about 10 km, with gentle north facing slopes and steep south facing slopes. The bottom of Fryxell Basin is occupied by Lakes Hoare and Bonney, separated by Canada Glacier. Lake Hoare is located at 73 m elevation and is a maximum of 34 m deep; Lake Fryxell is located at 18 m elevation and is a maximum of 34 m deep (Spigel and Priscu, 1998). Fryxell basin stretches about 15 km in length along the valley axis from Canada Glacier to McMurdo Sound and is separated from McMurdo Sound by a channel at 78 m elevation. This channel cuts across a large moraine complex near the Valley Mouth called Coral Ridge (Kellogg et al., 1980), which has an average elevation of about 100 m.

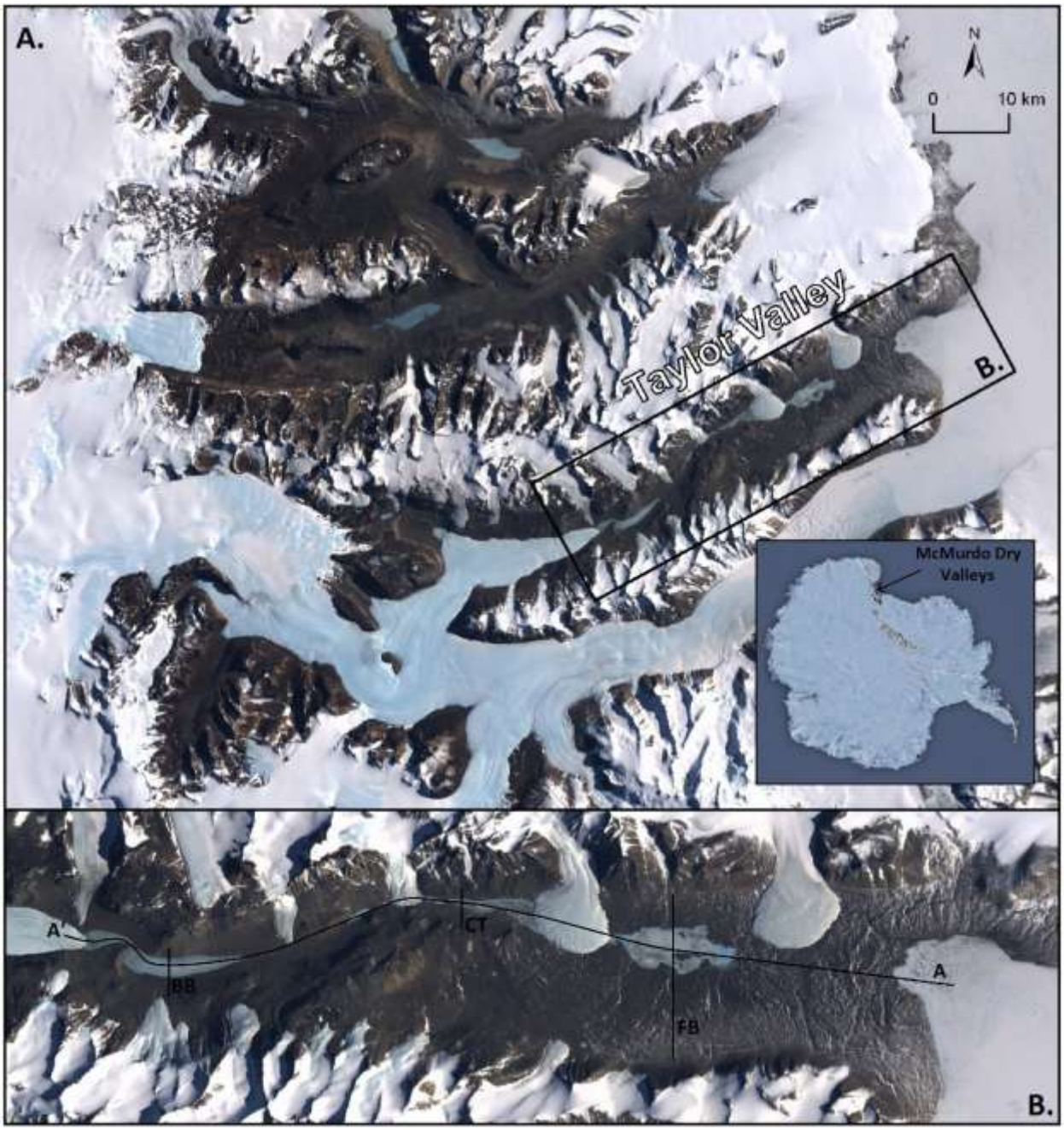


Figure 1.1. A. Landsat Image Mosaic of the McMurdo Dry Valleys and Antarctica (available at http://lima.usgs.gov/); B. Taylor Valley with transect lines used in Figure 1.2 and Figure 1.3. The transect line A-A' generally follows the valley bottom of Taylor Valley and the cross-section profile for this line is given in Figure 1.2. Cross-valley transect lines are given for Fryxell Basin (FB), central Taylor Valley (CT), and Bonney Basin (BB). The profiles for these cross sections are given in Figure 1.3.

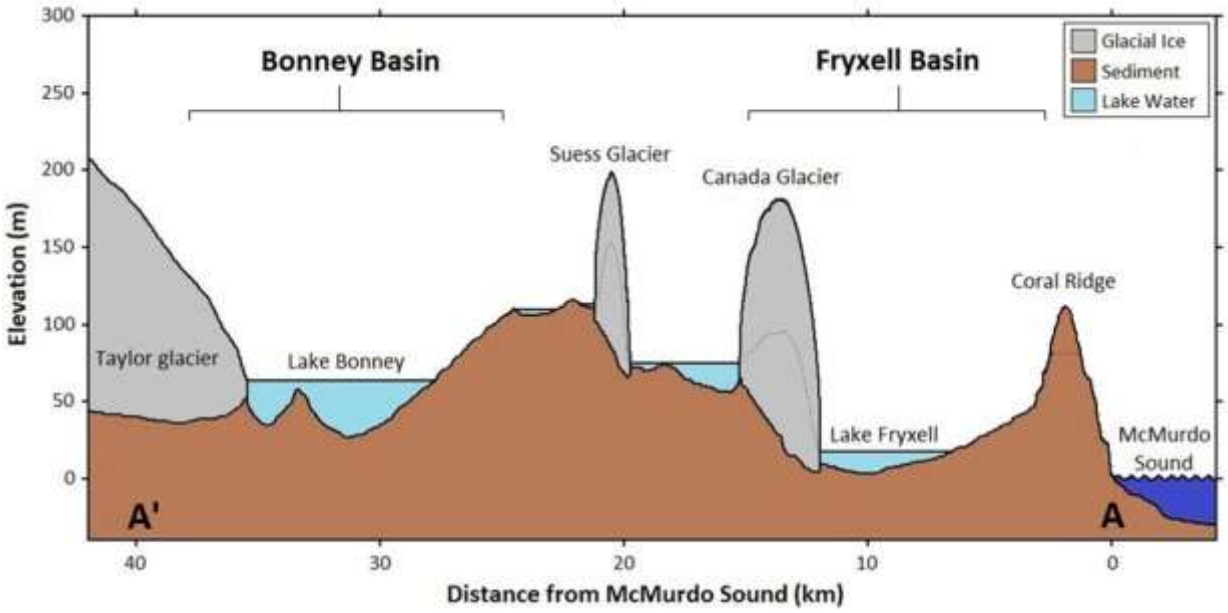


Figure 1.2. This is a scaled cross-section of major features in Taylor Valley including Taylor Glacier, Lake Bonney, Lake Fryxell, Suess Glacier, Canada Glacier, Coral Ridge, and McMurdo Sound. Fryxell and Bonney Basin are shown, with major thresholds at 116 m near the Suess Glacier and 78 m through Coral Ridge (Kellogg et al., 1980). This cross-section was constructed from elevations determined in ArcGIS using LIDAR maps of Taylor Valley (Csatho et al., 2005).

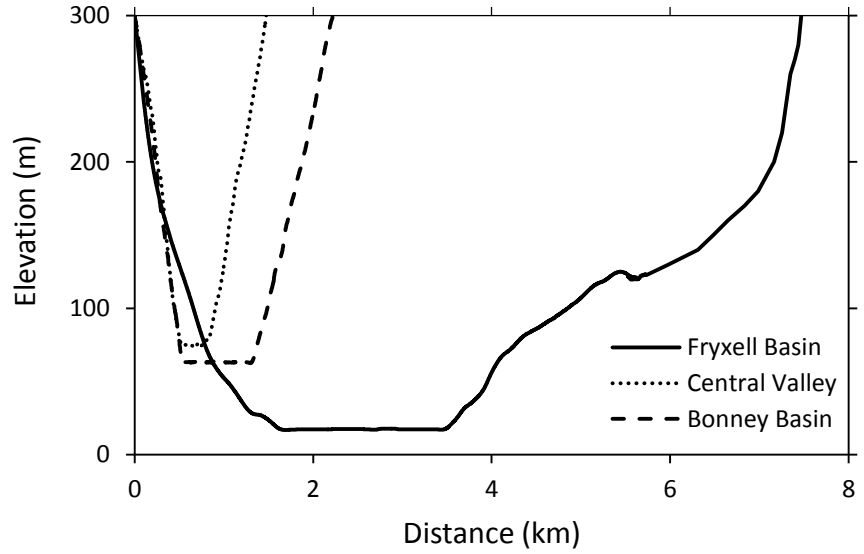


Figure 1.3. This shows cross-valley cross sections of Fryxell Basin, Central Taylor Valley, and Bonney Basin. The lines of cross section are shown in Figure 1.1. Fryxell Basin is much larger and broader than western or central Taylor Valley.

### *1.5.2. Climate*

Mean annual air temperatures in Taylor Valley average about -20°C, with maximum winter temperatures as low at -60°C and maximum summer temperatures as high at 10°C (Clow et al.,

1988; Doran et al., 2002a). Temperatures in western Taylor Valley are typically warmer than in eastern Taylor Valley by several degrees (Fountain et al., 1999). Precipitation in Taylor Valley is limited to snowfall or windblown snow from katabatic winds (Fountain et al., 2010) and is highly variable across the valley floor. Differences in snow accumulation across Taylor Valley are primarily influenced by the Nussbaum Riegel, which limits moisture from McMurdo Sound, making Bonney Basin drier than Fryxell Basin (Doran et al., 2002a; Fountain et al., 1999). Near McMurdo Sound, average snow accumulation rates are about 70 mm $yr^{-1}$, but can be as high as 100 mm $yr^{-1}$ in some years; further inland, average snow accumulation rates decrease to about 15 mm $yr^{-1}$ near Canada Glacier and decrease further to about 10 mm $yr^{-1}$ at Lake Bonney (Fountain et al., 2010). Wind is a major landscape shaping force in Taylor Valley, eroding rock surfaces (Gillies et al., 2008), transporting fine material (Lancaster, 2002), and transporting snow (Fountain et al., 2010). Winds in the Dry Valleys occurs as coastal winds from McMurdo sound (Clow et al., 1988; Doran et al., 2002a), adiabatically heated katabatic winds sweeping off the East Antarctic Ice Sheet that can reach speeds of 100 km $hr^{-1}$ (Clow et al., 1988; Doran et al., 2002a; Nylen et al., 2004), and foehn winds descending from local mountain slopes (Speirs et al., 2010).

### *1.5.3. Surficial Geology and Glacial History*

Sediments in eastern Taylor Valley, below approximately 300 m, are comprised of relatively young glacial, fluvial, and lacustrine sediments deposited by the LGM advance of the RSIS into eastern Taylor Valley (Denton et al., 1970; Hall et al., 2000; Stuiver et al., 1981). The age of this RSIS glaciation has been determined by extensive radiocarbon dating of fossil algae and marine shells found in glaciolacustrine sediments throughout the McMurdo Sound Region (Hall and Denton, 2000; Stuiver et al., 1981). However, there are conflicting interpretations on how RSIS sediments in Taylor Valley were deposited. According to Stuiver et al. (1981), RSIS sediments were deposited when a lobe of the RSIS penetrated deep into Taylor Valley, up to

present-day Lake Hoare, and dammed a proglacial lake up to about 300 m elevation (Figure 1.4). Following the maximum position of the RSIS lobe, the RSIS retreated with numerous fluctuations. Advances of the RSIS would have caused proglacial lakes to rise as lake water was displaced, while retreats of the RSIS would have caused proglacial lakes to lower as lake water filled space vacated by the RSIS lobe (Stuiver et al., 1981). The interpretation of Stuiver et al. (1981) is similar to the interpretation of Prentice et al. (2009), except that RSIS penetrated even deeper into Taylor Valley than in Stuiver et al. (1981) and proglacial lakes were much smaller (Figure 1.5). According to Prentice et al. (2009), sediments on the valley walls are glaciofluvial sediments deposited at the margins of the RSIS lobe, while sediments at lower elevations are glaciolacustrine sediments. In contrast, Hall et al. (2000) proposed that the RSIS never entered Taylor Valley beyond Coral Ridge, near the Valley Mouth. In this interpretation, sediments in Taylor Valley are lake-ice conveyor deposits (Hendy et al., 2000) that were transported throughout eastern Taylor Valley by a 300 m deep proglacial lake fronting the RSIS (Hall et al., 2000) (Figure 1.6).

The timing of paleolake levels in Taylor Valley is constrained by $^{14}C$ ages of fluvial terraces, which have been interpreted as deltas (Hall and Denton, 2000; Stuiver et al., 1981) (Figure 1.7). These deltas are the primary evidence for large paleolakes in Taylor Valley and $^{14}C$ dates of these terraces represent the elevation and timing of paleolake high stands. $^{14}C$ ages of fluvial terraces in Taylor Valley are highly scattered for any given elevation by about 5 – 10 Ka. This has been interpreted as an effect of millennium scale paleolake fluctuations in response to paleoclimate conditions in the Dry Valleys (Hall et al., 2010).

Above approximately 350 m elevation in eastern Taylor Valley, glacial sediments near the Nussbaum Riegel are composed of older glacial deposits from the RSIS and Taylor Glacier (Denton et al., 1970; Péwé, 1960). Near the Nussbaum Riegel, pre-LGM RSIS sediments are thought to be younger than 1.2 Ma (Denton et al., 1970). Sediments deposited by advances of

the Taylor Glacier are thought to have occurred during or before Taylor III drift (Denton et al., 1970), which has been dated to 208 – 335 Ka (Higgins et al., 2000). In general, older sediments at higher elevation in eastern Taylor Valley are more weathered and contain higher accumulations of salt than younger sediments at lower elevations (Bockheim et al., 2008b).

Soils in western Taylor Valley are primarily composed of tills from older glacial advances of Taylor Glacier, with ages on the order of 0.1 – 1 Ma (Figure 1.8) (Denton et al., 1989; Denton et al., 1993; Higgins et al., 2000). Most soils at lower elevations in western Taylor Valley are from the Taylor II glaciation, 113-120 Ka (Higgins et al., 2000), extending from above Lake Bonney to Canada Glacier. The Taylor II glaciation was not extensive enough to deposit till in higher elevation soils of eastern Taylor Valley (Denton et al., 1970). Above Taylor II till, even older sediments deposited by Taylor Glacier can be found with ages on the order of 1 Ma (Higgins et al., 2000; Wilch et al., 1993). In general, the degree of soil development measured by weathering stage soluble salt content is consistent with the age of tills in western Taylor Valley (Bockheim et al., 2008a; Bockheim et al., 2008b; Pastor and Bockheim, 1980).

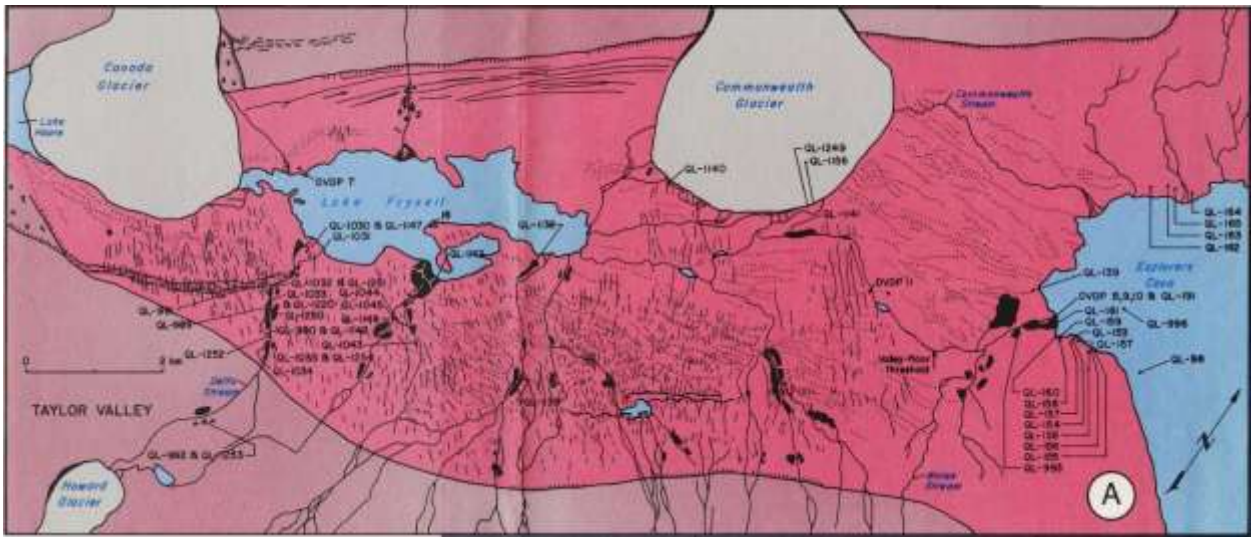


Figure 1.4. A map of RSIS sediments in eastern Taylor Valley from Stuiver et al. (1981) with permission. The maximum extent of the RSIS in Taylor Valley is indicated by the red area. Black deposits are interpreted as lacustrine deltas deposited in paleolakes fronting the RSIS.

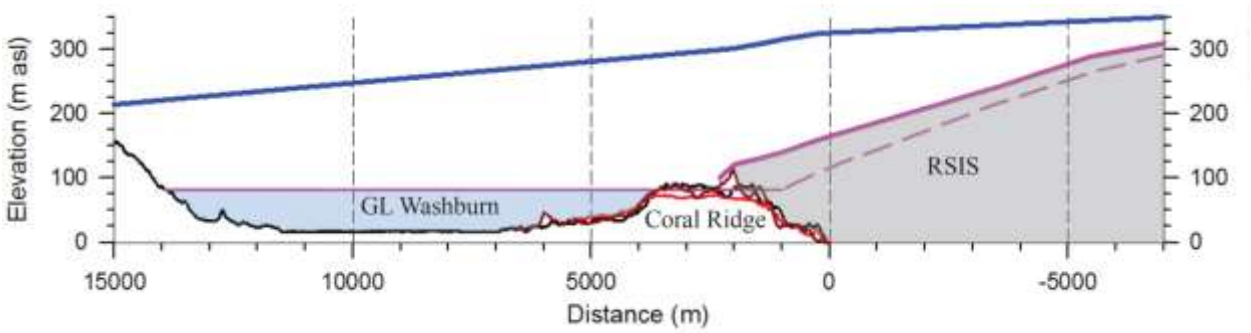


Figure 1.5. A schematic along the valley axis of Taylor Valley from Prentice et al. (2009), showing the maximum extent of the RSIS (blue line), and the maximum elevation of paleolakes (GL Washburn).

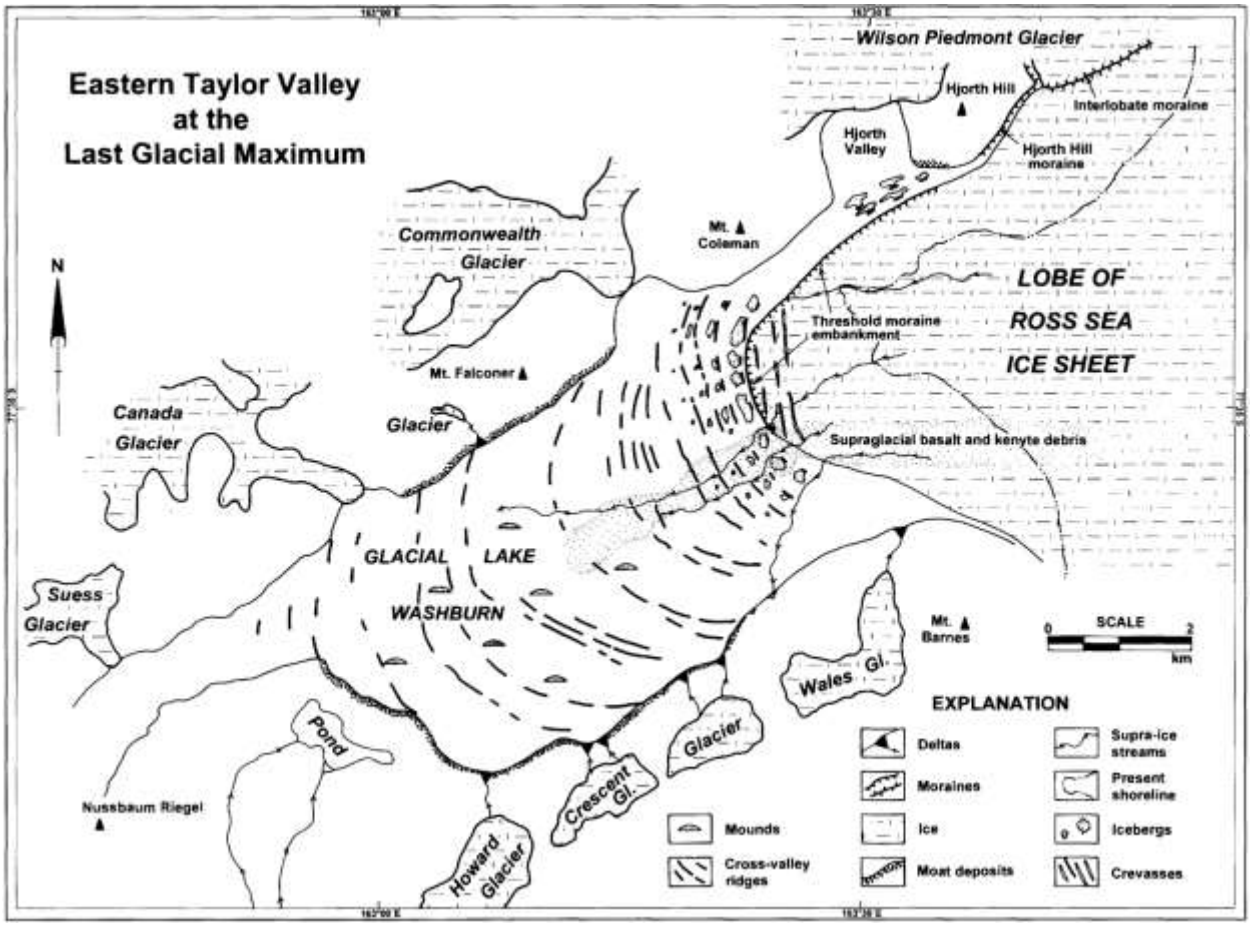


Figure 1.6. This is a drawing of glacial and lacustrine events in Taylor Valley from Hall et al. (2000) with permission, showing the RSIS and paleolakes (Glacial Lake Washburn) at their maximum extents in Taylor Valley. Sediments being transported by the lake-ice conveyor system are also shown in front of the RSIS lobe.

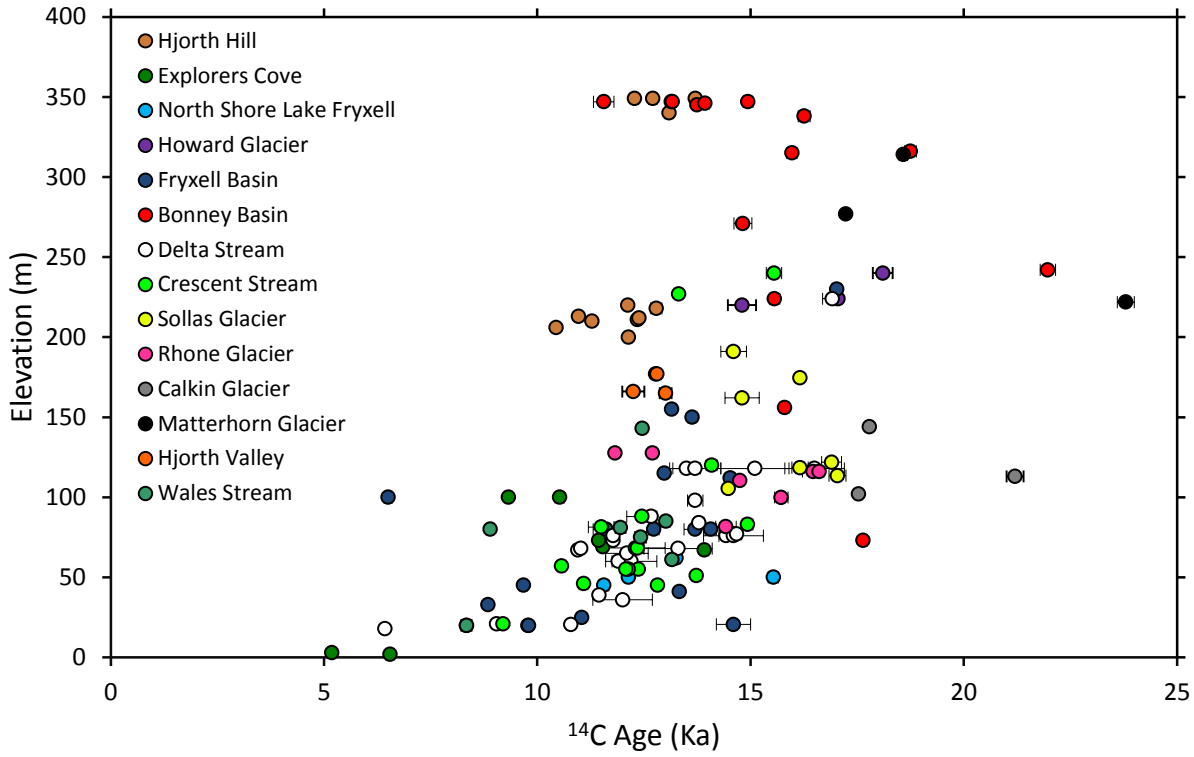


Figure 1.7. $^{14}C$ dates of algae found within Taylor Valley terraces, data from Hall et al. 2000 and Hall et al. 2010. The terraces are organized by the drainage or stream in which they are found.

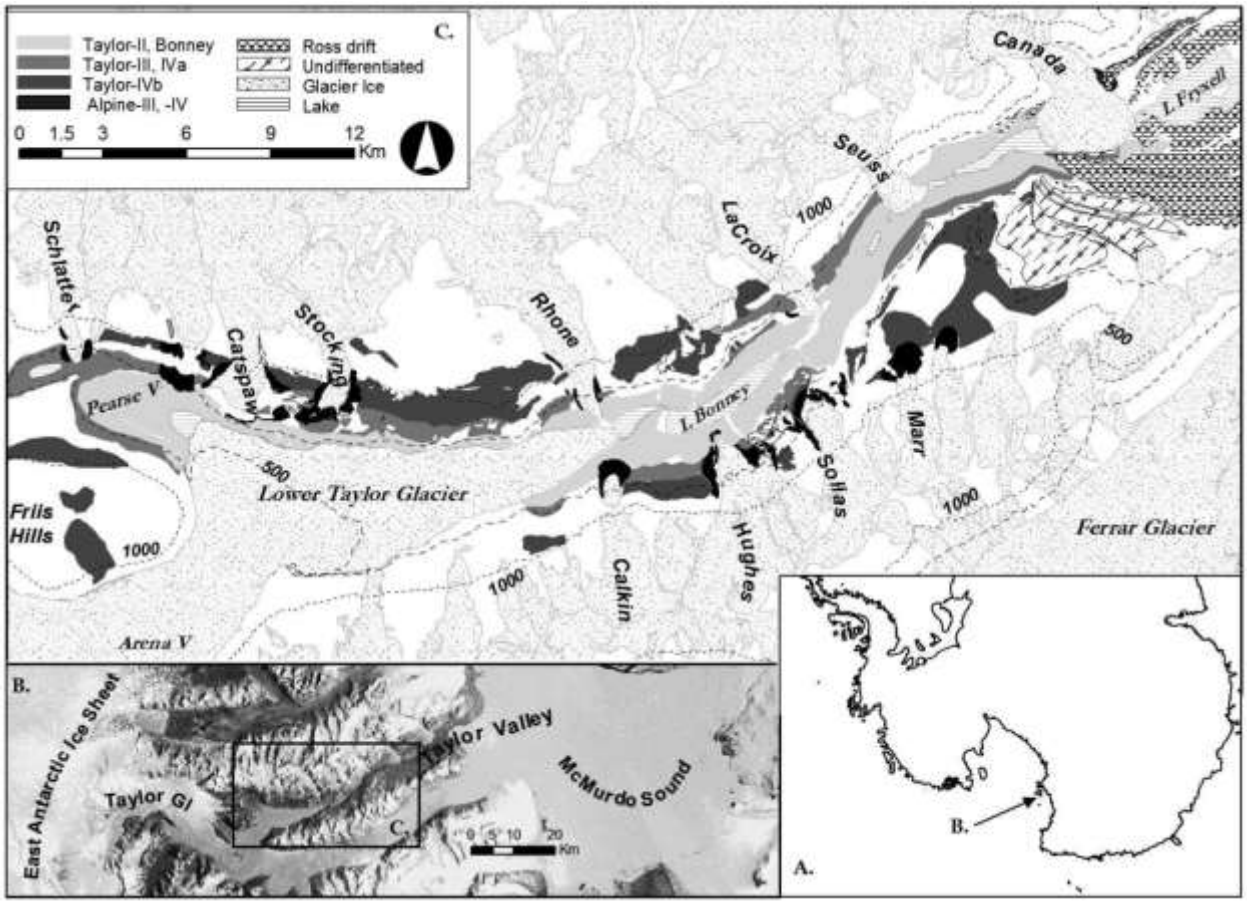


Figure 1.8. The distribution of tills of different age in western Taylor Valley from Bockheim et al. (2008b) with permission: Taylor II (113 – 120 Ka), Taylor III (208 – 335 Ka), Taylor IV (~1 Ma) (Higgins et al., 2000; Wilch et al., 1993).

### *1.5.4. Soils*

Under the World Reference Base for Soil Resources classification system, soils in the Dry Valleys, Antarctica, are classified as Gelisols (Soil Survey Staff, 2010). These are soils that must have permafrost within 100 cm of the soil surface. Soils in eastern Taylor Valley are primarily Typic Haploturbels (Figure 1.9), with Glacic Haploturbels occurring on young, ice-cored alpine moraines. To classify as Turbels, these soils must "have one or more horizons with evidence of cryoturbation in the form of irregular, broken, or distorted horizon boundaries, involutions, the accumulation of organic matter on top of the permafrost, ice or sand wedges, and oriented rock fragments" (Soil Survey Staff, 2010). Cryoturbation in eastern Taylor Valley is caused by the ubiquitous presence of ice-cemented soil (Bockheim et al., 2008b) (Figure 1.10),

which commonly occurs at about 30 cm depth. The expansion and contraction of ice-cemented soil in response to seasonal temperature variations results in the formation of sand-wedge polygonal patterned ground (Black and Berg, 1963). As the ice-cemented permafrost cools during the winter, tensile stresses induced by thermal contraction can overcome the tensile strength of the ice-cemented soil, causing the soil to crack (Lachenbruch, 1962). These cracks are filled by sand from overlying dry sediments, forming a sand wedge, which prevents the contraction cracks from completely expanding as temperatures increase during the summer. During repeated cycles of expansion and contraction, sand wedges progressively grow; the rate of growth in sand-wedge width is on the order of 0.1 – 1 mm $yr^{-1}$ (Sletten et al., 2003).

In western Taylor Valley, soils are primarily Typic Anhyorthels (Figure 1.9). Orthels are distinct from Turbels in that they have “little or no evidence of cryoturbation” (Soil Survey Staff, 2010). The absence of cryoturbation in soils of Bonney Basin is due to the lack of ice-cement in most soils (Figure 1.10), although there is evidence of past cryoturbation from sand-wedge casts (Bockheim et al., 2008b). Dry permafrost is common in older soils, such as in Bonney Basin, and is thought to be due to sublimation of the ice-cement over time (Campbell and Claridge, 2006). In the oldest, high elevation soils of Bonney Basin, and near the Nussbaum Riegel in eastern Taylor Valley, Salic and Petrosalic Anhorthels are common (Bockheim et al., 2008b). Salic soils contain visible salt accumulations within the soil profile, while Petrosalic soils contain a hardened salt pan.

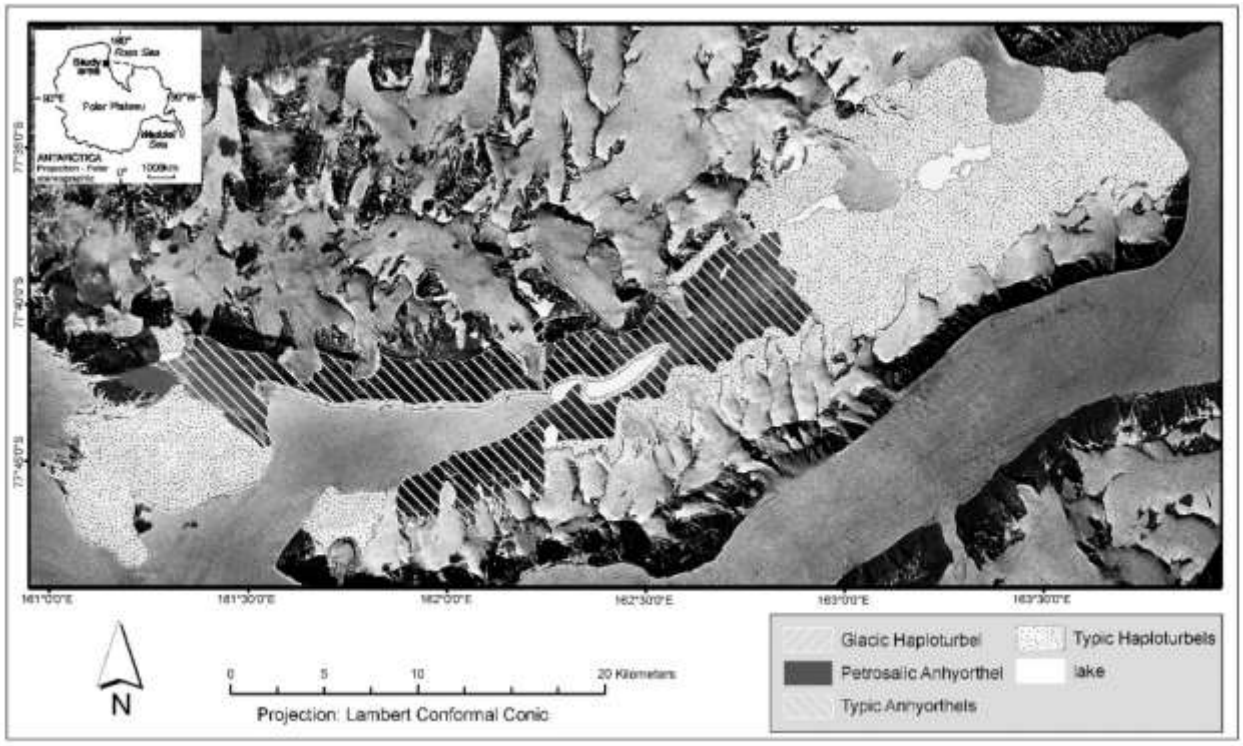


Figure 1.9. The distribution of soil types in Taylor Valley from Bockheim et al. (2008b) with permission.

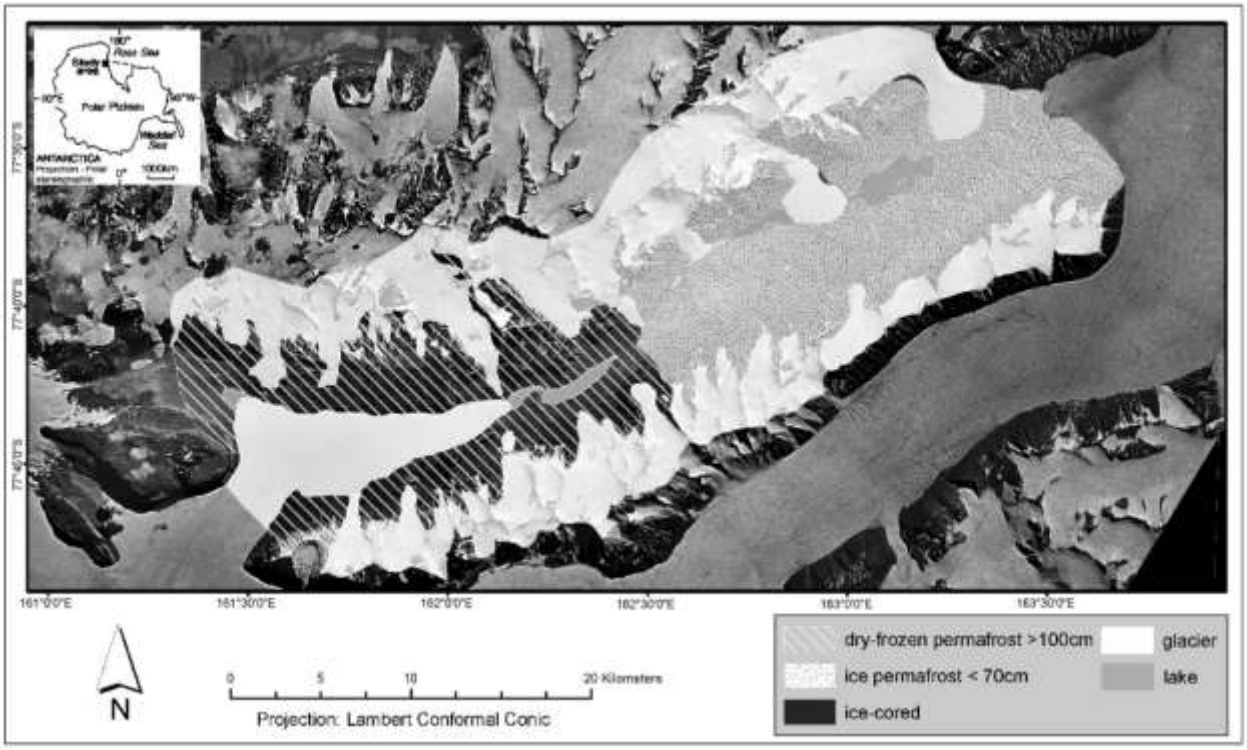


Figure 1.10. The distribution of permafrost types in Taylor Valley from Bockheim et al. (2008b) with permission.

### *1.5.5. Salt Accumulations*

Salt accumulations in Taylor Valley soils are thought to be derived from marine sources (Bao et al., 2008; Keys and Williams, 1981), aeolian dust (Foley et al., 2006; Fortner et al., 2005; Witherow et al., 2006), and relatively minor chemical weathering (Bao and Marchant, 2006; Miller, 2006). Salt phases that have been found in Taylor Valley include: halite (NaCl), sylvite (KCl), monohydrocalcite ($CaCO_3$), aragonite ($CaCO_3$), calcite ($CaCO_3$), thenardite ($Na_2SO_4$), gypsum ($CaSO_4 \cdot 2H_2O$), trona ($NaHCO_3 \cdot Na_2CO_3 \cdot 2H_2O$), thermonatrite ($Na_2CO_3 \cdot H_2O$), and darapskite ($Na_3(SO_4)(NO_3) \cdot H_2O$) (Keys, 1980; Nishiyama and Kurasawa, 1975). Nishiyama and Kurasawa (1975) studied the distribution of salt encrustations in Taylor Valley, and found that Na-carbonate salts, trona and thermonatrite, occur near the valley mouth region of Taylor Valley. These salts have not been found in any other soils of the Dry Valleys (Keys, 1980). Gypsum and mirabilite are also found throughout Taylor Valley, particularly in Bonney Basin (Nishiyama and Kurasawa, 1975). Calcite is ubiquitous in soils across Taylor Valley and occurs as lacustrine carbonates precipitated from evaporating paleolakes (Higgins et al., 2000; Lawrence and Hendy, 1989), surface coatings underneath desert pavement clasts (Foley et al., 2006; Keys, 1980; Nishiyama and Kurasawa, 1975), or marble disseminated in Ross Sea till (Blank et al., 1963; Haskell et al., 1965).

#### *1.5.5.1. Sources of Salt to the Landscape*

##### *1.5.5.1.1. Marine Aerosols*

Marine aerosols in the Dry Valley region are from two main sources: sea-spray aerosols near the coast and atmospheric aerosols found on the Antarctic Plateau. Salts from marine sea-spray aerosols are blown by coastal winds to inland regions of the Antarctica and contain high proportions of Na, Mg, and Cl ions (Benassai et al., 2005; Wagenbach et al., 1998). On the Antarctic Plateau, the influence of sea-spray aerosols is greatest near the ocean and decreases by two orders of magnitude 200 km from the sea (Benassai et al., 2005). Marine salt deposition from ocean sea-spray aerosol is active year round (Wagenbach et al., 1998); during the

summer months, sea-spray aerosols are formed by wind and wave action in the seasonally open waters in McMurdo Sound, while in winter, marine aerosols are derived from salt accumulations termed ‘frost flowers’ that form from thin brine films on the surface of sea ice (Rankin et al., 2000). Frost flowers have been found to be depleted in Na and $SO_4$ ions relative to seawater due to the precipitation of mirabilite ($Na_2SO_4 \cdot 10H_2O$) (Rankin et al., 2000). This source of fractionated marine salt is blown into the Dry Valleys by coastal winds during winter months. The flux of salt during the winter can be greater than the contribution of aerosols during the summer months (Wagenbach et al., 1998). In the Dry Valleys, the effect of marine inputs on salt accumulation is most pronounced near the source of marine sea-spray aerosols, McMurdo Sound (Claridge and Campbell, 1977). In lower elevation soils closer to McMurdo Sound, Na and Cl salt phases derived from sea-spray aerosols are more prevalent, while in higher elevation soils closer to the East Antarctic Ice Sheet, these salt phases are less common (Keys and Williams, 1981).

Atmospheric marine aerosols are distinct from sea-spray aerosols in that they are sourced from the East Antarctic Ice Sheet (Claridge and Campbell, 1968a). These aerosols are comprised mostly of nitrates and sulfates that reach the Dry Valleys through a series of pathways and processes initially described by Claridge and Campbell (1968a). Aerosols containing nitrogen and sulfur compounds from mid-latitude oceans are oxidized to nitrate and sulfate in the upper atmosphere, carried towards inland Antarctica by the Antarctic anti-cyclone, deposited in precipitating snow on the Antarctic Plateau, and then carried into the Dry Valleys by katabatic winds sweeping snow off the Antarctic Plateau towards the ocean (Claridge and Campbell, 1968a). Since atmospheric sulfate and nitrate are sourced inland, from the East Antarctic Ice Sheet, salts of $NO_3$ and $SO_4$ are more prevalent at higher elevations, further from McMurdo Sound (Keys and Williams, 1981). The upper atmospheric oxidation pathway for $SO_4$ and $NO_3$ deposited on the East Antarctic Ice Sheet has been confirmed by isotopic studies showing that

$SO_4$ and $NO_3$ in the Dry Valleys carry an anomalous $\Delta^{17}O$ signature resulting from upper atmospheric oxidation with ozone (Bao et al., 2000; Michalski et al., 2005). Ozone is one of the few naturally occurring compounds in which oxygen isotopes are fractionated independent of mass resulting in a $\Delta^{17}O$ anomaly (Thiemens, 2001). When marine nitrogen and sulfur compounds react with ozone in the upper atmosphere to form $SO_4$ and $NO_3$, the mass-independent $\Delta^{17}O$ anomaly in ozone is incorporated into the $SO_4$ and $NO_3$.

Blood Falls, a rust colored flow located in Western Taylor Valley at the snout of Taylor Glacier, is an important influx of inherited marine salts into Lake Bonney that is believed to originate from an ancient evaporite deposit located under Taylor Glacier (Black et al., 1965). Both Blood Falls and Lake Bonney have ionic compositions similar to seawater, which suggests that Blood Falls influences the chemistry of Lake Bonney (Lyons et al., 2005; Mikucki et al., 2004).

*1.5.5.1.2. Chemical Weathering*

Chemical weathering in Antarctic soils is limited by the cold-dry climate (Claridge and Campbell, 1984; Ugolini and Jackson, 1982) and is thought to occur as a result of high ionic strength brine films that remain liquid at extremely low temperatures. These brines allow oxygen and carbon-dioxide to come into close aqueous association with mineral surfaces and facilitate weathering reactions (Ugolini and Anderson, 1973). The occurrence of chemical weathering in the cold-dry soils of Antarctica has been demonstrated by the precipitation of secondary minerals (Claridge, 1965a; Jackson et al., 1977; Ugolini and Jackson, 1982) and alteration of primary minerals (Dickinson and Rosen, 2003; Glazovskaya, 1958). Over time, chemical weathering can also release salts to soils and influence the composition of salt accumulations (Claridge and Campbell, 1977). The composition of salts derived from chemical weathering has been shown to be dependent on the soil parent material (Claridge and Campbell, 1977; Keys and Williams, 1981). Claridge and Campbell (1977) showed that soils formed exclusively on dolerite bedrock have high proportions of Ca and Mg caused by the preferential weathering of ferromagnesian

minerals. Keys and Williams (1981) showed that Mg enriched salt chemistries are generally found in soils composed of mafic igneous rock minerals. In contrast, granitic soils contain higher proportions of K, which is attributed to weathering of muscovite and, to a lesser extent, K-feldspar (Claridge and Campbell, 1977).

Kelly and Zumberge (1961) have shown that $SO_4$ can be derived from weathering of igneous rocks. By studying the isotopic signature of oxygen atoms in soil $SO_4$, Bao and Marchant (2006) determined the relative proportions of $SO_4$ derived from marine aerosols and chemical weathering. They found that $SO_4$ derived from chemical weathering had the least contribution to the total $SO_4$ content, which indicates that $SO_4$ production from chemical weathering is of secondary importance to the influx of marine aerosols to the landscape. Jones and Faure (1978) also found evidence that salt derived from chemical weathering is of secondary importance to marine aerosols in coastal regions of Antarctica. $^{87}Sr/^{86}Sr$ ratios in Taylor Valley are more radiogenic in western Taylor Valley, furthest from McMurdo Sound, suggesting that Sr in these soils is partially derived from weathering of the soil. However, in eastern Taylor Valley $^{87}Sr/^{86}Sr$ ratios decrease to near seawater ratios, suggesting that seawater aerosols control the composition of salt accumulations near the coast.

There is abundant evidence that chemical weathering occurs in streams and lakes of Taylor Valley. Jones and Faure (1978) and Lyons et al. (2002) examined $^{87}Sr/^{86}Sr$ ratios in the lakes and streams of Taylor Valley and the generally radiogenic $^{87}Sr/^{86}Sr$ ratios they measured suggest that much of the Sr is derived from chemical weathering of primary carbonate and silicate minerals. Lyons et al. (2002) calculated that an average of 92% of the Sr in stream water is due to chemical weathering, although most of the weathering was attributed to carbonate dissolution and not silicate weathering. Chemical weathering in streams is also supported by studies of $HCO_3$ and $H_2SiO_4$ weathering products (Green et al., 1988; Lyons et al., 1998b; Nezat et al., 2001) and direct observations of mica alteration (Maurice et al., 2002).

*1.5.5.1.3. Aeolian Material*

The ability of wind to transport fine-grained particles makes wind an important mechanism for the redistribution of salt accumulations in the Dry Valleys because fine-grained particles have a high surface area that can absorb more salt than coarse-grained particles. Salt accumulations found in glacial snow are largely influence by the accumulation of aeolian material rich in carbonate and sulfate salts (Fortner et al., 2005; Lyons et al., 2003; Witherow et al., 2006). In particular, higher concentrations of $SO_4$ have been found on the up-valley side of Canada Glacier, which suggests that some of the $SO_4$ precipitated on Canada Glacier is from aeolian material blown off $SO_4$ rich soils from Bonney Basin (Fortner et al., 2005).

*1.5.5.1.4. Wetted Hydrologic Margins*

Soils near lake and stream margins are affected by evapoconcentration, a process in which water from lakes and streams moves upwards by capillary forces to the soil surface and evaporates (Barrett et al., 2009; Gooseff et al., 2007; Northcott et al., 2009). The activity of evapoconcentration in soils is indicated by visibly wetted margins around lakes and streams in the Dry Valleys (Figure 1.11). Near lake margins, soils wetted by capillary forces can extend up to 30 m horizontally and 1 m vertically from the lake surface (Gooseff et al., 2007). Near the soil surface, this lake water evaporates, depositing solutes entrained in the lake water into the upper soil (Barrett et al., 2009). Soils adjacent to streams are also influenced by evapoconcentration, but these soils have relatively low salt concentrations compared to lake margins (Barrett et al., 2009). This has been interpreted as an effect of the stability of stream wetted margins; wetted margins around lakes are stable, allowing evapoconcentration to operate for extended periods of time, but wetted margins around streams are unstable due to variable water fluxes (Barrett et al., 2009; Northcott et al., 2009). In addition, salt concentrations in streams are much lower than in lake waters (Lyons et al., 1998b), which will reduce the rate of salt accumulation from evapoconcentration.

Figure 1.11. Wetted hydrologic margin along Lake Joyce from Gooseff et al. (2007). Water wicking upward from the lake evaporates near the soil surface and deposits salts from the lake water.

The high salt concentrations produced by evapoconcentration along lake margins have been used to study the past extent of lakes in the Dry Valleys. Near Bull Pass in Wright Valley, the precipitation of salts from paleolakes has been used to explain sharp spikes in Cl, $NO_3$, and $SO_4$ accumulations in soils at lower elevations (Poage et al., 2008). In Taylor Valley, high soil salinities (measured by electroconductivity) have been found in soils near the south shores of Lakes Fryxell, Hoare, and Bonney. These salt accumulations are thought to be derived from evapoconcentration along paleolake margins (Barrett et al., 2010). Near Lakes Fryxell and Hoare, the soil salinity below 100 – 120 m elevation fluctuates from high to low values over small distances, but is uniformly low at higher elevations. In Bonney Basin, soil salinity is relatively high for all soils sampled. The accumulation and preservation of salts deposited at paleolake margins has been interpreted as a function of soil texture, paleolake margin stability, and subsequent leaching, which results in the complicated distribution of soil salinity observed in Taylor Valley (Barrett et al., 2010). In particular, soil salinity is strongly related to the fine-grained (clay and silt) fraction of soils; soils with more fine-grained material had higher salinities than soils with less fine-grained material (Barrett et al., 2010). This suggests a relationship between the fine-grained fraction and the amount of evapoconcentrated salt.

*1.5.5.2. Salt Leaching*

Salt accumulations deposited by aerosols, weathering, or along hydrologic margins can be altered by leaching (Bao et al., 2008; Keys, 1980). In studies attempting to use salt accumulations to study past events, it is important to understand how salt leaching can change salt distributions deposited in paleoenvironments and the potential effects of leaching on lakes, stream, and groundwater systems. Rates of leaching in the Dry Valleys are slow due to the perennially cold-dry climate and precipitation rates of less than 50 mm water equivalent per year (Fountain et al., 2010); however, over long timescales even slow leaching can potentially remove significant quantities of salt from the soils.

Salt leaching is thought to occur primarily during the summer, when liquid water is available from melting snowfall, permafrost, or glacial ice. Following transient snowfall events during the summer, the accumulated snow quickly melts and percolates down soil profiles. This melt water dissolves salts in the upper soil and moves them deeper into the soil, eventually reaching the ice-cemented permafrost (Dickinson and Rosen 2001, Hagedorn et al. 2010). In the seasonally thawed upper permafrost, known as the active layer, salts likely migrate both vertically and laterally across the relatively impermeable ice-cemented soil during the summer (Conovitz et al. 2006). Even when the active layer is frozen, salts have been observed migrating in thin, saline brine films that remain liquid at extremely low temperatures (Ugolini and Anderson 1973).

### *1.5.6. Ground Water*

Groundwater movement has been found throughout the Dry Valleys and occurs in both shallow and deep ground waters (Cartwright and Harris, 1981). Shallow ground waters occur near the soil surface above ice-cemented soil (Cartwright and Harris, 1981; Harris et al., 2007; Head et al., 2007; Levy et al., 2011; Webster et al., 2003). These flows have been found throughout Taylor Valley during the summer season and several have been traced to melting snow banks at higher elevations (Harris et al., 2007; Levy et al., 2011). The concentration of solutes in shallow groundwater is greater than in nearby streams or glacial ice and the water is isotopically

heavy, indicating modification of these waters by evaporation (Harris et al., 2007; Levy et al., 2011). Brines transported by shallow groundwaters are carried downslope and accumulate at the bottoms of basin and depressions. Depressions in the Dry Valleys are typically moist and contain high concentrations of salt, which is attributed to leaching of salts from surrounding soils (Campbell and Claridge, 1982).

A deep groundwater flow system has been found in Wright Valley near Don Juan Pond (Harris and Cartwright, 1979, 1981) and similar groundwaters are thought to underlie the permafrost in other regions of the Dry Valleys (Cartwright and Harris, 1981). The groundwaters near Don Juan Pond are unique in that they are composed of $CaCl_2$, a composition typically found in deep oil field brines, hydrothermal fluids, or evaporite deposits in other parts of the world (Garrett, 2004). The upwelling of this water to the surface at an average rate of 30 $m^3$ per day and evaporation has formed Don Juan Pond (Harris and Cartwright, 1979). Since $CaCl_2$ brine has a eutectic temperature below -51.8°C (Marion, 1997), Don Juan Pond remains unfrozen during much of the Antarctic winter and the groundwater remains liquid despite permafrost temperatures of -16 to -18°C (Harris and Cartwright, 1981). A similar, and possibly connected, groundwater system is thought to influence the chemistry of bottom waters in Lake Vanda, although Lake Vanda contains more Mg and Na than does Don Juan Pond (Green and Canfield, 1984).

A common property of groundwater brine in the Dry Valleys is enrichment in divalent Ca and Mg ions. Moist seeps in Bonney Basin and undrained hollows located throughout the Dry Valleys are enriched in Ca-Mg compared to surrounding soils (Campbell and Claridge, 1982). Suprapermafrost flows beneath the soil surface have elevated Ca-Mg concentrations compared to nearby surface snow or streams (Field, 1975; Levy et al., 2011; Webster et al., 2003; Wilson, 1979). In shallow groundwater systems, this Ca-Mg enrichment is thought to be controlled by the solubility, eutectic temperature, and hydroscopic properties of salts. Because Ca-Mg-Cl-

$NO_3$ salts have the highest solubilities, lowest eutectic temperatures, and are hygroscopic, they preferentially leach out of the soil over Na or K salts (Keys, 1980; Wilson, 1979). These Ca-Mg enriched brines then migrate to basin bottoms and accumulate, forming Ca-Mg enriched brines. The deep ground waters of Don Juan Pond are unlike any other groundwater brines in the Dry Valleys in that they are enriched in Ca, but highly depleted in Mg. The source of Ca enrichment is controversial and several different theories have been proposed including: hydrothermal fluids, water-rock interaction, and freezing or evaporation of seawater (Lyons and Mayewski, 1993).

# Chapter 2 Soluble Salt Accumulations in Taylor Valley, Antarctica: Implications for Paleolakes and the Ross Sea Ice Sheet

## *2.1. Abstract*

Soluble salt accumulations in Taylor Valley, Antarctica, provide a history of paleolakes and the advance of the Ross Sea Ice Sheet (RSIS). In western Taylor Valley, soluble salt accumulations are relatively high and are composed primarily of Na, Ca, Cl, and $SO_4$. In eastern Taylor Valley, soluble salt accumulations are much lower and are composed primarily of Na and $HCO_3$. Soluble Na-$HCO_3$ compositions in eastern Taylor Valley are formed through leaching, calcite dissolution, and cation exchange reactions and appear to influence the chemistry of nearby streams and lakes. The data presented here supports hypotheses that a lobe of the RSIS expanded into eastern Taylor Valley and dammed proglacial paleolakes. However, in contrast to previous studies, our findings indicate that the RSIS advanced deeper into Taylor Valley and that paleolakes were less extensive. By comparing soluble salt distributions across Taylor Valley, we conclude that a lobe of the RSIS filled all of eastern Taylor Valley and dammed paleolakes in western Taylor Valley up to 300 m elevation. Following ice retreat, smaller paleolakes formed in both western and eastern Taylor Valley up to about 120 m elevation, with prominent still stands controlled by the elevation of major valley thresholds. At higher elevations, soluble salt accumulations are consistent with older soils that have not been affected by the most recent RSIS advance.

*2.2. Introduction*

Soluble salt accumulations are common in the hyperarid soils of the McMurdo Dry Valleys, Antarctica, and have been studied for over forty years (Campbell and Claridge, 1987; Claridge and Campbell, 1968a; Keys and Williams, 1981). Soils accumulate salts over time from the input of marine sea-spray aerosols (Claridge and Campbell, 1968a, 1977; Keys and Williams, 1981), oxidized marine nitrogen and sulfur compounds deposited on the East Antarctic Ice Sheet (Bao et al., 2000; Claridge and Campbell, 1968a; Michalski et al., 2005), and chemical weathering (Claridge and Campbell, 1977; Keys and Williams, 1981). These salts are reworked across the landscape by aeolian processes (Fortner et al., 2005; Lyons et al., 2003; Witherow et al., 2006) and leaching (Hagedorn et al., 2010; Keys, 1980; Wilson, 1979). Salt accumulations have been used as an indicator of relative soil age (Bockheim, 1979, 1982, 1990; Everett, 1971; Pastor and Bockheim, 1980) because of hyperarid conditions that preserve salts in Dry Valley soils, potentially over million-year timescales (Bockheim, 1983; Hall et al., 1993; Marchant et al., 1994). Soluble salt accumulations can also be modified during inundation by lakes and are useful for studying past lacustrine events (Barrett et al., 2010; Bockheim et al., 2008a; Field, 1975; Morikawa et al., 1975; Poage et al., 2008), such as those that are thought to have occurred in Taylor Valley.

During Marine Isotope Stage (MIS) 2 (14.1 to 27.6 Ka), the Ross Sea Ice Sheet (RSIS) filled McMurdo Sound and abutted the Transantarctic Mountains near the McMurdo Dry Valleys (Denton et al., 1970; Stuiver et al., 1981). In front of the RSIS, proglacial lakes are believed to have formed in Taylor Valley (Hall et al., 2000; Péwé, 1960; Stuiver et al., 1981), Wright Valley (Hall et al., 2001), Victoria Valley (Hall et al., 2002), Marshall Valley (Hendy, 2000), and Miers Valley (Péwé, 1960) up to about 450 m above present lake levels. In Taylor Valley, contrasting theories have been proposed about the extent of paleolakes and the RSIS. According to Stuiver et al. (1981), proglacial paleolakes were dammed to a maximum elevation of 310 m by a

lobe of the RSIS that entered deep into Taylor Valley, so that much of eastern Taylor Valley was filled with ice. Prentice et al. (2009) proposed that the RSIS entered further into eastern Taylor Valley than Stuiver et al. (1981). In contrast, Hall et al. (2000) proposed that the RSIS was grounded at the valley mouth for about 10 Ka, forming a stable ice dam that resulted in the filling of all eastern and western Taylor Valley with proglacial paleolakes up to 350 m elevation.

These scenarios have different implications for the paleoclimate during and after MIS 2, the sensitivity of the RSIS to deglacial sea level rise and warming trends, and past hydrologic and climatic regimes in Taylor Valley. In the interpretation of Stuiver et al. (1981), paleolake fluctuations primarily reflect the movement of the RSIS in Taylor Valley as it advanced or retreated in response to deglacial sea level rise and climate change. During advances, the RSIS would have displaced lake water, raising lake levels; by retreating from Taylor Valley, lake water would have filled in areas vacated by the retreating ice, lowering lake levels (Stuiver et al., 1981). In contrast, Hall et al. (2000) proposed that lake levels fluctuated on the basis of changing climatic regimes, which influenced melt water production from the RSIS and surrounding alpine glaciers (Hall et al., 2010).

Salt distributions have been used to study the history of paleolakes in Taylor Valley by Foley et al. (2006), Bockheim et al. (2008a), and Barrett et al. (2010). Foley et al. (2006) mapped the distribution of pedogenic carbonates in near-surface soil horizons and attributed an increase in carbonates below 346 m elevation to lacustrine carbonate deposition. Bockheim et al. (2008a) analyzed the distribution of soluble salts in soils, primarily in western Taylor Valley, and concluded that salt accumulations are influenced primarily by soil age, not inundation by paleolakes. This conclusion was based on the interpretation that soils inundated by lakes are leached of soluble salts; however, Barrett et al. (2009) showed that salts can accumulate near wetted lake margins as lake water moves along water potential gradients towards an evaporation zone near the soil surface. Barrett et al. (2010) studied salt accumulations near

lakes Bonney, Hoare, and Fryxell by measuring the electroconductivity of soil-water mixtures and found evidence of salt accumulation along paleolake margins in all three areas. The influence of paleolakes on these salt accumulations was interpreted as a function of lake stability, lake salinity, soil texture, and leaching (Barrett et al., 2010).

These past studies on salt distribution in Taylor Valley are limited by either the method of analysis or the extent of soils studied. The pedogenic carbonates studied by Foley et al. (2006) are sparingly soluble and are not as sensitive to the influence of paleolakes as more soluble salts. The electroconductivity measurements in Barrett et al. (2010) cannot be used to determine the ionic composition of salts. Bockheim et al. (2008a) analyzed a large soluble salt dataset from soils in Taylor Valley, but few soils were sampled in eastern Taylor Valley and most soils were located at high elevations, above paleolake high-stands proposed by either Stuiver et al. (1981) or Hall et al. (2000). To use soluble salts as a tool to study the glacial and lacustrine history of Taylor Valley, a more detailed and comprehensive understanding of salt distribution is needed.

In this paper, we present data on the water soluble salt contents of 89 soils throughout Taylor Valley. By comparing salt distributions along elevational transects to modern salt accumulations and distributions along lake and ice margins, we present new evidence regarding the extent of the RSIS and paleolakes in Taylor Valley. Our results suggest that the RSIS advanced deep into Taylor Valley and that proglacial paleolakes did not fill all of Taylor Valley, but formed within separate basins in eastern and western Taylor Valley.

## *2.3. Methods*

### *2.3.1. Study Sites*

The McMurdo Dry Valleys are cold-dry deserts that are generally ice-free, with the exception of local alpine glaciers and ice-covered lakes. Minimal penetration by ice is due to the

Transantarctic Mountains, which divert ice from the East Antarctic away from McMurdo Sound (Chinn, 1990). Mean annual temperatures in the Dry Valleys average about -20°C (Doran et al., 2002c) and annual precipitation rates are less than 100 mm in the form of snow (Bromley, 1985; Fountain et al., 2010). Taylor Valley is the lowest elevation Dry Valley and is exposed to seasonally open seawater, making Taylor Valley the wettest and warmest of the McMurdo Dry Valleys (Doran et al., 2002c). Annual temperatures average -17°C, with average winter temperatures around -30°C and average summer temperatures near 0°C (Clow et al., 1988; Doran et al., 2002c).

Taylor Valley is bounded by Taylor Glacier, an outlet of the East Antarctic Ice Sheet, on the west, and McMurdo Sound to the east (Figure 2.1A). Within Taylor Valley, cold-based alpine glaciers descend from the Asgard Range and Kukri Hills. During the austral summer, melt water from these glaciers feeds numerous ephemeral streams that drain into closed basin lakes (McKnight et al., 1999). The largest of these lakes are Lake Fryxell at 18 m elevation, Lake Hoare at 73 m elevation, and Lake Bonney at 58 m elevation (Spigel and Priscu, 1998). These closed basin lakes are sensitive to stream flow variations during warmer and cooler summers (Conovitz et al., 1998; Doran et al., 2008). Since lake levels were first recorded in Taylor Valley by Scott (1905), lake levels have risen owing to greater melt water inputs from surrounding alpine glaciers (Bomblies et al., 2001; Chinn, 1981, 1993).

Soil transects presented here fall into three distinct regions: soils near the valley mouth (Valley Mouth), soils within the closed drainage basin of Lake Fryxell (Fryxell Basin), and soils within the closed drainage basin of Lake Bonney (Bonney Basin) (Figure 2.1B). These regions are further grouped into soils that occur in western Taylor Valley (Bonney Basin soils) and eastern Taylor Valley (Fryxell Basin and Valley Mouth soils). Fryxell Basin and Bonney Basin are the largest closed drainage basins within Taylor Valley and are distinctly different from each other. Bonney Basin is narrow (about 3 km wide), with steep valley walls, while Fryxell Basin is broad

(about 10 km wide), with gentle north-facing slopes and steep south-facing slopes. Fryxell Basin and Bonney Basin are separated from each other by a 116-m-high threshold below the terminus of the Suess Glacier (Figure 2.2) (Kellogg et al., 1980). Near this threshold, much of Taylor Valley is occupied by a distinct bedrock hill called the Nussbaum Riegel, which constricts the valley bottom into a narrow defile. The Nussbaum Riegel reaches an elevation of about 700 m and limits the penetration of moist air masses from McMurdo Sound, making Bonney Basin drier than Fryxell Basin (Fountain et al., 1999). As a result, average snow accumulation rates in Taylor Valley decrease from about 70 mm $yr^{-1}$ near the Valley Mouth to about 10 mm $yr^{-1}$ near Lake Bonney (Fountain et al., 2010). Fryxell Basin is separated from McMurdo Sound by Coral Ridge (Figure 2.2), a large moraine complex near the valley mouth that has an average elevation of about 100 m and is cut by a major channel at its lowest point of 78 m (Kellogg et al., 1980).

Soils in eastern Taylor Valley have formed on glacial, lacustrine, and fluvial sediments deposited during the MIS 2 advance of the RSIS into Taylor Valley (Denton et al., 1970; Hall et al., 2000; Stuiver et al., 1981). Older glacial deposits from the RSIS and Taylor Glacier crop out near the Nussbaum Riegel and above approximately 350 m elevation (Bockheim et al., 2008b; Denton et al., 1970; Péwé, 1960). Soils in western Taylor Valley are believed to have formed in glacial deposits from older advances of Taylor Glacier and alpine glaciations, with ages on the order of 0.1–4 Ma (Denton et al., 1970; Denton et al., 1989; Denton et al., 1993; Higgins et al., 2000; Krusic, 2009).

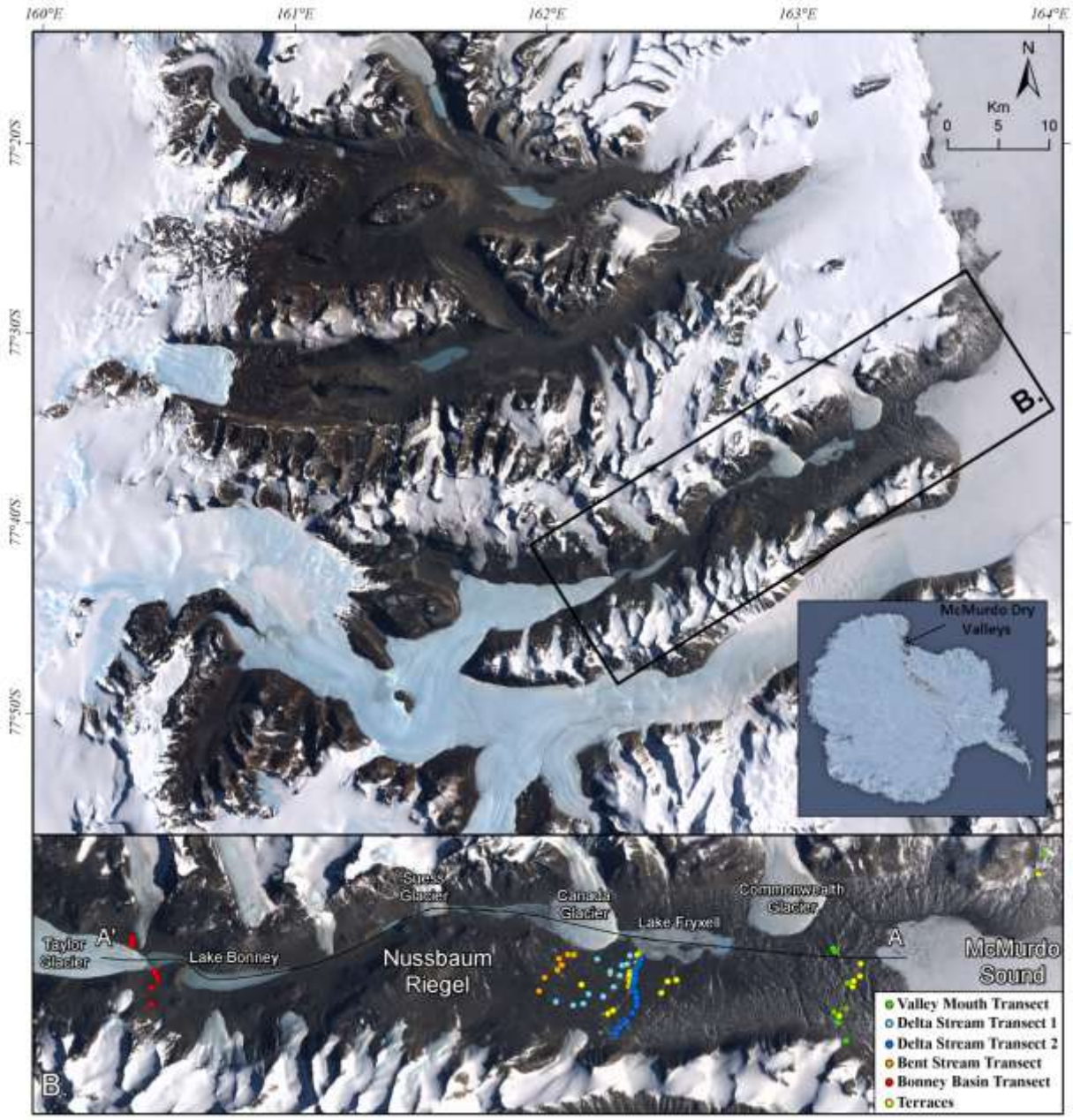


Figure 2.1. A. Landsat Image Mosaic of the McMurdo Dry Valleys and Antarctica (available at http://lima.usgs.gov/); B. Soil pits sampled in this study: Bonney Basin transect, Bent Stream transect, Delta Stream transects (1 and 2), Valley Mouth transect, and fluvial terraces. The black line A-A' generally follows the floor of Taylor Valley and the cross-section profile for this line is shown in Figure 2.

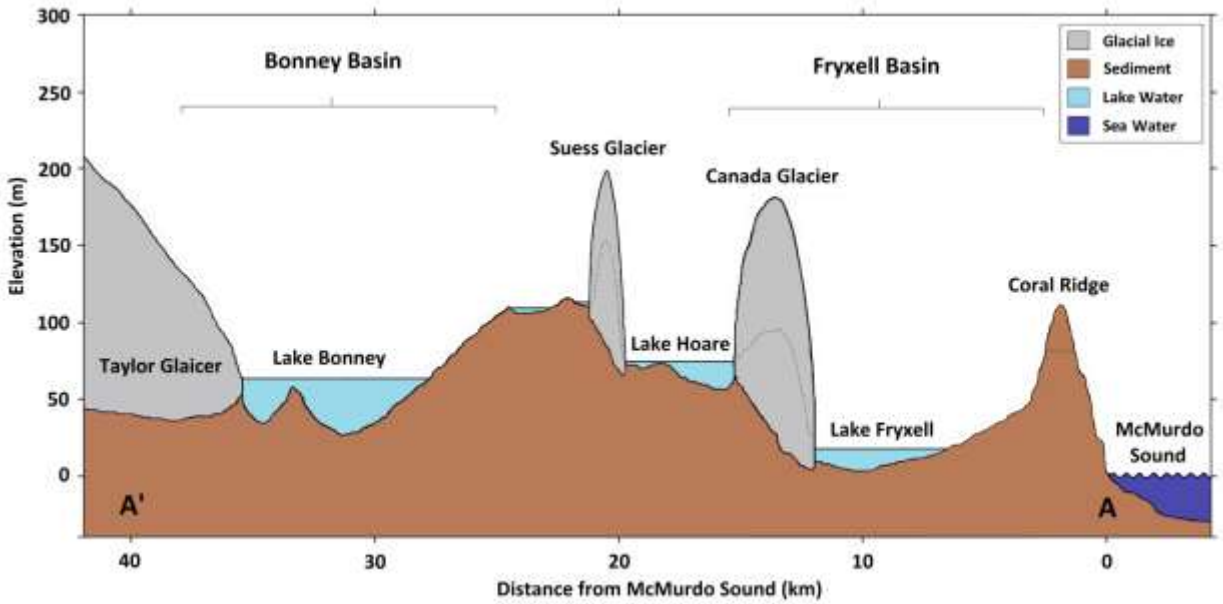


Figure 2.2. A scaled cross-section of major features in Taylor Valley including Fryxell Basin, Bonney Basin, Taylor Glacier, Lake Bonney, Lake Hoare, Lake Fryxell, Suess Glacier, Canada Glacier, Coral Ridge, and McMurdo Sound, constructed from elevations determined in ArcGIS using LIDAR maps of Taylor Valley (Csatho et al., 2005). The line of cross-section is the black line A–A' in Figure 2.1, which generally follows the valley bottom except near Suess Glacier, Canada Glacier, and Coral Ridge. The lowest possible cross-sections in these areas are near the margins of Suess and Canada Glaciers and in a channel through Coral Ridge at 78 m elevation; these lower transects are indicated by lightly dashed lines.

### *2.3.2. Sampling and Analysis*

Soils were sampled along five elevational transects: the Valley Mouth, Delta Stream 1, Delta Stream 2, Bent Stream, and Bonney Basin transects (Figure 2.1B). Additional soils were sampled from fluvial terraces throughout eastern Taylor Valley. Samples were collected from soils at level sites on local topographic highs. Soils were sampled from each soil horizon to the depth of the hard ice-cemented soil; the top few cm of the ice-cemented soil was sampled using a chisel. Typically, soil pits were about 30 cm deep, except for several soils in Bonney Basin, where no ice-cement was present and pits were excavated to 1 m depth. In general, if individual soil horizons were greater than 10 cm in thickness, the horizon was sampled at 10 cm intervals. For the Delta Stream 2 Transect, the top 10 cm of soil was bulk-sampled without regard to individual horizons. All samples were sieved in the field at 2 mm and the weight of each fraction was measured. Laboratory tests were conducted on the <2 mm fraction.

Past researchers have used a 1:5 soil-water extraction to measure soluble salts in Dry Valley soils (e.g., Bockheim, 1979; Claridge and Campbell, 1977; Gibson et al., 1983), but this may underestimate the amount of some ions (Bao et al., 2000). To determine the most efficient and complete extraction method, soluble salts were extracted from sample #159 (a soil with a relatively high concentration of soluble salt) using four different soil-water ratios: 1:10, 1:25, 1:50, and 1:100. Soluble salts were extracted sequentially three times; for each extraction cycle, the soil-water mixture was shaken for one hour, centrifuged, and the supernatant decanted. Based on the results of these extractions (Figure 2.3, Table 2.1), soluble salts were measured using three sequential 1:25 soil-water extractions.

Chemical analysis for major cations (Ca, Mg, Na, K) was conducted using Inductively Coupled Plasma–Optical Emission Spectrometry (Perkin-Elmer® Optima 3300DV) and major anions (Cl, $SO_4$, $NO_3$) using Ion Chromatography (Dionex® ICS-2500). Total inorganic carbon was determined using an OI700 Carbon Analyzer, which acidifies the sample and measures evolved $CO_2$. All inorganic carbon in the soil-water extractions is assumed to be bicarbonate ($HCO_3^-$), because the pH of extracting solutions is around pH 7. The accuracy of this analysis was checked by calculating the charge balance. In addition to the analysis of major soluble ions, soil pH was determined by shaking a 1:2 soil-water mixture for one hour, then allowing the mixture to rest for one hour before measuring the pH.

To calculate the total soluble salt content, it is necessary to determine the soil bulk density. Past studies have assumed bulk densities of 1.5 or 1.6 g $cm^{-3}$ to calculate soluble salt contents (e.g., Bockheim, 1979), but this can greatly overestimate the salt content in rocky soils, because most of the salt is in the <2 mm fraction. Following the method of Burnham and Sletten (2010), we correct for the effect of gravel and cobbles on the total salt content by calculating the whole soil bulk density ($\mathrm{BD}$) from the percent weight ($\%\mathrm{w}$) of the <2 mm and >2 mm soil fractions, the bulk density of the <2 mm soil fraction ($\rho_{<2\mathrm{mm}}$), and the grain density ($\rho_{\mathrm{g}}$):

$$\mathrm{BD}\ (\mathrm{g\ cm^{-3}}) = \left( \frac{100}{\frac{\%\mathrm{w}_{<2\ \mathrm{mm}}}{\rho_{<2\mathrm{mm}}} + \frac{100 - \%\mathrm{w}_{>2\ \mathrm{mm}}}{\rho_{\mathrm{g}}}} \right) \quad (1)$$

The grain density was measured using volume as determined from water displacement for several samples, which yielded a constant grain density of 2.72 g $cm^{-3}$. Because most soils in Taylor Valley are sandy, we use a bulk density of 1.55 g $cm^{-3}$ for the <2 mm fraction, a value typical for sandy soils (Rawls, 1983). To check the accuracy of whole soil bulk density calculations, 15 soils were measured for bulk density using a tin can with a diameter of 15 cm. The average measured bulk density for these soils was 1.76±0.16 g $cm^{-3}$, while the average calculated bulk density using equation (1) was 1.73±0.10 g $cm^{-3}$. The close agreement between measured and calculated values indicates that the bulk density corrections employed here are reasonable.

Salt contents in the soil (equivalents $m^{-2}$) are calculated by summing over all soil horizons the product of the salt concentration $\mathrm{C}$ (meq $kg^{-1}$), the horizon thickness $\mathrm{t}$ (m), the whole soil bulk density $\mathrm{BD}$ (g $cm^{-3}$), and the weight fraction of the <2 mm soil fraction for each soluble ion (Burnham and Sletten, 2010):

$$\mathrm{Salt\ Content}\ (\mathrm{eq\ m^{-2}}) = \sum_{\mathrm{horizon}} \mathrm{BD}_{\ \mathrm{horizon}} \times \mathrm{t}_{\mathrm{horizon}} \times \mathrm{C}_{\mathrm{horizon}} \times \left( \frac{\%\mathrm{w}_{<2\ \mathrm{mm}}}{100} \right)_{\mathrm{horizon}} \quad (2)$$

Total salt contents are the equivalent sum of all anions and cations. The results of this study are combined with soluble salt data compiled by Bockheim [2003] (available at http://nsidc.org/data/ggd221.html) and data from I. B. Campbell and G. G. C. Claridge compiled by Gibb et al. (2002) in the Antarctic Soil Database (available at http://soils.landcareresearch.co.nz/contents/index.aspx). Soluble salt contents in Bockheim (2003) and Gibb et al. (2002) are calculated from soluble salt and soil texture data using equation (2) and the whole soil bulk density in equation (1). Soil texture data was not available

for some soil pits in Bockheim (2003). For these soils, it was assumed that the bulk density was 1.75 g $cm^{-3}$, the average in this study. Also, because inorganic carbon, and often nitrate, was not measured in either Bockheim (2003) or Gibb et al. (2002), total soluble salt contents are calculated as the equivalent sum of the cations multiplied by two. This will give the total equivalent sum of anions and cations because charge balance requires that the equivalent sum of cations will equal the equivalent sum of anions.

## *2.4. Results*

### *2.4.1. Soluble Salt Extraction Procedure*

Tests on different soil-water extraction procedures show that measured soluble salts are strongly dependent on both the soil-water ratio and the number of sequential extractions performed (Figure 2.3, Table 2.1). Total equivalent ion concentrations (the equivalent sum of cations in the three sequential extractions multiplied by two) increase from 115 meq $kg^{-1}$ in the 1:10 extraction procedure to 154 meq $kg^{-1}$ in the 1:100 extraction procedure (Figure 2.3). All ion concentrations increase in higher soil-water extraction procedures except Cl. Na concentrations are slightly lower in the 1:10 extraction procedure and plateau in the 1:25, 1:50, and 1:100 extractions. $SO_4$, Ca, Mg, and K concentrations do not plateau, but increase at higher soil-water extraction procedures. In particular, Ca concentrations increase by an order of magnitude from the 1:10 to the 1:100 soil-water extraction procedures. With respect to ion concentrations measured in each sequential soil-water extraction, nearly all Cl and $SO_4$ in the soil was extracted in the first sequential extraction, independent of the soil-water ratio used (Table 2.1). In contrast, significant concentrations of Ca, Mg, Na, and K were liberated in the second and third sequential extractions. Na and K ions liberated in subsequent extractions are characterized by decreasing concentrations; in contrast, Ca and Mg increase in subsequent extractions. Based on total ion concentrations measured in the 1:100 extraction procedure (as in Figure 2.3), we calculate that if only a single 1:10 soil-water extraction procedure is used, the

total Na content in the soil will be underestimated by 31%, K by 75%, Mg by 80%, and Ca by 97%. However, Ca, Mg, Na, and K are high even in the third sequential 1:100 soil-water extraction, which suggests that the 1:100 extraction procedure also underestimates total ion concentrations.

These tests on extraction methods show that it is difficult to completely extract all soluble ions from the soil, even using sequential extractions at high soil-water ratios. The sequential 1:25 soil-water extraction procedure was selected for this study because it is clear that sequential extractions remove more soluble Na, K, and Mg ions from the soil and total extracted Na plateaus after the 1:25 extraction procedure. The extraction of nearly all Cl and possibly $SO_4$ in the first sequential extraction indicates that these ions will be comparable between the sequential 1:25 soil-water method used in this study and the 1:5 soil-water method used by Bockheim (2003) and Gibb et al. (2002). In contrast, the extraction of significant concentrations of Na, K, Mg, and Ca in the second and third sequential extractions indicates that these ion concentrations will vary depending on the extraction method.

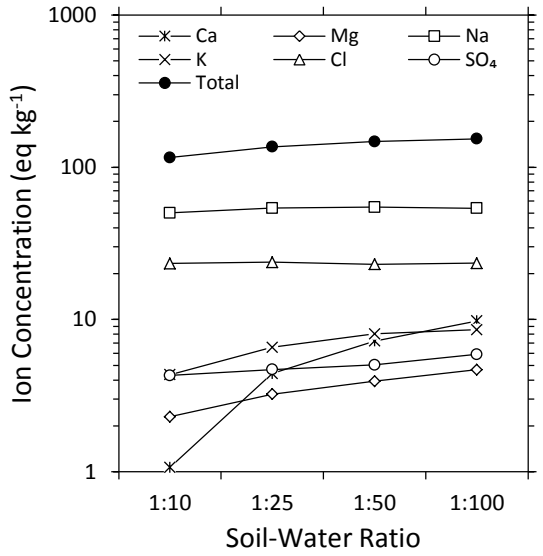


Figure 2.3. Graph of ion concentrations (the sum of all sequential extractions) measured at different soil-water ratios. The total ion concentration is the sum of the equivalent cation concentrations multiplied by two.

Table 2.1. Ion concentrations (mmol $kg^{-1}$) measured in individual extractions of the sequential soil-water extractions.

| Soil-Water Ratio | Extraction Step | Ca | Mg | Na | K | Cl | $SO_4$ |
|---|---|---|---|---|---|---|---|
| | | | | mmol $kg^{-1}$ | | | |
| 1:10 | 1 | 0.14 | 0.46 | 37.30 | 2.17 | 22.77 | 2.00 |
| | 2 | 0.11 | 0.33 | 9.12 | 1.14 | 0.84 | 0.13 |
| | 3 | 0.29 | 0.38 | 4.71 | 1.10 | 0.21 | 0.06 |
| 1:25 | 1 | 0.19 | 0.48 | 42.24 | 3.23 | 22.98 | 2.10 |
| | 2 | 0.58 | 0.55 | 8.89 | 2.00 | 0.71 | 0.16 |
| | 3 | 1.46 | 0.60 | 3.56 | 1.44 | 0.39 | 0.12 |
| 1:50 | 1 | 0.35 | 0.62 | 44.41 | 4.50 | 21.75 | 2.15 |
| | 2 | 1.33 | 0.66 | 7.90 | 2.21 | 0.91 | 0.22 |
| | 3 | 1.94 | 0.71 | 2.88 | 1.40 | 0.62 | 0.17 |
| 1:100 | 1 | 0.80 | 0.70 | 43.66 | 4.89 | 22.27 | 2.35 |
| | 2 | 1.84 | 0.81 | 7.98 | 2.43 | 1.09 | 0.31 |
| | 3 | 2.29 | 0.86 | 3.18 | 1.37 | 0.56 | 0.34 |

### *2.4.2. Total Salt Content Distributions*

The distribution of total soluble salt contents in Taylor Valley is shown in Figure 2.4 using the datasets of Bockheim (2003), Gibb et al. (2002), and data from this study. Soils in this study are located primarily in the Fryxell Basin and Valley Mouth regions. Soils from Bockheim (2003) and Gibb et al. (2002) are located primarily in Bonney Basin. Some of the variability in soluble salt contents in Figure 2.4 may be due to greater dissolution of gypsum and calcite in the 1:25 soil-water extraction used in this study than in the 1:5 soil-water extraction used by Bockheim (2003) and Gibb et al. (2002). However, measured sulfate concentrations are typically low in this study and carbonate dissolution can account only for about 20 eq $m^{-2}$ of the total salt content (based on an average $HCO_3$ content of 10 eq $m^{-2}$ and assuming that all $HCO_3$ is associated with equivalent concentrations of cations). Soluble salt contents in Figure 2.4 may also be influenced by the depth of soil pits. In Bonney Basin, the absence of ice-cemented soil allowed many soils to be excavated two to three times deeper than in eastern Taylor Valley, where ice-cemented soil occurs at about 30 cm depth. Greater pit depth could increase salt contents measured in Bonney Basin soils relative to eastern Taylor Valley. However, given the broad categories for salt contents in Figure 2.4, variability in total salt contents because of different extraction methods and pit depth is small relative to the value range of the categories.

The dominant characteristic of soluble salt distributions in Taylor Valley is the occurrence of low salt contents in eastern Taylor Valley (averaging 50 eq $m^{-2}$) and high salt contents in western

Taylor Valley (averaging 900 eq $m^{-2}$). Salt accumulations in Dry Valley soils are thought to be directly related to soil age (e.g., Bockheim, 1979) and, in general, salt distributions are consistent with differences in soil age between eastern and western Taylor Valley. In western Taylor Valley, soils are from MIS 5 or older advances of Taylor Glacier and alpine glaciations, while in eastern Taylor Valley, soils are primarily from the MIS 2 advance of the RSIS (Bockheim et al., 2008b). There are a number of exceptions to this overall trend in salt content; soils with low salt contents can be found in western Taylor Valley and soils with high salt contents are scattered throughout eastern Taylor Valley. Soils in western Taylor Valley that have low salt contents are typically ice-cemented near the surface. Ice-cemented soil is relatively rare in western Taylor Valley (Bockheim et al., 2007) and its presence suggests a higher local moisture regime that may have leached soluble salts from these soils. Several soils in western Taylor Valley with low salt contents are located on lateral moraines along alpine glacier margins and are younger than adjacent soils.

Although most soils sampled in eastern Taylor Valley have low salt accumulations, high salt accumulations are found on the eastern slopes of the Nussbaum Riegel in soils developing on pre-MIS 2 drift of the RSIS and Taylor Glacier. Salt contents in these older soils are generally lower than in similarly aged soils in western Taylor Valley. This suggests that salts in these soils are much more susceptible to leaching in the wetter climate of eastern Taylor Valley. Soils with relatively high salt contents are also scattered below approximately 120 m elevation in young RSIS sediments. Barrett et al. (2010) also found high salt accumulations below 120–100 m near Lake Fryxell and Hoare and concluded that these accumulations were deposited at the margins of paleolakes.

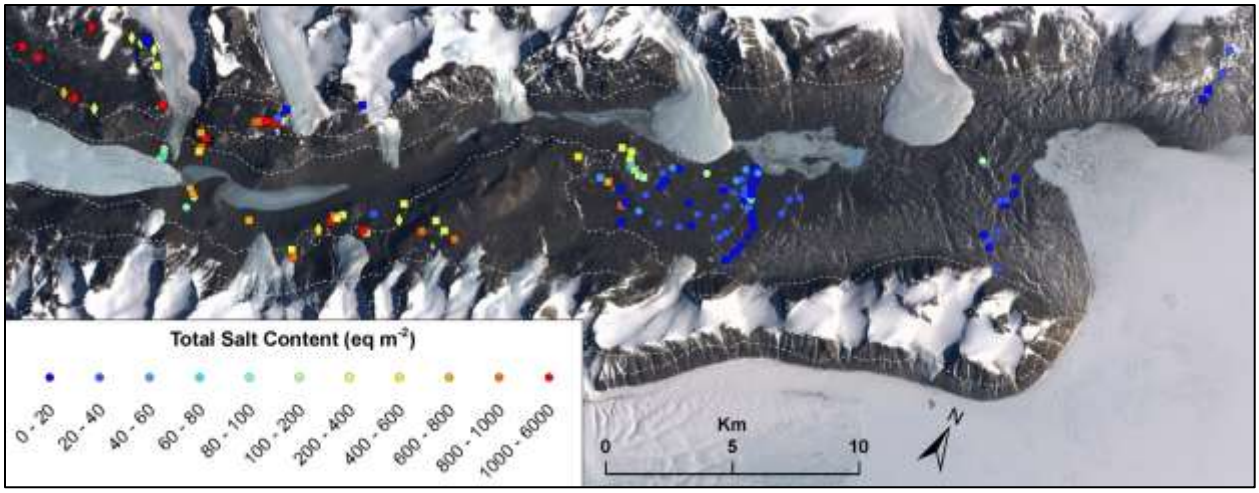


Figure 2.4. Map of total salt contents from this study (circles), Bockheim (2003) (squares), and Gibb et al. (2002) (diamonds) given in eq $m^{-2}$. Contour lines are given at 500-m intervals as dashed white lines.

### *2.4.3. The Chemical Composition of Salt Accumulations*

Average and median ion contents in Valley Mouth, Fryxell Basin, and Bonney Basin soils are given in Table 2.2. Only data from this study is considered in this section because tests on different soil-water extraction procedures indicate that the different soil-water extraction procedure used in Bockheim (2003) and Gibb et al. (2002) will have a large effect on Ca, Mg, Na, K, and possibly $SO_4$ concentrations. In eastern Taylor Valley, the concentration of all ionic species is low compared to western Taylor Valley, which reflects trends in total salt contents (Table 2.2). The greatest differences in ion contents between these two regions are found in Ca, Mg, Na, $SO_4$, Cl, and $NO_3$, while K and $HCO_3$ contents are only slightly higher in western Taylor Valley. Average ion concentrations are much higher than median ion concentrations, particularly in eastern Taylor Valley. This indicates that the distribution of salt contents in eastern Taylor Valley is characterized by mostly low salt contents, punctuated by relatively few soils with high salt contents. Soils with high salt contents in eastern Taylor Valley have higher Ca, Na, Cl, and $SO_4$ contents.

The composition of salts and soil pH varies with distance from McMurdo Sound. Valley Mouth soils are composed almost entirely of Na and $HCO_3$ ions and the average soil pH is 9.7 (Table

2.2). Further inland, in Fryxell Basin, Na and $HCO_3$ are still the dominant ions and the average soil pH is 9.6, but soils contain higher proportions of Ca and Mg. In Bonney Basin, located furthest from McMurdo Sound, soils have high proportions of Ca, Mg, Na, Cl, and $SO_4$ and the average soil pH decreases to 8.5. The trend in soil pH in Taylor Valley is similar to trends observed by Claridge and Campbell (1977); soils near the coast are alkaline with pH values around 9, while near the East Antarctic Ice Sheet pH decreases to as low as 6. Claridge and Campbell (1977) suggested that this is due to the accumulation of slightly alkaline marine aerosols near the coast and slightly acidic aerosols near the East Antarctic Ice Sheet.

Ionic ratios of soluble salts can be used to determine the source of salts to soils in Taylor Valley (Table 2.3). Near McMurdo Sound, average $SO_4$/Cl and $NO_3$/Cl ratios in soils are close to ratios in seawater, while further from McMurdo Sound $SO_4$/Cl and $NO_3$/Cl ratios increase. These trends in $SO_4$, $NO_3$, and Cl with distance from McMurdo Sound are similar to findings by Keys and Williams (1981) and are thought to be due to the influence of Cl rich marine sea-spray aerosols near McMurdo Sound and $SO_4$-$NO_3$ rich snow on the East Antarctic Ice Sheet (Claridge and Campbell, 1968a). $SO_4$ and $NO_3$ on the East Antarctic Ice Sheet are derived from marine nitrogen and sulfur compounds that have been oxidized to $SO_4$ and $NO_3$ in the upper atmosphere (Bao et al., 2000; Michalski et al., 2005). These ions are precipitated with snow onto the East Antarctic Ice Sheet and carried down to the Dry Valleys by katabatic winds (Claridge and Campbell, 1968a). $SO_4$ may also accumulate in Taylor Valley soils from chemical weathering (Bao and Marchant, 2006; Claridge and Campbell, 1977; Kelly and Zumberge, 1961) and $SO_4$-rich aeolian dust from soils in western Taylor Valley (Fortner et al., 2005).

With respect to other ionic ratios, soluble salts in Taylor Valley soils generally vary from seawater compositions. In Bonney Basin soils, Na/Cl ratios are similar to seawater but Ca/Cl, Mg/Cl, K/Cl, and $HCO_3$/Cl are higher than in seawater. In Fryxell Basin and Valley Mouth soils, Ca/Cl, Mg/Cl, Na/Cl, K/Cl, and $HCO_3$/Cl ratios are 1 to 2 orders of magnitude higher than in

seawater (Table 2.3). The large difference in soil Na/Cl ratios from the seawater ratio is surprising because Na/Cl ratios in Taylor Valley glaciers, streams, and lakes are relatively close to seawater ratios (Lyons et al., 1998b). Furthermore, Valley Mouth soils should be the most strongly influenced by marine sea-spray aerosols, but Na/Cl ratios in these soils deviate the most from the seawater ratios. As will be discussed in the following sections, ion ratios and compositions in these soils can be explained by mineral dissolution and cation exchange reactions.

Table 2.2. Average and median salt contents of major cations and anions in moles $m^{-2}$, and pH for Valley Mouth, Fryxell Basin, and Bonney Basin soils. The number of soils is given by n.

| | Region | n | pH | Ca | Mg | Na | K | Cl | $SO_4$ | $NO_3$ | $HCO_3$ | Total |
|---|---|---|---|---|---|---|---|---|---|---|---|---|
| | | | | | | | moles $m^{-2}$ | | | | | eq $m^{-2}$ |
| Average | Valley Mouth | 15 | 9.7 | 1.09 | 1.06 | 12.05 | 1.10 | 5.88 | 0.61 | 0.16 | 8.72 | 34.88 |
| | Fryxell Basin | 68 | 9.6 | 2.22 | 0.97 | 5.30 | 1.06 | 2.38 | 0.86 | 0.05 | 7.77 | 25.49 |
| | Bonney Basin | 7 | 8.5 | 18.96 | 13.98 | 65.76 | 3.86 | 88.44 | 15.05 | 1.28 | 10.64 | 271.00 |
| Median | Valley Mouth | 15 | 9.8 | 0.72 | 0.45 | 6.80 | 1.08 | 0.84 | 0.11 | 0.00 | 8.68 | 21.88 |
| | Fryxell Basin | 68 | 9.7 | 1.50 | 0.74 | 3.58 | 0.83 | 0.57 | 0.13 | 0.00 | 7.97 | 19.88 |
| | Bonney Basin | 7 | 8.4 | 16.12 | 6.02 | 19.71 | 1.88 | 20.01 | 10.35 | 0.80 | 10.90 | 113.41 |

Table 2.3. Average ionic ratios in Taylor Valley soils compared to ratios in seawater. The number of soils is given by n.

| | n | Ca/Cl | Mg/Cl | Na/Cl | K/Cl | $SO_4$/Cl | $NO_3$/Cl | $HCO_3$/Cl |
|---|---|---|---|---|---|---|---|---|
| Valley Mouth | 15 | 1.443 | 0.758 | 10.712 | 1.450 | 0.161 | 0.011 | 13.116 |
| Fryxell Basin | 68 | 3.553 | 1.519 | 7.243 | 1.956 | 0.402 | 0.017 | 16.981 |
| Bonney Basin | 7 | 0.584 | 0.204 | 0.828 | 0.084 | 0.444 | 0.032 | 0.300 |
| Seawater | – | 0.019 | 0.098 | 0.857 | 0.018 | 0.051 | 0.009 | 0.004 |

## *2.5. Discussion*

### *2.5.1. The Influence of Mineral Dissolution and Cation Exchange on Soil-Water Extractions*

Tests on different soil-water extraction procedures indicate that the measurement of soluble salts is strongly dependent on the soil-water ratio and the number of sequential extractions that are performed. The effects of different soil-water extraction procedures on soluble salts has been studied extensively by Eaton and Sokoloff (1935), Kelley (1939), and Reitemeier (1946). These authors found that the measurement of soluble ions in soil-water extractions is complicated by the effects of mineral dissolution and cation exchange. In particular, the dissolution of sparingly soluble gypsum or calcite increases Ca, $SO_4$, and $HCO_3$ concentrations

in soil-water extractions and causes Ca to exchange with Na, K, and Mg on the exchange complex. By increasing the water content in soil-water extractions, greater mineral dissolution occurs, which leads to even greater exchange of Ca for Na, K, and Mg.

Soil-water extractions in this study are likely affected by calcite dissolution and cation exchange because calcite is ubiquitous in Taylor Valley soils (Foley et al., 2006; Keys, 1980; Nishiyama and Kurasawa, 1975) and soluble salts are measured in dilute soil-water extractions. Calcite dissolution and cation exchange can be described by the following generalized reaction:

$$\mathrm{CaCO_3 + H_2CO_3 + (2Na, 2K, Mg)X_2 \leftrightarrow (2Na^+, 2K^+, Mg^{+2}) + 2HCO_3^- + CaX_2} \quad (3)$$

where X is an exchange site associated with an absorbed cation. The increase in Ca, Mg, Na, K, and $HCO_3$ concentrations predicted by equation (3) is consistent with high ratios of Ca, Mg, Na, K, and $HCO_3$ relative to Cl in soil-water extractions of eastern Taylor Valley. Furthermore, the alkalinity produced by this reaction has been shown to raise soil pH (Cruz-Romero and Coleman, 1975; Gupta et al., 1981; Reitemeier, 1946) and is consistent with the high pH values measured in this study.

To test the hypothesis that mineral dissolution and cation exchange is affecting the composition of water extractions, soluble salts in 33 samples were measured in a single 1:10 soil-water extraction (shaken for one hour) and then compared to cations measured in the three sequential 1:25 soil-water extractions (Figure 2.5). The results of this experiment show that all cation concentrations are higher in the sequential 1:25 soil-water extractions and that $Mg_{1:25}/Mg_{1:10}$, $K_{1:25}/K_{1:10}$, and $Na_{1:25}/Na_{1:10}$ ratios increase linearly with increasing $Ca_{1:25}/Ca_{1:10}$ ratios. On average, the increase in Ca, Mg, Na, and K concentrations in the 1:25 relative to the 1:10 soil-water extraction is 6.95, 1.90, 5.79, and 2.41 mmol $kg^{-1}$, respectively. This is consistent with higher Ca concentrations in the 1:25 extraction owing to increased mineral dissolution and the exchange of this Ca with exchangeable Na, K, and Mg. $Cation_{1:25}/cation_{1:10}$ ratios shown in

Figure 2.5 fall into distinct groups; in general, $Mg_{1:25}/Mg_{1:10} > K_{1:25}/K_{1:10} > Na_{1:25}/Na_{1:10}$. This relationship suggests the relative affinity of Mg, K, and Na for exchange sites in the order Mg > K > Na. For example, the higher $Mg_{1:25}/Mg_{1:10}$ ratio indicates that a higher proportion of Mg is removed from the soil in the 1:25 extraction relative to the 1:10 extraction and suggests that a higher proportion of Mg remained on the exchange complex in the 1:10 extraction. Relative cation affinities for exchange sites are also consistent with how quickly Mg, K, and Na are extracted from soils in sequential water extractions (Table 2.1). Nearly all the Na is removed in the first extraction, while high proportions of Mg and K remain in subsequent extractions.

Although mineral dissolution and cation exchange will influence the chemical composition of soil-water extractions, only mineral dissolution will affect total salt contents measured in equivalents because charge is conserved during exchange reactions. Furthermore, the effects of mineral dissolution and cation exchange on soil-water extractions will be limited by the solubility of calcite/gypsum and the Cation Exchange Capacity (CEC). Since the CEC of Antarctic soils is generally low, averaging about 40 meq $kg^{-1}$ for sandy soils (Cameron and Conrow, 1969; Cameron et al., 1970; Cameron et al., 1971), the addition of exchangeable Mg, Na, and K to soil-water extractions will be limited to a maximum of about 40 meq $kg^{-1}$. In soils with high soluble salt accumulations, such as in Bonney Basin, ions from mineral dissolution and cation exchange will have a relatively small effect on the total ion content. This is consistent with ratios of Ca, Mg, Na, K, and $HCO_3$ relative to Cl in Bonney Basin that are closer to seawater ratios. In contrast, mineral dissolution and cation exchange effects should dominate the chemistry of soil-water extractions in soils with low soluble salt accumulations, such as occur in eastern Taylor Valley.

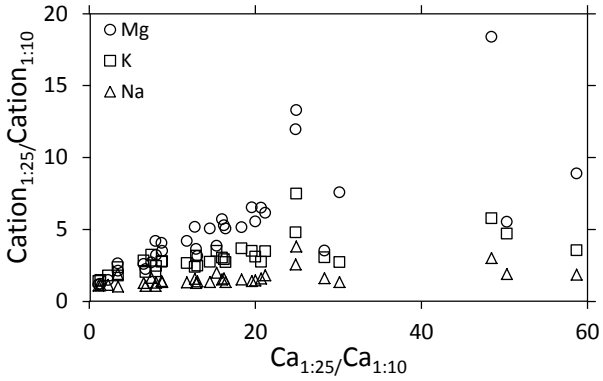


Figure 2.5. Graph showing the increase in Na, K, and Mg relative to the increase in Ca between 1:25 and 1:10 soil-water extractions. For all samples, cation concentrations are higher in the 1:25 extraction relative to the 1:10 extraction.

### *2.5.2. Na-$HCO_3$ Soils in Eastern Taylor Valley*

The influence of mineral dissolution and cation exchange observed in soil-water extractions suggests that these reactions also occur naturally in Taylor Valley soils to produce soil solutions enriched in Na-$HCO_3$. The formation of soluble Na-$HCO_3$ in soils has been studied extensively by authors investigating alkali (sodic) soils (e.g., de' Sigmond, 1927; Gedroiz, 1912; Kelley and Cummins, 1921) and is reviewed by Kelley (1951). In calcareous soils, such as occur in eastern Taylor Valley, Na-$HCO_3$ salts are thought to develop through a series of steps that include leaching with Na-rich salt solution, calcite dissolution, and cation exchange. This process was first demonstrated over a century ago by Mondésir (1888). By leaching a soil with Na-rich salt solution, such as NaCl, the exchange complex becomes saturated in Na. As Na absorbs onto exchange sites, exchangeable Ca, Mg, and K is displaced into the soil solution and leached from the soil. When wetted, calcareous soils with high proportions of exchangeable Na follow the reaction in equation (3); Ca from calcite dissolution exchanges with exchangeable Na, producing a Na-$HCO_3$-enriched soil solution (Gedroiz, 1912). Na-$HCO_3$ enrichment can also occur in the absence of calcite from the hydrolysis of exchangeable Na (Gedroiz, 1912):

$$H_2CO_3 + NaX = HX + Na^+ + HCO_3^- \quad (4)$$

Although this hydrolysis reaction is important for Na-$HCO_3$ formation in some soils, Cummins and Kelley (1923) demonstrated that Na-$HCO_3$ formation in the presence of calcite is far greater than what can be produced by hydrolysis in the absence of calcite.

In Taylor Valley, soils with high exchangeable Na likely form when Na-Cl rich salts from marine aerosols leach down soil profiles following snowfall events (Hagedorn et al., 2010). Since K ions are relatively minor in Dry Valley soils (Keys, 1980), downward-leaching Na will primarily displace exchangeable Ca and Mg:

$$2\mathrm{NaCl} + (\mathrm{Ca},\mathrm{Mg})\mathrm{X}_2 \leftrightarrow (\mathrm{Ca},\mathrm{Mg})\mathrm{Cl}_2 + 2\mathrm{NaX} \quad (5)$$

The Ca-Mg-Cl leachate predicted by this reaction may contribute to Ca-Mg-Cl enriched brines that have been found in groundwater seeps throughout Taylor Valley (Levy et al., 2011). Furthermore, Na absorbed onto the exchange complex in reaction (4) is no longer associated with Cl, which is leached from the soil with Ca and Mg. When the soil is wetted, this exchangeable Na can exchange with Ca from calcite dissolution to form Na-$HCO_3$-enriched soil solutions. The evaporation of Na-$HCO_3$ solutions following wetting events could account for trona ($NaHCO_3 \cdot Na_2CO_3 \cdot 2H_2O$) and thermonatrite ($Na_2CO_3 \cdot H_2O$) salt encrustations that occur in soils of eastern Taylor Valley (Nishiyama and Kurasawa, 1975). Similar leaching, mineral dissolution, and exchange processes have been found to occur in Egyptian desert soils by Smettan and Blume (1987). In these soils, downward-leaching Na from the soil surface has resulted in soluble Na-$HCO_3$ compositions near the soil surface and the migration of highly soluble Ca-Mg-Cl-$NO_3$ brine to depth (Smettan and Blume, 1987).

The process of Na-$HCO_3$ formation outlined above is dependent on leaching and wetting of the soil; leaching with Na-rich salt saturates exchange sites with Na and wetting soils with high exchangeable Na forms Na-$HCO_3$ rich soil solutions. The dependence of Na-$HCO_3$ formation on moisture suggests that Na-$HCO_3$ compositions will occur in regions with high precipitation

rates. In eastern Taylor Valley, precipitation rates are relatively high owing to the influence of moisture from McMurdo Sound (Fountain et al., 2010), which is consistent with the prevalence of soluble Na-$HCO_3$ compositions in eastern Taylor Valley. In addition, soluble Na-$HCO_3$ is often associated with the presence of calcite because of the combined effects of calcite dissolution and cation exchange (Kelley, 1951). Although calcite is found in many soils of the Dry Valleys, it is particularly prevalent in eastern Taylor Valley owing to the presence of marble in RSIS sediments, which dissolves and reprecipitates as a calcite pendants beneath soil clasts (Campbell and Claridge, 1987). Hence, the climate and mineralogy of soils in eastern Taylor Valley are well suited to the formation of soluble Na-$HCO_3$ salts.

Stream and lake waters in eastern Taylor Valley also have distinctive Na-$HCO_3$ compositions (Green et al., 1988), which suggests that soils influence water chemistries in eastern Taylor Valley. Na-$HCO_3$ from soils may enter nearby stream and lake water when Na-$HCO_3$ soil solutions are leached from soils during wetting. In addition, wind will disperse $Na_2CO_3$ salt precipitates and soil particles with high exchangeable Na into nearby stream and lake waters (Lancaster, 2002). Alternatively, stream waters eroding into sediments or the reactivation of relict stream channels (McKnight et al., 2007) would enrich stream waters in Na-$HCO_3$ because the introduction of water to these soils is roughly analogous to a soil-water extraction. The flux of Na-$HCO_3$ enriched stream waters into closed basin Lake Fryxell is thought to control the chemical evolution of Lake Fryxell, resulting in its Na-$HCO_3$ composition (Green et al., 1988). Similarly, in western Taylor Valley, the Na-Ca-Cl-$SO_4$ composition of soil-water extractions is reflected in stream compositions (Welch et al., 2010) and lake waters (Angino et al., 1964). These spatial relationships between soil chemistries, stream waters, and lake waters suggest that soils have a strong influence on solutes found in Dry Valley hydrologic systems.

### *2.5.3. Taylor Valley Paleolakes*

Soluble salts in Taylor Valley soils are thought to be sensitive indicators of past glacial and lacustrine events, such as the MIS 2 advance of the RSIS into Taylor and associated paleolakes (Barrett et al., 2010; Bockheim et al., 2008a). To interpret relict soluble salt distributions from these events, we consider present-day salt distributions along lake and glacier margins.

Lake water is thought to influence soluble salt accumulations in Dry Valley soils by leaching soluble salts from inundated soils during lake high-stands (Bockheim et al., 2008a; Keys, 1980) and accumulating soluble salts along wetted lake margins following lake level lowering (Barrett et al., 2009; Barrett et al., 2010; Poage et al., 2008). Salt accumulation along lake margins is driven by capillary forces that draw nearby lake water upwards against gravity, wetting soils around lake margins up to 30 m horizontally and 1 m vertically from the lake surface (Gooseff et al., 2007; Northcott et al., 2009). In a process that has been termed "evapoconcentration," this lake water evaporates near the soil surface, concentrating salts dissolved in the lake water into the upper soil (Barrett et al., 2009). Soluble salts in soils influenced by evapoconcentration have been sampled by Barrett et al. (2009) to 10 cm depth. Cl concentrations in these soils average about 100 mmol Cl $kg^{-1}$. Using this Cl concentration and an average bulk density of about 1.65 g $cm^{-3}$ measured by Barrett et al. (2009), the average Cl content calculated from equation (2) is 16.5 moles Cl $m^{-2}$. This value is relatively high and is similar to Cl contents measured in Bonney Basin soils, older soils near the Nussbaum Riegel, and soils below approximately 120 m elevation in eastern Taylor Valley.

Soils adjacent to streams are also influenced by evapoconcentration, but these soils contain relatively low concentrations of salt compared to soils along lake margins (Barrett et al., 2009). These lower salt concentrations are likely caused by the lower solute concentrations in streams relative to lakes (Lyons et al., 1998b) and the instability of stream wetted margins because of variable water fluxes (Barrett et al., 2009; Northcott et al., 2009). Wetted stream margins sampled by Barrett et al. (2009) have Cl concentrations averaging about 5 mmol $kg^{-1}$. The Cl

content of these soils calculated in equation (2) for a bulk density of 1.65 g $cm^{-3}$, as above for wetted lake margins, is 0.5 moles Cl $m^{-2}$. This value is consistent with the low Cl contents found in most soils of eastern Taylor Valley. Since melt water streams are commonly found along low-elevation glacier margins in the Dry Valleys (Atkins and Dickinson, 2008; Hambrey and Fitzsimons, 2010), we suggest that low salt concentrations associated with stream margins can be extrapolated to glacier margins.

Using the distinct differences in salt content produced at lake, stream, and possibly glacier margins, we propose a delineation of past lacustrine and glacial margins in Taylor Valley; soils influenced by paleolake margins will have high salt accumulations relative to soils influenced by streams near glacial margins. The lake and ice margins determined this way will represent the last episode of lake or ice retreat, because any soluble salts deposited prior to the last event will have been redistributed. We expect that relict soluble salt accumulations from past glacial and lacustrine events will be somewhat altered by leaching, mineral dissolution, and cation exchange reactions. This alteration will be more pronounced in the relatively low-salt-content soils of eastern Taylor Valley and less significant in the high-salt-content soils of Bonney Basin.

*2.5.3.1. Bonney Basin*

In Bonney Basin, strandlines and lacustrine sediments provide evidence of paleolake margins with maximum high-stands between 306 and 350 m elevation (Hall et al., 2000; Stuiver et al., 1981). Near the Rhone Glacier, lacustrine strandlines are etched into the valley walls from 116 to 306 m (Stuiver et al., 1981). Furthermore, terraces, which have been interpreted as deltas, are found throughout Bonney Basin up to 350 m elevation (Hall and Denton, 2000; Hall et al., 2010) and the elevation of several of these terraces coincides with lacustrine strandlines near the Rhone Glacier (Stuiver et al., 1981). The age and elevation of these terraces is thought to record the timing and height of paleolake levels in Bonney Basin (Hall and Denton, 2000; Hall et al., 2010; Stuiver et al., 1981). However, the interpretation that the terraces are deltas has been

challenged by ground penetrating radar (GPR) studies of terraces in eastern Taylor Valley, which have shown that the internal stratigraphy of most terraces lacks sedimentary architecture characteristic of deltas (Arcone et al., 2008; Horsman, 2007). Although no terraces were studied by GPR in Bonney Basin, the results in eastern Taylor Valley cause uncertainty as to whether terraces in Bonney Basin actually are deltas. Hall et al. (2000) note that foreset beds are common in Bonney Basin terraces, but rare in eastern Taylor Valley terraces. This suggests that terraces in Bonney Basin are more likely to be deltas than terraces in eastern Taylor Valley, although this must be confirmed by further study of the internal structure of these deposits.

The distribution of total soluble salt contents in Bonney Basin with elevation (this study; Bockheim, 2003; Gibb et al., 2002) is consistent with evidence of paleolakes below approximately 300 m elevation (Figure 2.6). Salts in Bonney Basin are characterized by relatively high salt contents above 300 m (averaging 960 eq $m^{-2}$), which sharply transition to relatively low salt contents below 300 m (averaging 284 eq $m^{-2}$). Soils above 300 m elevation in Bonney Basin have ages on the order of 0.1–4 Ma and the high salt contents in these soils are thought to be derived from long-term accumulation of aerosols (Bockheim et al., 2008a). A few soils above 300 m elevation have low salt contents; however, these soils typically contain ice-cement near the soil surface, which suggests that salts have been leached from these soils. Soils noted as containing ice-cement (marked with a “+” symbol in Figure 2.6) account for nearly all the soils with low salt contents above 300 m. Below 300 m elevation, soils in Bonney Basin are located on sediments deposited during the Taylor II glaciation between 113–120 Ka (Higgins et al., 2000). This suggests the possibility that the lower salt contents in soils below 300 m are due to differences in soil age; however, Taylor II soils are also found above 300 m elevation and have high salt contents somewhat lower, but similar to, older soils (Bockheim et al., 2008a; Bockheim et al., 2008b). This indicates that the difference in salt contents above

and below 300 m is not due to soil age; instead, the distribution of soluble salts, stand lines, and terraces with elevation is consistent with paleolakes having maximum high-stands up to approximately 300 m elevation.

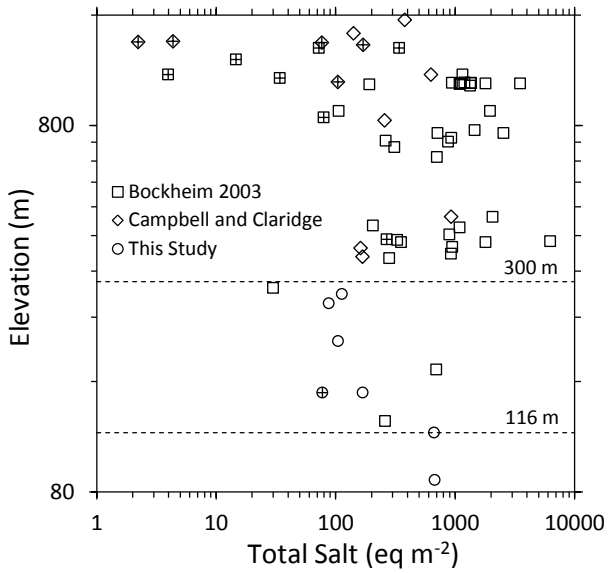


Figure 2.6. Graph of total salt contents of soils in Bonney Basin from this study, Gibb et al. (2002), and Bockheim (2003). Soils noted as containing ice-cement are indicated by a "+" symbol.

Below approximately 300 m elevation in Bonney Basin, paleolakes would have redistributed soluble salts in soils, leaching salts from inundated soils and accumulating salts by evapoconcentration along paleolake margins. The quantity of salt deposited by evapoconcentration is thought to be dependent primarily on the stability of paleolake margins (Barrett et al., 2009; Barrett et al., 2010; Northcott et al., 2009); along more stable lake margins, greater salt accumulation from evapoconcentration occurs. Paleolakes in Bonney Basin above 116 m elevation would have been proglacial lakes dammed behind the RSIS as it advanced into eastern Taylor Valley. Proglacial lakes in such a system are dynamic and unstable because lake levels would be sensitive to changes in glacial melt water inputs and the movement of the RSIS (Hall et al., 2010; Stuiver et al., 1981). As a result, lake level lowering may have occurred rapidly at times, limiting evapoconcentration along paleolake margins. In contrast, paleolakes below 116 m elevation would have been closed basin lakes controlled by the elevation of the

Bonney-Fryxell threshold at 116 m elevation. Lowering of lake water in closed basins occurs slowly as lake water evaporates or lake-ice sublimates (Clow et al., 1988), resulting in relatively stable lake levels. These differences in lake level stability above and below 116 m would result in relatively low salt accumulations above 116 m and high salt accumulations below 116 m elevation.

Evapoconcentrated salt accumulations in Bonney Basin are characterized by a trend of increasing salt contents at lower elevations (Figure 2.6, Figure 2.7), particularly below 116 m elevation. This is consistent with a transition from glacially dammed paleolakes above 116 m to closed basin paleolakes below 116 m elevation. Soils S046 and S047 were sampled at 86 and 116 m elevation and contain the highest salt contents measured in this study, averaging 672 eq $m^{-2}$ (Figure 2.7). Well-defined shorelines also occur at 86 and 116 m, indicating that at these elevations paleolake margins were stable. The elevation of the higher of these two soils at 116 m corresponds to the elevation of the threshold separating Bonney Basin from Fryxell Basin (Kellogg et al., 1980). This threshold makes 116 m elevation a natural limit for paleolake expansions in Bonney Basin because an increase in lake levels above 116 m would cause lake waters to spill over into Fryxell Basin. The soil at 86 m elevation is not associated with an obvious threshold, but indicates a major still-stand as closed basin lakes within Bonney Basin evaporated. A soil sampled by Bockheim (2003) at 172 m elevation in Bonney Basin below the Hughes Glacier (soil 76-25) has a high salt content (698.5 eq $m^{-2}$) similar to soils S046 and S047, suggesting that a major still-stand occurred at this elevation as proglacial paleolakes lowered.

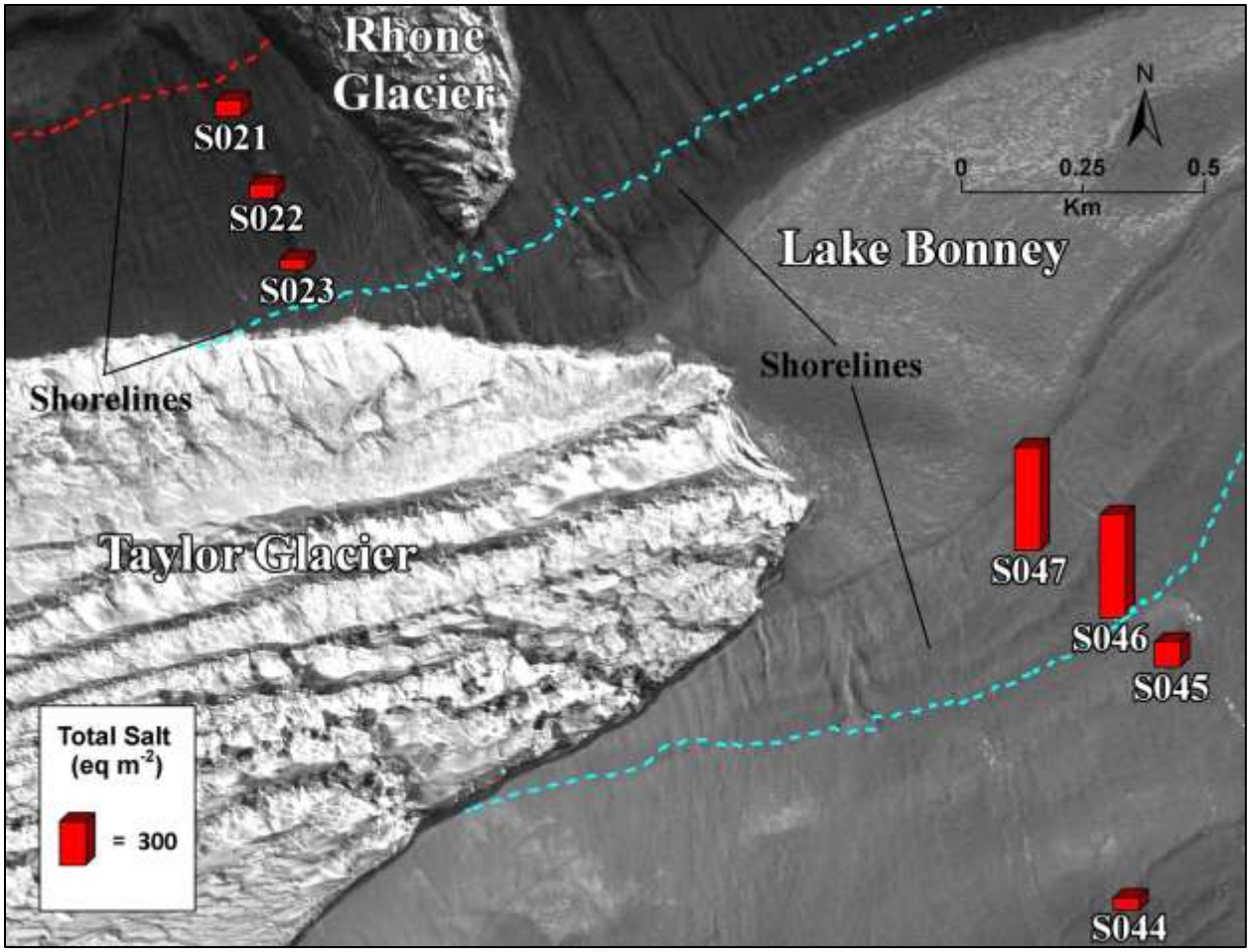


Figure 2.7. Map of total soluble salt contents measured in Bonney Basin soils overlain on a high-resolution satellite image of Bonney Basin. The proposed limit of paleolakes in Bonney Basin is shown as the blue line at 116 m. The red line indicates 300 m elevation, the approximate limit of paleolake proposed by Stuiver et al. (1981). Shorelines below 116 m can be seen on the south shore of Lake Bonney. Faint shorelines can also be seen on the north wall of Bonney Basin, west of the Rhone Glacier, from 116 to 306 m elevation. The 1997 level of Lake Bonney is at 58 m elevation (Spigel and Priscu, 1998).

Because soluble salts in soils below approximately 300 m in Bonney Basin are derived largely from paleolake waters, ionic ratios in these soils can be used to examine the chemical composition of paleolakes. In Table 2.4, ionic ratios in soils below 116 m elevation and soils between 116–300 m elevation (this study only) are compared to possible ionic compositions for paleolake waters, including: Blood Falls, surface waters of West Lake Bonney (WLB) above 6 m depth, highly concentrated hypolimnia in WLB below 15 m depth, and seawater. Blood Falls is a saline discharge from the snout of Taylor Glacier thought to derive from marine evaporite deposits beneath Taylor Glacier (Black et al., 1965). This discharge has ionic ratios similar to

seawater and is thought to influence the chemistry of waters in WLB (Lyons et al., 2005). Near-surface lake waters in WLB are currently evapoconcentrating in wetted margins along Lake Bonney (Barrett et al., 2009) and represent a possible composition for evapoconcentrating lake waters; however, the composition of surface waters in Bonney Basin paleolakes may have been different in the past. In the hypolimnia of WLB, salt concentrations are much higher than in surface waters (about 2.25 M Cl) (Angino et al., 1964). These hypolimnia may be derived from lake waters concentrated as paleolakes in Bonney Basin evaporated below current levels (Hendy et al., 2000). As a result, ionic ratios in WLB hypolimnia may represent the original composition of paleolake waters in Bonney Basin, although altered by evaporative concentration.

Table 2.4. Ratios of salts in Bonney Basin soils (this study only) compared to ratios in WLB surface water (above 6 m depth), WLB hypolimnia (below 15 m depth), Blood Falls, and seawater. Ion ratios for WLB and Blood Falls are determined from the average of MCM-LTER data.

| | Ca/Cl | Mg/Cl | Na/Cl | K/Cl | $SO_4$/Cl | $NO_3$/Cl | $HCO_3$/Cl |
|---|---|---|---|---|---|---|---|
| Soils below 116 m Elevation | 0.12 | 0.14 | 0.72 | 0.03 | 0.10 | 0.01 | 0.07 |
| Soils between 116–300 m Elevation | 0.77 | 0.23 | 0.87 | 0.10 | 0.58 | 0.04 | 0.27 |
| WLB Hypolimnia | 0.03 | 0.16 | 0.71 | 0.02 | 0.03 | – | – |
| WLB Surface Water | 0.10 | 0.13 | 0.83 | 0.02 | 0.10 | – | – |
| Blood Falls | 0.25 | 0.10 | 1.05 | 0.02 | 0.34 | – | – |
| Seawater | 0.02 | 0.10 | 0.86 | 0.02 | 0.05 | – | – |

Soils between 116–300 m elevations have high Mg/Cl, Na/Cl, and K/Cl ratios compared to most other soils and waters in Table 2.4. The $HCO_3$/Cl ratio (0.27) is also high, which suggests that cation ratios relative to Cl in these soils are influenced by mineral dissolution and cation exchange, similar to soils in eastern Taylor Valley, but of a lesser magnitude. This makes it uncertain as to whether ionic ratios in soils between 116–300 m are influenced by paleolake compositions or the soil-water extraction procedure. In soils below 116 m elevation, the $HCO_3$/Cl ratio is low and soluble salt concentrations are the highest in this study, indicating the mineral dissolution and cation exchange has a minimal effect on ionic ratios. Na/Cl ratios in soils below 116 m elevation (0.72) and WLB hypolimnia (0.71) are distinct from Na/Cl ratios in seawater (0.86), WLB surface water (0.83), and Blood Falls (1.05). K/Cl ratios are similar in all

waters in Table 2.4 and soils below 116 m elevation (0.02–0.03), as are Mg/Cl ratios (0.1–0.16). Since K, Mg, Na, and Cl are conservative solutes during closed basin lake evolution (Eugster and Jones, 1979; Hardie and Eugster, 1970), the similarity in Mg/Cl, Na/Cl, and K/Cl ratios in soils below 116 m elevation and WLB hypolimnia, particularly the unique similarity in Na/Cl ratios, suggests that WLB hypolimnia represent the original composition of paleolake waters in Bonney Basin, which have since evaporated into concentrated brine.

$SO_4$/Cl and Ca/Cl ratios in Bonney Basin soils between 116–300 m elevation (0.58 and 0.77, respectively) are higher than in soils below 116 m (0.1 and 0.12, respectively). The change in these ratios above and below 116 m is consistent with proglacial paleolake waters dammed by the RSIS between 116–300 m that transition into a closed basin regime below 116 m. In evaporating lake water, gypsum, mirabilite, and calcite are often the first salts to precipitate, whereas highly soluble chloride salts remain in solution, causing $SO_4$/Cl and Ca/Cl ratios to decrease in evaporating lake waters (Eugster and Jones, 1979). Assuming that the WLB hypolimnia are concentrated from a larger paleolake in Bonney Basin, the lower Ca/Cl and $SO_4$/Cl ratios in WLB hypolimnia compared to soils below 116 m elevation is consistent with precipitation of Ca and $SO_4$ in gypsum as lake levels lowered.

The distribution of evapoconcentrated salt accumulations in Bonney Basin soils with depth suggests that soluble salts have undergone significant postdepositional leaching (Figure 2.8). Salts accumulating from evapoconcentration are initially concentrated near the soil surface, as indicated by Cl concentration profiles with depth in lake-marginal soils sampled by Barrett et al. (2009). However, in Bonney Basin soils influenced by paleolakes, the highest Cl concentrations are commonly found 10–50 cm below the soil surface. This indicates that evapoconcentrated Cl has been partially leached down soil profiles following paleolake level lowering. The timescale for this Cl leaching is between 3–10 Ka, based on evidence of the last Lake Bonney low-stand sometime prior to 3 Ka (Poreda et al., 2004) and $^{14}C$ dates of terraces that possibly date the last

paleolake high-stand in Bonney Basin (Hall et al., 2010). Leaching of near-surface Cl accumulations down 10–50 cm over the Holocene represents a significant rate of leaching and is consistent with Cl migration observed by Ugolini and Anderson (1973) in Wright Valley soils. $SO_4$ concentrations are highest directly beneath the soil surface, which indicates that $SO_4$ has experienced much less leaching than Cl. The close correlation between $SO_4$ and Ca in Bonney Basin suggests that $SO_4$ has combined with Ca to precipitate gypsum. Gypsum is a sparingly soluble salt that is not as easily leached from soils as more soluble chloride salts. This evidently preserves evapoconcentrated $SO_4$ in its original position near the soil surface.

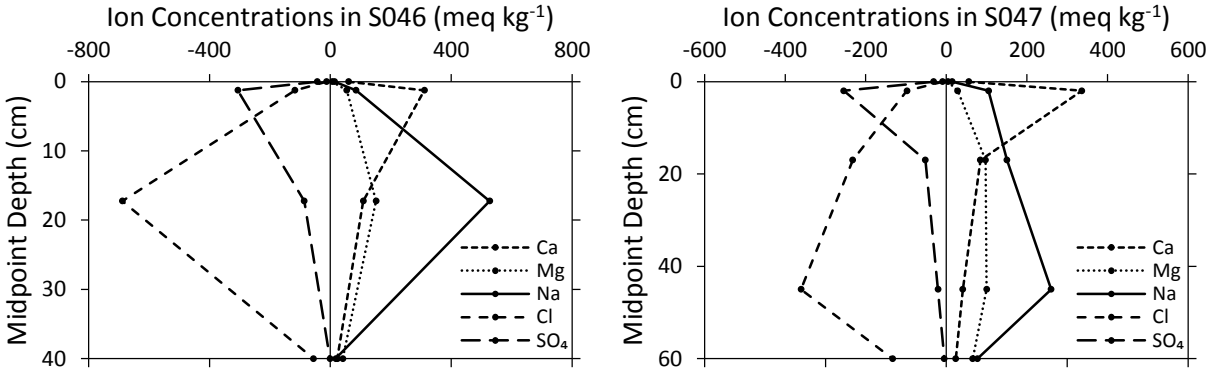


Figure 2.8. Graph showing the depth distribution of major anions and cations in two soils from Bonney Basin. Soil S046 is located at 86 m elevation, and soil S047 is located at 116 m elevation. Ion distributions indicate that significant leaching of Cl salts has occurred following evapoconcentration of salts near the soil surface.

### *2.5.3.2. Eastern Taylor Valley: Fryxell Basin and Valley Mouth*

In eastern Taylor Valley, soluble salt accumulations are low and are strongly influenced by the dissolution of calcite or gypsum minerals and cation exchange in the soil-water extraction. This obscures salt distributions and compositions that may have been influenced by glacial and lacustrine paleoenvironments. To study the history of eastern Taylor Valley, we consider only total Cl accumulations because Cl concentrations measured in different soil-water extraction procedures are comparable and Cl is a conservative ion in the soil that does not participate in exchange reactions. The dominant distribution of Cl contents in eastern Taylor Valley soils is that of higher Cl accumulations near the Nussbaum Riegel, lower Cl accumulations above approximately 120 m, and higher Cl accumulations below approximately 120 m (Figure 2.9).

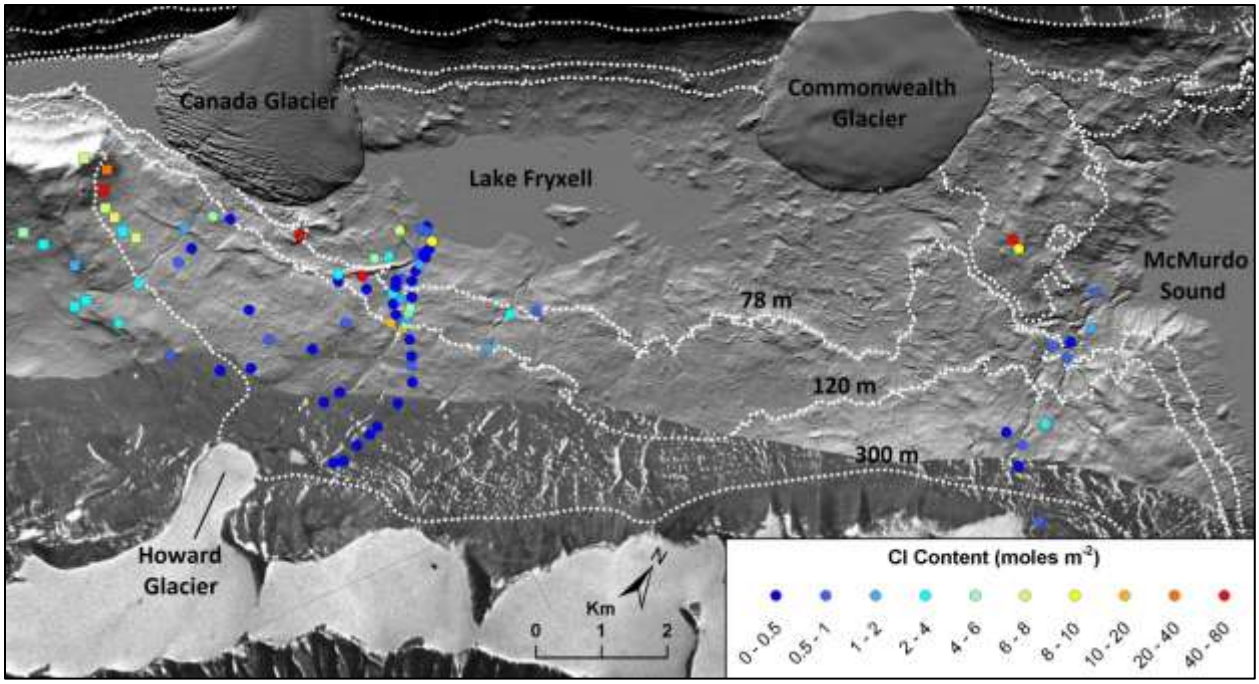


Figure 2.9. Map of total Cl contents in eastern Taylor Valley glacial sediments, including fluvial terraces. Square data points are from Bockheim (2003) and circle data points are from this study. Contour lines are given at 78 m and 120 m, the elevation of major thresholds in Taylor Valley (Kellogg et al., 1980), and at 300 m, approximately the maximum high-stand of paleolakes based on evidence from Bonney Basin.

Above approximately 120 m elevation, Cl contents in eastern Taylor Valley are generally consistent with soil age. Cl contents in older soils are generally higher than in MIS 2 RSIS sediments at lower elevations. However, Cl contents in older soils within eastern Taylor Valley are not as high as in older soils within Bonney Basin. This is likely due to greater leaching of soluble salts in the wetter climate of eastern Taylor Valley relative to western Taylor Valley. Because soluble salt contents vary from extremely high to low values, this leaching appears to be highly variable across the landscape. Heterogeneous leaching may occur as a result of different snow accumulation patterns, soil texture, aspect, and slope (Keys, 1980). For example, in soils located at 221 and 307 m elevation along the Bent Stream Transect, excavated soil pits were visibly moist within 10 cm of the soil surface. These soils were located on warmer north-facing slopes on small benches, which suggests that leaching may be caused by melt water from upslope snow drifts or ice-cemented soil. Leaching was also found to vary within individual soils. For example, in a soil located at 384 m elevation on the Bent Stream

transect (S016), large white soluble salt precipitates several centimeters thick were found beneath clasts between 3–21 cm depth (Figure 2.11). Given this visible evidence of high salt content, it was expected that soluble salts extracted from the soil surrounding these precipitates would also be high, but measured soluble salts were fairly low (2.96 mol Cl $m^{-2}$). This suggests that salts in S016 preferentially accumulated in areas of low leaching; in this case, beneath clasts in the soil. The heterogeneous distribution of salts in soil S016 also suggests that bulk sampling of numerous soil pits on individual landscape elements is needed to accurately determine soil age from soluble salt contents.

Below 320 m in eastern Taylor Valley, all soils sampled in this study, except for higher elevation soils on the Bent Stream Transect located on pre-MIS 2 deposits, are located on deposits from the MIS 2 advance of the RSIS. Cl contents in these MIS 2 soils are primarily characterized by low Cl contents above 120–140 m elevation, consistent with the young age of RSIS sediments, and high Cl contents below 120–140 m elevation, similar to older soils. In the Valley Mouth transect, two soils located at 120 m elevation on Coral Ridge have Cl contents of 9.6 and 67.4 mol Cl $m^{-2}$, which is much higher than Cl contents averaging 0.9 moles Cl $m^{-2}$ in all other Valley Mouth soils. In the Delta Stream transects, Cl contents in soils between 264–134 m elevation are uniformly low, averaging 0.3 mol Cl $m^{-2}$. At 128 m elevation, Cl contents spike to 15.4 mol Cl $m^{-2}$ and are variable but generally high below 128 m elevation. Fluvial terraces in Fryxell Basin are characterized by two distinct spikes in Cl content near 78 and 121 m elevation and low Cl contents at all other elevations (Figure 2.10). Cl contents in the spikes are as high as 3.8 mol Cl $m^{-2}$ at 77 m elevation and 12.6 mol Cl $m^{-2}$ at 121 m elevation. In the Bent Stream Transect, fewer soils were excavated and the boundary where Cl contents increase is not clear, but the Cl content in a soil at 143 m elevation is relatively high (4.9 mol Cl $m^{-2}$). High Cl contents measured in recent RSIS sediments below 120–140 m elevation are much higher than

Cl contents found in RSIS sediments at higher elevations. These high Cl contents at lower elevations are inconsistent with the young age of these soils.

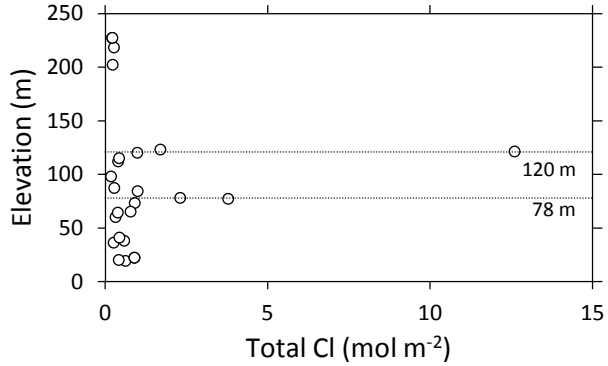


Figure 2.10. Graph of Cl contents in Fryxell Basin fluvial terraces. Cl contents in these soils contain two distinct spikes at 78 and 121 m elevation, which correspond to the elevations of major thresholds in Taylor Valley.

Similar increases in salt contents below approximately 120 m, in addition to increases in organic matter and fines (clay and silt), have been found in soils near Lake Fryxell by Barrett et al. (2010) and were attributed to evapoconcentration along paleolake margins. Barrett et al. (2010) found that above approximately 120 m salt contents, organic carbon, and fines are uniformly low, while below 120 m salt contents, organic carbon, and fines are generally high but positively covary from high to low values over short distances. The distribution of fines, organic carbon, and salt contents in eastern Taylor Valley soils suggests that paleolakes occupied Fryxell Basin below 120 m, but not above 120 m. Although clay and silt content was not determined for soils in the current study, we observed that soils with the highest Cl contents were commonly found in fine-grained soils below 120 m. In particular, a soil sampled on a silt rich moraine in front of Canada Glacier at 110 m elevation (soil S057) contained 43 moles Cl $m^{-2}$ and a soil composed of stratified, silty lacustrine sediment at 86 m elevation (soil S056) contained 47.5 moles Cl $m^{-2}$. Soils sampled along Coral Ridge at 120 m (soil CR03 and CR04) were composed almost entirely of silt and had the highest measured Cl contents in the Valley Mouth region, 16.7 and 64.0 moles Cl $m^{-2}$. These Cl contents are much higher than in nearby soils and are similar to high salt contents found in older soils.

The association between fine-grained soils and salinity may be caused by increased deposition of clay and silt along stable lake margins or lower rates of leaching in fine-grained soils (Barrett et al., 2010). It is likely that both of these mechanisms influence the relationship between soil texture and salinity. If silt and clay deposition is associated with paleolakes, then increases in silt and clay contents may be useful as an additional indicator of paleolake levels, similar to soluble salts. Silty soils will also slow down the rate of salt leaching because fine-grained soils absorb water more strongly than coarse-grained soils (Hunt et al., 2007), reducing downwards percolation of snow melt. This mechanism of salt preservation is consistent with the distribution of soil texture and soil salinity in soils influenced by evapoconcentration below 120 m elevation; Cl contents are the highest in silty soils (S056, S057, CR03, and CR04) and are lower in sandy soils (terrace soils and most soils along the Delta Stream Transect).

Paleolakes filling eastern Taylor Valley were likely controlled by the elevation of the threshold separating Fryxell Basin from McMurdo Sound at 78 m elevation. A large terrace is also found at 78 m elevation that has been confirmed as a delta having foreset stratigraphy by GPR (Horsman, 2007). This delta indicates that paleolakes existed in eastern Taylor Valley at least up to 78 m elevation (Prentice et al., 2009) and is consistent with evidence of evapoconcentration in terraces. Below 78 m elevation, paleolakes in eastern Taylor Valley would have been closed-basin lakes. Above 78 m elevation, paleolakes were likely proglacial lakes dammed by the RSIS because, without an ice dam, lake waters would spill over into McMurdo Sound (although it is possible that the valley mouth-Fryxell Basin threshold was higher in the past and has since eroded down from its maximum elevation). The upper limit of higher Cl contents suggests that the maximum high-stand of these paleolakes was approximately 120 m elevation. The height of these paleolakes may have been limited by the Fryxell-Bonney threshold at 116 m elevation. To raise lake levels up to 116 m, water needs to fill Fryxell Basin, but to raise lake levels higher than 116 m requires the filling of both Fryxell and

Bonney Basin. Alternatively, the elevation of paleolakes in Fryxell Basin may have been controlled by the elevation of the RSIS grounding line in eastern Taylor Valley.

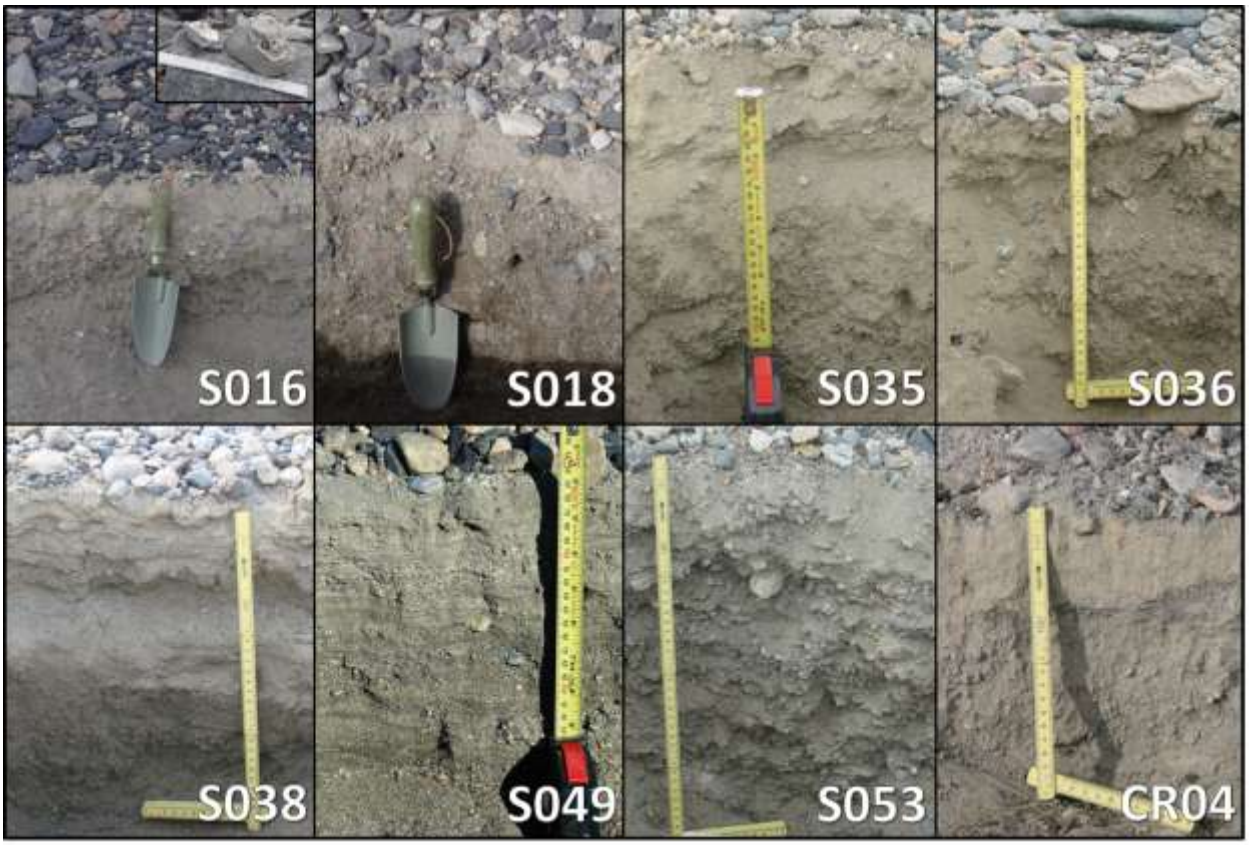


Figure 2.11. Soils representative of pits sampled in eastern Taylor Valley. S016: soil at 386 m on the Bent Stream transect, with salt encrustations found beneath clasts shown in the inset; S018: visibly moist soil at 221 m on the Bent Stream transect; S035: silty soil at 362 m on the Delta Stream 1 transect; S036: gravelly soil at 329 m on the Delta Stream 1 transect; S038: soil with laminated sands at 170 m on the Delta Stream 1 transect; S049: fluvial terrace with cross bedded stratification at 77 m along Crescent Stream; S053: gravelly sandy soil at 289 m on the Delta Stream 1 transect; CR04: silty soil on Coral Ridge at 120 m along the Valley Mouth transect.

#### *2.5.3.3. Valley-Wide Glaciolacustrine History*

Stuiver et al. (1981) and Hall et al. (2000) proposed that Taylor Valley was filled by valley wide paleolakes (filling both eastern and western Taylor Valley) that extended to a maximum elevation of approximately 300–350 m. The minimum elevation of a valley wide paleolake in Taylor Valley must have been at 116 m, since below 116 m separate paleolakes would fill Fryxell Basin and Bonney Basin divided by the 116-m-high threshold near the Suess Glacier. As a result, soils affected by valley wide paleolakes in Taylor Valley will lie between

approximately 116 and 350 m elevation. We expect that the formation of valley wide paleolakes would result in similar soluble salt accumulations from evapoconcentration in soils across Taylor Valley because the stability of lake margins and the concentration of solutes in lake water would be similar along the length of the paleolake. However, between 116 and 350 m elevation, salt contents in western Taylor Valley are much higher than salt contents in eastern Taylor Valley.

The difference in soluble salt accumulations between eastern and western Taylor Valley could be explained as the result of higher leaching rates in eastern Taylor Valley. In eastern Taylor Valley soils below 120 m elevation, evapoconcentrated salt accumulations are generally lower than evapoconcentrated accumulations in Bonney Basin, which is consistent with leaching; however, leaching has not completely removed evapoconcentrated salt accumulations because high salt accumulations do occur. Similarly, salts in older soils near the Nussbaum Riegel have been leached so that salt accumulations in these soils are not as high as similarly aged soils in Bonney Basin, but relatively high salt accumulations remain in places. These two cases indicate that while leaching occurs, it does not uniformly flush salts from the landscape. As a result, it is difficult to explain the uniformly low salt contents measured in MIS 2 soils of eastern Taylor Valley between 116 and 350 m elevation as the result of leaching. Below 120 m elevation, 36% of the soils sampled on MIS 2 RSIS sediments have significant Cl contents above 5 moles Cl $m^{-2}$ (excluding terrace soils), but such high Cl contents occur in only one out of thirty soils between 120–350 m elevation.

Because differences in soluble salt accumulations between eastern and western Taylor Valley are difficult to explain as a result of leaching, we conclude that soluble salt distributions in Taylor Valley are not consistent with valley wide paleolake hypotheses. Instead, soluble salt distributions suggest that western Taylor Valley was filled with paleolakes up to approximately 300 m elevation, while eastern Taylor Valley was filled with paleolakes up to only 120 m elevation. This interpretation is also consistent with the distribution of fines, organic carbon, and

salt accumulations found by Barrett et al. (2010). To reconcile the occurrence of low soluble salt distributions in MIS 2 RSIS sediments above 120 m elevation in eastern Taylor Valley with evidence of evapoconcentration from paleolakes up to approximately 300 m elevation in Bonney Basin, paleolakes in Bonney Basin must have been dammed by a lobe of the RSIS that filled eastern Taylor Valley to at least 300 m elevation in Fryxell Basin. The margins of the RSIS in eastern Taylor Valley would have been characterized by ice-marginal streams that would leach soluble salts from soils. This RSIS lobe probably abutted against the Nussbaum Riegel, forming an ice dam in the narrow valley defile near the Suess Glacier. During the retreat of the RSIS from Taylor Valley, paleolake levels in Bonney Basin would have lowered from the high-stand as lake water filled space vacated by retreating ice (Stuiver et al., 1981) or paleolakes may have lowered in response to decreased melt water inputs from alpine glaciers and the RSIS (Hall et al., 2010). Lowering of paleolakes during deglaciation could explain the preservation of low salt accumulations in RSIS sediments above 120 m elevation from the influence of paleolakes.

The MIS 2 RSIS expansion into Taylor Valley proposed here is more extensive than in Stuiver et al. (1981) and Hall et al. (2000). Compared to the maximum position of the RSIS lobe in Stuiver et al. (1981), the maximum elevation of ice proposed here is about 150 m higher near Canada Glacier. Hall et al. (2000) proposed that the RSIS never extended beyond Coral Ridge near the Valley Mouth and that RSIS sediments throughout eastern Taylor Valley were deposited in a lake-ice conveyor system (Hendy et al., 2000). Many of the sediments that have been interpreted as lake-ice conveyor deposits, including cross-valley ridges, sinuous ridges, and mounds, are found below 120 m elevation on the valley floor (Hall et al., 2000). The primary evidence for high paleolakes above 120 m elevation in eastern Taylor Valley comes from radiocarbon dates of algae buried in terraces (Hall and Denton, 2000; Stuiver et al., 1981). In Fryxell Basin, most terraces occur below 120 m elevation; out of a total of 78 fluvial terraces that have been radiocarbon dated, 70 are located below 120 m elevation while only 8 are

located above 120 m elevation. Hence, evidence for valley wide paleolake levels above 120 m elevation rests on relatively few radiocarbon dates from terraces. Several terraces near 220 m along Delta Stream were explored with GPR to determine if the internal stratigraphy was deltaic, but foreset beds were not found (Horsman, 2007). This suggests that these features are not deltas deposited in large paleolakes, but may be stream sediments deposited at the margins of the RSIS (Prentice et al., 2009). The only terrace investigated with GPR that was confirmed as a delta was located at 78 m elevation (Horsman, 2007), which is consistent with the paleolake extents proposed here. Even if terraces above 120 m elevation are interpreted as deltas, this does not provide conclusive evidence for a valley wide paleolake filling Fryxell Basin, because deltas could also have been deposited in ponds marginal to the RSIS lobe.

### *2.6. Conclusions*

This study uses soluble salt accumulations in Taylor Valley, Antarctica, to determine the history of paleolakes believed to have been dammed by the RSIS. Results from this study indicate that soluble salt distributions are controlled by soil age, distance from the sea (McMurdo Sound), leaching, soil texture, cation exchange, and past glacial and lacustrine events. Soils in western Taylor Valley have relatively high soluble salt contents and salt compositions are similar to seawater; in contrast, soils in eastern Taylor Valley have relatively low salt contents and salt compositions are dominated by Na and $HCO_3$. The peculiar Na-$HCO_3$ composition of salts in eastern Taylor Valley is consistent with mineral dissolution and cation exchange reactions in the presence of relatively high leaching rates. These reactions result in Cl being leached from soils as Ca-Mg-Cl brine and the association of Na with $HCO_3$ from calcite dissolution.

Soluble salt contents in soils are primarily determined by soil age. Soils developing on glacial sediments from the MIS 2 advance of the RSIS have much lower salt contents than soils developing on glacial sediments from older advances of Taylor Glacier, the RSIS, and alpine glaciations. This relationship between soil age and salt content is not uniform because salts are

leached in the wetter climate of eastern Taylor Valley. Paleolakes have also redistributed soluble salts in lower elevation soils through evapoconcentration along paleolake margins. Soils in Bonney Basin are consistent with a history of evapoconcentration along paleolake margins up to approximately 300 m elevation, which agrees with paleolake high-stands inferred from lacustrine strandlines and terraces. In eastern Taylor Valley, salt distributions indicate maximum paleolake high-stands up to 120 m. Differences in salt accumulations between eastern and western Taylor Valley are not consistent with the hypothesis that valley wide lakes filled all of eastern and western Taylor Valley during the MIS 2 advance of the RSIS. We conclude that high paleolakes in Bonney Basin were dammed by a lobe of the RSIS that entered deep into eastern Taylor Valley, filling Fryxell Basin to at least 300 m elevation.

# Chapter 3 The Formation of Ca-Cl Enriched Brines by Cation Exchange Reactions in Taylor Valley, Antarctica

## *3.1. Abstract*

Ca-Cl enriched brines have been found in shallow subsurface flows, groundwater systems, lakes, and ponds throughout the Dry Valleys of Antarctica. The apparent abundance of Ca-Cl enriched water near the surface is unusual compared to global surface water compositions and a number of theories have been proposed to explain the genesis of these brines. We show that an ice-cemented soil developing on fluvial sediment in Taylor Valley also contains Ca-Cl enriched brine. The distribution of soluble ions, exchangeable cations, and stable isotopes down to 2.1 m depth in the soil suggests that this Ca-Cl enriched brine was formed by cation exchange reactions during downward reactive transport of Na-Cl brine from the soil surface. To explore the implications of exchange reactions for the formation of Ca-Cl enriched brine, Ca-Na and Ca-Mg exchange properties were measured in dilute, 0.1 M, and 4.75 M solutions. Low-temperature reactions and brine transport were modeled in PHREEQC by incorporating FREZCHEM Pitzer parameters and solubility products into PHREEQC. Modeling shows that by freezing soils in equilibrium with Dry Valley surface waters, a strong Ca-Mg-Cl enrichment of the soil solution is caused by the exchange of aqueous Na with exchangeable Ca and Mg. Ca-Mg-Cl enrichment also occurs as Na-Cl brine from the soil surface advects into ice-cemented soil. By modeling this process in the borehole soil, trends in ion distributions with depth can be predicted. Brine compositions from cation exchange reactions are consistent with Ca-Cl enriched brine compositions in the Dry Valleys, although additional water-rock interaction is proposed to account for the low Mg concentrations in Don Juan Pond. Furthermore, the amount of $CaCl_2$ that can be produced by exchange reactions is consistent with estimated amounts of $CaCl_2$ in groundwaters beneath Don Juan Pond. This suggests that cation

exchange reactions can explain the Ca-Cl enriched composition of the enigmatic Don Juan Pond and other brines in the Dry Valleys.

*3.2. Introduction*

Ca-Cl waters have been found throughout the McMurdo Dry Valleys, Antarctica, in shallow subsurface flows (Field, 1975; Levy et al., 2011; Webster et al., 2003; Wilson, 1979), deep groundwaters (Cartwright and Harris, 1981; Harris and Cartwright, 1981), local depressions (Campbell and Claridge, 1982), and saline lakes and ponds (Angino and Armitage, 1963; Healy et al., 2006; Lyons et al., 2011). Don Juan Pond in Wright Valley contains concentrated Ca-Na-Cl brine that remains unfrozen to temperatures as low as -51°C (Marion, 1997). This brine is fed by upwelling Ca-Na-Cl groundwater from a confined aquifer within fractured Ferrar Dolerite underlying the Don Juan Pond basin (Harris and Cartwright, 1981). The bottom water of Lake Vanda, also in Wright Valley, contains a concentrated Ca-Mg-Na-Cl brine (Angino and Armitage, 1963). This brine is thought to derive from mixing of deep Ca-Na-Cl groundwaters, similar to those found near Don Juan Pond, with dilute inflow water from the Onyx River (Carlson et al., 1990; Green and Canfield, 1984). Ca-Cl enrichment is also common in shallow subsurface flows found in Taylor and Wright Valley (Cartwright and Harris, 1981; Levy et al., 2011; Webster et al., 2003). These subsurface flows wet the soil surface due to upward wicking water and are visible as dark streaks on hill slopes (Head et al., 2007; Levy et al., 2011). Ca-Cl enriched brines in the Dry Valleys are of considerable interest as an analog for Ca-Cl brines that may exist on Mars (Burt and Knauth, 2003; Head et al., 2007; Wynn-Williams et al., 2001). It is thought that groundwater may occur in the Martian subsurface as a Ca-Cl brine (Burt and Knauth, 2003; Knauth and Burt, 2002), which could remain unfrozen in the cold conditions of Mars due to the low eutectic temperature of $CaCl_2$, -50.4°C (Marion, 1997). Kreslavsky and Head (2009) speculate that dark slope streaks on Mars, similar to those observed in the Dry Valleys, may originate from shallow subsurface flows of Ca-Cl brine.

Ca-Cl brine is rare on the earth's surface (Garrett, 2004), but appears to be relatively common in the Dry Valleys. To explain the formation of Ca-Cl brines within the Dry Valleys, Wilson

(1979) and Keys (1980) proposed that Ca-Cl can be fractionated from surface waters based on the physical properties of salts. Since Ca-Cl salts have the highest solubility, lowest eutectic temperature, and greatest deliquescence, they are thought to be the most mobile salt phase in soils and preferentially accumulate in closed basins over salts of Na, K, and Mg. Following Green and Canfield (1984) and Lyons and Mayewski (1993), this mechanism of Ca-Cl formation can be evaluated using the model of closed basin brine evolution developed by Hardie and Eugster (1970). According to this model, concentrated Ca-Cl brines can only develop from surface waters when the equivalent concentration of Ca is greater than the equivalent concentration of carbonate and sulfate species. When this condition is not met, Ca depleted brines develop. This is because calcite ($CaCO_3$) and gypsum ($CaSO_4 \cdot 2H_2O$) precipitate early during freezing or evaporation, removing Ca from solution (c.f. "Chemical Divides" in Drever, 1982). Since most surface and groundwaters in the world have greater equivalent concentrations of bicarbonate than Ca (Langmuir, 1997), they do not evolve into Ca-Cl enriched brines. This is also true of stream, lake, and glacial ice in the Dry Valleys (Green et al., 1988; Green and Canfield, 1984). As a result, Green and Canfield (1984) and Lyons and Mayewski (1993) argue that Ca-Cl enriched brines found in the Dry Valleys have not evolved from surface waters.

After reviewing a number of existing models of Ca-Cl enrichment, Lyons and Mayewski (1993) conclude that subsurface water-rock interaction is responsible for the chemistry of Don Juan Pond, possibly due to hydrothermal waters (Hardie, 1990) or fracturing of felsic rocks containing Ca-Cl fluid inclusions (Nordstrom et al., 1989), although they note that there is little evidence to support either hypothesis. Garrett et al. (2004) proposed that the Ca-Cl enrichment in Don Juan Pond is the result of low-temperature dolomitization and albitization of accumulating seawater aerosols. However, the extensive dolomite minerals expected from this water-rock interaction

have not been found in Dry Valley Drilling Project (DVDP) sediment cores near Don Juan Pond (Mudrey et al., 1975).

A mechanism for Ca-Cl enrichment that has received little attention in the Dry Valleys is cation exchange. Cation exchange reactions can produce Ca-Cl enriched brines by exchanging aqueous Na with exchangeable Ca. This exchange reaction has been observed to produce Ca-Cl enrichment in desert soils by Smettan and Blume (1987) and in groundwater systems by Sanford et al. (1992), Bjerg and Christensen (1993), and Howard and Lloyd (1983). In groundwaters, Ca-Cl enrichment due to cation exchange is commonly associated with the intrusion of saline Na-Cl water into freshwater sediments highly saturated with exchangeable Ca (e.g. Bjerg and Christensen, 1993; Howard and Lloyd, 1983). Infiltrating saline waters are chromatographically separated by exchange reactions, causing the front of the infiltrating brine to become enriched in Ca-Cl (Appelo et al., 1990; Beekman and Appelo, 1990; Bjerg and Christensen, 1993; Cates et al., 1996).

In the Dry Valleys, evidence for Ca-Cl enrichment by cation exchange is limited. Nakaya et al. (1979) hypothesized that the Ca-Mg-Cl brine in Lake Vanda is caused by exchange of Na and K in lake water with exchangeable Ca and Mg in sediments during evaporation. In support of this, Nakaya et al. (1979) observed that Ca and Mg exchanged into solution when sediments from near Lake Vanda were immersed in seawater. Ugolini and Anderson (1973) found that Cl migrated faster than Na in soils using radioactive $^{22}Na$ and $^{36}Cl$ tracers and suggested that the retarded Na velocity was due to absorption onto exchange sites. To conserve charge balance, Na absorption must be balanced by the release of ions to the soil solution. The ions involved in this exchange were likely Ca and Mg since K is relatively minor in Dry Valley soils. A detailed analysis of soluble salts in Taylor Valley soils by Toner et al. (2012b) suggests that exchange reactions strongly influence the chemistry of soil solutions, salt precipitates, and surface waters. In particular, high Na/Cl ratios measured in soils of eastern Taylor Valley suggest that Na from

accumulating seawater aerosol has adsorbed onto the soil and displaced exchangeable Ca and Mg (Toner et al., 2012b). The Ca-Mg-Cl brine predicted by this exchange reaction appears to have leached from the soil and may contribute to the Ca-Cl enrichment found in shallow groundwaters by Levy et al. (2011).

In this paper, we present evidence that cation exchange reactions can explain the Ca-Cl enrichment in Dry Valley groundwaters based on soluble ion, exchangeable cation, and stable isotope distributions in a 210 cm deep soil profile. The implications of exchange reactions for brine chemistry are explored by measuring the exchange properties of Taylor Valley soils and modeling reactive transport using the geochemical programs PHREEQC (Parkhurst and Appelo, 1999) and FREZCHEM (Marion and Grant, 1994).

### *3.3. Methods*

#### *3.3.1. Site Description*

Taylor Valley is a cold-dry desert within the McMurdo Dry Valleys, Antarctica. Annual temperatures average about -17°C (Clow et al., 1988; Doran et al., 2002b) and precipitation rates are less than 100 mm $yr^{-1}$ in the form of snow (Fountain et al., 2010). The results presented here are based on the analysis of a soil located at 36 m elevation (-77.62638 S, 163.11592 W) on a terrace adjacent to Delta Stream (Figure 3.1). This terrace has a deposition age of about 5 Ka, based on luminescence dating (Toner et al., 2012a). The terrace surface is capped by a gravelly desert pavement surface, which is underlain by gravelly sand. Above 30 cm depth the soil is dry and has cross-bedded stratigraphy. Below 30 cm depth, the soil is cemented by ice and has foreset beds inclining downstream at 14°. Ground Penetrating Radar studies of this terrace by Horsman et al. (2007) indicate that the foreset beds extend to about 200 cm depth below the soil surface and are underlain by crudely stratified sediments.

Figure 3.1. The terrace sampled in this study, located at 36 m elevation adjacent to Delta Stream. The white string is leveled, which highlights the inclined foreset beds found below 30 cm depth in ice-cemented soil. Above the white string is dry sediment with cross bedded stratigraphy.

### *3.3.2. Borehole Sampling and Analysis*

Samples were collected from the ice-cemented soil (ICS) at 10 cm intervals to a depth of 210 cm below the soil surface using an auger drill and were kept frozen below -20°C before further preparation. The top 30 cm of dry soil above the ICS was also sampled. In the lab, about 20 g of ICS was used to determine the gravimetric water content by oven drying. The remaining ICS was thawed overnight at 40°C in closed polyethylene bags and the melted water was collected by centrifuging in a double-bottomed centrifuge cup (a perforated cup inside a sealed cup). This extracted water was filtered at 0.45 µm and analyzed for water soluble salts and exchangeable cations. Water soluble salts in the top 30 cm of dry soil were determined in a 1:10 soil-water extraction by shaking 5 g of soil in 50 ml of water for one hour and filtering at 0.45 µm.

To determine exchangeable Ca, Mg, and Na, 40 ml of 1 M KCl was added to 5 g of soil, shaken for one hour, centrifuged, and the supernatant decanted. This KCl extraction was done three times and all three supernatants were combined for analysis of Ca, Mg, and Na. Ca that may have gone into solution due to calcite dissolution was corrected for using the method of Amrhein and Suarez (1990). To determine exchangeable K, a similar extraction procedure was performed using a 1 M $NH_4Cl$ extraction. The Cation Exchange Capacity (CEC) is calculated as the equivalent sum of exchangeable Ca, Mg, Na, and K. Some of the Ca, Mg, Na, and K in the KCl and $NH_4Cl$ extractions may be from soluble salts. In the ICS, these soluble salts are corrected for by subtracting soluble cations in the remaining melt water from cations measured in the KCl and $NH_4Cl$ extractions. In the top 30 cm of dry soil, a similar correction is not possible. The potential influence of soluble salts in the dry soil on the exchangeable cation determination was estimated from the 1:10 soil-water extractions. Assuming that all $HCO_3$ in the 1:10 extraction is from calcite dissolution, the correction for soluble salts in the top 30 cm of dry soil is about 10% of the CEC, which will have a minimal effect on exchangeable cations.

Chemical analysis for cations (Na, K, Ca, Mg) was conducted using Inductively Coupled Plasma – Optical Emission Spectrometry (Perkin-Elmer® Optima 3300 DV) and anions (Cl, $SO_4$, and $NO_3$) using Ion Chromatography (Dionex® ICS-2500). Total inorganic carbon was determined by an OI-700 Carbon Analyzer, which acidifies the sample and measures evolved $CO_2$. The accuracy of this analysis was checked by calculating the charge balance, assuming that all inorganic carbon is bicarbonate. The particle size distribution of all soil samples was measured by a laser diffraction particle size analyzer (Beckman-Coulter LS 13 320) under sonication in a solution of 10% sodium hexametaphosphate. $\delta D$ was measured by converting water into hydrogen gas using the chromium reduction method and analyzing the evolved hydrogen with a Finnigan DeltaPlus mass spectrometer. $\delta^{18}O$ was measured by equilibrating

the water with $CO_2$ gas and measuring $CO_2$ on a Micromass IsoPrime mass spectrometer. Isotope values are given with respect to the VSMOW standard:

$$\delta(‰) = 1000\left[\frac{R_{sample}}{R_{STD}} - 1\right]$$

where $\mathbf{R_{sample}}$ and $\mathbf{R_{STD}}$ are ratios of the heavy to light isotope for the sample and standard. The precision is ±0.08‰ for $\delta^{18}O$ and ±1‰ for δD. Chemical and isotopic data are tabulated in Appendix C.

*3.3.3. Cation Exchange Experiments*

Cation exchange properties were determined by equilibrating soils in 4.75 M, 0.1 M, and dilute solutions of Cl (prepared from reagent grade NaCl, $CaCl_2 \cdot 2H_2O$, and $MgCl_2 \cdot 6H_2O$), followed by extraction of exchangeable cations in 1 M KCl solution. Equilibrating solution concentrations and compositions were chosen to represent a range of soil solutions that may exist in the Dry Valleys; from dilute solutions found in streams (<1 mM) to concentrated brines (>1 M). 0.1 M and 4.75 M equilibrating solutions were composed of various proportions of Ca-Na and Ca-Mg. The soil used for these experiments was a typical sandy loam collected in Taylor Valley. Four different soils were equilibrated with a Ca-Mg-Na-Cl solution similar to the average composition of Taylor Valley Streams monitored by the Long-Term Ecological Research (LTER) group (excluding K): Ca = 0.37, Mg = 0.11, and Na = 0.46 mM.

For a given equilibrating solution, 40 ml of solution was added to 5 g of soil, the mixture was shaken for one day, centrifuged, and the supernatant decanted. This equilibration procedure was repeated until the composition of the equilibrating solution was constant. After the final equilibration, the equilibrating solution was decanted and saved for analysis, and the mass of equilibrating solution remaining in the soil was determined gravimetrically. For the 4.75 M equilibrating solutions the final soil-solution mixture was centrifuged over filter paper in a

double-bottomed centrifuge cup to remove as much of the equilibrating solution as possible. Exchangeable cations were extracted with 1 M KCl using the method described above for extracting exchangeable cations in the borehole soil. To calculate exchangeable Ca, Mg, and Na (mmol $\mathrm{kg}_{\mathrm{soil}}^{-1}$), cations in the residual equilibrium solution were subtracted from cations in the saturating solution:

$$\mathrm{Na} = \left(\mathrm{Na}_{\mathrm{sat}} - \mathrm{Na}_{\mathrm{eq}} \times \frac{\mathrm{V}_{\mathrm{eq}}}{\mathrm{V}_{\mathrm{sat}}}\right) \times \frac{\mathrm{V}_{\mathrm{sat}}}{\mathrm{soil\ (g)}}$$

$$\mathrm{Mg} = \left(\mathrm{Mg}_{\mathrm{sat}} - \mathrm{Mg}_{\mathrm{eq}} \times \frac{\mathrm{V}_{\mathrm{eq}}}{\mathrm{V}_{\mathrm{sat}}}\right) \times \frac{\mathrm{V}_{\mathrm{sat}}}{\mathrm{soil\ (g)}}$$

$$\mathrm{Ca} = \left(\mathrm{Ca}_{\mathrm{sat}} - \frac{\mathrm{HCO}_3}{2} - \mathrm{Ca}_{\mathrm{eq}} \times \frac{\mathrm{V}_{\mathrm{eq}}}{\mathrm{V}_{\mathrm{sat}}}\right) \times \frac{\mathrm{V}_{\mathrm{sat}}}{\mathrm{soil\ (g)}}$$

where $\mathrm{V}_{\mathrm{sat}}$ and $\mathrm{V}_{\mathrm{eq}}$ (ml) are the volume of saturating and equilibrating solutions, and $\mathrm{Na}_{\mathrm{sat}}$, $\mathrm{Na}_{\mathrm{eq}}$, $\mathrm{Mg}_{\mathrm{sat}}$, $\mathrm{Mg}_{\mathrm{eq}}$, $\mathrm{Ca}_{\mathrm{sat}}$, $\mathrm{Ca}_{\mathrm{eq}}$, and $\mathrm{HCO}_3$ (mM) are concentrations of ions in saturating and equilibrating solutions. Since equilibrating and saturating solutions were measured gravimetrically, gravimetric weights were converted to volumes ($\mathrm{V}_{\mathrm{sat}}$ and $\mathrm{V}_{\mathrm{eq}}$) using solution density. Solution densities were calculated from molar concentrations using FREZCHEM version 12.2 (Marion, 2007).

Cation exchange is modeled with the Rothmund-Kornfeld equation, which has been shown to accurately describe cation exchange in variable composition soil solutions (Bond, 1995; Langmuir, 1997). For a binary cation exchange reaction, the general form of the Rothmund-Kornfeld equation is given by (Bond, 1995):

$$\mathrm{K}^{\mathrm{ij}} = \frac{\mathrm{A}_{\mathrm{i}}^{\mathrm{z_j}}}{\mathrm{A}_{\mathrm{j}}^{\mathrm{z_i}}}\left[\frac{\mathrm{a}_{\mathrm{j}}^{\mathrm{z_i}}}{\mathrm{a}_{\mathrm{i}}^{\mathrm{z_j}}}\right]^{\mathrm{n}^{\mathrm{ij}}} \tag{6}$$

where $\mathrm{K}^{\mathrm{ij}}$ is the Rothmund-Kornfeld parameter for exchange involving cations $\mathrm{i}$ and $\mathrm{j}$, $\mathrm{A}_{\mathrm{i}}$ is the exchangeable cation activity, $\mathrm{a}_{\mathrm{i}}$ is the aqueous cation activity, $\mathrm{z}_{\mathrm{i}}$ is the cation charge, and $\mathrm{n}^{\mathrm{ij}}$ is

an empirically derived parameter. The aqueous cation activity is related to the measured cation concentration $C_i$ by $a_i = \gamma_i C_i$, where $\gamma_i$ is the activity coefficient. $\gamma_i$ can be determined from thermodynamic equilibrium models such as the Pitzer model. For exchangeable cation activities we employ the Gaines-Thomas convention, which defines exchangeable cation activity as $A_i = g_i N_i$, where $g_i$ is the exchange phase activity coefficient and $N_i$ is the equivalent fraction (Gaines and Thomas, 1953). The equivalent fraction of an exchangeable cation with concentration $c_i$ is defined as $N_i = z_i c_i / CEC$. Exchangeable cation activity coefficients are assumed to be equal to aqueous cation activity coefficients for the same cation species ($g_i = \gamma_i$) since it has been observed that cation exchange parameters are more constant under this assumption when the solution concentration varies (Appelo, 1994).

Data from the cation exchange experiments is fitted to the Rothmund-Kornfeld equation by plotting $\log(A_j^{z_i} / A_i^{z_j})$ versus $\log(a_j^{z_i} / a_i^{z_j})$. If cation exchange obeys the Rothmund-Kornfeld formula, then this plot will be linear, with the parameter $n^{ij}$ obtained from slope of the line and $\log K^{ij}$ by the intercept (Bond, 1995).

*3.3.4. Geochemical Modeling: PHREEQC and FREZCHEM*

The geochemical programs PHREEQC version 2.18 and FREZCHEM version 7.2 are used to model the high concentration and low temperature conditions found in ICS. PHREEQC is capable of speciation, precipitation, 1-dimensional transport, and exchange calculations (Parkhurst and Appelo, 1999). The Rothmund-Kornfeld model for cation exchange can also be used in PHREEQC (Appelo and Parkhurst, 2002). To calculate activity coefficients in concentrated solutions, PHREEQC uses the Pitzer virial-coefficient model (Pitzer, 1981), but the current Pitzer database used in PHREEQC only describes solutions near 25°C. FREZCHEM is also based on the Pitzer ion interaction approach and can model freezing and evaporation of concentrated solutions over a wider temperature range from -70 to 25°C (Marion, 2001, 2002;

Marion and Farren, 1999; Marion and Grant, 1994). A full description of the Pitzer approach used in FREZCHEM can be found in Marion and Kargel (2008).

To update PHREEQC for lower temperatures, Pitzer parameters and solubility products from FREZCHEM version 7.2 in the system Ca-Mg-Na-K-H-OH-Cl-$SO_4$-$HSO_4$-$NO_3$-$CO_3$-$HCO_3$-$CO_2$-$H_2O$ were incorporated into PHREEQC and several changes were made to the PHREEQC code. In FREZCHEM, the temperature dependence of Pitzer parameters ($P$) and solubility products ($K$) at a given temperature $T$ (°K) is given by (Marion, 2002):

$$P(T) = \ln K(T) = a_1 + a_2 T + a_3 T^2 + a_4 T^3 + \frac{a_5}{T} + a_6 \ln T + a_7 T^4 + \frac{a_8}{T^2} \quad (7)$$

where the virial-coefficients $a_i$ are empirical constants. PHREEQC uses a different equation, in which the temperature dependence of Pitzer parameters is given by:

$$P(T) = a_1 + a_2\left(\frac{1}{T} - \frac{1}{T_R}\right) + a_3 \ln\left(\frac{T}{T_R}\right) + a_4(T - T_R) + a_5\left(T^2 - {T_R}^2\right) + a_6\left(\frac{1}{T^2} - \frac{1}{{T_R}^2}\right) \quad (8)$$

and the temperature dependence of solubility products by:

$$\log K(T) = a_1 + a_2 T + \frac{a_3}{T} + a_4 \ln T + \frac{a_5}{T^2} + a_6 T^2 \quad (9)$$

where $T_R$ is 298.15° K. To incorporate the temperature dependence of Pitzer parameters and solubility products used in FREZCHEM into PHREEQC, values calculated from equation (7) were fitted to equations (8) and (9) using a least-squares fitting method over the temperature range -70 to 25°C.

When applying the Pitzer parameterization used in one model to another, it is important that the Debye-Hückel constant ($A_\phi$) is internally consistent with the new set of parameters (Marion and Kargel, 2008). $A_\phi$ is integral to the Pitzer model but is treated differently in FREZCHEM and

PHREEQC. In FREZCHEM, the temperature dependence of $A_\phi$ is described by virial-coefficients as in equation (7), while in PHREEQC $A_\phi$ is given by:

$$A_\phi = \frac{1}{3}\left(\frac{2\pi N_A d_w}{1000}\right)^{1/2}\left(\frac{e^2}{\varepsilon kT}\right)^{3/2} \quad (10)$$

where $N_A$ is Avogadro's number, $d_w$ is the density of water, $e$ is the charge of an electron, $\varepsilon$ is the dielectric constant, and $k$ is the Boltzmann constant. As discussed by Spencer et al. (1990), the application of equation (10) to low temperature solutions is limited because the density of water is only known to -34°C and the dielectric constant is not known below 0°C. To address this issue, the PHREEQC code was changed so that the FREZCHEM equation for $A_\phi$ is used instead. Another issue is that PHREEQC fails to converge when it attempts to find the density of water below -33°C, forcing the program to stop. Since the solution density is not needed to calculate Pitzer activity coefficients when $A_\phi$ is determined by the FREZCHEM equation, this issue was addressed by forcing a value of 1 g $cm^{-3}$ to the density of water when the density routine in PHREEQC fails to converge.

The updated Pitzer parameterization in PHREEQC is verified by modeling seawater freezing using the seawater composition given in Marion et al. (2010) (Figure 3.2). Ion concentrations modeled in PHREEQC are in excellent agreement with ion concentrations modeled in FREZCHEM. Both programs follow the Gitterman pathway for seawater freezing (Marion et al., 1999) and predict a eutectic temperature of -36.1°C for seawater. A major advantage of this low-temperature version of PHREEQC is that ice formation and salt precipitation can be modeled in conjunction with the reaction and transport capabilities in PHREEQC. This makes it possible to model cation exchange and reactive transport in ICS.

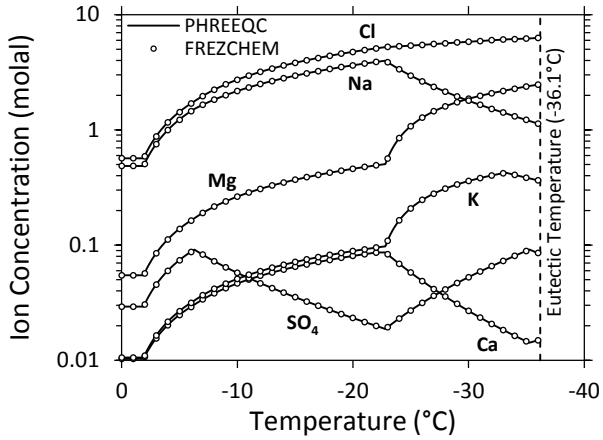


Figure 3.2. A Graph showing seawater freezing modeled with PHREEQC and FREZCHEM. The initial composition of seawater was: Ca = 0.01074, Mg = 0.05474, Na = 0.48610, K = 0.01058, Cl = 0.56672, $SO_4$ = 0.02927, and $HCO_3$ = 0.00238 molal in equilibrium with atmospheric $CO_2$. Although not shown, pH and inorganic carbon species calculated with the updated PHREEQC are also in excellent agreement with FREZCHEM.

## *3.4. Results*

### *3.4.1. Borehole Physical and Chemical Properties*

In Figure 3.3, ion concentrations in the thawed ICS are given in units of mM (grey circles), while 1:10 soil-water extractions in the upper 30 cm of dry soil are given in units of mmol $kg^{-1}$ (white circles). To compare soluble ions above and below the ICS boundary, ion concentrations in the thawed ICS are also given in units of mmol $kg^{-1}$ using the conversion mmol $kg^{-1}$ = mM x $\%H_2O/100$ (white circles) (Figure 3.3). Water contents ($\%H_2O$) used in this conversion are characterized by generally low values in the upper 40 cm of ICS that increase with depth and relatively constant values below this averaging 22% (Table 3.1). Soluble salts in the upper 30 cm of dry soil measured in 1:10 soil-water extractions are primarily composed of Na-$HCO_3$, which is likely due to calcite dissolution and cation exchange (Toner et al., 2012b). The composition of melt water extracted from the ICS is characterized by Na-Mg-Cl brine near the ICS surface, Ca-Mg-Na-Cl brine centered at approximately 150 cm depth, and Na-Mg-Cl brine at depth. Cl concentrations in the borehole increase with depth and have two distinct peaks in concentration near 150 cm and 210 cm depth. These Cl peaks correspond to peaks in divalent cations and monovalent cations. Divalent cations (Ca and Mg) covary with depth and have a

distinct peak in concentration at about 150-170 cm depth, while monovalent cations (Na and K) sharply increase at 200-210 cm depth. $SO_4$ and $NO_3$ trends are more variable, but are generally highest in the upper borehole soil and decrease with depth.

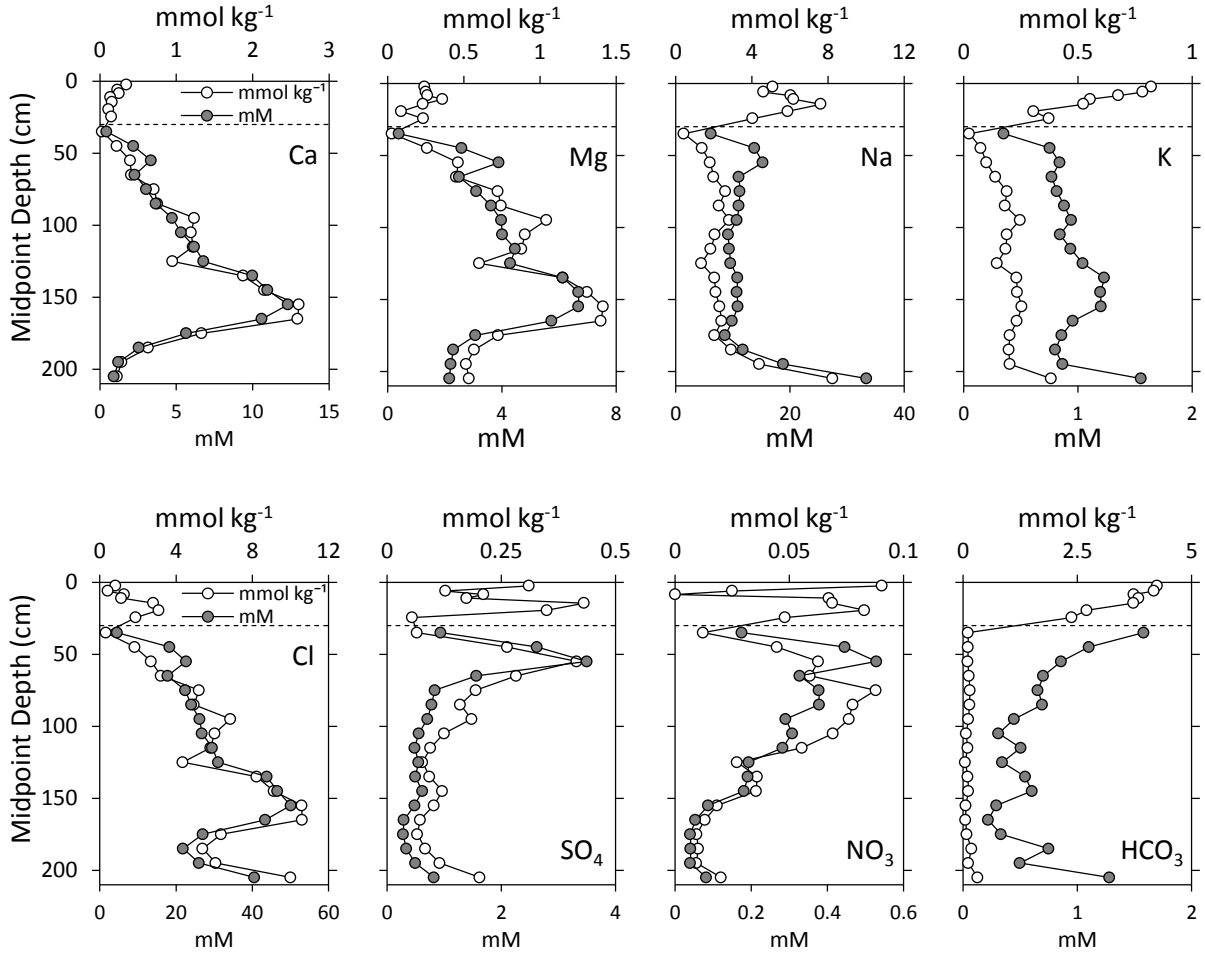


Figure 3.3. Graphs showing Ca, Mg, Na, K, Cl, $SO_4$, $NO_3$, and $HCO_3$ profiles with depth in the borehole soil. The grey circles indicate ion concentrations measured in the thawed ice-cement (in units of mM). The white circles are ion concentrations measured in the thawed ice-cement converted into units of mmol $kg^{-1}$ and ion concentrations from the in the 1:10 soil-water extractions in the upper 30 cm of dry soil with (units of mmol $kg^{-1}$). The depth to ice-cement is indicated by the dashed line at 30 cm depth.

Trends in exchangeable cations with depth (Figure 3.4) generally parallel trends in soluble cations. In the upper 30 cm of dry soil, exchangeable Na and Mg covary and have distinct peaks near 15 cm depth, while exchangeable Ca is highest near the soil surface and the ICS boundary. In the ICS, exchangeable Ca gradually increases below the ICS surface from 37% of the exchange complex at 30-40 cm depth to 50% of the exchange complex at 170-180 cm

depth. This increase in exchangeable Ca is mirrored by a decrease in exchangeable Na and Mg below the ICS surface. From 180 to 210 cm depth exchangeable Na and Mg increase, while exchangeable Ca decreases.

The CEC of the borehole is relatively constant in the upper 150 cm of soil, averaging 25 meq $kg^{-1}$. Below 150 cm, the CEC steadily increases to a maximum of 60 meq $kg^{-1}$ at 200-210 cm depth. These trends in CEC reflect trends in the clay and silt content of the borehole (Table 3.1), which is expected since clays and silts have high surface area and contribute the most to the total CEC (Malcolm and Kennedy, 1970). The relatively low CEC of the upper borehole soil is consistent with the sandy, fluvial nature of the upper soil, which contains little clay and silt. At depth, the CEC in the borehole increases as the sediment becomes more fine-grained. The occurrence of more fine-grained material near 200 cm depth is consistent with the textural shift in sediment indicated by Ground Penetrating Radar (Horsman et al., 2007). The silt rich sediment underlying the sandy fluvial sediment may be from past glaciolacustrine systems in Taylor Valley (Denton et al., 1970; Hall et al., 2000; Stuiver et al., 1981). Barrett et al. (2010) and Toner et al. (2012b) observed that silty soils in eastern Taylor Valley often contain high concentrations of soluble salts, presumably from paleolakes. This suggests that the sharp increase in aqueous and exchangeable Na, Mg, and Cl near 200 cm depth in the borehole is due to a saline paleosol that has been buried by fluvial sediment.

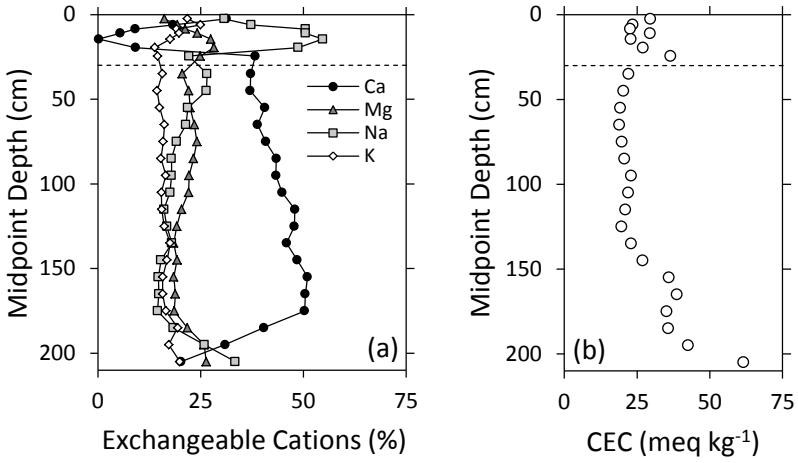


Figure 3.4. Graphs showing: (a) the equivalent percentage of exchangeable Ca, Mg, Na, and K; (b) the CEC profile with depth. The depth to ice-cement is indicated by the dashed line at 30 cm depth.

Table 3.1. Physical properties for the borehole including: clay, silt, and sand in the <2 mm size fraction, the gravimetric <2 mm size fraction (<2 mm), and the gravimetric water content ($H_2O$).

| Depth (cm) | Clay (%) | Silt (%) | Sand (%) | <2 mm (%) | $H_2O$ (%) |
|---|---|---|---|---|---|
| 0-5 | 1.5 | 3.0 | 95.6 | 41.9 | – |
| 5-7 | 1.2 | 1.3 | 97.5 | 96.5 | – |
| 7-10 | 0.3 | 0.8 | 98.9 | 57.6 | – |
| 10-12 | 0.5 | 0.9 | 98.6 | 90.0 | – |
| 12-17 | 0.3 | 0.7 | 98.9 | 71.9 | – |
| 17-22 | 0.4 | 0.8 | 98.8 | 85.6 | – |
| 22-30 | 0.4 | 1.0 | 98.6 | 76.2 | – |
| 30-40 | 0.7 | 2.3 | 97.0 | 93.8 | 7.0 |
| 40-50 | 0.9 | 2.9 | 96.3 | 77.3 | 10.0 |
| 50-60 | 1.1 | 3.6 | 95.3 | 92.4 | 11.9 |
| 60-70 | 1.6 | 5.5 | 92.9 | 88.3 | 18.1 |
| 70-80 | 1.5 | 5.2 | 93.3 | 88.5 | 23.2 |
| 80-90 | 1.3 | 4.4 | 94.3 | 94.5 | 20.6 |
| 90-100 | 1.7 | 5.6 | 92.8 | 96.3 | 26.2 |
| 100-110 | 1.5 | 5.0 | 93.5 | 98.4 | 22.5 |
| 110-120 | 1.4 | 4.7 | 93.9 | 89.2 | 19.7 |
| 120-130 | 1.5 | 5.1 | 93.4 | 89.1 | 14.0 |
| 130-140 | 1.6 | 5.5 | 92.8 | 92.0 | 18.8 |
| 140-150 | 1.7 | 6.0 | 92.2 | 92.8 | 19.6 |
| 150-160 | 1.8 | 6.4 | 91.8 | 95.2 | 21.2 |
| 160-170 | 2.5 | 8.5 | 89.1 | 95.9 | 24.4 |
| 170-180 | 3.2 | 10.6 | 86.2 | 99.7 | 23.6 |
| 180-190 | 4.0 | 13.0 | 83.0 | 99.2 | 24.7 |
| 190-200 | 3.8 | 12.9 | 83.3 | 99.7 | 23.3 |
| 200-210 | 5.4 | 17.4 | 77.1 | 98.8 | 24.7 |

$\delta^{18}O$ and $\delta D$ values in the ICS fall along the line $\delta D = 5.1\delta^{18}O - 87.3$ ($R^2 = 0.99$) and intersect the Global Meteoric Water Line (GMWL: $\delta D = 10 + 8\delta^{18}O$) at $\delta^{18}O$ = -33.9‰ and $\delta D$ = -261.1‰ (Figure 3.5a). Isotopic values for snow, ice-cement, and groundwater in Taylor Valley from Levy

et al. (2011) plot along the line of isotope values in the borehole (Figure 3.5a). The distribution of stable isotopes in the borehole with depth shows a systematic enrichment in heavy isotopes near the ICS surface (Figure 3.5b). At depth, the isotopic composition of the ICS is similar to snow in Taylor Valley, while near the surface the isotopic composition is similar to isotopically enriched ICS sampled by Levy et al. (2011). Shallow subsurface flows in Taylor Valley are isotopically Intermediate between near surface ICS and snow (Levy et al., 2011), which suggests that shallow groundwaters are derived from a mixture of melt from ICS and snow. In the upper ICS, highly negative deuterium excess values, given by $d_{excess} = \delta D - 8\delta^{18}O$ (Dansgaard, 1964), suggest kinetic fractionation due to evaporation (Figure 3.5c). Similar isotope profiles have been measured in a Victoria Valley soil by Hagedorn et al. (2010) and are thought to be caused by migration of brine from evaporated snowmelt into the ICS (Dickinson and Rosen, 2003; Hagedorn et al., 2010). The offset in the isotope profile from Hagedorn et al. (2010) relative to the Taylor Valley borehole is likely due to the greater elevation and distance from the coast of the Victoria Valley soil, resulting in more depleted isotope values in Victoria Valley (Gooseff et al., 2006; Matsubaya et al., 1979b).

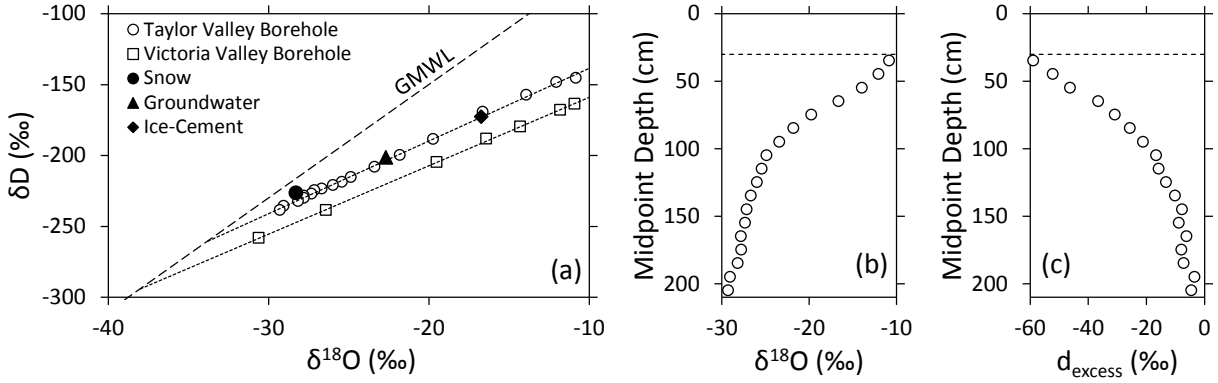


Figure 3.5. Graphs showing stable isotopic trends in the Taylor Valley borehole compared to stable isotopes values from a Victoria Valley borehole (Hagedorn et al., 2010) and values from snow, groundwater, and ice-cement in Taylor Valley (Levy et al., 2011) (a); $\delta^{18}O$ depth profile (b); $d_{excess}$ depth profile (c). The depth to ice-cement is indicated by the dashed line at 30 cm depth.

### *3.4.2. Cation Exchange Properties*

Exchange isotherms for Ca-Na and Ca-Mg exchange in 0.1 M and 4.75 M solutions are shown in Figure 3.6 using the data from exchange experiments (Table 3.2 and Table 3.3). The 0.1 M Ca-Na exchange isotherm is distinct from the 4.75 M Ca-Na exchange isotherm; for the same equivalent fraction of Ca in solution, 4.75 M Ca-Na soil solutions have about 40% less exchangeable Ca compared to 0.1 M soil solutions. This indicates that Ca is more strongly partitioned onto exchange sites (and Na into solution) as the solution concentration increases from 0.1 M to 4.75 M. Ca-Mg exchange isotherms are similar for both 0.1 M and 4.75 M solutions and indicate that Ca is more strongly partitioned onto exchange sites than Mg. In the dilute cation exchange experiments, exchange sites are dominated by exchangeable Ca and Mg, even though a significant fraction of the equilibrating solution is composed of Na (Table 3.4).

The exchange properties noted here are consistent with a concentration effect known as the 'ratio law' (McBride, 1994). As formulated by Schofield (1947), the ratio law states that if the exchange composition is held constant, the ratio $a_j^{z_i}/a_i^{z_j}$ will also be constant as the concentration of the soil solution changes. A major consequence of the ratio law is that in heterovalent exchange reactions, such as Ca-Na exchange, aqueous monovalent cations (Na and K) will exchange with exchangeable divalent cations (Ca and Mg) as the solution is concentrated, enriching the soil solution in divalent cations. Conversely, as the soil solution is diluted, aqueous divalent cations will exchange with exchangeable monovalent cations, enriching the soil solution in monovalent cations. With respect to homovalent exchange reactions, such as Ca-Mg exchange, the ratio law predicts that the relative proportions of aqueous cations will be unaffected by changes in solution concentration. These effects are consistent with the stronger Na adsorption in 4.75 M solutions relative to 0.1 M solutions, the high Ca and Mg saturation in the simulated stream solution, and the similarity in Ca-Mg exchange at different concentrations.

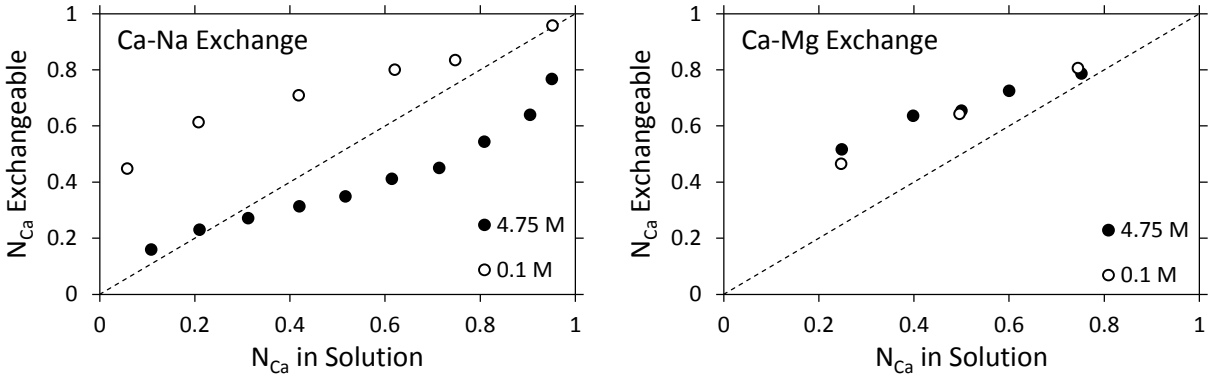


Figure 3.6. Cation exchange isotherms derived using data in Table 3.2 and Table 3.3 for 0.1 M and 4.75 M solutions. $N_{Ca}$ is the equivalent fraction of Ca in either the solution or exchange phase. The dashed line is the isotherm for which cations are equally partitioned between exchange and aqueous phases.

Table 3.2**.** Data from Ca-Na exchange experiments. The CEC is the equivalent sum of exchangeable cations.

| Experiment | Equilibrating Solutions (M) | | Exchange Composition (meq $kg^{-1}$) | | |
|---|---|---|---|---|---|
| | Ca | Na | $CaX_2$ | NaX | CEC |
| 4.75 M | 0.258 | 4.223 | 13.2 | 69.9 | 83.1 |
| | 0.494 | 3.705 | 18.3 | 61.7 | 80.0 |
| | 0.742 | 3.256 | 21.0 | 56.6 | 77.6 |
| | 1.007 | 2.779 | 25.1 | 55.0 | 80.1 |
| | 1.206 | 2.249 | 29.2 | 54.7 | 83.9 |
| | 1.465 | 1.838 | 29.8 | 42.7 | 72.5 |
| | 1.700 | 1.360 | 35.3 | 43.3 | 78.7 |
| | 1.950 | 0.918 | 41.5 | 34.9 | 76.5 |
| | 2.201 | 0.460 | 45.4 | 25.6 | 71.0 |
| | 2.283 | 0.234 | 56.4 | 17.2 | 73.6 |
| 0.1 M | 0.003 | 0.086 | 33.4 | 46.7 | 80.1 |
| | 0.010 | 0.075 | 49.8 | 31.6 | 81.4 |
| | 0.020 | 0.056 | 59.2 | 24.4 | 83.5 |
| | 0.031 | 0.038 | 63.0 | 15.8 | 78.8 |
| | 0.041 | 0.027 | 66.4 | 13.3 | 79.6 |
| | 0.048 | 0.005 | 75.1 | 3.4 | 78.5 |

Table 3.3**.** Data from Ca-Mg exchange experiments. The CEC is the equivalent sum of exchangeable cations.

| Experiment | Equilibrating Solutions (M) | | Exchange Composition (meq $kg^{-1}$) | | |
|---|---|---|---|---|---|
| | Ca | Mg | $CaX_2$ | $MgX_2$ | CEC |
| 4.75 M | 0.603 | 1.820 | 41.7 | 39.2 | 81.0 |
| | 0.977 | 1.472 | 48.3 | 27.7 | 76.0 |
| | 1.217 | 1.216 | 41.4 | 21.9 | 63.3 |
| | 1.467 | 0.974 | 53.3 | 20.3 | 73.6 |
| | 1.841 | 0.605 | 55.3 | 15.1 | 70.3 |
| 0.1 M | 0.013 | 0.038 | 35.7 | 41.2 | 76.9 |
| | 0.025 | 0.026 | 49.3 | 27.5 | 76.9 |
| | 0.038 | 0.013 | 61.5 | 14.9 | 76.3 |

Table 3.4**.** Data from dilute exchange experiments. Soils 464 and 510 are from silty tills, and soils 651 and 830 are from sandy terraces. The CEC is the equivalent sum of exchangeable cations.

| Soil | Equilibrating Solutions (mM) | | | Exchange Composition (meq $kg^{-1}$) | | | |
|---|---|---|---|---|---|---|---|
| | Ca | Mg | Na | $CaX_2$ | $MgX_2$ | NaX | CEC |
| 464 | 0.406 | 0.111 | 0.457 | 41.4 | 9.1 | 4.7 | 55.2 |
| 510 | 0.360 | 0.100 | 0.504 | 78.9 | 16.9 | 7.9 | 103.7 |
| 651 | 0.352 | 0.109 | 0.438 | 34.0 | 7.8 | 4.7 | 46.5 |
| 830 | 0.371 | 0.111 | 0.454 | 36.4 | 7.9 | 5.9 | 50.2 |

To determine if measured cation exchange properties obey the Rothmund-Kornfeld model of cation exchange, $\log(A_j^{z_i}/A_i^{z_j})$ is plotted versus $\log(a_j^{z_i}/a_i^{z_j})$ in Figure 3.7. Data plotted in Figure 3.7 includes data from the dilute, 0.1 M, and 4.75 M exchange experiments (Table 3.2, Table 3.3, and Table 3.4), as well as data from the thawed borehole samples. The borehole is included in Figure 3.7 because solutes in the thawed ICS should have equilibrated with exchange sites due to the rapid kinetics of cation exchange (Malcolm and Kennedy, 1970). As a result, the measurement of solutes and exchangeable cations in the borehole is considered to be a quaternary cation exchange experiment involving Ca, Mg, Na, and K. This permits a calculation of cation exchange parameters under natural soil conditions and allows an estimation of exchange parameters for K.

The linear nature of experimental data points in Figure 3.7 indicates that the Rothmund-Kornfeld model provides a good description of cation exchange at varying exchange compositions and solution concentrations. Parameters $\log K^{ij}$ and $n^{ij}$ (determined from the intercept and the slope of the line respectively) are given in Table 3.5. Manipulating equation (6) shows that if a single set of Rothmund-Kornfeld parameters are used to describe cation exchange and the exchange composition is held constant, the ratio $(a_j{}^{z_i}/a_i{}^{z_j})^{n^{ij}}$ will also be constant. This is nearly identical to the ratio law formulated by Schofield (1947) and indicates that the ratio law is a useful conceptual framework for understanding the effects of solution concentration on cation exchange reactions in Dry Valley soils.

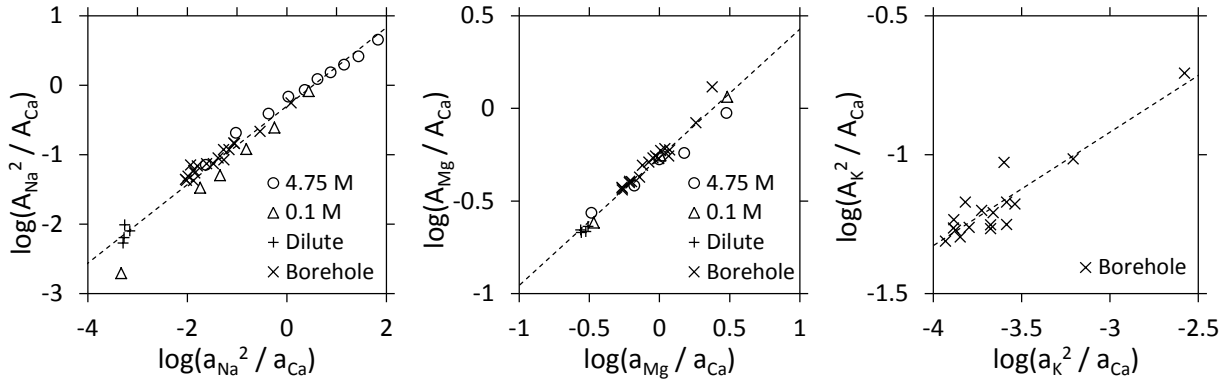


Figure 3.7. Plots of $\log(A_j^{z_i}/A_i^{z_j})$ versus $\log(a_j^{z_i}/a_i^{z_j})$ for Ca-Mg, Ca-Na, and Ca-K exchange for all exchange experiments. The dashed lines are a linear fit to the experimental data, with the Rothmund-Kornfeld parameter $n^{ij}$ obtained from the slope and $\log K^{ij}$ from the intercept.

Table 3.5. Parameters for the Rothmund-Kornfeld equation calculated by fitting data from exchange experiments and data from the borehole analysis to equation (6).

| | $\log K^{ij}$ | $n^{ij}$ | $R^2$ |
|---|---|---|---|
| Ca-Na | 0.303 | 0.565 | 0.97 |
| Ca-Mg | 0.265 | 0.691 | 0.96 |
| Ca-K | -0.306 | 0.408 | 0.86 |

*3.5. Discussion*

Ca-Cl enrichment is defined here as an excess of Ca in solution subject to the condition $2Ca > HCO_3 + 2SO_4$ (Lerman, 1970). This identifies the Ca component associated with Cl and predicts that when a Ca-Cl enriched solution is concentrated through freezing or evaporation significant concentrations of Ca will remain as highly soluble $CaCl_2$ after the precipitation of relatively insoluble calcium carbonates and sulfates. Using this definition, the ICS between 60 and 200 cm depth in the borehole soil is strongly enriched in Ca-Cl (Figure 3.8). Ca-Cl enrichment is highest at 150-160 cm depth, near the peak concentration of divalent cations. It is unlikely that this Ca-Cl enriched brine has been influenced by groundwater because the study site is located on a raised, flat-topped terrace and groundwater indicators, such as wetted soil surfaces or nearby snow banks (Levy et al., 2011; Levy et al., 2012), were not present. This suggests that the Ca-Cl enrichment in the borehole was produced *in situ* less than two meters from the soil surface. This argues against mechanisms of subsurface Ca-Cl enrichment as reviewed by Lyons and Mayewski (1993) and contrasts with the view of Green and Canfield

(1984) and Lyons and Mayewski (1993) that Ca-Cl brines cannot evolve near the surface. Furthermore, the initial chemistry of ice-cement in the borehole soil was likely derived from surface waters in Taylor Valley. Given that present-day surface waters in Fryxell Basin are Na-$HCO_3$ waters with high concentrations of $HCO_3$ relative to Ca (Green et al., 1988), the ICS should not have developed Ca-Cl brine. Instead, it appears that Ca-Cl enrichment does evolve from surface waters, even in the extreme case where the ice-cement initially had a Na-$HCO_3$ composition.

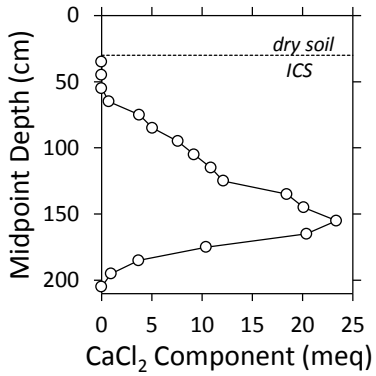


Figure 3.8. A graph of the $CaCl_2$ component in the borehole, defined as the equivalent concentration of Ca in excess of $HCO_3$ and $SO_4$ ($CaCl_2 = 2Ca - HCO_3 - 2SO_4$). The depth to ice-cement is indicated by the dashed line at 30 cm depth.

The distribution of stable isotopes in the borehole soil with depth suggests that isotopically enriched brine from evaporated snowmelt is advecting downwards into the ICS, enriching the upper ICS in heavy isotopes (Hagedorn et al., 2010). Since downward advecting brine will be highly saline, the brine is likely enriched in Ca by Ca-Na exchange, similar to cases in more temperate regions where infiltrating saline groundwater is enriched in Ca by cation exchange (e.g. Bjerg and Christensen, 1993; Howard and Lloyd, 1983; Sanford et al., 1992). To explore the hypothesis that cation exchange is responsible for the Ca-Cl enrichment in the borehole, we develop the following conceptual model of reactive transport in ICS.

Sediments deposited in surface environments will initially be saturated with divalent cations (Ca and Mg). This is due to the relatively high proportion of divalent ions in Dry Valley surface

waters (Lyons et al., 1998b) and the strong affinity of divalent cations for exchange surfaces in dilute waters (McBride, 1994). Following deposition, soils will begin accumulating Na-Cl rich marine aerosols. These salts will then be transported towards the ICS by percolating water from snowmelt (Dickinson and Rosen, 2003; Hagedorn et al., 2010; McKay et al., 1998). Once in the ICS, melt water will be concentrated by freezing and transported downwards as thin brine films (Dickinson and Rosen, 2003; Hagedorn et al., 2010; Ugolini and Anderson, 1973). In the high concentration solutions produced by freezing, the ratio law predicts that the unfrozen soil solution will be enriched in divalent ions (Ca and Mg) relative to monovalent ions (Na and K). We predict that the advection of Na-Cl brines into frozen soil that is highly saturated with exchangeable Ca will result in strong Ca-Na exchange and Ca-Cl enrichment in the soil solution.

*3.5.1. The Exchange Chemistry of Soils in Equilibrium with Surface Waters*

In this section, PHREEQC is used to determine the initial composition of exchangeable cations in soils after deposition by surface waters in the Dry Valleys. Due to the rapid kinetics of ion exchange, the exchangeable cation composition of soils deposited in surface environments would have equilibrated with surface waters. To determine possible exchange compositions that can be produced from equilibration with surface waters, PHREEQC is used to model exchangeable cations in soils in equilibrium with Dry Valley stream and lake chemistries monitored by the LTER group (Table 3.6). For lake waters, only the composition of surface water (above 8 m depth) is used to model exchangeable cations because this is the water that soils will be in contact with prior to lake retreat.

Modeled exchange compositions in Table 3.6 are characterized by high exchangeable Ca and Mg concentrations, even in waters with high proportions of Na. Sediments in equilibrium with stream waters have exchangeable cation compositions in the order Ca >> Mg > K > Na, while sediments in equilibrium with lake waters have higher exchangeable Mg, Na, and K. Exchange

surfaces in contact with stream waters in Bonney Basin contain higher proportions of Na and Mg than in Fryxell Basin, while exchange surfaces in contact with Hoare Basin streams contain the highest exchangeable Ca. Even though near-surface lake water in Lake Fryxell and Lake Bonney contain much higher concentrations of Na than Ca or Mg, exchange surfaces in equilibrium with these waters contain more than 50% exchangeable Ca and Mg. For all waters modeled here, the proportion of K on exchange surfaces is relatively high compared to K in streams and lakes.

Table 3.6**.** The exchangeable cation composition of sediments in equilibrium with stream and lake surface waters in Taylor and Wright Valleys modeled using PHREEQC. n is the total number of water samples modeled and the concentration of bicarbonate is determined from charge balance: $HCO_3 = 2Ca + 2Mg + Na + K – Cl – 2SO_4$. The exchange composition of soils in equilibrium with surface water is enriched in Ca and Mg.

| | | | Average Ion Concentration (mM) | | | | | | | Exchange Composition (%) | | | |
|---|---|---|---|---|---|---|---|---|---|---|---|---|---|
| | | n | Ca | Mg | Na | K | Cl | $SO_4$ | $HCO_3$ | $CaX_2$ | $MgX_2$ | NaX | KX |
| Streams | Fryxell Basin | 832 | 0.28 | 0.07 | 0.33 | 0.05 | 0.28 | 0.05 | 0.70 | 70.7 | 15.2 | 6.0 | 8.0 |
| | Hoare Basin | 176 | 0.23 | 0.02 | 0.07 | 0.01 | 0.07 | 0.03 | 0.46 | 85.0 | 7.8 | 2.7 | 4.5 |
| | Bonney Basin | 397 | 0.55 | 0.19 | 0.80 | 0.06 | 0.77 | 0.44 | 0.69 | 65.5 | 19.7 | 7.2 | 7.6 |
| | Onyx River | 100 | 0.10 | 0.04 | 0.17 | 0.02 | 0.16 | 0.04 | 0.23 | 65.0 | 18.5 | 7.3 | 9.2 |
| Lakes | Lake Fryxell | 176 | 1.65 | 1.91 | 15.86 | 0.95 | 13.90 | 0.73 | 8.55 | 37.5 | 21.1 | 24.0 | 17.3 |
| | Lake Hoare | 130 | 0.70 | 0.48 | 2.60 | 0.28 | 2.26 | 0.44 | 2.11 | 52.1 | 21.2 | 13.1 | 13.6 |
| | Lake Bonney | 236 | 1.84 | 2.51 | 16.28 | 0.47 | 19.53 | 1.72 | 2.47 | 39.2 | 25.2 | 24.7 | 10.9 |
| | Lake Vanda | 6 | 1.83 | 0.81 | 2.17 | 0.34 | 6.96 | 0.17 | 0.50 | 58.5 | 18.1 | 10.0 | 13.4 |

### *3.5.2. The Effects of Freezing on Aqueous and Exchangeable Cations*

After Dry Valley soils are deposited by surface waters, the soil pore water will freeze, forming ICS. To determine the equilibrium chemistry of frozen soils initially saturated with the surface waters in Table 3.6, PHREEQC is used to model pore water freezing at -19°C, approximately the average temperature in Taylor Valley (Clow et al., 1988; Doran et al., 2002b). In Table 3.7, pore water freezing is modeled in equilibrium with exchangeable cations. The saturated gravimetric water content of the soil prior to freezing is assumed to be 25% and the CEC is assumed to be 40 meq $kg^{-1}$, a value typical for soils found throughout Antarctica (Cameron and Conrow, 1969; Cameron et al., 1970; Cameron et al., 1971). For comparison, freezing of soil solutions is also modeled in the absence of exchange reactions in Table 3.8.

When soils initially saturated with surface waters are frozen they form concentrated Ca-Mg-Cl enriched brine (Table 3.7). Freeze-concentrated soils initially saturated with stream water evolve to nearly pure Ca-Mg-Cl brine with very low concentrations of Na and K. Soils initially saturated with lake waters also evolve brine with high concentrations of divalent ions, but Na concentrations are higher, up to about 20% of the equivalent aqueous cation composition. Most pore waters in Table 3.6 prior to freezing are characterized by the condition $2Ca < HCO_3 + 2SO_4$, which suggests pore waters should evolve into Ca depleted brine during freeze-concentration. That Ca-Cl enrichment occurs instead is due to cation exchange reactions. As soil solutions are freeze-concentrated, aqueous Na and K ions exchange with exchangeable Ca and Mg, increasing the concentration of Ca and Mg in soil solutions. This process can be seen in the lower exchangeable divalent ions and higher exchangeable monovalent ions in Table 3.7 compared to Table 3.6. Ratios of divalent ions to monovalent ions in freeze-concentrated soil solutions range from 2 to 270 and are much higher than ratios in unfrozen waters ranging from 0.2 to 3.

Table 3.7**.** Unfrozen brine and exchangeable cation chemistries in frozen soils at -19°C modeled in PHREEQC using pore water chemistries and exchange compositions in Table 3.6. For all solutions, gypsum and calcite precipitate during freezing.

| | | Average Ion Concentration (molal) | | | | | | | Exchange Composition (%) | | | |
|---|---|---|---|---|---|---|---|---|---|---|---|---|
| | | Ca | Mg | Na | K | Cl | $SO_4$ | $HCO_3 + CO_3$ | $CaX_2$ | $MgX_2$ | NaX | KX |
| Streams | Fryxell Basin | 1.72 | 0.51 | 0.03 | 0.00 | 4.48 | 0.00 | 0.00 | 70.1 | 15.0 | 6.5 | 8.3 |
| | Hoare Basin | 2.02 | 0.22 | 0.01 | 0.00 | 4.46 | 0.00 | 0.00 | 84.0 | 7.3 | 3.2 | 5.4 |
| | Bonney Basin | 1.38 | 0.77 | 0.04 | 0.00 | 4.33 | 0.00 | 0.00 | 63.9 | 19.2 | 8.5 | 8.4 |
| | Onyx River | 1.13 | 0.92 | 0.02 | 0.00 | 4.11 | 0.00 | 0.00 | 64.9 | 18.5 | 7.4 | 9.2 |
| Lakes | Lake Fryxell | 0.58 | 1.11 | 0.72 | 0.04 | 4.13 | 0.01 | 0.00 | 29.6 | 18.3 | 34.7 | 17.4 |
| | Lake Hoare | 0.87 | 1.11 | 0.12 | 0.02 | 4.10 | 0.00 | 0.00 | 47.9 | 20.1 | 16.9 | 15.1 |
| | Lake Bonney | 0.66 | 1.13 | 0.65 | 0.01 | 4.23 | 0.01 | 0.00 | 32.7 | 21.7 | 34.7 | 10.9 |
| | Lake Vanda | 1.12 | 0.91 | 0.08 | 0.02 | 4.15 | 0.00 | 0.00 | 54.5 | 15.8 | 14.0 | 15.8 |

The increase in divalent ions with respect to monovalent ions during freeze-concentration is consistent with the ratio law. As the solution is concentrated by freezing, the ratio law predicts that equilibrium conditions will favor the exchange of aqueous monovalent cations with exchangeable divalent cations. To demonstrate this effect, we model the freezing of a soil solution initially saturated with pore water having the average composition of Lake Fryxell

surface water in Figure 3.9. Above 0°C, the soil solution is unfrozen and dilute, and the soluble composition is dominated almost entirely by Na. Below 0°C, the soil solution is concentrated by freezing, which causes divalent ions to increase relative to monovalent ions due to ratio law effects. The increase in divalent ions is most rapid immediately after freezing begins, and becomes gradual afterwards. This is due to the rapid increase in solute concentration near 0°C. From 0 to -3°C Cl concentrations increase by a factor of 120 (0.014 to 1.65 molal), while from -3 to -39°C Cl concentrations increase by a smaller factor of 4.2 (1.65 to 6.77 molal).

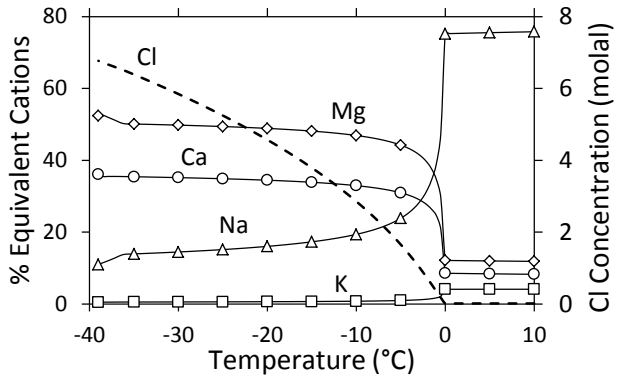


Figure 3.9. Graph showing the equilibrium freezing of a soil solution initially saturated with water having the average composition of Lake Fryxell surface water. Aqueous Ca, Mg, Na, and K are shown as equivalent %, while Cl is given in molal concentration.

The importance of exchange reactions for Ca-Cl enrichment is highlighted by modeling freezing of surface waters without exchange reactions (Table 3.8). This results in Ca-depleted brine for all surface waters except Lake Vanda. Lake Vanda surface waters are already enriched in Ca ($2Ca > HCO_3 + 2SO_4$) and evolve into Ca-Mg-Na-Cl brine similar in composition to the saline hypolimnia of Lake Vanda. The Ca enriched composition of Lake Vanda surface water is not found in its main inflow water, the Onyx River, and is likely due to upward diffusion of brine from the hypolimnia of Lake Vanda (Green and Canfield, 1984). The formation of Ca-depleted brine from surface waters in the absence of exchange reactions (or groundwater influence) is consistent with the observations of Green et al. (1988) that higher equivalent concentrations of $HCO_3$ in surface waters relative to Ca favors the loss of Ca through precipitation of calcite. We add that $SO_4$ is also unfavorable for Ca-Cl formation due to the precipitation of gypsum.

In the absence of cation exchange reactions, our modeling predicts that $CaCO_3$, $CaSO_4 \cdot 2H_2O$, $Na_2SO_4 \cdot 10H_2O$, $3MgCO_3 \cdot Mg(OH)_2 \cdot 3H_2O$, $Na_2CO_3 \cdot 10H_2O$, and KCl will precipitate from surface waters (Table 3.8). Equilibrium conditions also indicate that dolomite ($CaMg(CO_3)_2$) and magnesite ($MgCO_3$) are supersaturated and could precipitate during freezing; however, these minerals are prevented from precipitating in PHREEQC because their formation is kinetically inhibited at low temperatures (Land, 1998; Langmuir, 1965). When freezing is modeled with cation exchange reactions included, only $CaCO_3$ and $CaSO_4 \cdot 2H_2O$ precipitate from soil solutions (Table 3.7). Additional salt phases that form in the absence of cation exchange are due to excess $HCO_3$ and $SO_4$ relative to Ca in most surface waters. After the precipitation of $CaCO_3$ and $CaSO_4 \cdot 2H_2O$, excess $HCO_3$ and $SO_4$ remain to precipitate with Na, K, and Mg. Exchangeable Ca can alter the balance between aqueous $HCO_3$, $SO_4$, and Ca by exchanging into solution. As soil solutions are frozen, solute concentrations increase, causing Ca to precipitate as $CaCO_3$ and $CaSO_4 \cdot 2H_2O$. This Ca loss from solution is compensated as exchangeable Ca is pulled into the soil solution until equilibrium is attained between aqueous and exchangeable Ca. Since the solubility of $CaCO_3$ and $CaSO_4 \cdot 2H_2O$ is low, this process continues until either all of the Ca is removed from the exchange complex or all of the $SO_4$ and $HCO_3$ has precipitated with Ca. This suggests that in soil solutions, Ca-Cl enrichment has the potential to occur during freezing when both exchangeable and aqueous Ca are greater than $HCO_3$ and $SO_4$ ($2Ca_{(aq)} + 2Ca_{(exch)} > HCO_3 + 2SO_4$).

Table 3.8**.** Unfrozen brine in soils at -19°C modeled without exchange reactions in PHREEQC using pore water compositions in Table 3.6. Common salt phases are defined as phases present in more than 10% of the samples modeled: Cal (Calcite, $CaCO_3$), Mir (Mirabilite, $Na_2SO_4 \cdot 10H_2O$), Gyp (Gypsum, $CaSO_4 \cdot 2H_2O$), Hmag (Hydromagnesite, $3MgCO_3 \cdot Mg(OH)_2 \cdot 3H_2O$), Nat (Natron, $Na_2CO_3 \cdot 10H_2O$), and Syl (Sylvite, KCl). In the absence of cation exchange, the unfrozen solution typically evolves into Na-Mg-K-Cl brine.

| | | Average Concentration (molal) | | | | | | | Common Salt Phases |
|---|---|---|---|---|---|---|---|---|---|
| | | Ca | Mg | Na | K | Cl | $SO_4$ | $HCO_3 + CO_3$ | |
| Streams | Fryxell Basin | 0.01 | 0.32 | 3.39 | 0.96 | 4.66 | 0.05 | 0.17 | Cal, Mir, Gyp, Hmag, Nat, Syl |
| | Hoare Basin | 0.04 | 1.12 | 1.59 | 0.91 | 4.47 | 0.16 | 0.01 | Cal, Mir, Gyp, Hmag, Syl |
| | Bonney Basin | 0.02 | 0.82 | 2.41 | 0.62 | 4.55 | 0.07 | 0.02 | Cal, Mir, Gyp, Hmag |
| | Onyx River | 0.01 | 0.64 | 2.76 | 0.68 | 4.65 | 0.05 | 0.01 | Cal, Mir, Hmag |
| Lakes | Lake Fryxell | 0.00 | 0.01 | 4.72 | 0.33 | 4.66 | 0.04 | 0.22 | Cal, Mir, Hmag, Nat |
| | Lake Hoare | 0.00 | 0.31 | 3.59 | 0.58 | 4.73 | 0.03 | 0.01 | Cal, Mir, Hmag |
| | Lake Bonney | 0.07 | 0.53 | 3.32 | 0.11 | 4.56 | 0.03 | 0.01 | Cal, Mir, Gyp |

| | | | | | | | | |
|---|---|---|---|---|---|---|---|---|
| Lake Vanda | 0.94 | 0.54 | 1.44 | 0.22 | 4.59 | 0.00 | 0.00 | Cal, Gyp |

*3.5.3. The Frozen State of the Borehole Soil*

Soluble and exchangeable ions in the borehole soil were measured in thawed sediment but, as shown in the previous section, the distribution of ions between aqueous, solid, and exchange phases will be different in frozen soil. In this section, we model freeze-concentration of the unfrozen borehole in PHREEQC to determine the state of the borehole soil under frozen conditions. When frozen, the distribution of ions between aqueous, solid, and exchange phases will depend on the soil temperature.

To estimate the temperature profile in the borehole at time $t$ and depth $z$, a mathematical model of soil temperature variation is used (Campbell, 1977):

$$T(z,t) = T_a + A_0 e^{-z/\delta} \sin(\omega t - z/\delta) \quad (11)$$

where $T_a$ is the average annual soil temperature, $A_0$ is the seasonal amplitude of temperature variation, $\omega$ is the frequency of the annual wave, and $\delta$ is the damping depth. $T_a$ and $A_0$ are determined by fitting equation (11) to soil surface temperature data at the Lake Fryxell LTER meteorology station from 1995 – 2010: $T_a$ = -19°C and $A_0$ = 25°C. $\delta$ Is assumed to be 1.4 m for dry soil and 2.8 m for ICS, as in McKay et al. (1998). In this study, we are primarily interested in the state of the borehole when downward reactive transport is occurring. Brine transport in the ICS is thought to occur during the austral summer when snowmelt forms and temperature gradients cause water potential gradients that drive moisture downwards (Dickinson and Rosen, 2003; Hagedorn et al., 2010). Since snowmelt will only form when surface temperatures are above 0°C, the average temperature profile during transport is assumed to be the average temperature field in equation (11) when the soil surface is above 0°C (a time period of 78 days during the austral summer). The resulting temperature profile (Figure 3.10) shows that average temperatures during transport in the upper 30 cm of dry soil are above 0°C, while below 30 cm

depth average temperatures are below 0°C. This is consistent with the ICS boundary at 30 cm depth.

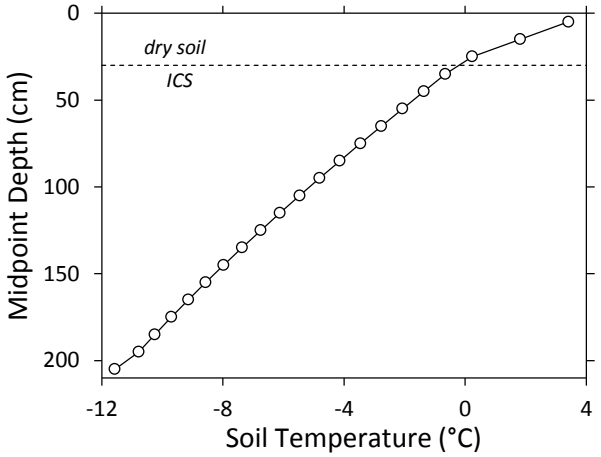


Figure 3.10. A graph of the average temperature profile for the Taylor Valley borehole when the soil surface is above 0°C. This was modeled using equation (11) and soil temperature data from the Lake Fryxell LTER met station. The depth to ice-cement is indicated by the dashed line at 30 cm depth.

The equilibrium state of ICS in the borehole is modeled in PHREEQC using measured soluble ions, exchangeable cations, water contents, and the modeled temperature profile (Figure A.1.) Modeled trends in ion concentration with depth are inversely correlated with the temperature profile due to freeze-concentration. Ion concentrations are low near the ICS surface where temperatures are high and ion concentrations are high at depth where temperatures are low. The gravimetric water content of the unfrozen brine is relatively constant with depth, averaging 0.32%. In the upper ICS, this unfrozen brine is high in Na-Mg-Cl, while at depth the composition becomes enriched in Ca. In the deepest portion of the borehole where the sediment texture becomes more fine-grained, the unfrozen brine transitions into a Na-Mg-Cl composition. The overall distribution of aqueous ions is similar to those measured in the thawed borehole sediment, except that the ratio of aqueous divalent to monovalent ions is greater. This is due to the ratio law concentration effect during freezing, which causes aqueous monovalent ions to exchange with exchangeable divalent ions as the soil solution becomes more concentrated. The increase in Ca concentration, from both cation exchange and freezing, results in

precipitation of calcite and gypsum. In particular, gypsum precipitates in a distinct spike at 50-60 cm depth below the soil surface (Figure 3.11c).

The modeled distribution of exchangeable cations with depth shows that the exchangeable Mg and Na increase near the ICS surface, while exchangeable Ca decreases. This is consistent with the adsorption of Na and Mg from downward advecting brines, and displacement of exchangeable Ca. In the following sections, we develop a model to test the hypothesis that reactive transport involving cation exchange can result in the chemical distributions modeled in Figure 3.11.

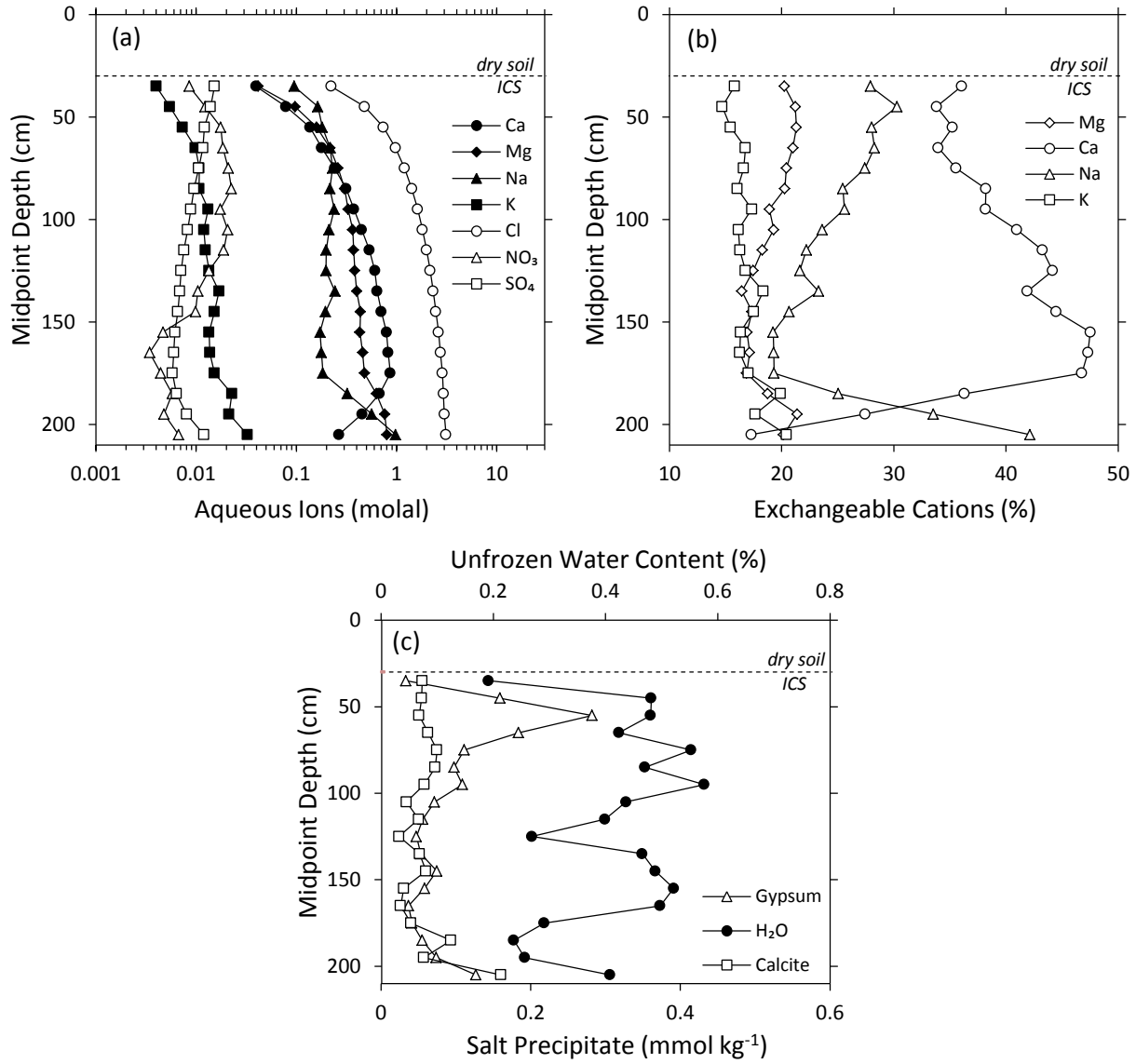


Figure 3.11. Graphs showing (a) the distribution of aqueous ions in unfrozen brines, (b) exchangeable cations, (c) gravimetric water contents, calcite precipitates, and gypsum precipitates predicted from modeling freezing of the borehole soil in PHREEQC. The depth to ice-cement is indicated by the dashed line at 30 cm depth.

### *3.5.4. Modeling Reactive Transport in Ice-Cemented Soil*

As has been shown by Hagedorn et al. (2010), the infiltration of brine into the borehole ICS can be described by advective dispersive reactive transport. In PHREEQC, advective dispersive reactive transport is given by (Appelo and Postma, 2005):

$$\frac{\partial \mathrm{C}}{\partial \mathrm{t}} = -\mathrm{v}\frac{\partial \mathrm{C}}{\partial \mathrm{x}} + \mathrm{D}^{*}\frac{\partial^{2}\mathrm{C}}{\partial \mathrm{x}^{2}} - \frac{\partial \mathrm{Q}}{\partial \mathrm{t}} \qquad (12)$$

In this equation, $C$ is the concentration of aqueous chemical species advecting downward, $Q$ is the concentration of a stationary exchange or solid phase, and $D^*$ is the hydrodynamic dispersion given by $D^* = D_e + \alpha v$, where $D_e$ ($m^2\ s^{-1}$) is the effective diffusion coefficient and α (m) is the dispersivity. The mobile phase consists of saline brine in equilibrium with ice advecting downward along interconnected films with average linear velocity $v$ ($m\ s^{-1}$). This brine is in contact with mineral grain surfaces during transport and chemically interacts with the exchange complex. The equilibration between the brine and exchange surfaces is considered to be instantaneous because the timescale for complete exchange in soils is rapid (Malcolm and Kennedy, 1970).

In addition to transport in the ICS, it is important to model transport in the upper 30 cm of dry soil because reactive transport in the upper dry soil will alter the composition of brine reaching the ICS. Following the conceptual model of Hagedorn et al. (2010), brine transport in the upper 30 cm of dry soil is characterized by intermittent unsaturated flow following episodic snowmelt events. A rigorous model of this type of transport over long timescales would require an understanding of the frequency, duration, and magnitude of snowmelt events (Marion et al., 2008); however, these events are poorly understood in Dry Valley soils (Fountain et al., 2010; Seybold et al., 2010). As a result, we approximate reactive transport in the upper 30 cm of dry soil by modeling only advection, so that $D^* = 0$ in equation (12).

*3.5.4.1. Parameterization of the Transport Model*

*3.5.4.1.1. Advection Velocity and Dispersivity*

The velocity of advecting brine in the borehole is estimated from the apparent position of the advective front with respect to the soil surface and the age of the soil. The position of the advecting front is suggested by the extent of Ca-Cl enrichment in the borehole, to about 180 cm depth below the soil surface. Below this is Na-Cl brine, which should have been displaced if the Ca-Cl brine had advected further downwards. A more accurate estimation of the advection

length can be determined using $NO_3$ as a tracer for downward advecting brines from the soil surface. $NO_3$ concentrations and $NO_3$/Cl ratios in the borehole sediment are high near the soil surface and quickly decrease near 150 cm depth to low values (Figure 3.12). Since $NO_3$ concentrations are extremely low in Taylor Valley stream and lake waters, on the order of 1-10 µM (Green et al., 1989), the $NO_3$ in the upper borehole must not have been initially present in the ice-cement. Instead, the distribution of $NO_3$ in the borehole suggests that $NO_3$ has advected downwards from the soil surface. The advecting front of downward moving brine is suggested by the sharp decrease in $NO_3$ at 150 cm below the soil surface. This depth is also near where the Ca-Cl enrichment in the ICS is the highest. For a total advection length of about 150 cm and a soil age of 5 Ka, the calculated average advection velocity is $9.5 \times 10^{-12}$ m $s^{-1}$. This value is close to advection velocities of $10^{-10}$-$10^{-11}$ m $s^{-1}$ determined from isotope profiles in a Victoria Valley soil by Hagedorn et al. (2010).

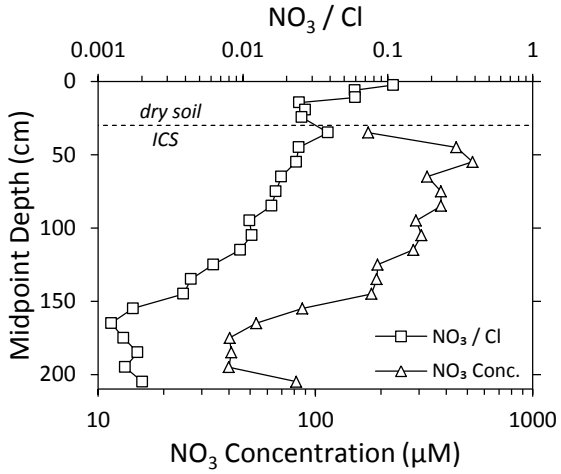


Figure 3.12. A graph showing $NO_3$ concentrations and $NO_3$/Cl ratios with depth in the borehole. The depth to ice-cement is indicated by the dashed line at 30 cm depth.

Advecting brines will be spread out by hydrodynamic dispersion, $D^* = D_e + \alpha v$, which is the sum of mechanical dispersion ($\alpha v$) and molecular diffusion ($D_e$) (Bear, 1972). At low moisture fluxes, mechanical dispersion is low and hydrodynamic dispersion is dominated by diffusion along thin unfrozen water films (Toride et al., 2003). Given the low unfrozen water contents and advection velocity in this study, mechanical dispersion is assumed to be negligible and only molecular

diffusion is modeled. Effective diffusion coefficients measured in frozen soils decrease sharply near 0°C, and slowly decrease at lower temperatures; at a temperature of -3°C, $D_e$ in frozen soil is on the order of $10^{-11}$ $m^2$ $s^{-1}$ (Murrmann, 1973).

*3.5.4.1.2. Initial Soil Conditions*

The initial source of water in the borehole sediment must have been surface water in Taylor Valley, although it is uncertain if this sediment was deposited in lake water as a delta or in stream water (Horsman, 2007) or what the compositions of lake and stream waters were in the past. As a result, the initial conditions of the borehole are inferred based on modern surface waters and the distribution of exchangeable cations in the borehole. Below the downward advecting front of surface brine at 150 cm depth, exchangeable cations are constant from 150 to 180 cm; above 150 cm exchangeable Mg and Na increase. This suggests that exchange compositions at 150-180 cm depth represent the initial exchange composition of the borehole sediment, which has not been significantly altered by downward advecting brines. The average exchange composition of the frozen borehole at 150-180 cm depth is $CaX_2$ = 47.0 %, $MgX_2$ = 17.0 %, NaX = 19.5 %, and KX = 16.5 % (Figure 3.11). This is similar to exchange compositions predicted for ICS initially saturated with water from Lake Hoare (Table 3.7).

*3.5.4.1.3. Infiltrating Brine*

The initial composition of snowmelt water percolating into the soil will reflect ions found in surface snow, which contains salts derived primarily from aeolian dust (Lyons et al., 2003; Witherow et al., 2006) and marine aerosols (Claridge and Campbell, 1977; Keys and Williams, 1981). We approximate the composition of surface snow at the borehole site using the average composition of fresh surface snow from nearby Canada Glacier determined in Lyons et al. (2003) normalized to Cl concentrations: Ca = 0.35, Mg = 0.18, Na = 0.87, K = 0.15, Cl = 1.00, $SO_4$ = 0.08, and $NO_3$ = 0.07. The flux of salt to the soil in the transport model is based on Cl because Cl is a conservative tracer of transport in the soil. In the model, Cl is added to the soil

surface at a constant flux $J_{Cl}$ (mmol $m^{-2}$ $a^{-1}$) and all other ions are added to the soil in proportion to Cl, as in Canada Glacier snow. If all Cl in the upper 150 cm of the borehole soil is derived from downward advecting brine, $J_{Cl}$ is given by the total Cl in the upper 150 cm of soil divided by the soil age. The total Cl content in the upper 150 cm of soil is 10.25 mol Cl $m^{-2}$, calculated as in Toner et al. (2012b), and the average Cl flux to the soil is $J_{Cl}$ = 2.05 mmol Cl $m^{-2}$ $a^{-1}$ for a soil age of 5 Ka.

Salt added to the soil surface will advect downwards into the soil as brine. In the ICS, advecting brine will be in equilibrium with ice, which will determine the concentration of ions in solution and the brine volume. In the upper 30 cm of dry soil, the concentration of ions in solution will depend on the water content of the soil. As a rough approximation of unsaturated transport in the upper dry soil, we assume a constant water content distribution with depth. By modeling isotope ratios during evaporation, Hagedorn et al. (2010) suggests that if snowmelt initially saturates the upper soil layers, infiltrating water reaching the ICS surface is about 95% evaporated. Based on a soil porosity of 0.4, a value typical for sandy soils, this suggests that the pore volume of evaporated brine advecting in the upper dry soil is 0.02.

*3.5.4.1.4. Model Results*

From the above discussion, parameters for advective-dispersive-reactive transport are summarized in Table 3.9. Transport is modeled using the temperature profile in Figure 3.10 and measured CECs. Ion distributions from transport modeling closely correspond to ion distributions determined by modeling the frozen state of the borehole soil (Figure 3.13). Exchangeable Ca and Na in the transport model are inversely correlated, with Na generally increasing near the soil surface and Ca decreasing. Near the ICS boundary, there is a small increase in Ca and decrease in Na which also occurs in the frozen borehole. This feature is due to reduced freeze-concentration in the higher temperatures near the ICS boundary, which results in a more dilute soil solution favoring more Ca ion on the exchange complex. K

concentrations are generally low and show almost no variation with depth. The depth profile of Mg in the transport model is significantly different from the frozen borehole soil. In the transport model Mg decreases near the soil surface, while in the frozen borehole Mg increases near the soil surface. The transport model predicts the precipitation of gypsum near the top of the ICS with a distinct peak at 50-60 cm depth (Figure 3.14). This correlates well with a spike in precipitated gypsum in the modeled frozen state of the borehole. Gypsum is precipitated in the transport model due to freeze-concentration of $SO_4$ in the infiltrating brine as it enters the ICS, coupled with high Ca concentrations from the exchange of Na with Ca.

Table 3.9**.** Summary of reactive transport parameters and initial conditions used in PHREEQC.

| | |
|---|---|
| $D^*$ ($m^2$ $s^{-1}$) | $10^{-11}$ |
| v (m $s^{-1}$) | 9.5 x $10^{-12}$ |
| $J_{Cl}$ (mmol $m^{-2}$ $a^{-1}$) | 2.05 |
| Cell Length (cm) | 10 |
| Time (Ka) | 5 |
| Time Step (Ka) | 0.33 |
| Steps (#) | 15 |
| $H_2O$ in Dry Soil (%) | 1.3 |
| $CaX_2$ (%) | 47.0 |
| $MgX_2$ (%) | 17.0 |
| NaX (%) | 19.5 |
| KX (%) | 16.5 |

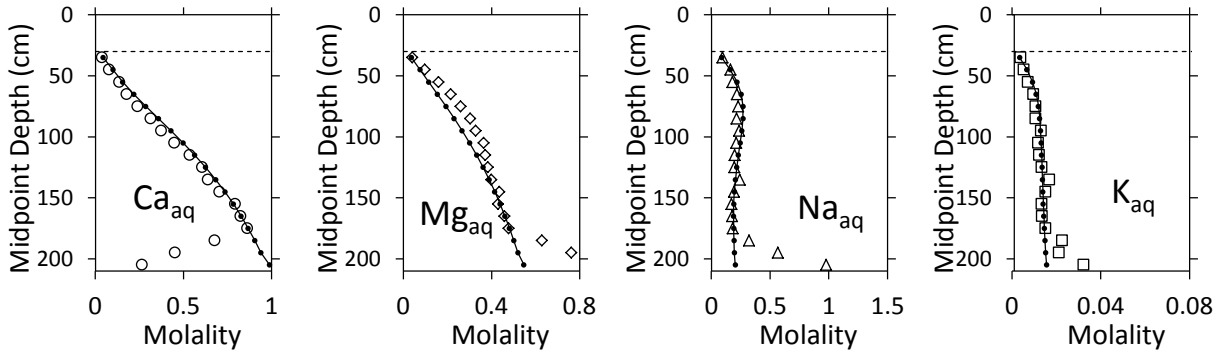

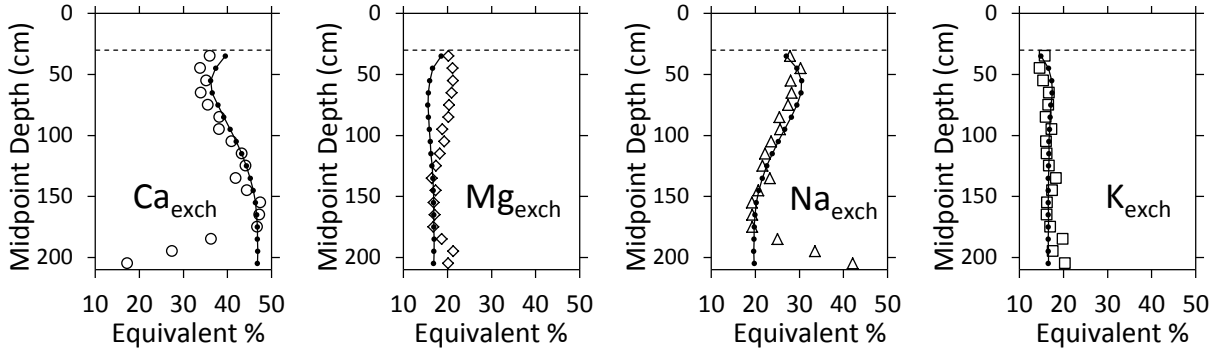


Figure 3.13. Graphs showing the distribution of aqueous (aq) and exchangeable (exch) cations predicted from the transport model compared to the modeled frozen state of the borehole. Black points connected by lines indicate values from the transport model, while white data points are values from modeling freezing of the borehole in Figure 3.11. The depth to ice-cement is indicated by the dashed line at 30 cm depth.

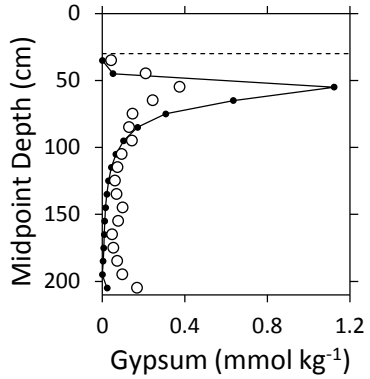


Figure 3.14. A graph showing the distribution of precipitated gypsum predicted in the transport model (black circles connected by lines) compared to the modeled frozen state of the borehole (open circles). The depth to ice-cement is indicated by the dashed line at 30 cm depth.

### *3.5.5. The Formation of Ca-Cl Enriched Groundwaters by Cation Exchange Reactions*

The Ca-Cl enrichment measured in the Taylor Valley borehole and modeled Ca-Cl enrichment in ICS suggests that cation exchange reactions will strongly influence the chemistry of groundwaters in the Dry Valleys. Ca-Cl enriched brines produced by exchange reactions will be highly mobile in soils due to their low eutectic temperature, high solubility, and high deliquescence, and will migrate downslope towards valley bottoms (Keys, 1980; Wilson, 1979). Melting of ICS enriched in Ca-Cl and lateral groundwater movement along the relatively impermeable ICS surface could explain the Ca-Cl enrichment found in shallow groundwater flows in Taylor and Wright Valleys (Cartwright and Harris, 1981; Levy et al., 2011; Webster et al., 2003; Wilson, 1979). Downslope migration and accumulation of these subsurface flows

could explain the Ca-Cl enrichment found in ponds (Cartwright and Harris, 1981; Healy et al., 2006; Lyons et al., 2011) and moist depressions (Campbell and Claridge, 1982). Ca-Cl brines advecting downwards into the ICS could also accumulate within deep groundwaters, which could explain the Ca-Cl enrichment found in upwelling deep groundwaters feeding Don Juan Pond.

To determine if cation exchange reactions are consistent with the chemistry of Ca-Cl enriched waters, we compare measured and modeled Ca/Na, Ca/Mg, and Na/K ratios in cation exchange brines with Ca-Cl enriched waters in the Dry Valleys (Table 3.10). Ca/Na ratios can be indicative of cation exchange reactions because cation exchange strongly fractionates Na and Ca ions due to ratio law effects. Ca/Na ratios will be more indicative of cation exchange reactions than Mg/Na ratios because Mg enrichment can also occur in the absence of cation exchange. Ca/Na ratios in the thawed borehole average 0.5 (ranging from 0.05 to 1.1), while Ca/Na ratios under the frozen borehole conditions modeled in Figure 3.11 average 4.6 (ranging from 0.4 to 10.1). Modeled freeze-concentration of soil-water mixtures in Table 3.7 predicts Ca/Na ratios that range from 0.81 in sediment initially saturated with Lake Fryxell surface water to ~300 in sediment initially saturated with stream waters in Hoare Basin. These Ca/Na ratios are consistent with the high Ca/Na ratios found in Ca-Cl enriched waters.

Table 3.10**.** Ion concentrations (mM) and ratios in a representative selection of Ca-Cl enriched ground and surface waters in the Dry Valleys. Ca-Cl enrichment is defined as $2Ca > HCO_3 + 2SO_4$.

| Source | Ca | Mg | Na | K | Cl | $SO_4$ | $HCO_3$ | Ca/Na | Ca/Mg | Na/K |
|---|---|---|---|---|---|---|---|---|---|---|
| Don Juan Pond Surface Water[a] | 4105 | 96 | 423 | 6 | 8836 | – | – | 9.7 | 42.8 | 70.5 |
| Don Juan Pond Groundwater[b] | 1800 | 41 | 300 | 2 | 3944 | 1 | – | 6.0 | 43.7 | 128.6 |
| Lake Vanda (66 m depth)[c] | 606 | 316 | 294 | 20 | 2137 | 8 | – | 2.1 | 1.9 | 15.0 |
| South Fork Flow, Wright Valley[d] | 453 | 288 | 430 | 16 | 1730 | 0.1 | – | 1.1 | 1.6 | 26.4 |
| VXE-6 Pond, Wright Valley[b] | 130 | 70 | 126 | 3 | 451 | 9 | – | 1.0 | 1.9 | 43.9 |
| GW5 Flow, Wright Valley[e] | 35 | 26 | 74 | 6 | 178 | 13 | 6 | 0.5 | 1.3 | 11.4 |
| Lime60 Pond, Victoria Valley[f] | 103 | 153 | 285 | 5 | 707 | 23 | 2 | 0.4 | 0.7 | 55 |
| Parera Pond West, Taylor Valley[g] | 9 | 25 | 52 | 6 | 113 | 6 | 1 | 0.2 | 0.4 | 8.4 |
| "Water Track" Flows, Taylor Valley[h] | – | – | – | – | – | – | – | 0.7 | – | 5.9 |

[a]average in Marion (1997); [b]Cartwright and Harris (1981) ; [c]Angino and Armitage (1963); [d]Wilson (1979); [e]Webster et al. (2003); [f]Healy et al. (2006); [g]Lyons et al. (2011); [h]Levy et al. (2011).

With respect to homovalent Ca-Mg or Na-K cation exchange, ratio law effects do not occur and the relative proportions of Na versus K and Ca versus Mg in soil solutions will be determined by the relative affinity of these cations for exchange sites. For cations of the same charge, the relative affinity is primarily influenced by hydration radius, with cations of smaller hydration radius being more strongly adsorbed to exchange sites (Shainberg and Kemper, 1966). Since the hydration radius of Mg and Na is greater than Ca and K respectively, exchange sites will adsorb Ca more strongly than Mg and K more strongly than Na. This indicates that aqueous Ca/Mg ratios will be lower than exchangeable Ca/Mg ratios, and that aqueous Na/K ratios will be greater than exchangeable Na/K ratios. Modeling of cation exchange reactions in freeze-concentrated soil solutions (Table 3.7) predicts aqueous Ca/Mg ratios ranging from 0.4 to 6, which is less than exchangeable Ca/Mg ratios (1.5 to 12.5). With respect to Na-K exchange, modeled aqueous Na/K ratios in Table 3.7 (2.8 to 38.5) are much greater than exchangeable Na/K ratios (0.6 to 3.4). In the modeled frozen borehole (Figure 3.11), aqueous Ca/Mg ratios range from 0.4 to 1.8 and Na/K ratios range from 8.8 to 21.8.

For most surface and groundwaters in Table 3.10, Ca/Mg and Na/K ratios are well within the range of ratios expected from cation exchange reactions. The exception is Don Juan Pond. Don Juan Pond contains a more pure Ca-Cl brine than any other ground or surface water in the Dry Valleys, with high concentrations of Ca relative to Na, K, and Mg. Ca/Mg and Na/K ratios in Don Juan Pond are much higher than ratios predicted from cation exchange reactions. High Na/K ratios could be due to non-reversible fixation of K onto exchange sites between clay interlayers (Martion and Sparks, 1985). Keys (1980) found evidence of K fixation from high Na/K ratios in Blood Falls, a saline discharge from Taylor Glacier, and in soils. Although high Na/K ratios could be due to K fixation onto clays, high Ca/Mg ratios in Don Juan Pond are difficult to explain with cation exchange because exchange reactions do not strongly fractionate Ca and Mg ions.

*3.5.5.1. The Role of Water-Rock Interactions in Don Juan Pond*

As first noted by Green and Canfield (1984), the chemistry of Don Juan Pond is similar to highly saline Ca-Cl enriched brines found deep in crystalline basement rocks (e.g. Fritz and Frape, 1982; Herut et al., 1990; Nordstrom et al., 1989). These deep brines commonly have high Ca/Mg ratios that can be on the order of 1000 (Bottomley et al., 1999; Fritz and Frape, 1982; Nordstrom et al., 1989) and high Na/K ratios (Bottomley and Clark, 2004). Low Mg concentrations in these brines have been attributed to the removal of Mg by water-rock interactions, including dolomitization of calcite (Bottomley et al., 2005; Bottomley et al., 1999) and the formation of Mg-silicates such as chlorite, Mg-smectite, or sepiolite (Frape and Fritz, 1984; Herut et al., 1990). Mg-K depletion and Ca enrichment due to water-rock interaction is known to occur in hydrothermal vents (Hardie, 1983, 1990) and seafloor basalts (Larwrence et al., 1975), and has been demonstrated in experiments with basalt and seawater at 70-150 °C (Seyfried and Bischoff, 1979). In Don Juan Pond, high ratios of F/Cl (Webster and Goguel, 1988), Li/Na (Lyons and Welch 1997), $^{36}Cl/Cl$ (Carlson et al., 1990), and $^{87}Sr/^{86}Sr$ (Jones and Faure, 1978) have been attributed to the influence of water-rock interaction. This suggests the possibility that water-rock interactions could explain the Ca enriched and Mg-K depleted chemistry of Don Juan Pond. However, as pointed out by Lyons and Mayewski (1993), although water-rock interactions can produce brines depleted in Mg, K, and Na, the resulting brines have much lower Ca/Na ratios than are found in Don Juan Pond.

Water-rock interactions can explain the high Ca/Mg ratios in Don Juan Pond, but cannot account for the high Ca/Na ratios. On the other hand, cation exchange can explain the high Ca/Na ratios in Don Juan Pond, but cannot account for the high Ca/Mg ratios. This suggests that the brine in Don Juan Pond is the result of both cation exchange and water-rock interaction. We speculate that Ca-Mg-Cl brine derived from cation exchange reactions could have been modified to Ca-Cl brine by Mg removal during water-rock interaction.

Freeze concentrated brines in the Dry Valleys are thought to be highly reactive and corrosive (Dickinson and Rosen, 2003; Ugolini and Jackson, 1982), resulting in mineral alteration and authigenic mineral formation despite the freezing temperatures (Dickinson and Bleakley, 2005; Dickinson and Rosen, 2003; Gibson et al., 1983). This suggests the possibility that Mg could be depleted in soil solutions by low-temperature water-rock interactions; however, little is known about how water-rock interactions influence the soluble chemistry in frozen soils. To determine if water-rock interactions can remove Mg from soil solutions at low-temperatures, we consider the chemistry of Beacon ground ice (Table 3.11), a remnant of Taylor Glacier thought to be at least 100 Ka old (Ng et al., 2005a; Sugden et al., 2002b). Sediment in Beacon ground ice contains clasts of Ferrar Dolerite, Beacon Sandstone, and possibly granites (Marchant et al., 2002), which is lithologically similar to sediments and bedrock near Don Juan Pond (Harris and Cartwright, 1981). The ice content of the frozen sediment is high, averaging about 95% by weight. This suggests that Beacon ice has remained a largely closed chemical system since it was deposited. Hence, old Beacon ground ice represents a unique opportunity to determine the influence of water-rock interaction in frozen sediments over long timescales.

A total of 29 samples were collected from the Beacon ground ice by coring down to a depth of 19 m and sampling laterally across the ice surface. Melt water was extracted from these samples and analyzed using the methods described in this paper. To determine if cation compositions in the ice have been altered by water-rock interaction, we examine cation concentrations relative to the conservative ion Cl. The chemistry of Beacon ice is uniform for all samples and is characterized by high proportions of Ca, Na, $SO_4$, and $HCO_3$ and low proportions of Mg and K (Table 3.11). Ca/Cl, Na/Cl, $SO_4$/Cl, and $HCO_3$/Cl ratios in the Beacon ice are similar to ratios in nearby glacial ice and snow. In contrast, Mg/Cl and K/Cl ratios in Beacon ice are much lower than ratios in nearby glacial ice and snow, but are similar to ratios in Don Juan Pond. The Beacon ice is not enriched in Ca-Cl since $2Ca < HCO_3 + 2SO_4$.

The pronounced depletion in Mg and K in the Beacon ground ice relative to nearby snow and ice suggests that soluble Mg and K have been quantitatively removed by water-rock interaction. In addition, the absence of Ca-Cl enrichment in the Beacon ground ice suggests that low-temperature water-rock interaction does not produce Ca-Cl enrichment. K depletion in the ground ice could be caused by non-reversible K fixation onto clays. Mg may have been removed by formation of Mg-silicates since weathering in Dry Valley soils is known to form Mg-silicates (Claridge, 1965b; Claridge and Campbell, 1984; Ugolini and Jackson, 1982).

Table 3.11**.** The chemistry of snow and ice in Beacon Valley and Don Juan Pond groundwater in Wright Valley, where n is the number of samples collected.

| Source | n | Ca/Cl | K/Cl | Mg/Cl | Na/Cl | $SO_4$/Cl | $HCO_3$/Cl |
|---|---|---|---|---|---|---|---|
| Taylor Glacier[a] | 2 | 0.371 | 0.117 | 0.163 | 1.022 | 0.129 | 0.949 |
| Mullins Glacier[a] | 1 | 0.593 | 0.117 | 0.332 | 1.482 | 0.204 | 2.043 |
| Fresh Snow[a] | 1 | 0.295 | 0.053 | 0.126 | 0.713 | 0.136 | 0.336 |
| Beacon Ground Ice[a] | 29 | 0.349 | 0.009 | 0.006 | 1.170 | 0.162 | 0.565 |
| Don Juan Pond Groundwater[b] | 2 | 0.456 | 0.001 | 0.010 | 0.076 | 0.000 | 0.010 |

[a]Data from Beacon Valley.
[b]Harris and Cartwright (1981).

### *3.5.5.2. Estimating the Flux of $CaCl_2$ to Don Juan Pond*

Cation exchange reactions can potentially explain the distinct Ca-Cl enrichment found in many Dry Valley waters, including Don Juan Pond. To determine if cation exchange is consistent with the large quantity of Ca-Cl enriched brine found in groundwaters beneath Don Juan Pond (Torii et al., 1977) we estimate the potential contribution of $CaCl_2$ derived from exchange reactions to Don Juan Pond basin as follows. The volume of sediment beneath Don Juan Pond basin is about $3.1 \times 10^6$ $m^3$, based on an average sediment depth to bedrock of 13 m (Harris and Cartwright, 1981) and a surface area of $2.4 \times 10^5$ $m^2$ (determined with ArcGIS). Assuming that this sediment is saturated with groundwater and a sediment porosity of 0.4, the volume of groundwater beneath Don Juan Pond is estimated to be $1.2 \times 10^9$ L. Based on the concentration of Ca measured in groundwater beneath Don Juan Pond (1.8 M) (Harris and Cartwright, 1981), Don Juan Pond basin is estimated to contain $2.2 \times 10^9$ mol $CaCl_2$.

We estimate the potential contribution of $CaCl_2$ from cation exchange to the subsurface as follows for a soil column of one meter depth, bulk density of 1550 kg $m^{-3}$, CEC of 40 meq $kg^{-1}$, and initial exchange composition 50% saturated with Ca (0.01 mol $Ca_{exch}$ $kg^{-1}$). If downward advecting NaCl completely displaces exchangeable Ca, the amount of $CaCl_2$ that could be produced by cation exchange per $m^{-2}$ of soil surface area is given by: (1550 kg $m^{-3}$) x (1 m) x (0.01 mol $Ca_{exch}$ $kg^{-1}$) = 15.5 mol $CaCl_2$ $m^{-2}$. For a drainage area to Don Juan Pond of 1.08 x $10^8$ $m^2$ (determined with ArcGIS using a 30 m Digital Elevation Model) an estimated 1.7 x $10^9$ mol $CaCl_2$ could be produced by exchange reactions from one meter of sediment. This quantity of $CaCl_2$ is close to the total estimated $CaCl_2$ in groundwaters beneath Don Juan Pond (2.2 x $10^9$ mol $CaCl_2$) and suggests that exchange reactions could account for the magnitude of Ca-Cl enrichment found in Don Juan Pond and other Dry Valley groundwaters.

*3.6. Conclusions*

The abundance of Ca-Cl enriched brines throughout the Dry Valleys of Antarctica is distinct from global surface water compositions. We suggest that this Ca-Cl enrichment is caused by cation exchange reactions in frozen soils. To explore the implications of exchange reactions for Dry Valley soils, we measured the exchange properties of Taylor Valley soils over a range of solution concentrations from ~0.1 mM to 4.75 M and developed a model for brine transport in frozen soil. Cation exchange experiments indicate that Rothmund-Kornfeld equation models cation exchange behavior well and that heterovalent exchange is strongly influenced by solution concentration. Reactive transport modeling using the geochemical programs PHREEQC and FREZCHEM shows that by freezing soils, a strong Ca-Cl enrichment of the soil solution is caused by the exchange of aqueous Na with exchangeable Ca. Furthermore, advection of Na-Cl rich brines into frozen soil displaces adsorbed Ca, enriching the soil solution in Ca-Cl. The strong adsorption of Na relative to Ca measured and modeled in frozen soils is caused by the highly concentrated nature of brine in frozen soil. This high concentration environment

results in a ‘ratio law’ effect that enriches the soil solution in divalent ions (Ca and Mg) relative to monovalent ions (K and Na).

Ca-Cl enrichment by cation exchange can account for variations in the Ca, Mg, Na, and K composition of Ca-Cl enriched waters in the Dry Valleys, although additional water-rock interaction is necessary to explain the low Mg concentration in Don Juan Pond. Cation exchange is also consistent with estimated amounts of $CaCl_2$ in groundwaters beneath Don Juan Pond. The occurrence of Ca-Cl enrichment by cation exchange under freezing conditions suggests that cation exchange may be important for the Ca-Cl enriched brines that have been found in other permafrost areas (Shouakar-Stash et al., 2007; Stotler et al., 2009) and regions that have been historically glaciated (Katz et al., 2011; Starinsky and Katz, 2003). Ca-Cl enriched brines that are thought to exist in the Martian subsurface could also be formed by cation exchange reactions.

# Chapter 4 Luminescence Ages of Fluvial Terraces in Taylor Valley, Antarctica

## *4.1. Abstract*

Alluvial terrace deposits are found throughout Taylor Valley up to 350 m elevation and are important for understanding the glaciolacustrine history of this region. We used single-grain luminescence dating of quartz (OSL) and feldspar (IRSL) to date terraces in eastern Taylor Valley. Luminescence ages range from 4 to 10 Ka and indicate that terraces were deposited during warm climate conditions following deglaciation, but not during periods of late-Holocene cooling. We suggest that warmer deglacial conditions favored the deposition of terraces due to greater melt water production from alpine glaciers, stream flows, and sedimentation rates; in contrast, terraces were not deposited during colder climate conditions due to low melt water production, stream flows, and sedimentation rates. Luminescence dates are 5 to 12 Ka younger than previously determined $^{14}C$ ages of algal deposits from the same terraces. Based on differences in age, sample texture, position within terraces, and presence of algal material between luminescence and $^{14}C$ samples, we suggest that $^{14}C$ samples were sampled directly from older glaciolacustrine sediments underlying or adjacent to younger, terrace sediments. We interpret the $^{14}C$ ages as dating the retreat of the Ross Sea Ice Sheet from Taylor Valley, which is correlated with temperature increases after the Last Glacial Maximum as recorded in Taylor Dome ice core data. In contrast, luminescence ages date the deposition age of terraces during warm climate conditions that followed deglaciation.

*4.2. Introduction*

During the Last Glacial Maximum (LGM), an ice sheet, known as the Ross Sea Ice Sheet (RSIS), expanded across McMurdo Sound and entered Taylor Valley, Antarctica (Denton et al., 1970; Hall et al., 2000; Stuiver et al., 1981). Behind the RSIS, it is thought that Taylor Valley filled with proglacial paleolakes (Denton et al., 1970; Hall et al., 2000; Péwé, 1960; Stuiver et al., 1981; Toner et al., 2012) fed by melt water from the RSIS (Hall et al., 2010). The timing of these paleolakes and the RSIS retreat from Taylor Valley has largely been inferred from about 200 perched terraces, ranging in elevation from sea level to 350 m elevation. These terraces have been interpreted as remnants of deltas deposited by melt water streams flowing into proglacial paleolake waters (Hall et al., 2000; Péwé, 1960; Stuiver et al., 1981). $^{14}$C dates of algal layers buried within the terraces are thought to record the age of paleolake levels in Taylor Valley, with $^{14}$C ages ranging from 5 to 25 $^{14}$C Ka (Hall and Denton, 2000; Stuiver et al., 1981). The paleolake fluctuations implied by these ages have implications for the timing of climate changes in the Southern Hemisphere (Hall et al., 2010) and the deglaciation history of the RSIS from Taylor Valley (Hall et al., 2000; Stuiver et al., 1981).

In periglacial environments, such as Taylor Valley, $^{14}$C dating can be problematic because datable material in periglacial sediments is often low and cold-dry conditions preserve relict organic carbon (Bateman, 2008; Thrasher et al., 2009). Another pervasive complication to $^{14}$C dating in the Dry Valleys is the preservation of relict inorganic carbon in stagnant lakes and glacial ice, known as the radiocarbon reservoir effect (Doran et al., 1999). Algae growing within lakes or near ice margins can take up relict inorganic carbon, resulting in inherited $^{14}$C ages on the order of 1-10 $^{14}$C Ka (Doran et al., 1999; Hall and Henderson, 2001; Hendy and Hall, 2006; Takahashi et al., 1999). The potentially large and variable nature of radiocarbon reservoir effects have made it difficult to obtain $^{14}$C chronologies from Dry Valley lake sediments (Doran et al., 1999; Wagner et al., 2006; Wagner et al., 2011; Whittaker et al., 2008).

To address the potential for inherited age components in $^{14}C$ dating of terraces, Stuiver et al. (1981) postulated that deltas prograding into paleolakes would have buried algae growing *in situ* within lake moats. Since near-shore lake water is well equilibrated with atmospheric $CO_2$, algae growing within lake moats would presumably not have been affected by radiocarbon reservoir effects. This interpretation is based on present-day observations of algal mats in lake moats and stream environments (McKnight et al., 1998; Wharton et al., 1983) and is supported by the generally modern $^{14}C$ age of dissolved inorganic carbon and algae in proglacial streams and lake moats (Doran et al., 1999; Hendy and Hall, 2006). However, recent work with Ground Penetrating Radar (GPR) on terraces in eastern Taylor Valley shows that, although the surficial expressions of these features appear deltaic, the internal architecture of most terraces is not characteristic of deltas (Arcone et al., 2008; Horsman, 2007). If terraces in Taylor Valley are not deltas, then $^{14}C$ ages of these sediments may not be immune to radiocarbon reservoir effects or recycling of relict algae.

Our purpose here is to determine the age of terraces using single-grain Optically Stimulated Luminescence (OSL) and Infrared Stimulated Luminescence (IRSL) dating. Berger and Doran (2001) and Berger et al. (2010) have demonstrated that both OSL and IRSL dating can successfully date lake bottom sediments in Lake Hoare, Taylor Valley, that are influenced by large radiocarbon reservoir effects. We use single-grain luminescence dating because single-grain age distributions can be used to detect and control for incomplete resetting of the luminescence signal known as ‘partial bleaching’ (Duller, 2004, 2006, 2008; Olley et al., 1999), which is common in periglacial sediments (Bateman, 2008; Fuchs and Owen, 2008; Thrasher et al., 2009). Quartz is the ideal mineral for luminescence dating because OSL dating has been verified with independent dating methods (Murray and Olley, 2002; Wallinga, 2002), the quartz signal is stable over time (Aitken, 1998), and the quartz signal is reset within seconds after exposure to sunlight (Godfrey-Smith et al., 1988). However, in Dry Valley sediments, quartz

sensitivity is low, making quartz difficult to work with (Berger et al., 2010; Bristow et al., 2010). Feldspar luminescence signals are much brighter than quartz (Krbetschek et al., 1997) and the sensitivity of feldspar grains in Antarctic sediments to IR stimulation is high (Berger and Doran, 2001; Krause et al., 1997).

## *4.3. Methods*

### *4.3.1. Study sites*

Samples for luminescence dating were collected from terraces in eastern Taylor Valley, primarily along Delta and Crescent Streams in Fryxell Basin and terraces near the valley mouth (Figure 4.1). Although terraces are also found in western Taylor Valley, no samples were collected from this region. Pits were excavated on level surfaces at the apex of terraces several meters from the sloping terrace front. Samples were collected from the center of polygonal pattered ground cryoturbation features, to ensure that samples had not been disturbed since deposition. Ten terraces sampled in this study are from terraces that have also been $^{14}C$ dated (S027, S032, S033, S034, S041, S048, S049, S051, S066, and G121-006). Three terraces in this study (S061, S062, and S071) have not been previously $^{14}C$ dated. Corresponding $^{14}C$ dates of terraces are determined using the map of terraces in eastern Taylor Valley provided in Hall and Denton (2000). For samples S032, S034, and S041, it is uncertain if $^{14}C$ samples are from the same terrace as luminescence samples since it is difficult to distinguish individual terrace features using the map in Hall and Denton (2000) and latitude-longitude coordinates are not provided. The remaining luminescence samples were collected from distinct, isolated terraces and could be correlated with $^{14}C$ samples from the same feature.

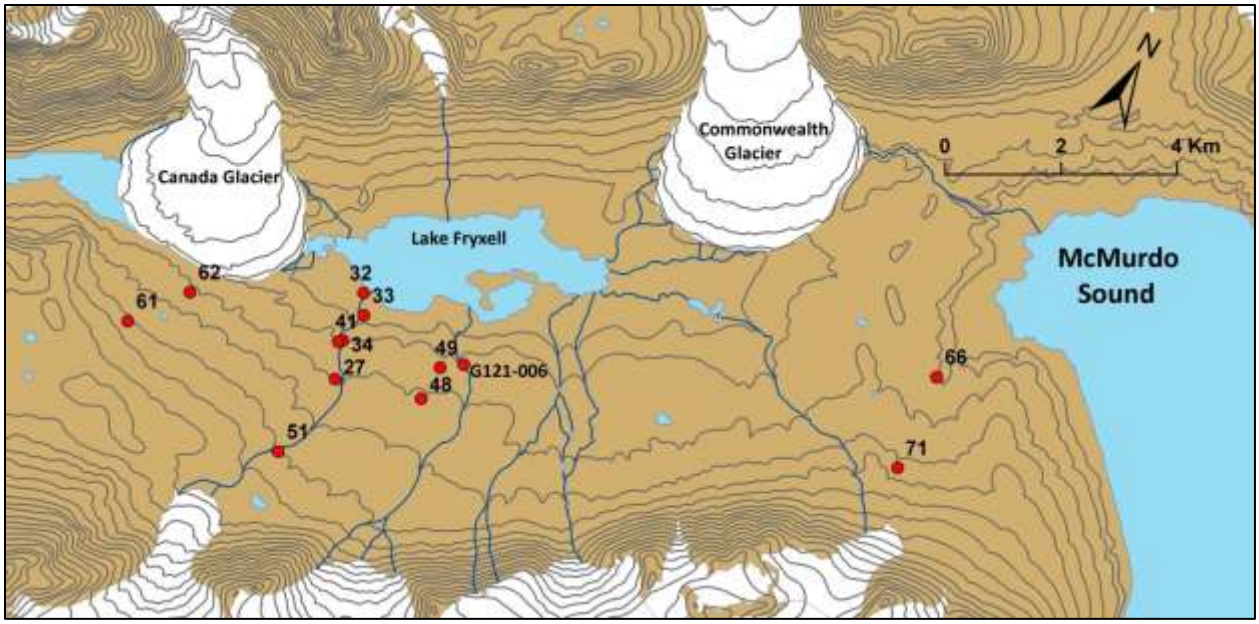


Figure 4.1. The location of the 13 luminescence samples collected in eastern Taylor Valley. The contour interval is 50 m.

*4.3.2. Sample Collection and Preparation*

Luminescence samples were collected by driving light-tight tubes of ABS piping into sediments. Tubes of ABS piping 5 cm in diameter and 25 cm long were prepared before entering the field by sharpening one end of the tube and placing a plastic sliding plug near the sharpened end. To sample a soil, the pit was excavated and a cross section of the soil was exposed. After scraping off surface sediment, the ABS tube was pressed horizontally into the soil, keeping the same soil depth, until the tube was filled with sediment and the plastic plug had slid to the other end of the tube. The entire tube was then excavated from the soil and the sharpened end was capped with a PVC test cap so that the soil in the tube was tightly compacted. These ends were further sealed with duct tape to ensure that sediment was not exposed to light. Sample G121-006 was sampled by drilling a 10 cm diameter core to a depth of 20 cm into the ice-cemented soil. This core sample was kept frozen below -20°C before further preparation.

In the lab, sediment from each sampling tube was extracted under red light (Berger and Kratt, 2008). About 5 cm of sediment near the ends of each tube was extracted and used for radiation

measurements. The remaining sediment was saved for luminescence analysis. For the G121-006 core sample, the sides of the core were removed and used for dose rate analysis, while the central, unexposed portion of the core was used for luminescence analysis.

Sediment for the luminescence analysis was treated with HCl to remove carbonates, with $H_2O_2$ to remove organic material, and then sieved to obtain various size fractions. Quartz and feldspar fractions were separated using sodium polytungstate solutions at a specific gravity of 2.67 g $cm^{-3}$ for quartz separation and 2.58 g $cm^{-3}$ for feldspar separation, saving the light fractions. The quartz fraction was etched in HF for 50 min at 48% concentration to remove the outer surface of the quartz grains and to dissolve feldspars. Several quartz samples required several HF etches to completely remove feldspar contamination. Feldspar grains between 200-250 µm were saved for analysis, while for quartz several size fractions were used: S027 (90-150 µm), S032 (150 µm), S033 (150-225 µm), S066 (90-150 µm), and G121-006 (150-225 µm). The 200-250 µm grain size used in the feldspar analysis give single-grain resolution since the diameter of holes in single grain discs is 300 µm. Smaller size fractions were used in the quartz analysis so that several grains would fit into single grain disc holes. This effectively gave single-grain resolution because the sensitivity of the quartz was low.

The moisture content of the soil profile is important, since water absorbs radiation at a different rate than in dry soil, reducing the dose rate to the sample. Moisture samples were collected at various depths in the soil, including the ice-cemented soil, and placed in sealed moisture tins. The moisture content was determined in McMurdo Station by weight loss after oven drying. The particle size distribution of some soil samples was measured by a laser diffraction particle size analyzer (Beckman-Coulter LS 13-320) under sonication in a solution of 10% sodium hexametaphosphate.

*4.3.3. Luminescence Analysis*

Feldspar and quartz grains were analyzed using a single-grain aliquot (SAR) protocol (Murray and Wintle, 2000; Wallinga et al., 2000). In addition, the 150 μm quartz fraction in samples S032 and S033 was analyzed in multi-grain aliquots by adhering grains to stainless steel discs with silicon oil at diameters of 7 and 4 mm respectively. Feldspar IRSL was analyzed at the University of Washington, while quartz OSL was analyzed at the Desert Research Institute by Dr. Glenn Berger. Parameters for these measurements are given in Table 4.1. A relatively large machine error (12%) is used for quartz to account for the possibility of variable irradiation from the beta source and other intrinsic errors in quartz dating, as suggested by Thompsen et al. (2007). To test for the presence of feldspar contamination in the quartz, samples were given IR stimulation at the end of the measurement sequence as described in Berger et al. (2010). For feldspar, a small machine error is used (2%) and additional errors in the IRSL analysis are determined directly from dose recovery tests.

In the dose recovery test, the natural signal is first removed by light stimulation and then all grains are given a constant laboratory dose. These grains are then analyzed with the SAR method to test if the measured equivalent dose, $D_e$, is the same as the given laboratory dose. This procedure simulates the natural resetting of the luminescence signal by exposure to light and tests the ability of the luminescence dating method to reproduce a known laboratory dose (Wintle and Murray, 2006). In addition, the scatter in the dose recovery test can be used to determine the intrinsic error in the luminescence measurements (e.g. Thompsen et al., 2007).

The feldspar IRSL signal is subject to fading over time (Spooner, 1994; Wintle, 1973), resulting in significant age underestimates if fading is not accounted for (Balescu et al., 2003; Huntley and Lamothe, 2001; Lamothe and Auclair, 1999; Wallinga et al., 2001). The effect of fading on the IRSL age is corrected following Huntley and Lamothe (2001) by measuring fading rates on single-grain aliquots using the procedures of Auclair et al. (2003). Huntley and Lamothe (2001) found that by measuring the rate of fading and correcting for the signal loss, IRSL ages are well

correlated with independent dating methods for samples younger than 20 Ka old. Fading was measured for up to two to six days of storage following irradiation and are expressed as g-values, which is the percent loss per decade, where a decade is a power of ten and the values are normalized to two days.

The environmental dose rate is the sum of external radiation sources (cosmic radiation and radiation from surrounding sediments) and, in feldspars, internal radiation from potassium. Radiation in the sediment was determined by thick source alpha counting, using the pairs technique for $^{238}U$ and $^{232}Th$ concentrations and flame photometry for K concentrations. $^{238}U$, $^{232}Th$, and K concentrations were converted to dose rates following Adamiec and Aitken (1998). $\%K_2O$ of individual feldspar grains was determined for several samples using a JEOL Model 733 Electron Microprobe. The internal dose rate from potassium in K-feldspar was calculated using the $\%K_2O$ content of feldspar grains as in Mejdahl (1983). The effect of ice-cemented soil at depth on dose rates is corrected for using the tables in Aitken (1985), Appendix H. Given the prevailing cold-dry conditions in the Dry Valleys, we assume that water contents in soil have remained constant over time.

Table 4.1. Summary of luminescence measurement parameters used in this study.

| Parameter | IRSL Analysis | OSL Analysis |
|---|---|---|
| System | Risø TL-DA-20 | Risø TL-DA-20 |
| Excitation | 830 nm IR laser 90% power | 532 nm laser 90% power |
| Emission | 7 mm blue-filter pack (350-450 nm) | 7 mm U340 |
| Preheat | 250°C, 60 s | 220-240°C, 10 s |
| Optical Stimulation | 50°C, 60 s | 50°C, 3 s (125°C, 1 s for S027) |
| Signal | first 0.06 s | first .068 s |
| Background | 0.65-0.8 s | 0.068-0.255 s |
| Test Dose | 6 Gy | 20 Gy (31 Gy for G121-006) |
| Test Dose Preheat | 250°C, 60 s | 180-200°C |
| Machine Error | 2% | 12% |

*4.4. Terrace Characteristics*

Terraces sampled in this study are flat-topped deposits capped with a desert pavement surface of gravel about 1 to 3 cm thick (Figure 4.3). Larger cobbles and boulders were absent from the majority of terrace surfaces, but were abundant on nearby glacial sediments. The desert

pavement overlies and protects about 30 cm of dry, loosely consolidated sand with some gravel clasts. All luminescence samples, with the exception of G121-006, were sampled from this dry soil at about 15 cm depth. The analysis of grain-size distributions in the <2 mm fraction of luminescence samples indicates that the <2 mm fraction is composed of medium to coarse-grained sand with low silt and clay components (Figure 4.2, Table 4.2). Grain size distribution curves follow either a normal distribution with a peak near 400 µm or a bimodal distribution with peaks near 400 µm and 1000 µm. At a depth of about 30 cm, dry soil abruptly transitions into hard ice-cemented soil with an average gravimetric water content of 12%.

All terraces in this study exhibit either cross-bedding or dipping beds. Both S033 and S041 had dipping beds inclined at 20° facing downstream, while S034 had dipping beds inclined at 30° facing downstream. S051 also had dipping beds facing downstream, as shown in Figure 4.3, but these beds became horizontal after about 50 cm. The fluvial stratification was undisturbed in all soil pits, indicating that these soils were not affected by cryoturbation from nearby sand wedges. No algal flakes or layers were seen in any of the terraces sampled in this study.

Table 4.2. The location, sample depth (cm), gravimetric water content in the ice-cemented soil (ICS), and texture characterization for terraces.

| Sample | Latitude | Longitude | Elevation M | Depth cm | ICS $H_2O$ % | $D_{50}$ mm | Clay % | Silt % | Sand % | < 2mm % |
|---|---|---|---|---|---|---|---|---|---|---|
| S027 | -77.63657 | 163.12134 | 121 | 18 | 16.6 | 0.520 | 0.9 | 2.0 | 97.1 | 87 |
| S032 | -77.62285 | 163.10808 | 20 | 14 | 6.6 | 0.436 | 0.7 | 1.5 | 97.8 | 75 |
| S033 | -77.62582 | 163.11623 | 36 | 16 | 7.9 | 0.553 | 0.4 | 0.7 | 98.9 | 86 |
| S034 | -77.63083 | 163.11212 | 67 | 12 | 14.1 | 0.446 | 0.5 | 0.8 | 98.7 | 93 |
| S041 | -77.63131 | 163.10977 | 67 | 20 | 12.9 | 0.506 | 0.9 | 1.6 | 97.6 | 81 |
| S048 | -77.63248 | 163.18210 | 121 | 14 | 14.6 | 0.392 | 0.7 | 1.7 | 97.7 | 88 |
| S049 | -77.62691 | 163.18273 | 82 | 17.5 | 18.8 | 0.451 | 1.4 | 2.4 | 96.2 | 89 |
| S051 | -77.65063 | 163.11203 | 218 | 13 | – | 0.935 | 0.3 | 0.7 | 99.0 | 60 |
| S061 | -77.64486 | 162.97084 | 215 | 10 | – | – | – | – | – | – |
| S062 | -77.63620 | 162.99936 | 115 | 14 | 9.6 | 0.442 | 1.2 | 1.4 | 97.4 | 85 |
| S066 | -77.58944 | 163.49459 | 70 | 12.5 | 14.3 | 0.398 | 0.5 | 0.9 | 98.6 | 96 |
| S071 | -77.60458 | 163.50340 | 194 | 13 | 13.5 | 0.508 | 0.5 | 0.9 | 98.6 | 81 |
| G121-006 | -77.62464 | 163.19630 | 81 | 40 | 10.1 | – | – | – | – | – |

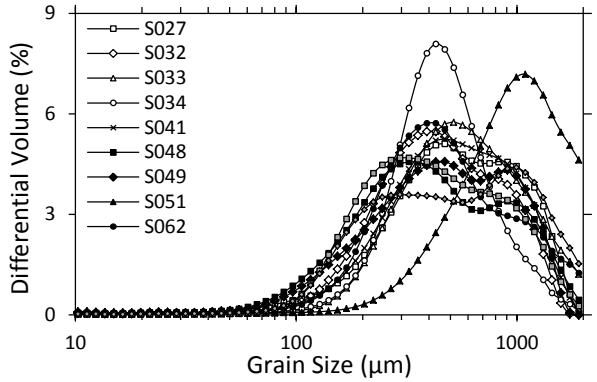


Figure 4.2. Grain size distributions in luminescence samples.


Figure 4.3. Soil profiles in terraces sampled for luminescence dating. All soils are composed of medium to coarse-grained sand and have either cross-bedded or foreset fluvial stratification.

*4.5. Dose Recovery Tests*

Dose recovery tests are analyzed using the dose recovery ratio ($D_e$ / laboratory dose), which will equal one if the equivalent dose is equal to the laboratory dose (Table 4.3). For feldspars, the weighted average of dose recovery ratios, calculated using the Central Age Model (CAM) of Galbraith et al. (1999), is close to unity (1.01±0.01) for all grains tested. The over dispersion ranges from 9.8 to 21.7% in individual samples and has a weighted mean of 20.3±0.5% for all samples. These results indicate that the SAR IRSL measurement parameters used in this study

are appropriate, but that there is significant scatter in the IRSL signal. To account for the error caused by this scatter, the over dispersion measured in dose recovery tests is added to the single-grain error in quadrature.

Few single-grain quartz signals were measured during dose recovery tests because the quartz luminescence sensitivity was low. Dose recovery tests were not obtained for S032 and G121-006 due to limited amounts of sample and the low quartz sensitivity. To obtain a statistically significant dose recovery result, all quartz dose recovery tests are combined, for a total of 30 data points. The weighted mean of the quartz dose recovery ratios is 1.11±0.08 with an over dispersion of 25.2±7.6%. The sample size in quartz dose recovery tests were so low that removing several outlying dose recovery ratio causes the over dispersion to become zero. As a result, over dispersion in quartz is assumed to be minimal.

Table 4.3. Feldspar dose recovery test results using the dose recovery ratio ($D_e$ / dose), where a perfect dose recovery result gives a dose recovery ratio of 1. Dose recovery results are given as the weighted mean, using the CAM. Error is ± 1 σ.

| | Sample | n | Weighted Mean | Over Dispersion (%) |
|---|---|---|---|---|
| Feldspar | S027 | 95 | 1.06±0.02 | 19.4±1.6 |
| | S032 | 66 | 0.88±0.02 | 15.0±1.6 |
| | S033 | 58 | 0.94±0.02 | 13.8±1.7 |
| | S034 | 61 | 1.02±0.02 | 15.6±1.9 |
| | S041 | 39 | 1.08±0.02 | 9.8±1.8 |
| | S048 | 109 | 1.16±0.02 | 20.7±1.6 |
| | S049 | 64 | 1.08±0.03 | 19.2±2.0 |
| | S051 | 64 | 0.92±0.03 | 21.7±2.1 |
| | S061 | 97 | 0.98±0.02 | 20.7±1.7 |
| | S062 | 108 | 0.98±0.02 | 21.7±1.7 |
| | S066 | 87 | 0.95±0.02 | 16.0±1.5 |
| | S071 | 76 | 1.09±0.02 | 16.1±1.7 |
| | G121-006 | 63 | 0.93±0.02 | 19.3±2.0 |
| | All | 887 | 1.01±0.01 | 20.3±0.5 |
| Quartz | S027 | 13 | 0.96±0.08 | 0±0 |
| | S033 | 6 | 1.13±0.18 | 31.8±14.0 |
| | S066 | 11 | 1.32±0.17 | 26.8±14.2 |
| | All | 30 | 1.11±0.08 | 25.2±7.6 |

*4.6. Luminescence Ages*

Results from OSL, IRSL, and previously published $^{14}C$ dates of terraces are presented in Table 4.5. Luminescence ages are determined by: 1) calculating the age of each aliquot by dividing the measured equivalent dose ($D_e$) by the environmental dose rate, 2) correcting for fading in

feldspars, and 3) analyzing the distribution of ages using an appropriate age model. The environmental dose rate in feldspars averages 3.09 Gy $Ka^{-1}$ and is significantly higher than the average dose rate in quartz, 2.52 Gy $Ka^{-1}$, due to the contribution of internal potassium to the total radiation dose in feldspars. Microprobe analysis of individual feldspar grains indicates that most feldspar grains have between 13 to 16 $\%K_2O$, but that a significant proportion of feldspar has lower $\%K_2O$ contents. It was observed that the lower $\%K_2O$ values are caused by striations or inclusions of plagioclase feldspar within grains of K-feldspar. To calculate the internal dose rate in feldspars, the average $\%K_2O$ value of 11.6±5.1 % is used. Fading rates determined for feldspar samples are closely grouped near 6-7 % $decade^{-1}$, which is similar to average fading rates determined by Huntley and Lamothe (2001).

Table 4.4. Measurements of $\%K_2O$, $^{238}U$, and $^{232}Th$ in sediments. The dose rate is the sum of internal and external radiation sources to mineral grains, and is assumed to be constant over time.

| Sample | $\%K_2O$ | $^{238}U$ (ppm) | $^{232}Th$ (ppm) | Dose Rate (Gy $Ka^{-1}$) | |
|---|---|---|---|---|---|
| | Flame Photometry | Alpha Counting | Alpha Counting | Feldspar | Quartz |
| S027 | 1.43±0.23 | 1.32±0.11 | 4.67±0.85 | 2.59±0.33 | 2.06±0.17 |
| S032 | 2.19±0.22 | 1.01±0.10 | 4.92±0.79 | 3.12±0.30 | – |
| S033 | 2.14±0.22 | 0.66±0.10 | 6.22±0.91 | 3.09±0.31 | 2.56±0.16 |
| S034 | 1.95±0.04 | 0.83±0.11 | 6.71±1.65 | 3.00±0.26 | – |
| S041 | 1.80±0.08 | 0.92±0.11 | 7.06±0.98 | 2.97±0.26 | – |
| S048 | 2.30±0.08 | 1.02±0.11 | 5.83±0.85 | 3.24±0.26 | – |
| S049 | 1.99±0.07 | 1.38±0.11 | 3.52±0.74 | 2.94±0.25 | – |
| S051 | 2.45±0.09 | 1.00±0.11 | 6.07±0.88 | 3.39±0.26 | – |
| S061 | 1.52±0.07 | 1.12±0.12 | 6.78±1.03 | 2.74±0.26 | – |
| S062 | 2.33±0.08 | 1.53±0.12 | 4.31±0.82 | 3.30±0.26 | – |
| S066 | 1.96±0.08 | 1.71±0.13 | 6.21±0.92 | 3.38±0.28 | 2.85±0.13 |
| S071 | 2.05±0.15 | 1.84±0.15 | 7.01±1.07 | 3.37±0.28 | – |
| G121-006 | 2.33±0.08 | 1.18±0.11 | 4.84±0.87 | 3.04±0.28 | 2.51±0.13 |

### *4.6.1. Single-Grain OSL and IRSL Ages*

To determine the luminescence age of a sample, the distribution of single-grain ages must be analyzed using an appropriate age model. A number of different age models have been developed for analyzing age distributions (e.g. Galbraith et al., 1999; Lepper et al., 2000; Olley et al., 1998) and the choice of one age model over another can have a large influence on the final luminescence age (Bailey and Arnold, 2006). Age distributions in fluvial sediments are commonly affected by incomplete resetting of the luminescence signal prior to deposition, an effect known as partial bleaching (Rittenour, 2008). Partially bleached grains will have an

inherited age component and are mixed with younger age signals that were completely reset prior to deposition. These younger age signals represent the true age of the sediment. Terrace single-grain age distributions are consistent with the presence of partial bleaching because there is significant over dispersion in excess of over dispersion measured in dose recovery tests (Olley et al., 2004) and the age distributions are positively skewed (Lepper et al., 2000; Olley et al., 1999). The minimum age model (MAM) can control for partial bleaching by isolating the youngest statistically significant group of ages in an age distribution containing inherited age signals (Galbraith et al., 1999).

Luminescence MAM ages of terraces range from 2 to 10 Ka (Table 4.5). OSL and IRSL ages are generally consistent with each other, but for samples where both OSL and IRSL ages were determined, ages are significantly different. For samples S027, G121-006, and S066, the IRSL age is lower than the OSL age, with the largest age difference of 2 Ka in sample S066. In sample S032 and S033 the reverse occurs, the IRSL age are older than the OSL ages. The IRSL age of S032 is within error terms of the OSL age, but the IRSL age of S033 is about 3 Ka older than the OSL age. However, the OSL age of sample S033 is a poorly constrained date since only 19 grains were dated, which is too low for the MAM age to be robust (Rodnight, 2008). Differences between single-grain OSL and IRSL ages for the same terrace may be due to uncertainties in both intrinsic and extrinsic sources of error, which can significantly affect the age calculated with the MAM (Olley et al., 2004). Although intrinsic errors in the luminescence analysis can be estimated with dose recovery tests, extrinsic errors such as heterogeneity in the environmental dose rate can cause additional over dispersion in luminescence ages but are difficult to determine (Mayya et al., 2006; Nathan et al., 2003). Furthermore, intrinsic errors in the OSL analysis are uncertain given that data from the quartz dose recovery was sparse and dose recovery tests were not performed on samples S032 and G121-006.

### *4.6.2. Multi-Grain OSL Ages*

MAM OSL ages determined for multi-grain aliquot samples S032 and S033 are older than single-grain OSL ages but within error terms of the IRSL ages. These multi-aliquot ages may be influenced by partially bleached grains in each aliquot (Olley et al., 1999). The total number of grains in multi-grain aliquots was ~2000 for S032 and ~700 for S033. Based on the number of usable grains in the single-grain OSL analysis for samples S032 and S033 (2.2% and 0.4% respectively), the average number of signals in each multi-grain disc was about 50 for S032 and 3 for S033. Usable OSL signals in the single-grain analysis were characterized by many weak signals with a scattered few bright signals. This suggests OSL measured in multi-grain aliquots will be dominated by only a few bright grains, effectively giving single-grain resolution.

### *4.6.3. Comparing Luminescence and $^{14}C$ Ages*

Both OSL and IRSL luminescence ages of terraces are much younger than $^{14}C$ dates from the same terrace. This age difference ranges from 5 to 12 $^{14}C$ Ka and averages 7 $^{14}C$ Ka. Sample S051, the highest terrace at 218 m elevation, has the oldest $^{14}C$ age (17.06±0.06 $^{14}C$ Ka) and a relatively young luminescence age (5.6±0.8 Ka), resulting in the largest age difference measured in this study. The age differences between luminescence and $^{14}C$ dates are a minimum since calibrated $^{14}C$ dates will be somewhat older than the uncalibrated dates given in Table 4.5. Even if the weighted mean from the CAM is used as the terrace luminescence age, the age difference between luminescence and $^{14}C$ ages is still large. One possibility for this large age difference is that by assuming that the water content in the upper soil is low over the burial history, the environmental dose rate is overestimated. This would result in underestimated luminescence ages. However, even if the soil was continuously saturated with water the dose rate would only decrease by about 20-30%, which cannot account for the factor of 2-3 difference between luminescence and $^{14}C$ ages.

Table 4.5. Results from luminescence dating of terraces in Taylor Valley compared to $^{14}C$ dates. The number of grains used in luminescence age calculations are given, with the percentage of these grains relative to all grains analyzed in parentheses. Weighted skewness of the age distribtions are calculated as in Bailey and Arnold (2006).

The weighted mean and over dispersion age distributions, as well as fading rates (g), are calculated using the CAM. All errors are ± 1 σ.

| | Sample | Grains | g % decade$^{-1}$ | Skewness | Weighted Mean Ka | Over Disp. % | MAM Ka | $^{14}$C Age[a] $^{14}$C Ka |
|---|---|---|---|---|---|---|---|---|
| Feldspar (IRSL) | S027 | 140 (35%) | 6.4±0.3 | 1.2±0.2 | 10.0±0.4 | 22.9±4.2 | 8.5±1.0 | 16.5±0.7 |
| | S032 | 153 (51%) | 9.2±0.5 | 1.5±0.2 | 6.1±0.2 | 19.0±5.8 | 5.3±0.7 | 10.8±0.1 |
| | S033 | 193 (48%) | 6.4±0.3 | 1.3±0.2 | 6.0±0.1 | 9.6±4.6 | 5.4±0.6 | 11.5±0.1 |
| | S034 | 93 (46%) | 6.2±0.2 | 2.1±0.2 | 6.6±0.2 | 12.7±5.0 | 5.5±0.2 | 13.3±0.8 |
| | S041 | 109 (54%) | 6.0±0.3 | 1.3±0.2 | 7.0±0.2 | 21.7±3.2 | 5.3±0.8 | 12.1±0.5 |
| | S048 | 55 (11%) | 5.7±0.3 | 2.7±0.3 | 8.6±0.4 | 17.1±6.6 | 8.2±1.1 | 14.1±0.1 |
| | S049 | 69 (14%) | 7.3±0.4 | 2.3±0.3 | 9.0±0.4 | 13.7±6.8 | 8.5±0.5 | 14.9±0.1 |
| | S051 | 131 (66%) | 6.4±0.3 | 0.9±0.2 | 7.3±0.3 | 21.2±4.6 | 5.6±0.8 | 17.1±0.1 |
| | S061 | 97 (24%) | 6.5±0.3 | 1.2±0.2 | 10.6±0.5 | 20.3±6.1 | 8.5±0.7 | – |
| | S062 | 99 (20%) | 6.9±0.4 | 2.6±0.2 | 9.6±0.5 | 29.1±5.5 | 6.6±0.8 | – |
| | S066 | 203 (51%) | 6.0±0.2 | 1.8±0.2 | 5.7±0.1 | 18.4±2.9 | 5.2±0.2 | 12.4±0.1 |
| | S071 | 147 (37%) | 5.4±0.2 | 4.1±0.2 | 8.7±0.3 | 21.7±3.3 | 8.1±0.7 | – |
| | G121-006 | 179 (45%) | 6.3±0.3 | 2.0±0.2 | 6.3±0.2 | 31.1±3.8 | 4.2±0.4 | 12.4±0.1 |
| Quartz (OSL) | S027 | 66 (2.6%) | – | 2.5±0.3 | 15.9±1.2 | 45.6±6.8 | 9.7±1.4 | 16.5±0.7 |
| | S032 | 54 (2.2%) | – | 2.7±0.3 | 7.1±0.5 | 35.7±7.5 | 4.6±0.7 | 10.8±0.1 |
| | S032 (mg)[b] | – | – | 0.8±0.5 | 6.4±0.4 | 0 | 6.4±1.0 | 10.8±0.1 |
| | S033 | 19 (0.4%) | – | 1.5±0.6 | 4.3±0.6 | 46.2±13.0 | 2.2±0.5 | 11.5±0.1 |
| | S033 (mg)[b] | – | – | 0.7±0.5 | 6.5±0.5 | 22.0±9.3 | 5.0±0.8 | 11.5±0.1 |
| | S066 | 44 (1.8%) | – | 0.3±0.4 | 7.5±0.4 | 0±0 | 7.5±0.6 | 12.4±0.1 |
| | G121-006 | 49 (1.1%) | – | 4.1±0.3 | 10.4±0.2 | 39.5±7.5 | 5.6±0.9 | 12.5±0.1 |

[a]Dates are uncalibrated $^{14}$C dates from the map provided in Hall and Denton (2000) and are coreolated to luminescence samples as follows: S027 (QL- 1034), S032 (QL-1147), S033 (AA-13559), S034 (AA-13560), S041 (QL-1033), S048 (AA-14036), S049 (UGA-6861), S051 (QL-1253 and QL-992), S066 (QL-1913), and G121-006 (QL-1044, QL-1045, and QL-1149).
[b]Multi-grain OSL.

### *4.7. Inherited Radiocarbon Ages in Terraces*

A common cause of inherited $^{14}$C ages in Taylor Valley are radiocarbon reservoir effects found in stagnant water below stratified lake surfaces, in open moats surrounding lake ice-rafts, and in proglacial lakes fed by sub-glacial melt water (Doran et al., 1999; Hendy and Hall, 2006). The influence of reservoir effects on $^{14}$C ages depends on the degree of equilibration between atmospheric $CO_2$ and dissolved inorganic carbon in water supporting algal growth. Algae growing in stagnant water near the bottom of stratified lakes or in water directly fed by glacial melt, have yielded high inherited $^{14}$C ages on the order of 1 – 10 Ka (Hall and Henderson, 2001; Hendy and Hall, 2006). In contrast, algae growing in streams and lake moats have near modern $^{14}$C ages because dissolved inorganic carbon in these systems equilibrates quickly with atmospheric $CO_2$ (Doran et al., 1999; Hendy and Hall, 2006). The difference between luminescence and $^{14}$C ages in this study is similar to radiocarbon reservoir effects measured in lake bottoms and in glacial ice, but radiocarbon reservoir effects associated with lake bottom

sediments are not consistent with the fluvial nature of terraces. Terraces, whether interpreted as deltas or another form of fluvial sedimentation, are deposited in either stream or lake moat environments and algae growing within these environments should have a minimal radiocarbon reservoir effect (Doran et al., 1999; Hall and Denton, 2000; Hendy and Hall, 2006).

If the algae sampled for $^{14}C$ dating grew *in situ* within fluvial or lake moat environments, it is difficult to explain the consistently large age difference between $^{14}C$ and luminescence ages in terraces as a reservoir effect. This suggests that the algae sampled within terraces did not grow *in situ*, but is ultimately sourced from older algae within older sediments. The most likely source of this older algae is from glaciolacustrine deposits that cover the floor of eastern Taylor Valley up to approximately 350 m elevation (Hall et al., 2000). Algal flakes and layers are abundant in these sediments and over 100 $^{14}C$ dates of the algae have been determined by Hall and Denton (2000). Glaciolacustrine sediments have $^{14}C$ dates ranging from 7 to 19.1 $^{14}C$ Ka (averaging 13.6±2.3 $^{14}C$ Ka), which is similar to $^{14}C$ dates in terraces that range from 5.2 – 18.1 $^{14}C$ Ka (averaging 12.3±2.3 $^{14}C$ Ka) (Figure 4.4). This similarity in $^{14}C$ ages between terraces and glaciolacustrine sediments suggests that algae sampled for $^{14}C$ dating in terraces is sourced from algae in nearby glaciolacustrine sediments.

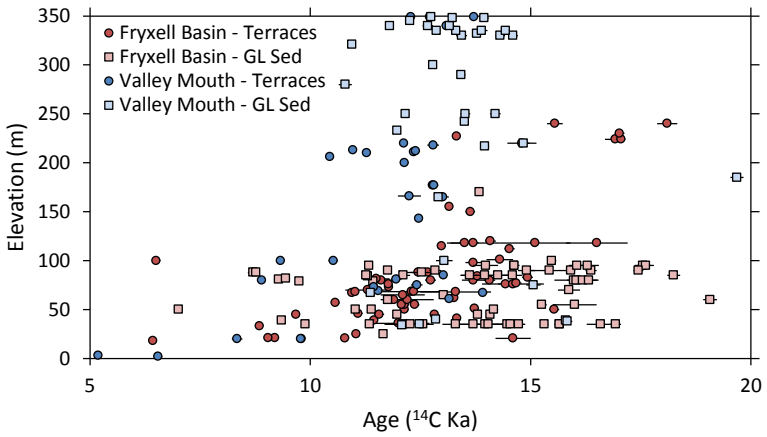


Figure 4.4. $^{14}C$ dates of terraces and glaciolacustrine sediments in Taylor Valley.

In Hall and Denton (2000) and Stuiver et al. (1981), short descriptions are provided of sediment texture and the approximate sample location within terraces where $^{14}C$ samples were collected. A comparison of these descriptions with luminescence samples collected in this study indicates that sediments sampled for $^{14}C$ dating vary from luminescence samples with respect to texture, presence of algal material, and position within terraces. 83.5% of the sediments sampled for $^{14}C$ dating in eastern Taylor Valley are described as silty or fine-grained, 12.1% are described simply as sand or are not described for texture, and 4.4% are specified as medium to coarse-grained sand in texture. 58.2% of the $^{14}C$ samples were collected below the surface of the terrace, within stream cuts, near the toe of the terrace, or on the sloping terrace front. Combined, sediments sampled for $^{14}C$ dating in terraces were either fine-grained or below the upper terrace surface in 88% of all samples from eastern Taylor Valley. In contrast, all luminescence samples in this study were collected from the apex of terraces and were uniformly composed of medium to coarse-grained sand. Twelve other terraces sampled for soluble salts by Toner et al. (2012) were also collected near the apex of the terrace and were composed of medium to coarse-grained sand. In addition, although algal layers were described in nearly all terraces sampled for $^{14}C$ dating, no algal layers or flakes were found near the apex of any terraces in this study or in Toner et al. (2012).

Differences in age, texture, algal material, and sample location between $^{14}C$ and luminescence samples are consistent with the hypothesis that $^{14}C$ samples are dating older, fine-grained glaciolacustrine sediments, while luminescence samples are dating younger, coarse-grained fluvial sediments. This suggests that 1) either algae found within terraces is reworked algae from nearby glaciolacustrine sediments or 2) $^{14}C$ samples have been sampled directly from glaciolacustrine sediments adjacent to or underlying terraces. With respect to the first possibility, glaciolacustrine sediments containing algae could have been eroded by streams, redepositing relict algae within terraces along with fine-grained material. However, this is not

consistent with observations of *in situ* algal layers in most $^{14}C$ samples. If sediments sampled for $^{14}C$ dating had been reworked by streams, then the algae should be distributed throughout the reworked sediment as algal flakes, not as algal layers. Instead, the *in situ* appearance of algal layers in $^{14}C$ sample suggests the second possibility, that $^{14}C$ samples were sampled directly from glaciolacustrine sediments.

GPR studies of terraces in eastern Taylor Valley indicate that most terraces are thin deposits mantling the landscape and are often about one to two meters thick (Horsman, 2007). Below sandy terrace sediments are crudely stratified deposits. Using a auger drill, Toner and Sletten (2012) sampled the sediments underling the terrace near luminescence sample S033 and found a transition from sandy terrace sediments to silt-rich saline sediments near two meters depth. Saline, fine-grained sediments in Taylor Valley are associated with glaciolacustrine deposits (Barrett et al., 2010; Toner et al., 2012) and fine-grained sediments are common in RSIS deposits (Hall et al., 2000). Since many $^{14}C$ samples were collected from terrace fronts or in stream cuts up to several meters from the terrace surface, a likely explanation for the large age difference between luminescence and $^{14}C$ samples is that $^{14}C$ samples were taken from older fine-grained glaciolacustrine sediments underlying or adjacent to younger terrace sediments.

Sample G121-006 was sampled from the only terrace in eastern Taylor Valley that was confirmed as a delta having foreset stratigraphy with GPR (Horsman, 2007) . Three $^{14}C$ samples have been dated on this terrace with relatively consistent ages of 12.3±0.7 $^{14}C$ Ka (QL-1044), 12.3±0.1 $^{14}C$ Ka (QL-1149), and 11.5±0.3 $^{14}C$ Ka (QL-1045). The OSL and IRSL luminescence dates for this same terrace are 5.6±0.9 Ka and 4.2±0.4 Ka respectively. From this, the inherited $^{14}C$ age component is about 7 $^{14}C$ Ka, near the average for all terraces sampled in this study. The large inherited $^{14}C$ age component of G121-006 indicates even if terraces are interpreted as deltas, they are not immune to inherited age components. This casts uncertainty on the significance of many other $^{14}C$ dates that have been collected on

terraces in western Taylor Valley (Hall and Denton, 2000; Hall et al., 2010), Wright Valley (Hall et al., 2001), and Victoria Valley (Hall et al., 2002). As in eastern Taylor Valley, $^{14}C$ ages of terraces in other Dry Valleys may be sourced from nearby sediments.

### *4.8. Interpreting Luminescence and Radiocarbon Ages of Terraces*

#### *4.8.1. Radiocarbon Ages – A Deglaciation History*

A comparison of terrace $^{14}C$ ages in eastern Taylor Valley with ice core δD profiles at Taylor Dome and Vostok shows that the $^{14}C$ ages are associated with warming trends following the LGM (Figure 4.5). During these warming trends, $^{14}C$ ages in terraces show a significant trend of decreasing terrace age with decreasing elevation, particularly in Fryxell Basin. $^{14}C$ ages in Fryxell Basin decrease from about 16 $^{14}C$ Ka near 220 m elevation to 10 $^{14}C$ Ka near the current elevation of Lake Fryxell. A linear fit to the $^{14}C$ ages in Fryxell Basin in Figure 4.5 gives a slope of 5.9 $^{14}C$ Ka per 100 m elevation and a $R^2$ value of 0.43. In addition, $^{14}C$ ages near the Valley Mouth (closer to McMurdo Sound) are generally younger than $^{14}C$ ages within Fryxell Basin (further from McMurdo Sound). We interpret these trends and the timing of $^{14}C$ ages as broadly dating the deglaciation of Taylor Valley following the LGM. The general trend of decreasing $^{14}C$ ages with elevation in the terraces is consistent with a deglaciation trend produced as the floor of Taylor Valley was progressively uncovered by retreating ice from the RSIS and lowering of associated paleolakes. Furthermore, the occurrence of younger ages at similar elevations near the valley mouth relative to Fryxell Basin is consistent with uncovering of surfaces deeper in Taylor Valley earlier in deglaciation.

$^{14}C$ ages in Figure 4.5 are given as uncalibrated ages because algae in glaciolacustrine sediments throughout eastern Taylor Valley may be influenced by potentially large and variable radiocarbon reservoir effects (Hall and Denton, 2000). Based on reservoir effects measured in Trough Lake, a proglacial lake that may have been similar to proglacial paleolakes that

occupied Taylor Valley, the radiocarbon reservoir effect could be up to about 4 $^{14}$C Ka (Hendy and Hall, 2006). This potential reservoir effect is consistent with the large scatter in $^{14}$C ages at similar elevations and causes some uncertainty about the timing of events associated with $^{14}$C dates of terraces.

If algae sampled for $^{14}$C dating is sourced from glaciolacustrine sediments underlying fluvial terrace sediments, then $^{14}$C ages do not indicate the elevation of paleolake levels as in the interpretation of Stuiver et al. (1981), Hall and Denton (2000), and Hall et al. (2010). Algal mats are common throughout the Dry Valleys and algae within glaciolacustrine sediments may have grown in proglacial lakes fronting the RSIS or in ice marginal streams and ponds. By analyzing salt distributions in Taylor Valley, Toner et al. (2012) found that Fryxell Basin was occupied by paleolakes up to approximately 120 m elevation during deglaciation. This suggests that algae sampled for $^{14}$C dating above 120 m elevation in Fryxell Basin grew in ice marginal environments, while algae below 120 m elevation grew in paleolake environments. The strong trend of decreasing $^{14}$C ages with elevation below 120 m elevation in Fryxell Basin is likely due to paleolake lowering during deglaciation.

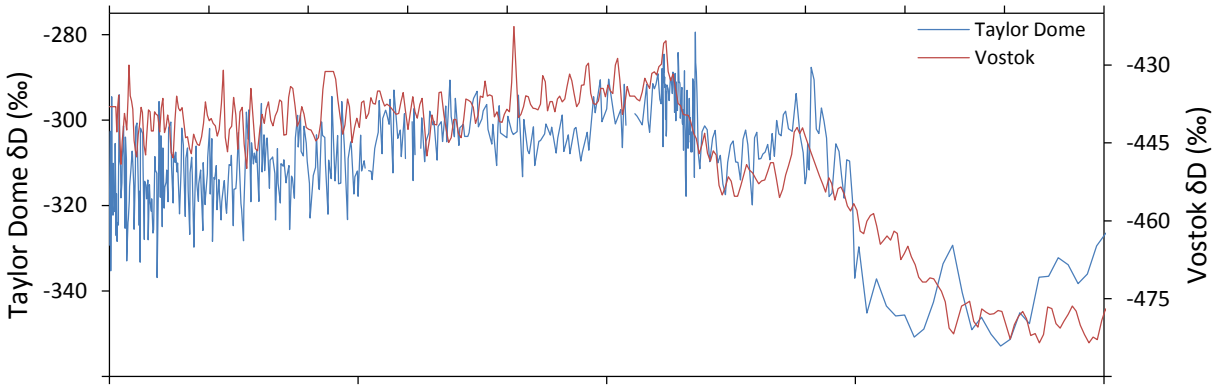

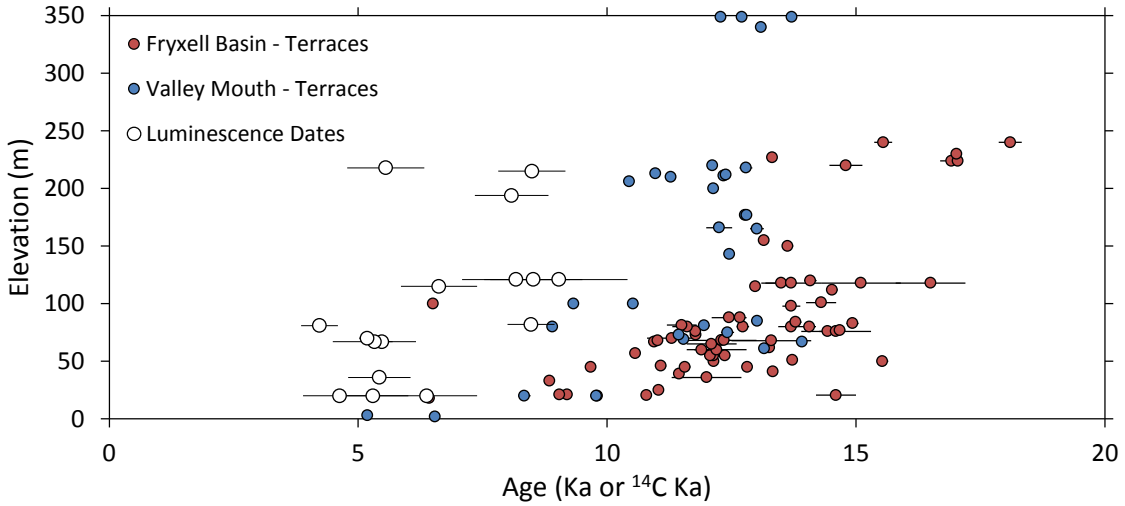


Figure 4.5. A comparison of feldspar and quartz luminescence ages measured in this study, and the δD record (a proxy for temperature changes) of the Taylor Dome ice core (Steig et al., 2000) and the Vostok ice core (Petit et al., 2001). $^{14}C$ ages are associated with temperature increases following the LGM while luminescence ages all occur during early-Holocene temperature highs.

### *4.8.2. Luminescence Ages – Periods of Fluvial Sedimentation*

Luminescence ages indicate that terraces were deposited during separate events after the retreat of the RSIS from Taylor Valley. Ice core records indicate that the period of time when terraces were deposited (4-10 Ka) was characterized by warmer atmospheric and oceanic conditions that followed deglaciation (Steig et al., 2000). After 6 Ka, the δD record at Taylor Dome indicates that the regional climate cooled, which is well correlated with evidence of sea ice increases and increased diatom productivity in McMurdo Sound (Steig et al., 1998). In the Dry Valleys, lake levels lowered to saline remnants during cold, dry conditions in the Holocene (Doran, 1994). Based on diffusion modeling of Cl (Matsubaya et al., 1979; Wilson, 1964), stable isotopes (Lyons et al., 1998), and $^{3}He/^{4}He$ profiles (Poreda et al., 2004) in lake Fryxell, Hoare, Bonney, and Vanda, this period of lake level lowering and desiccation occurred between 1 to 4 Ka. The deposition of fluvial terraces during warm conditions and their absence during cooler, drier conditions suggests that the climate between 4-10 Ka favored fluvial sedimentation of terraces.

Sedimentation by streams in the Dry Valleys is strongly influenced by climate conditions (Shaw and Healy, 1980) and melt water production from alpine glaciers (Hawke and McConchie, 2001; Mosley, 1988). Greater melt water production from alpine glaciers increases stream discharge, which has been shown to be directly related to bedload transport in the Onyx River (Mosley, 1988) and in melt water streams within Miers Valley (Hawke and McConchie, 2001). Observations of Dry Valley hydrologic systems during warm and cool summers indicate that glacial melt water production and stream discharge are sensitive to changes in climate (Chinn, 1981; Conovitz et al., 1998; Doran et al., 2008; Poreda et al., 2004). Warmer conditions in the Dry Valleys increase melt water production on glaciers, resulting in greater stream discharge. Similarly, cooler conditions reduce melt water from glaciers, resulting in decreased stream discharge. These observations suggest that during the warmer climatic conditions that followed deglaciation, melt water production from alpine glaciers increased, leading to greater fluvial sedimentation and the deposition of terraces in eastern Taylor Valley.

Based on the luminescence age of sample G121-006, which was confirmed as a delta by GPR (Horsman, 2007), the deposition of terraces was associated with a paleolake level up to 78 m elevation. Since the elevation of this paleolake lies at the threshold elevation between Fryxell Basin and McMurdo Sound, this paleolake level could have formed without the presence of a RSIS dam near the Valley Mouth. Lake levels in the Dry Valleys are thought to be sensitive to increased melt water inputs from alpine glaciers (Bomblies et al., 2001; Chinn, 1981, 1993) and greater stream discharge (Doran et al., 2008). A rise in lake levels to 78 m elevation is consistent with sedimentation of fluvial terraces during times of greater stream discharge. This is similar to the conclusions of Shaw and Healy (1980) that greater stream discharge in the Onyx River is related to both increased alluvial activity and higher paleolake levels in Lake Vanda.

Greater sedimentation by Dry Valley streams has also been linked to the availability of sediment for transport; loose sediments are more easily eroded and can greatly contribute to bedload transport in Dry Valley streams (Hawke and McConchie, 2001; Mosley, 1988; Shaw and Healy, 1980). The presence of the RSIS in eastern Taylor Valley would have deposited an abundant supply of loose sediment, which would be readily mobilized by periglacial mass-wasting and fluvial processes following deglaciation (Church and Ryder, 1972). These processes are most active immediately following deglaciation and rapidly decrease as surfaces are stabilized and loose sediment is redistributed towards valley bottoms (Fitzsimons, 1990, 1996).

The large time gap between $^{14}C$ and luminescence ages of terraces suggests that greater sedimentation did not occur immediately after deglaciation. No luminescence ages occur prior to 10 Ka, even though some of the highest deglacial temperatures occurred during this time period. This hiatus in fluvial sedimentation during a period of time that should have been characterized by high fluvial sedimentation may be due to a reduction in the size of alpine glaciers supplying melt water to streams. Alpine glaciers in the Dry Valleys are thought to fluctuate asynchronously with ice sheet advances in the Ross Sea (Clapperton and Sugden, 1990). As ice sheets fill the Ross Sea, the Dry Valley region becomes starved of moisture and snow accumulation decreases, causing alpine glaciers to recede; in contrast, during warmer interglacial time periods, alpine glaciers readvance in response to higher snow accumulation rates (Clapperton and Sugden, 1990; Dort, 1970). Snow accumulation rates at Taylor Dome indicate that accumulation during the LGM was lower than during the Holocene (Morse et al., 1999; Steig et al., 2000), with particularly high snow accumulation rates occurring between 6-8 Ka (Steig et al., 2000). Currently, alpine glaciers in Taylor Valley are thought to have advanced since the LGM and are now at their maximum extent (Higgins et al., 2000; Stuiver et al., 1981). This suggests that the after deglaciation alpine glaciers would have been much smaller than at

present, resulting in low melt water production and low stream discharge in spite of the warm climate conditions.

*4.9. Conclusions*

Dating glacial sediments in the Dry Valleys is difficult due to the lack of datable materials, problems of sediment recycling, and inherited age components. Luminescence dating can resolve these issues because datable material is abundant (quartz and feldspar within sediments) and inherited age signals can be controlled for by looking at age distributions. By applying luminescence dating to terraces in eastern Taylor Valley we find that terraces range in age from 4 to 10 Ka and are 5 to 12 $^{14}$C Ka younger than previously determined $^{14}$C dates from the same terrace. The most likely explanation for this consistently large age difference is that $^{14}$C samples were sampled from older, algae-rich, fine-grained sediments while luminescence samples were sampled from younger, coarse-grained fluvial sediments. This large age difference calls into question other chronologies in the Dry Valleys based on $^{14}$C dating of buried algae. The distribution of terrace luminescence ages suggests that the formation of these terraces is linked to past climate, melt water production from alpine glaciers, stream flow, lake levels, and sedimentation rates. During warmer climates, glacial melt water production increases, resulting in higher stream discharge, higher lake levels, and fluvial sedimentation of terraces; during colder climates, glacial melt water production decreases, leading to a hiatus in fluvial sedimentation.

# Chapter 5 Conclusions and Future Work

## *5.1. Conclusions*

Soluble salts in Taylor Valley, Antarctica, were investigated to determine the history of paleolakes and the RSIS during the LGM RSIS expansion. The initial working hypothesis of this thesis was that paleolakes would have leached soluble salts from soils and that maximum paleolake high stands would be indicated by a sharp decrease in soluble salt accumulations at lower elevations. Over the course of this study, it was found that mechanisms controlling the distribution of soluble salts in Taylor Valley are much more complicated than is suggested by this simple interpretation. It was found that soluble salts in soils of Taylor Valley are influenced by a variety of factors including soil age, leaching, distance from McMurdo Sound, soil texture, and past glacial and lacustrine events.

In western Taylor Valley, salt accumulations are rich in Na, Ca, Cl, and $SO_4$ and ion ratios are similar to seawater. In eastern Taylor Valley, salt accumulations are rich in Na and $HCO_3$ and ion ratios vary considerably from seawater. The unusual Na-$HCO_3$ composition of salts in eastern Taylor Valley is due to mineral dissolution and cation exchange reactions in the presence of high leaching rates. These reactions result in Cl being leached from soils as Ca-Mg-Cl brine and the association of Na with $HCO_3$ from calcite dissolution. Mineral dissolution and cation exchange reactions also influence the chemistry of soil:water extractions. It is important to consider the influence of these reactions when interpreting soluble salt concentrations measured in soil:water extractions.

The distribution of total soluble salt contents (the equivalent sum of all ions with depth) in Taylor Valley is primarily determined by soil age; soils developing on younger glacial sediments have much lower salt contents than soils developing on older glacial sediments. Since soils in Taylor Valley are generally older further inland and at higher elevations, the distribution of salts in

Taylor Valley is broadly characterized by higher salt contents in western Taylor Valley and lower salt contents in eastern Taylor Valley. This relationship between soil age and salt content has been altered by salt leaching, primarily in the wetter climate of eastern Taylor Valley, and paleolakes. Soils in Bonney Basin are consistent with a history of evapoconcentration along paleolake margins up to approximately 300 m elevation; in eastern Taylor Valley, salt distributions indicate maximum paleolake high stands up to approximately 120 m. To explain the absence of paleolakes between approximately 120 and 300 m elevation in eastern Taylor Valley, paleolakes in Bonney Basin must have been dammed by a lobe of the RSIS that filled all of eastern Taylor Valley to at least 300 m elevation. Following the retreat of the RSIS, paleolakes quickly lowered and formed separate paleolakes within Fryxell and Bonney Basin. This interpretation is a significant departure from previous theories on paleolakes and the RSIS in Taylor Valley. In contrast to these previous theories, this study concludes that the RSIS penetrated deeper into Taylor Valley and that paleolakes fronting this ice lobe were not valley-wide paleolakes, but filled separate basins within Taylor Valley.

By studying the distribution of soluble salts in Taylor Valley, it was found that leaching, mineral dissolution, and cation exchange processes strongly influence the amount and composition of soluble salts in soils. These processes were studied in detail in a terrace soil sampled to 2.1 m depth. Soluble salts in the borehole soil are characterized by Ca-Cl enrichment, a relatively rare aqueous chemistry that is shared only with groundwaters in the Dry Valleys, particularly Don Juan Pond. The distribution of stable isotopes with depth indicates that evaporated brines originating from the soil surface are advecting downwards, resulting in a systematic isotopic depletion in the upper meter of soil. Furthermore, the distribution of soluble salts and exchangeable cations with depth suggests that aqueous ions in downward advecting brines are reacting with exchangeable cations to produce the Ca-Cl enrichment.

To explore the implications of Ca-Cl formation by reactive transport, the exchange properties of Taylor Valley soils were measured and an advective dispersive model of brine transport was developed. Cation exchange was studied for Ca-Na, Ca-Mg, and Ca-K exchange over a range of solution concentrations that may exist in the Dry Valleys, from dilute solutions (~0.1 mM) to concentrated brine (4.75 M). It was found that exchange reactions in the borehole soil could be modeled with the Rothmund-Kornfeld formula over a wide range of solution compositions and ionic strengths. By modeling reactive transport using the geochemical programs PHREEQC and FREZCHEM, it was found that by freezing soils, a strong Ca-Cl enrichment of the soil solution is caused by the exchange of aqueous Na with exchangeable Ca. Furthermore, advection of Na-Cl rich brines from the soil surface displaces absorbed Ca in the soil, enriching the soil solution in Ca-Cl. Ca-Cl enrichment by reactive transport involving cation exchange is consistent with the ionic composition of most groundwater chemistries in the Dry Valleys and the amount of Ca-Cl enriched groundwater found beneath Don Juan Pond. This suggests that cation exchange can explain the Ca-Cl enrichment often found in shallow groundwaters, deep groundwaters, and ponds and lakes influenced by groundwaters.

The alteration of soluble salt accumulations by secondary soil processes such as leaching, cation exchange, and mineral dissolution makes it difficult to date sediments using salt contents in the soil and accumulation rates determined on nearby glaciers. In general, dating glacial sediments in the Dry Valleys is difficult due to the paucity of organic material for $^{14}C$ dating, sediment recycling, and inherited age components. To date terrace sediments in eastern Taylor Valley, luminescence dating was used because datable material is abundant (quartz and feldspar within sediments) and inherited age signals can be controlled for by looking at age distributions.

Luminescence ages of terraces range in age from 4 to 10 Ka and are 5 to 12 $^{14}C$ Ka younger than previously determined $^{14}C$ dates from the same terrace. The most likely explanation for

this consistently large age difference is that $^{14}C$ samples were sampled from older, algae-rich glaciolacustrine sediments, while luminescence samples were sampled from younger, coarse-grained fluvial sediments. $^{14}C$ ages are interpreted as dating the deglacial retreat of the RSIS and associated paleolakes from Taylor Valley. This interpretation is consistent the timing of $^{14}C$ ages near deglacial warming trends (as recorded in ice core records at Taylor Dome and Vostok) and general trends of decreasing $^{14}C$ ages with decreasing elevation. Luminescence ages suggest that fluvial terraces were deposited during periods of high stream flow following deglaciation between 4 to 10 Ka, but were not deposited during cooler, drier periods after 4 Ka. High stream flows are linked to warm climate conditions, which influences melt water production from alpine glaciers. During warm periods, glacial melt water production increases, resulting in higher stream discharge, higher lake levels, and fluvial sedimentation; during colder periods, glacial melt water production decreases, leading to a hiatus in fluvial sedimentation.

*5.2. Future Work*

The work presented here can be expanded upon and points to a number of areas needing further research. Salt distributions determined in this study, although more extensive than in previous studies, could be improved upon. Salt contents in an area were determined with a single soil pit, but the results of this study suggest that there is significant local variability in salt contents. This variability could be resolved by bulk sampling multiple soils in an area to more accurately reflect salt contents in the landscape. In addition, a more precise determination of the elevation of lacustrine events could be determined with greater sampling resolution with elevation, particularly near the elevation of events described in this thesis. Also, areas of Taylor Valley exist that have not been extensively analyzed for soluble salts, including: soils below 300 m elevation in Bonney Basin, central Taylor Valley near the Suess Glacier and Lake Hoare, the Nussbaum Riegel, the north slopes of Fryxell Basin, Fryxell Basin between Coral Ridge and Crescent Stream, and Hjorth Hill.

Soils pits sampled in Bonney Basin at 116 m and 86 m elevation indicate that evapoconcentrated salt accumulations initially deposited near the soil surface have migrated downwards over the Holocene. These soils are ideal for studying salt leaching down soil profiles because the initial salt distribution of the soil is known and the soils are homogeneous in texture (silty). A detailed sampling of these soils with depth could be coupled with unsaturated transport modeling, possibly using the recently developed richPHREEQC extension of PHREEQC, to model leaching processes.

Exchange properties in this study were based on only a few soils in Taylor Valley. A more comprehensive determination of cation exchange properties needs to be performed on different soils at a variety of ionic strengths. Exchangeable K was largely neglected in this thesis because it is relatively minor in Dry Valley soils and cation exchange involving K can be complicated by irreversible K fixation. Also, exchangeable cations in equilibrium with lake and stream waters in the Dry Valleys were determined by modeling. These modeling results should be tested by analyzing exchangeable and aqueous cations in stream and lake waters.

The hypothesis that Ca-Cl enriched brines are formed by cation exchange reactions could be studied by analyzing shallow groundwater and ground ice chemistries in the Dry Valleys. For example, a number of seeps have been observed above Don Juan Pond and may have a Ca-Cl composition. The formation of Ca-Cl brine by reactive transport could be studied by analyzing the borehole soil for trace metals and minor aqueous species. Trace metals have been studied on glaciers, snow, streams, lakes, and groundwaters in the Dry Valleys. The determination of these species in the borehole soil could further inform mechanisms that influence trace metals in the Dry Valleys.

Luminescence dates of terraces are restricted to terraces in Fryxell Basin, but many other terraces have been $^{14}C$ dated in Bonney Basin, Wright Valley, and Victoria Valley. $^{14}C$ dates of

terraces throughout the Dry Valleys have been used to support the existence and timing of large paleolakes up to 400 m above present levels. The large discrepancy between $^{14}C$ and luminescence dates found in eastern Taylor Valley may apply to these other regions as well. If so, conclusions that have been based on the $^{14}C$ dates (such as the existence of high paleolakes) need to be reevaluated.

In Taylor Valley, only terraces were dated using luminescence dating, but luminescence dating could also be applied to glacial and lacustrine sediments. This would further test the interpretation that samples for $^{14}C$ dating were collected from older glaciolacustrine sediment underlying younger terrace sediments. If luminescence ages of glaciolacustrine sediments were equivalent to the $^{14}C$ ages, then this would provide strong evidence for this interpretation.

# Bibliography

Adamiec, G., Aitken, M.J., 1998. Dose rate conversion factors: Update. Ancient TL 16, 37-50.

Aitken, M.J., 1985. Thermoluminescence Dating. Academic Press, London.

Aitken, M.J., 1998. An Introduction to Optical Dating: The Dating of Quaternary Sediments by the Use of Photon-Stimulated Luminescence. Oxford University Press.

Amrhein, C., Suarez, D.L., 1990. Procedure for determining sodium-calcium selectivity in calcareous and gypsiferous soils. Soil Science Society of America Journal 54, 999-1007.

Anderson, D.M., 1970. Phase boundary water in frozen soils. Cold Regions Research and Engineering Lab, Hanover, NH, p. 17

Angino, E.E., Armitage, K.B., 1963. A geochemical study of Lakes Bonney and Vanda, Victoria Land, Antarctica. The Journal of Geology 71, 89-95.

Angino, E.E., Armitage, K.B., Tash, J.C., 1964. Physicochemical limnology of Lake Bonney, Antarctica. Limnology and Oceanography 9, 207-217

Appelo, C.A.J., 1994. Cation and proton exchange, pH variations, and carbonate reactions in a freshening aquifer. Water Resources Research 30, 2793-2805.

Appelo, C.A.J., Parkhurst, D.L., 2002. Calculating cation exchange with PHREEQC (version 2).

Appelo, C.A.J., Postma, D., 2005. Geochemistry, Groundwater and Pollution, Second Edition ed. CRC Press, Boca Raton, Fl.

Appelo, C.A.J., Willemsen, A., Beekman, H.E., Griffioen, J., 1990. Geochemical calculations and observations on salt water intrusions. II Validation of a geochemical model with laboratory experiments. Journal of Hydrology 120, 225-250.

Arcone, S.A., Delaney, A.J., Prentice, M.L., Horsman, J.L., 2008. GPR reflection profiles of sedimentary deposits in lower Taylor Valley, Antarctica, Twelfth international conference on ground penetrating radar, Birmingham, UK.

Arnold, L.J., Bailey, R.M., Tucker, G.E., 2007. Statistical treatment of fluvial dose distributions from southern Colorado arroyo deposits. Quaternary Geochronology 2, 162-167.

Atkins, C.B., Dickinson, W.W., 2008. Landscape modification by meltwater channels at margins of cold-based glaciers, Dry Valleys, Antarctica. Boreas 36, 47-55.

Auclair, M., Lamothe, M., Huot, S., 2003. Measurement of anomalous fading for feldspar IRSL using SAR. Radiation Measurements 37, 487-492.

Bailey, R.M., Arnold, L.J., 2006. Statistical modelling of single grain quartz $D_e$ distributions and an assessment of procedures for estimating burial dose. Quaternary Science Reviews 25, 2475-2502.

Balescu, S., Lamothe, M., Mercier, N., Huot, S., Balteanu, D., Billard, A., Hus, J., 2003. Luminescence chronology of Pleistocene loess deposits from Romania: testing methods of age correction for anomalous fading in alkali feldspars. Quaternary Science Reviews 22, 967-973.

Bao, H., Barnes, J.D., Sharp, Z.D., Marchant, D.R., 2008. Two chloride sources in soils of the McMurdo Dry Valleys, Antarctica. Journal of Geophysical Research 113.

Bao, H., Campbell, D.A., Bockheim, J.G., Thiemens, M.H., 2000. Origins of sulphate in Antarctic dry-valley soils as deduced from anomalous $^{17}O$ compositions. Nature 407, 499-502.

Bao, H., Marchant, D.R., 2006. Quantifying sulfate components and their variations in soils of the McMurdo Dry Valleys, Antarctica. Journal of Geophysical Research 11.

Barbraud, C., Weimerskirch, H., 2001. Emperor penguins and climate change. Nature 411, 183-186.

Barrett, J.E., Gooseff, M.N., Takacs-Vesbach, C., 2009. Spatial variation in soil active-layer geochemistry across hydrologic margins in polar desert ecosystems. Hydrology and Earth System Sciences Discussions 13, 2349–2358.

Barrett, J.E., Poage, M.A., Gooseff, M.N., Takacs-Vesbach, C., 2010. The legacy of aqueous environments on soils of the McMurdo Dry Valleys: contexts for future exploration of

Martian soils, in: Doran, P.T., Lyons, B.W., McKnight, D.M. (Eds.), Life in Antarctic Deserts and other Cold Dry Environments. Cambridge Astrobiology, New York.

Bateman, M.D., 2008. Luminescence dating of periglacial sediments and structures. Boreas 37, 574-588.

Bear, J., 1972. Dynamics of Fluids in Porous Media. American Elsevier Pub. Co., New York.

Beekman, H.E., Appelo, C.A.J., 1990. Ion chromatography of fresh- and salt-water displacement: laboratory experiments and multicomponent transport modelling. Journal of Contaminant Hydrology 7, 21-37.

Benassai, S., Becagli, S., Gragnani, R., Magand, O., Proposito, M., Fattori, I., Traversi, R., Udisti, R., 2005. Sea-spray deposition in Antarctic coastal and plateau areas from ITASE traverses. Annals of Glaciology 41, 32-40.

Berger, G.W., Doran, P.T., 2001. Luminescence-dating zeroing tests in Lake Hoare, Taylor Valley, Antarctica. Journal of Paleolimnology 25, 519-529.

Berger, G.W., Doran, P.T., Thomsen, K.J., 2010. Single-grain and multigrain luminescence dating of on-ice and lake-bottom deposits at Lake Hoare, Taylor Valley, Antarctica. Quaternary Geochronology 5, 679-690.

Berger, G.W., Kratt, C., 2008. LED laboratory lighting. Ancient TL 26, 11-13.

Bjerg, P.L., Christensen, T.H., 1993. A field experiment on cation exchange-affected multicomponent solute transport in a sandy aquifer. Journal of Contaminant Hydrology 12, 269-290.

Black, R.F., Berg, T.E., 1963. Patterned ground in Antarctica, Permafrost International Conference. Nat. Acad. of Sci.-Nat, Res. Counc., Washington, D. C.

Black, R.F., Jackson, M.L., Berg, T.E., 1965. Saline discharge from Taylor Glacier, Victoria Land, Antarctica. The Journal of Geology 73, 175-181.

Blank, H.R., Cooper, R.C., Wheeler, R.H., Willis, I.A.G., 1963. Geology of the Koettlitz-Blue Glacier region, south Victoria Land Region, Antarctica. Transactions of the Royal Society of New Zealand - Geology 2, 79-100.

Bockheim, J.G., 1979. Relative age and origin of soils in eastern Wright Valley, Antarctica. Soil Science 128, 142-153.

Bockheim, J.G., 1982. Properties of a chronosequence of Ultraxerous soils in the Trans-Antarctic Mountains. Geoderma 28, 239– 255.

Bockheim, J.G., 1983. Use of soils in studying the behaviour of the McMurdo ice dome, in: James, P.R., Jago, J.B. (Eds.), Antarctic Earth Science: Fourth International Symposium. Cambridge University Press, New York, pp. 457-460.

Bockheim, J.G., 1990. Soil development rates in the Transantarctic Mountains. Geoderma 47, 59-77.

Bockheim, J.G., 2003. University of Wisconsin Antarctic Soils Database. National Snow and Ice Data Center/World Data Center for Glaciology, Boulder, CO.

Bockheim, J.G., Campbell, I.B., Malcolm, M., 2007. Permafrost distribution and active-layer depths in the McMurdo Dry Valleys, Antarctica. Permafrost and Periglacial Processes 18, 217-227.

Bockheim, J.G., Campbell, I.B., McLeod, M., 2008a. Use of soil chronosequences for testing the existence of high-water-level lakes in the McMurdo Dry Valleys, Antarctica. Catena 74, 144-152

Bockheim, J.G., Prentice, M.L., McLeod, M., 2008b. Distribution of glacial deposits, soils, and permafrost in Taylor Valley, Antarctica. Arctic, Antarctic, and Alpine Research 40, 279-286.

Bomblies, A., McKnight, D.M., Andrews, E.D., 2001. Retrospective simulation of lake-level rise in Lake Bonney based on recent 21-year record: indication of recent climate change in the McMurdo Dry Valleys, Antarctica. Journal of Paleolimnology 25, 477-492.

Bond, W.J., 1995. On the Rothmund-Kornfeld description of cation exhange. Soil Science Society of America Journal 59, 436-443.

Bottomley, D.J., Clark, I.D., 2004. Potassium and boron co-depletion in Canadian Shield brines: evidence for diagenetic interactions between marine brines and basin sediments. Chemical Geology 203, 225-236.

Bottomley, D.J., Clark, I.D., Nicholas, B., Tom, K., 2005. Geochemical and isotopic evidence for a genetic link between Canadian Shield brines, dolomitization in the Western Canada. Canadian Journal of Earth Sciences 42, 2059-2071.

Bottomley, D.J., Katz, A., Chan, L.H., Starinsky, A., Douglas, M., Clark, I.D., Raven, K.G., 1999. The origin and evolution of Canadian Shield brines: evaporation or freezing of seawater? New lithium isotope and geochemical evidence from the Slave craton. Chemical Geology 155, 295-320.

Bristow, C.S., Augustinus, P.C., Wallis, I.C., Jol, H.M., Rhodes, E.J., 2010. Investigation of the age and migration of reversing dunes in Antarctica using GPR and OSL, with implications for GPR on Mars. Earth and Planetary Science Letters 289, 30-42.

Bromley, A., 1985. Weather observations, Wright Valley, Antarctica. New Zealand Meteorological Service, Wellington N.Z.

Burnham, J.H., Sletten, R.S., 2010. Spatial distribution of soil organic carbon in northwest Greenland and underestimates of high Arctic carbon stores. Global Biogeochemical Cycles 24.

Burt, D.M., Knauth, L.P., 2003. Electrically conducting, Ca-rich brines, rather than water, expected in the Martian subsurface. Journal of Geophysical Research 108.

Cameron, R.E., Conrow, H.P., 1969. Antarctic Dry Valley soil, microbial incubation and gas composition. Antarctic Journal of the United States 4, 28-33.

Cameron, R.E., King, J., David, C.N., 1970. Soil microbial ecology of Wheeler Valley, Antarctica. Soil Science 109, 110-120.

Cameron, R.E., Lacy, G.H., Morelli, F.A., 1971. Farthest south soil microbial and ecological investigations. Antarctic Journal of the United States 6, 105-106.

Campbell, I.B., Claridge, G.G.C., 1975. Morphology and age relationships of Antarctic soils, in: Suggate, R.P., Cresswell, M.M. (Eds.), Ninth INQUA congress; Quaternary studies. The Royal Society of New Zealand, Christchurch, New Zealand, pp. 83-88.

Campbell, I.B., Claridge, G.G.C., 1982. The influence of moisture on the development of soils of the cold deserts of antarctica. Geoderma 28, 221-238.

Campbell, I.B., Claridge, G.G.C., 1987. Antarctica: Soils, Weathering Processes, and Environment. Elsevier Amsterdam, Netherlands.

Campbell, I.B., Claridge, G.G.C., 2006. Permafrost properties, patterns and processes in the Transantarctic Mountains region. Permafrost and Periglacial Processes 17, 215-232.

Carlson, C.A., Phillips, F.M., Elmore, D., Bentley, H.W., 1990. Chlorine-36 tracing of salinity sources in the Dry Valleys of Victoria Land, Antarctica. Geochimica et Cosmochimica Acta 54, 311-318.

Cartwright, K., Harris, H.J.H., 1981. Hydrogeology of the dry valley region, Antarctica, in: McGinnis, L.D. (Ed.), Dry Valley Drilling Project. American Geophysical Union, Washington, D. C., pp. 193-214.

Cates, D.A., Knox, R.C., Sabatini, D.A., 1996. The impact of ion exchange processes on subsurface brine transport as observed on piper diagrams. Ground Water 34, 532–544.

Chinn, T.J.H., 1981. Hydrology and climate in the Ross Sea area. Journal of the Royal Society of New Zealand 11, 373-386.

Chinn, T.J.H., 1990. The dry valleys in Antarctica: the Ross Sea region. Department of Scientific and Industrial Research, Wellington, NZ, pp. 137-153.

Chinn, T.J.H., 1993. Physical hydrology of the Dry Valleys lakes, in: Green, W.J., Friedman, E.I. (Eds.), Physical and Biogeochemical Processes in Antarctic Lakes. American Society of Limnology and Oceanography, Waco, Texas, pp. 1–51.

Church, J.A., Gregory, J.M., Huybrechts, P., Kuhn, M., Lambeck, K., Nhuan, M.T., Qin, D., 2001. Changes in sea level, Climate Change 2001: Changes in sea level Cambridge University Press, New York, pp. 639-694.

Church, M., Ryder, J.M., 1972. Paraglacial sedimentation: A consideration of fluvial processes conditioned by glaciation. Geological Society of America Bulletin 83, 3054-3072.

Clapperton, C.M., Sugden, D.E., 1990. Late Cenozoic glacial history of the Ross Embayment, Antarctica. Quaternary Science Reviews 9, 253-272.

Claridge, G.G.C., 1965a. The chemistry and clay mineralogy of some soils from the Ross Dependency, Antarctica. New Zealand Journal of Geology and Geophysics 8, 186-220.

Claridge, G.G.C., 1965b. The clay mineralogy and chemistry of some soils from the Ross dependency, Antarctica. New Zealand Journal of Geology and Geophysics 8, 186-220.

Claridge, G.G.C., Campbell, I.B., 1968a. Origin of nitrate deposits. Nature 217, 428 - 430.

Claridge, G.G.C., Campbell, I.B., 1968b. Soils of the Shackleton Glacier region, Queen Maud Range, Antarctica. New Zealand Journal of Science 11, 171-218.

Claridge, G.G.C., Campbell, I.B., 1977. The salts in Antarctic soils, their distribution and relationship to soil processes. Soil Science 123, 377-384.

Claridge, G.G.C., Campbell, I.B., 1984. Mineral transformation during the weathering of dolerite under cold arid conditions in Antarctica. New Zealand Journal of Geology and Geophysics 27, 537-545.

Clow, G.D., McKay, C.P., Simmons, G.M., Jr., Wharton, R.A., Jr., 1988. Climatological observations and predicted sublimation rates at Lake Hoare, Antarctica. Journal of Climate 1, 715-728.

Conovitz, P.A., McKnight, D.M., MacDonald, L.H., Fountain, A.G., House, H.R., 1998. Hydrologic processes influencing streamflow variation in Fryxell Basin, Antarctica, in: Priscu, J.C. (Ed.), Ecosystem dynamics in a polar desert; the McMurdo Dry Valleys, Antarctica. American Geophysical Union, Washington, D. C., pp. 93-108.

Cook, A.J., Fox, A.J., Vaughan, D.G., Ferrigno, J.G., 2005. Retreating glacier fronts on the Antarctic Peninsula over the past half-century. Science 308, 541-544.

Cruz-Romero, G., Coleman, N.T., 1975. Reactions responsible for high pH of Na-saturated soils and clays. European Journal of Soil Science 26, 169-175.

Csatho, B., Schenk, T., Krabill, W., Wilson, T., Lyons, W.B., McKenzie, G., Hallam, C., Manizade, S., Paulse, T., 2005. Airborne laser scanning for high-resolution mapping of Antarctic. Eos Trans. AGU 86, 237–238.

Cummins, A.B., Kelley, W.P., 1923. The formation of sodium carbonate in soils. Calif. Agr. Expt. Sta. Tech. Paper 3, 1-35.

Dansgaard, W., 1964. Stable isotopes in precipitation. Tellus 16, 436-468.

de' Sigmond, A.A.J., 1927. Contribution to the theory of the origin of alkali soils. Soil Science 21, 455-480.

Denton, G.H., Armstrong, R.L., Stuiver, M., 1970. Late Cenozoic glaciation in Antarctica; the record in the McMurdo Sound region. Antarctic Journal of the United States 5, 15-21.

Denton, G.H., Bockheim, J.G., Wilson, S.C., Stuiver, M., 1989. Late Wisconsin and early Holocene glacial history, inner Ross Embayment, Antarctica. Quaternary Research 31, 151-182.

Denton, G.H., Sugden, D.E., Marchant, D.R., Hall, B.L., Wilch, T.I., 1993. East Antarctic Ice Sheet sensitivity to Pliocene climatic change from a Dry Valleys perspective. Geografiska Annaler. Series A, Physical Geography 75, 155-204.

Dickinson, W.W., Bleakley, N.L., 2005. Facies control on diagenesis in frozen sediments: The Sirius Group: Table Mountain and Mt. Feather, Dry Valleys, Antarctica. Terra Antarctica 12, 25-34.

Dickinson, W.W., Rosen, M.R., 2003. Antarctic permafrost: An analogue for water and diagenetic minerals on Mars. Geology 31, 199 -202.

Doran, P.T., 1994. Paleolimnology of the McMurdo Dry Valleys, Antarctica. Journal of Paleolimnology 10, 85-114.

Doran, P.T., Berger, G.W., Lyons, W.B., Wharton, R.A., Davisson, M.L., Southon, J., Dibb, J.E., 1999. Dating Quaternary lacustrine sediments in the McMurdo Dry Valleys, Antarctica. Palaeogeography, Palaeoclimatology, Palaeoecology 147, 223-239.

Doran, P.T., McKay, C.P., Clow, G.D., Dana, G.L., Fountain, A.G., 2002a. Valley floor climate observations from the McMurdo dry valleys, Antarctica, 1986-2000. Journal of Geophysical Research 107.

Doran, P.T., McKay, C.P., Clow, G.D., Dana, G.L., Fountain, A.G., 2002b. Valley floor climate observations from the McMurdo dry valleys, Antarctica, 1986-2000 (DOI 10.1029 2001JD002045). Journal of Geophysical Research 107.

Doran, P.T., McKay, C.P., Clow, G.D., Dana, G.L., Fountain, A.G., Nylen, T., Lyons, W.B., 2002c. Valley floor climate observations from the McMurdo dry valleys, Antarctica, 1986–2000. Journal of Geophysical Research 107, 4772.

Doran, P.T., McKay, C.P., Fountain, A.G., Nylen, T., McKnight, D.M., Jaros, C., Barrett, J.E., 2008. Hydrologic response to extreme warm and cold summers in the McMurdo Dry Valleys, East Antarctica. Antarctic Science 20, 499-509.

Dort, W., 1970. Climatic causes of alpine glacier fluctuation, southern Victoria Land, International Symposium on Antarctic Glaciological Exploration. International Association of Scientific Hydrology and SCAR, pp. 358-362.

Drever, J.I., 1982. The Geochemistry of Natural Waters. Prentice-Hall, Englewood Cliffs, NJ.

Duller, G.A.T., 2004. Luminescence dating of quaternary sediments: recent advances. Journal of Quaternary Science 19, 183–192.

Duller, G.A.T., 2006. Single grain optical dating of glacigenic deposits. Quaternary Geochronology 1, 296-304.

Duller, G.A.T., 2008. Single-grain optical dating of Quaternary sediments: why aliquot size matters in luminescence dating. Boreas 37, 589–612.

Eaton, F.M., Sokoloff, V.P., 1935. Absorbed sodium in soils as affected by the soil-water ratio. Soil Science 40, 237-248.

Eugster, H.P., Jones, B.F., 1979. Behavior of major solutes during closed-basin brine evolution. American Journal of Science 279, 609-631.

Everett, K.R., 1971. Soils of the Meserve Glacier area, Wright Valley, South Victoria Land, Antarctica. Soil Science 112, 425-438.

Field, A.B., 1975. The geochemistry of soluble salts in the Wright and Taylor Valleys, South Victoria, Antarctica. University of Waikato, Hamilton, New Zealand.

Fitzsimons, S.J., 1990. Ice-marginal depositional processes in a polar maritime environment. Antarctic Journal of Glaciology 36, 279-286.

Fitzsimons, S.J., 1996. Paraglacial redistribution of glacial sediments in the Vestfold Hills, East Antarctica. Geomorphology 15, 93-108.

Foley, K.K., Lyons, W.B., Barrett, J.E., Virginia, R.A., 2006. Pedogenic carbonate distribution within glacial till in Taylor Valley, southern Victoria Land, Antarctica. Geological Society of America Special Papers 416, 89-103.

Fortner, S.K., Tranter, M., Fountain, A., Lyons, W.B., Welch, K.A., 2005. The geochemistry of supraglacial streams of Canada Glacier, Taylor Valley (Antarctica), and their evolution into proglacial waters. Aquatic Geochemistry 11, 391-412.

Fountain, A.G., Lyons, W.B., Burkins, M.B., Dana, G.L., Doran, P.T., Lewis, K.J., McKnight, D.M., Moorhead, D.L., Parsons, A.N., Priscu, J.C., Wall, D.H., Robert, A.W.J., Virginia, R.A., 1999. Physical controls on the Taylor Valley ecosystem, Antarctica. Bioscience 49, 961-971.

Fountain, A.G., Nylen, T.H., Monaghan, A., Basagic, H.J., Bromwich, D., 2010. Snow in the McMurdo Dry Valleys, Antarctica. International Journal of Climatology 30, 633-642.

Frape, S.K., Fritz, P., 1984. Water-rock interaction and chemistry of groundwaters from the Canadian Shield. Geochimica et Cosmochimica Acta 48, 1617-1627.

Fritz, P., Frape, S.K., 1982. Saline groundwaters in the Canadian Shield - a first overview. Chemical Geology 36, 179-190.

Fuchs, M., Owen, L.A., 2008. Luminescence dating of glacial and associated sediments: a review, recommendations and furture directions. Boreas 37, 636-659.

Gaines, G.L., Thomas, H.C., 1953. Adsorption studies on clay minerals. II. A formulation of the thermodynamics of exchange adsorption. The Journal of Chemical Physics 21, 714-718.

Galbraith, R.F., Roberts, R.G., Laslett, G.M., Yoshida, H., Olley, J.M., 1999. Optical dating of single and multiple grains of quartz from Jinmium Rock Shelter, northern Australia: Part I, experimental design and statistical models. Archaeometry 41, 339-364.

Garrett, D., 2004. Handbook of Lithium and Natural Calcium Chloride: Their Deposits, Processing, Uses, and Properties, 1st ed. Elsevier Academic Press, Amsterdam.

Gedroiz, K.K., 1912. Colloidal chemistry as related to soil science. I. Colloidal substances in the soil solution. Formation of sodium carbonate in the soil. Alkali soils and saline soils. Russian Journal of Experimental Agronomy 13, 363-412.

Gibb, R.G., Campbell, I.B., Claridge, G.G.C., 2002. 35 years of Ross Sea region soil studies on-line, in: Snape, I., Warren, R. (Eds.), Third International Conference on Contaminants in Freezing Ground. Australian Antarctic Division, Kingston, Tasmania, pp. 28-29.

Gibson, E.K., Wentworth, S.J., McKay, D.S., 1983. Chemical weathering and diagenesis of a cold desert soil from Wright Valley, Antarctica: an analog of Martian weathering processes, The Thirteenth Lunar and Planetary Science Conference. Journal of Geophysical Research, pp. A912-A928.

Gillies, J.A., Nickling, W.G., Tilson, M., 2008. Ventifacts and wind-abraded rock features in the Taylor Valley, Antarctica. Geomorphology 107, 149-160.

Glazovskaya, M.S., 1958. Weathering and primary soil formation in Antarctica. Scientific reports of Moscow University, Faculty of Geography 1, 63-76.

Godfrey-Smith, D.I., Huntley, D.J., Chen, W.H., 1988. Optical dating studies of quartz and feldspar sediment extracts. Quaternary Science Reviews 7, 373-380.

Gooseff, M.N., Barrett, J.E., Doran, P.T., Fountain, A., Lyons, W.B., Parsons, A., Porazinska, D., Virginia, R.A., Wall, D.H., 2003. Snow-patch Influence on soil biogeochemical processes and invertebrate distribution in the McMurdo Dry Valleys, Antarctica. Arctic, Antarctic, and Alpine Research 35, 91-99.

Gooseff, M.N., Barrett, J.E., Northcott, M.L., Bate, B.D., Hill, K.R., Zeglin, L.H., Bobb, M., Takacs-Vesbach, C.D., 2007. Controls on the spatial dimensions of wetted hydrologic margins of two Antarctic lakes. Vadose Zone Journal 6, 841-848.

Gooseff, M.N., Lyons, W.B., McKnight, D.M., Vaughan, B.H., Fountain, A.G., Dowling, C., 2006. A stable isotopic investigation of a polar desert hydrologic system, McMurdo Dry Valleys, Antarctica. Arctic, Antarctic, and Alpine Research 38, 60-71.

Graham, I.J., 2002. Dating Antarctic soils using atmosphere-derived $^{10}$Be and nitrate. Bulletin - Royal Society of New Zealand 35, 429-436.

Green, W.J., Angle, M.P., Chave, K.E., 1988. The geochemistry of Antarctic streams and their role in the evolution of four lakes of the McMurdo Dry Valleys. Geochimica et Cosmochimica Acta 52, 1265-1274.

Green, W.J., Canfield, D.E., 1984. Geochemistry of the Onyx River (Wright Valley, Antarctica) and its role in the chemical evolution of Lake Vanda. Geochimica et Cosmochimica Acta 48, 2457-2467.

Green, W.J., Gardner, T.J., Ferdelman, T.G., Angle, M.P., Varner, L.C., Nixon, P., 1989. Geochemical processes in the Lake Fryxell Basin (Victoria Land, Antarctica). Hydrobiologia 172, 129-148.

Gupta, R.K., Chhabra, R., Abrol, I.P., 1981. The relationship between pH and exchangeable sodium in a sodic soil. Soil Science 131, 215-219.

Hagedorn, B., Sletten, R.S., Hallet, B., McTigue, D.F., Steig, E.J., 2010. Ground ice recharge via brine transport in frozen soils of Victoria Valley, Antarctica: Insights from modeling $\delta^{18}O$ and δD profiles. Geochimica et Cosmochimica Acta 74, 435-448.

Hall, B.L., Denton, G.H., 2000. Radiocarbon chronology of Ross Sea Drift, eastern Taylor Valley, Antarctica: Evidence for a grounded ice sheet in the Ross Sea at the Last Glacial Maximum. Geografiska Annaler. Series A, Physical Geography 82, 305-336.

Hall, B.L., Denton, G.H., Fountain, A.G., Hendy, C.H., Henderson, G.M., 2010. Antarctic lakes suggest millennial reorganizations of Southern Hemisphere atmospheric and oceanic circulation. Proceedings of the National Academy of Sciences 107, 21355 -21359.

Hall, B.L., Denton, G.H., Hendy, C.H., 2000. Evidence from Taylor Valley for a grounded ice sheet in the Ross Sea, Antarctica. Geografiska Annaler. Series A, Physical Geography 82, 275-303.

Hall, B.L., Denton, G.H., Lux, D.R., Bockheim, J.G., 1993. Late Tertiary Antarctic paleoclimate and ice-sheet dynamics inferred from surficial deposits in Wright Valley. Geografiska Annaler. Series A, Physical Geography 75, 239-267.

Hall, B.L., Denton, G.H., Lux, D.R., Schlüchter, C., 1997. Pliocene paleoenvironment and Antarctic ice sheet behavior: Evidence from Wright Valley. The Journal of Geology 105, 285-294.

Hall, B.L., Denton, G.H., Overturf, B., 2001. Glacial Lake Wright, a high-level Antarctic lake during the LGM and early Holocene. Antarctic Science 13, 53-60.

Hall, B.L., Denton, G.H., Overturf, B., Hendy, C.H., 2002. Glacial Lake Victoria, a high level Antarctic Lake inferred from lacustrine deposits in Victoria Valley. Journal of Quaternary Science 17, 697-706.

Hall, B.L., Henderson, G.M., 2001. Use of uranium-thorium dating to determine past $^{14}C$ reservoir effects in lakes: examples from Antarctica. Earth and Planetary Science Letters 193, 565-577.

Hambrey, M.J., Fitzsimons, S.J., 2010. Development of sediment-landform associations at cold glacier margins, Dry Valleys, Antarctica. Sedimentology 57, 857-882.

Hardie, L.H., 1983. Origin of $CaCl_2$ brines by basalt-seawater interaction: Insights provided by some simple mass balance calculations. Contributions to Mineralogy and Petrology 82, 205-213.

Hardie, L.H., 1990. The roles of rifting and hydrothermal $CaCl_2$ brines in the origin of potash evaporites; an hypothesis. American Journal of Science 290, 43-106.

Hardie, L.H., Eugster, H.P., 1970. The evolution of closed-basin brines. Mineralogical Society of America Special Paper 3, 273-290.

Harris, H.J.H., Cartwright, K., 1979. Dynamic chemical equilibrium in a polar desert pond: A sensitive index of meteorological cycles. Science 204, 301 -303.

Harris, H.J.H., Cartwright, K., 1981. Hydrology of the Don Juan Basin, Wright Valley, Antarctica. Antarctic Research Series 33, 161-184.

Harris, K.J., Carey, A.E., Lyons, W.B., Welch, K.A., Fountain, A.G., 2007. Solute and isotope geochemistry of subsurface ice melt seeps in Taylor Valley, Antarctica. Geological Society of America Bulletin 119, 548-555.

Harwood, D., Levy, R., Cowie, J., Florindo, F., Naish, T., Powell, R., Pyne, A., 2006. Deep drilling with the ANDRILL program in Antarctica. Scientific Drilling 3.

Haskell, T.R., Kennett, J.P., Prebble, W.M., Smith, G., Willis, I.A.G., 1965. The geology of the Middle and Lower Taylor Valley of South Victoria Land, Antarctica. Transactions of the Royal Society of New Zealand - Geology 2, 169-186.

Hawke, R.M., McConchie, J.A., 2001. Bedload transport in a meltwater stream, Miers Valley, Antarctica: controls and prediction. New Zealand Journal of Hydrology 40, 1-18.

Head, J.W., Marchant, D.R., Dickson, J.L., Levy, J.S., Morgan, G.A., 2007. Slope streaks in the Antarctic Dry Valleys: Characteristics, candidate formation mechanisms, and implications for slope streak formation in the Martian environment, Seventh international conference on Mars. Lunar and Planetary Institute, Pasadena, CA.

Healy, M., Webster-Brown, J.G., Brown, K.L., Lane, V., 2006. Chemistry and stratification of Antarctic meltwater ponds II: Inland ponds in the McMurdo Dry Valleys, Victoria Land. Antarctic Science 18, 525-533.

Hendy, C.H., 2000. Late Quaternary lakes in the McMurdo Sound region of Antarctica. Geografiska Annaler. Series A, Physical Geography 82, 411-432.

Hendy, C.H., Hall, B.L., 2006. The radiocarbon reservoir effect in proglacial lakes: Examples from Antarctica. Earth and Planetary Science Letters 241, 413-421.

Hendy, C.H., Sadler, A.J., Denton, G.H., 2000. Proglacial lake-ice Conveyors: A new mechanism for deposition of drift in polar environments. Geografiska Annaler: Series A, Physical Geography 82, 249-270.

Herut, B., Starinsky, A., Katz, A., Bein, A., 1990. The role of seawater freezing in the formation of subsurface brines. Geochimica et Cosmochimica Acta 54, 13-21.

Higgins, S.M., Denton, G.H., Hendy, C.H., 2000. Glacial geomorphology of Bonney Drift, Taylor Valley, Antarctica. Geografiska Annaler. Series A, Physical Geography 82, 365-389.

Horsman, J.L., 2007. The origin of sandy terraces in eastern Taylor Valley, Antarctica, from Ground Penetrating Radar: A test of the Glacial Lake Washburn delta interpretation, Environmental Science and Policy. Plymouth State University, Plymouth, New Hampshire, p. 258.

Horsman, J.L., Prentice, M.L., Arcone, S.A., Delaney, A.J., 2007. Ground-Penetrating Radar studies of Late Pleistocene-Holocene lacustrine deltas in Lower Taylor Valley, Antarctica: Implications for lake history. Eos Trans. AGU 88, Fall Meet. Suppl., Abstract NS33A-08.

Howard, K.W.F., Lloyd, J.W., 1983. Major ion characterization of coastal saline ground waters. Ground Water 21, 429-437.

Hunt, H.W., Treonis, A.M., Wall, D.H., Virginia, R.A., 2007. A mathematical model for variation in water-retention curves among sandy soils. Antarctic Science 19, 427-436.

Huntley, D.J., Lamothe, M., 2001. Ubiquity of anomalous fading in K-feldspars and the measurement and correction for it in optical dating. Canadian Journal of Earth Sciences 38, 1093-1106.

Jackson, M.L., Lee, S.Y., Ugolini, F.C., Helmke, P.A., 1977. Age and uranium content of soil micas from Antarctica by the fission particle track replica method. Soil Science 123, 241-248.

Jones, L.M., Faure, G., 1978. A study of strontium isotopes in lakes and surficial deposits of the ice-free valleys, Southern Victoria Land, Antarctica. Chemical Geology 22, 107-120.

Katz, A., Starinsky, A., Marion, G.M., 2011. Saline waters in basement rocks of the Kaapvaal Craton, South Africa. Chemical Geology 289, 163-170.

Kelley, W.P., 1939. Effect of dilution on the water-soluble and exchangeable bases of alkali soils, and its bearing on the salt tolerance of plants. Soil Science 47, 367-375.

Kelley, W.P., 1951. Alkali Soils: Their Formation, Properties, and Reclamation. Reinhold, New York.

Kelley, W.P., Cummins, A.B., 1921. Chemical effect of salts on soils. Soil Science 11, 139-159.

Kellogg, D.E., Stuiver, M., Kellogg, T.B., Denton, G.H., 1980. Non-marine diatoms from Late Wisconsin perched deltas in Taylor Valley, Antarctica. Palaeogeography, Palaeoclimatology, Palaeoecology 30, 157-189.

Kelly, W.C., Zumberge, J.H., 1961. Weathering of a quartz diorite at Marble Point, McMurdo Sound, Antarctica. The Journal of Geology 69, 433-446.

Keys, J.R.H., 1980. Salts and their distribution in the McMurdo Region, Antarctica. Victoria University, Wellington, New Zealand.

Keys, J.R.H., Williams, K., 1981. Origin of crystalline, cold desert salts in the McMurdo region, Antarctica. Geochimica et Cosmochimica Acta 45, 2299-2309.

Knauth, L.P., Burt, D.M., 2002. Eutectic brines on Mars: Origin and possible relation to young seepage features. Icarus 158, 267-271.

Krause, W.E., Krbetschek, M.R., Stolz, W., 1997. Dating of quaternary lake sediments from the schirmacher oasis (East Antarctica) by infra-red stimulated luminescence (IRSL) detected at the wavelength of 560 NM. Quaternary Science Reviews 16, 387-392.

Krbetschek, M.R., Götze, J., Dietrich, A., Trautmann, T., 1997. Spectral information from minerals relevant for luminescence dating. Radiation Measurements 27, 695-748.

Kreslavsky, M.A., Head, J.W., 2009. Slope streaks on Mars: A new “wet” mechanism. Icarus 201, 517-527.

Krusic, A.G., 2009. Climatic implications of reconstructed early-mid Pliocene equilibrium-line altitudes in the McMurdo Dry Valleys, Antarctica. Annals of Glaciology 50, 31-36.

Lachenbruch, A.H., 1962. Mechanics of thermal contraction cracks and ice-wedge polygons in permafrost. Geological Society of America Special Papers 70.

Lamothe, M., Auclair, M., 1999. A solution to anomalous fading and age shortfalls in optical dating of feldspar minerals. Earth and Planetary Science Letters 171, 319-323.

Lancaster, N., 2002. Flux of eolian sediment in the McMurdo Dry Valleys, Antarctica: A preliminary assessment. Arctic, Antarctic, and Alpine Research 34, 318-323.

Land, L.S., 1998. Failure to precipitate dolomite at 25 °C from dilute solution despite 1000-fold oversaturation after 32 years. Aquatic Geochemistry 4, 361-368.

Langmuir, D., 1965. Stability of carbonates in the system $MgO-CO_2-H_2O$. The Journal of Geology 73, 730-754.

Langmuir, D., 1997. Aqueous environmental geochemistry. Prentice Hall, Upper Saddle River, NJ.

Larwrence, J.R., Gieskes, J.M., Broecker, W.S., 1975. Oxygen isotope and cation composition of DSDP pore waters and the alteration of layer II basalts. Earth and Planetary Science Letters 27, 1-10.

Lawrence, M.J.F., Hendy, C.H., 1989. Carbonate deposition and Ross Sea ice advance, Fryxell basin, Taylor Valley, Antarctica. New Zealand Journal of Geology and Geophysics 32, 267-278.

Lepper, K., Larsen, N.A., McKeever, S.W.S., 2000. Equivalent dose distribution analysis of Holocene eolian and fluvial quartz sands from Central Oklahoma. Radiation Measurements 32, 603-608.

Lerman, A., 1970. Chemical equilibria and evolution of chloride brines, in: Morgan, B.A. (Ed.), 50th Anniversary Symposium Mineralogical Society Special Paper, pp. 291-306.

Levy, J.S., Fountain, A.G., Gooseff, M.N., Welch, K.A., Lyons, W.B., 2011. Water tracks and permafrost in Taylor Valley, Antarctica: Extensive and shallow groundwater connectivity in a cold desert ecosystem. Geological Society of America Bulletin.

Levy, J.S., Fountain, A.G., Welch, K.A., Lyons, W.B., 2012. Hypersaline “wet patches” in Taylor Valley, Antarctica. Geophysical Research Letters 39.

Linkletter, G.O., 1972. Weathering and soil formation in the dry valleys of Southern Victoria Land: A possible origin for the salts in the soils. Antarctic Geol. Geophys. Symp. Antarct. Geol. Solid Earth Geophys Ser. B, 441–446.

Lyons, W.B., Mayewski, P.M., 1993. The geochemical evolution of terrestrial waters in the Antarctic: The role of rock-water interactions, in: Green, W.J., Friedman, E.I. (Eds.), Physical and Biogeochemical Preocesses in Antarctic Lakes. American Geophysical Union, Washington, D. C., pp. 135-143.

Lyons, W.B., Nezat, C.A., Benson, L.V., Bullen, T.D., Graham, E.Y., Kidd, J., Welch , K.A., Thomas, J.M., 2002. Strontium isotopic signatures of the streams and lakes of Taylor

Valley, Southern Victoria Land, Antarctica: Chemical weathering in a polar climate. Aquatic Geochemistry 8, 75-95.

Lyons, W.B., Tyler, S.W., Wharton, R.A., McKnight, D.M., Vaughn, B.H., 1998a. A Late Holocene desiccation of Lake Hoare and Lake Fryxell, McMurdo Dry Valleys, Antarctica. Antarctic Science 10, 247-256.

Lyons, W.B., Welch , K.A., 1997. Lithium in waters of a polar desert. Geochimica et Cosmochimica Acta 61, 4309-4319.

Lyons, W.B., Welch, K.A., Fountain, A.G., Dana, G.L., Vaughn, B.H., McKnight, D.M., 2003. Surface glaciochemistry of Taylor Valley, southern Victoria Land, Antarctica and its relationship to stream chemistry. Hydrological processes. 17, 115-130.

Lyons, W.B., Welch, K.A., Gardner, C.B., Jaros, C., Moorhead, D.L., Knoepfle, J.L., Doran, P.T., 2011. The geochemistry of upland ponds, Taylor Valley, Antarctica. Antarctic Science, 1-12.

Lyons, W.B., Welch, K.A., Neumann, K., Toxey, J.K., McArthur, R., Williams, C., McKnight, D.M., Moorhead, D.L., 1998b. Geochemical linkages among glaciers, streams, and lakes within the Taylor Valley, Antarctica, in: Priscu, J.C. (Ed.), Ecosystem Dynamics in a Polar Desert: The McMurdo Dry Valleys, Antarctica. American Geophysical Union, Washington, D. C., pp. 77-92.

Lyons, W.B., Welch, K.A., Snyder, G., Olesik, J., Graham, E.Y., Marion, G.M., Poreda, R.J., 2005. Halogen geochemistry of the McMurdo dry valleys lakes, Antarctica: Clues to the origin of solutes and lake evolution. Geochimica et Cosmochimica Acta 69, 305-323.

Malcolm, R.L., Kennedy, V.C., 1970. Variation of cation exchange capacity and rate with particle size in stream sediment. Journal (Water Pollution Control Federation) 42, 153-160.

Marchant, D.R., Denton, G.H., 1996. Miocene and Pliocene paleoclimate of the Dry Valleys region, Southern Victoria land: A geomorphological approach. Marine Micropaleontology 27, 253-271.

Marchant, D.R., Denton, G.H., Bockheim, J.G., Wilson, S.C., Kerr, A.R., 1994. Quaternary changes in level of the upper Taylor Glacier, Antarctica: Implications for paleoclimate and East Antarctic Ice Sheet dynamics. Boreas 23, 29-43.

Marchant, D.R., Denton, G.H., Swisher, C.C., 1993. Miocene-Pliocene-Pleistocene glacial history of Arena Valley, Quartermain Mountains, Antarctica. Geografiska Annaler. Series A, Physical Geography 75, 269-302.

Marchant, D.R., Denton, G.H., Swisher, C.C., Potter, N., 1996. Late Cenozoic Antarctic paleoclimate reconstructed from volcanic ashes in the Dry Valleys region of southern Victoria Land. Geological Society of America Bulletin 108, 181-194.

Marchant, D.R., Lewis, A.R., Phillips, W.M., Moore, E.J., Souchez, R.A., Denton, G.H., Sugden, D.E., Potter, N.J., Landis, G.P., 2002. Formation of patterned ground and sublimation till over Miocene glacier ice in Beacon Valley, southern Victoria Land, Antarctica. GSA Bulletin 114, 718-730.

Marion, G.M., 1997. A theoretical evaluation of mineral stability in Don Juan Pond, Wright Valley, Victoria Land. Antarctic Science 9, 92-99.

Marion, G.M., 2001. Carbonate mineral solubility at low temperatures in the Na-K-Mg-Ca-H-Cl-$SO_4$-OH-$HCO_3$-$CO_3$-$CO_2$-$H_2O$ system. Geochimica et Cosmochimica Acta 65, 1883–1896.

Marion, G.M., 2002. A molal-based model for strong acid chemistry at low temperatures (<200 to 298°K). Geochimica et Cosmochimica Acta 66, 2499–2516.

Marion, G.M., 2007. Adapting molar data (without density) for molal models. Computers & Geosciences 33, 829-834.

Marion, G.M., Farren, R.E., 1999. Mineral solubilities in the Na-K-Mg-Ca-Cl-$SO_4$-$H_2O$ system: A re-evaluation of the sulfate chemistry in the Spencer-Møller-Weare model. Geochimica et Cosmochimica Acta 63, 1305–1318.

Marion, G.M., Farren, R.E., Komrowski, A.J., 1999. Alternative pathways for seawater freezing. Cold Regions Science and Technology 29, 259-266.

Marion, G.M., Grant, S.A., 1994. FREZCHEM: A chemical-thermodynamic model for aqueous solutions at subzero temperatures. Cold Regions Research and Engineering Lab, Hanover, NH.

Marion, G.M., Kargel, J.S., 2008. Cold aqueous planetary geochemistry with FREZCHEM: From modeling to the search for life at the limits. Springer, Berlin/Heidelberg.

Marion, G.M., Mironenko, M.V., Robers, M.W., 2010. FREZCHEM: A geochemical model for cold aqueous solutions. Computers & Geosciences 36, 10-15.

Marion, G.M., Verburg, P.S.J., McDonald, E.V., Arnone, J.A., 2008. Modeling salt movement through a Mojave Desert soil. Journal of Arid Environments 72, 1012-1033.

Martion, H.W., Sparks, D.L., 1985. On the behavior of nonexchangeable potassium in soils. Communications in Soil Science and Plant Analysis 16, 133-162.

Matsubaya, O., Sakai, H., Torii, T., Burton, H., Kerry, K., 1979a. Antarctic saline lakes—Stable isotopic ratios, chemical compositions and evolution. Geochimica et Cosmochimica Acta 43, 7-25.

Matsubaya, O., Sakai, H., Torii, T., Burton, H., Kerry, K., 1979b. Antarctic saline lakes - stable isotopic ratios,chemical compositions and evolution. Geochimica et Cosmochimica Acta 43, 7-25.

Maurice, P.A., McKnight, D.M., Leff, L., Fulghum, J.E., Gooseff, M.N., 2002. Direct observations of aluminosilicate weathering in the hyporheic zone of an Antarctic Dry Valley stream. Geochimica et Cosmochimica Acta 66, 1335–1134.

Mayya, Y.S., Morthenkai, P., Murari, M.K., Singhvi, A.K., 2006. Towards quantifying beta microdosimetric effects in single-grain quartz dose distribution. Radiation Measurements 41, 132-1039.

McBride, M.B., 1994. Environmental Chemistry of Soils. Oxford University Press, New York.

McKay, C.P., Mellon, M.T., Friedmann, E.I., 1998. Soil temperatures and stability of ice-cemented ground in the McMurdo Dry Valleys, Antarctica. Antarctic Science 10, 31-38.

McKnight, D.M., Alger, A., Shupe, T.G., Spaulding, S.A., 1998. Longitudinal patterns in algal abundance and species distribution in meltwater streams in Taylor Valley, southern Victoria Land, Antarctica. Antarctic Research Series 72, 109-127.

McKnight, D.M., Niyogi, D.K., Alger, A.S., Bomblies, A., Conovitz, P.A., Tate, C.M., 1999. Dry Valley streams in Antarctica: Ecosystems waiting for water. BioScience 49, 985-995.

McKnight, D.M., Tate, C.M., Andrews, E.D., Niyogi, D.K., Cozzetto, K., Welch , K.A., Lyons, W.B., Capone, D.G., 2007. Reactivation of a cryptobiotic stream ecosystem in the McMurdo Dry Valleys, Antarctica: A long-term geomorphological experiment. Geomorphology 89, 186-204.

Mejdahl, V., 1983. Feldspar inclusion dating of ceramics and burnt stones. European PACT Journal, 351-364.

Michalski, G., Bockheim, J.G., Kendall, C., Thiemens, M., 2005. Isotopic composition of Antarctic Dry Valley nitrate: Implications for $NO_y$ sources and cycling in Antarctica. Geophysical Research Letters 32.

Mikucki, J.A., Foreman, C.M., Sattler, B., Lyons, W.B., Priscu, J.C., 2004. Geomicrobiology of Blood Falls: An iron-rich saline discharge at the terminus of the Taylor Glacier, Antarctica. Aquatic Geochemistry 10, 199–220.

Miller, E.A., 2006. A qualitative approach to understanding the rate of weathering, Taylor Valley, Antarctica. The Ohio State University.

Mondésir, P., 1888. Sur le rôle du pouvoir des terres dans la formation des carbonates des soude naturels. Comptes Rendus 160, 459-462.

Morikawa, H., Minato, I., Ossaka, J., Hayashi, T., 1975. The distribution of secondary minerals and evaporites at Lake Vanda, Victoria Land, Antarctica. Memoirs of National Institute of Polar Research. Special issue 4, 45-59.

Morse, D.L., Waddington, E.D., Marshall, H.P., Neumann, T.A., Steig, E.J., Dibb, J.E., Winebrenner, D.P., Arthern, R.J., 1999. Accumulation rate measurements at Taylor Dome, East Antarctica: Techniques and strategies for mass balance measurements in polar environments. Geografiska Annaler: Series A, Physical Geography 81, 683-694.

Mosley, M.P., 1988. Bedload transport and sediment yield in the Onyx River, Antarctica. Earth Surface Processes and Landforms 13, 51-67.

Mudrey, M.G.J., Torii, T., Harris, H.J.H., 1975. Geology of DVDP 13; Don Juan Pond, Wright Valley, Antarctica. Bulletin - Dry Valley Drilling Project 5, 78-93.

Murray, A.S., Olley, J.M., 2002. Precision and accuracy in the optically stimulated luminescence dating of sedimentary quartz: A status review. Geochronometria 21, 1-16.

Murray, A.S., Wintle, A.G., 2000. Luminescence dating of quartz using an improved single-aliquot regenerative-dose protocol. Radiation Measurements 32, 57-73.

Murrmann, R.P., 1973. Ionic Mobility in Permafrost. National Academy of Science Press, Washington, DC, Yakutsk, U.S.S.R., pp. 352-359.

Nakaya, S., Motoori, Y., Nishimura, M., 1979. One aspect of the evolution of saline lakes in the dry valleys of South Victoria Land, Antarctica, Proceedings of the Seminar III on Dry Valley Drilling Project. National Institute of Polar Research, Tokyo, Japan, pp. 49-52.

Nathan, R.P., Thomas, P.J., Jain, M., Murray, A.S., Rhodes, E.J., 2003. Environmental dose rate heterogeneity of beta radiation and its implications for luminescence dating: Monte Carlo modelling and experimental validation. Radiation Measurements 37, 305-313.

Nezat, C.A., Lyons, W.B., Welch, K.A., 2001. Chemical weathering in streams of a polar desert (Taylor Valley, Antarctica). Geological Society of America Bulletin 113.

Ng, F., Hall, B., Sletten, R.S., Stone, J.O., 2005a. Fast-growing till over ancient ice in Beacon Valley, Antarctica. Geology 33, 121-124.

Ng, F., Hallet, B., Sletten, R.S., Stone, J.O., 2005b. Fast-growing till over ancient ice in Beacon Valley, Antarctica. Geology 33.

Nishiyama, T., Kurasawa, H., 1975. Distribution of secondary minerals from Taylor Valley. Bulletin - Dry Valley Drilling Project, 120-133.

Nordstrom, D.K., Ball, J.A., Donahoe, R.J., Whittemore, D., 1989. Groundwater chemistry and water-rock interactions at Stripa. Geochimica et Cosmochimica Acta 53, 1727-1740.

Northcott, M.L., Gooseff, M.N., Barrett, J.E., Zeglin, L.H., Takacs-Vesbach, C.D., Humphrey, J., 2009. Hydrologic characteristics of lake- and stream-side riparian wetted margins in the McMurdo Dry Valleys, Antarctica. Hydrological processes. 23, 1255-1267.

Nylen, T.H., Fountain, A.G., Doran, P.T., 2004. Climatology of katabatic winds in the McMurdo dry valleys, southern Victoria Land, Antarctica. Journal of Geophysical Research 109.

Olley, J.M., Caitcheon, G., Murray, A.S., 1998. The distribution of apparent dose as determined by optically stimulated luminescence in small aliquots of fluvial quartz: Implications for dating young sediments. Quaternary Geochronology 17, 1033-1040.

Olley, J.M., Caitcheon, G.G., Roberts, R.G., 1999. The origin of dose distributions in fluvial sediments, and the prospect of dating single grains from fluvial deposits using optically stimulated luminescence. Radiation Measurements 30, 207-217.

Olley, J.M., Pietsch, T., Roberts, R.G., 2004. Optical dating of Holocene sediments from a variety of geomorphic settings using single grains of quartz. Geomorphology 60, 337-358.

Parkhurst, D.L., Appelo, C.A.J., 1999. User's guide to PHREEQC (version 2) - A computer program for speciation, reaction-path, 1D-transport, and inverse geochemical calculations, pp. 99-4259.

Pastor, J., Bockheim, J.G., 1980. Soil development on moraines of Taylor Glacier, Lower Taylor Valley, Antarctica. Soil Science Society of America Journal 44, 341-348.

Petit, J.R., Jouzel, J., Raynaud, D., Barkov, N.I., Barnola, J.M., Basile, I., Bender, M., Chappellaz, J., Davis, J., Delaygue, G., Delmotte, M., Kotlyakov, V.M., Legrand, M., Lipenkov, V., Lorius, C., Pépin, L., Ritz, C., Saltzman, E., Stievenard, M., 2001. Vostok

ice core data for 420,000 years, in: Program, N.N.P. (Ed.). World Data Center for Paleoclimatology Data, Boulder CO, USA.

Péwé, T.L., 1960. Multiple glaciation in the McMurdo Sound Region, Antarctica: A progress report. The Journal of Geology 68, 498-514.

Pitzer, K., 1981. Characteristics of very concentrated aqueous solutions, Physics and Chemistry of the Earth, pp. 249-272

Poage, M.A., Barrett, J.E., Virginia, R.A., Wall, D.H., 2008. The influence of soil beochemistry on nematode distribution, McMurdo Dry Valleys, Antarctica. Arctic, Antarctic, and Alpine Research 40, 119-128.

Poreda, R.J., Hunt, A.G., Lyons, W.B., Welch, K.A., 2004. The helium isotopic chemistry of Lake Bonney, Taylor Valley, Antarctica: Timing of late Holocene climate change in Antarctica. Aquatic Geochemistry 10, 353-371.

Prentice, M.L., Arcone, S.A., Horsman, J.L., Medley, E., Toner, J.D., Sletten, R., Shoemaker, K., 2009. Response of the Ross Sea Ice Sheet to the last deglaciation: New evidence from Taylor Valley, Antarctica. Eos Trans. AGU 90, Fall Meet. Suppl., Abstract C23A-0492.

Quayle, W.C., 2002. Extreme responses to climate change in Antarctic lakes. Science 295, 645-645.

Rankin, A.M., Auld, V., Wolff, E.W., 2000. Frost flowers as a source of fractionated sea salt aerosol in the polar regions. Geophysical Research Letters 27, 3469-3472.

Rawls, W.J., 1983. Estimating soil bulk density from particle size analysis and organic matter content. Soil Science 135, 123-125.

Reitemeier, R.F., 1946. Effect of moisture content on the dissolved and exchangeable ions of soils of arid regions. Soil Science 61, 195-214.

Rittenour, T.M., 2008. Luminescence dating of fluvial deposits: Applications to geomorphic, palaeoseismic, and archaeological research. Boreas 37, 613-635.

Rodnight, H., 2008. How many equivalent dose values are needed to obtain a reproducible distribution? . Ancient TL 26, 3-9.

Sanford, W.E., Wood, W.W., Councell, T.B., 1992. Calcium chloride-dominated brines: An ion-exchange model, in: Kharaka, Y.K., Maest, A.S. (Eds.), 7th international symposium on Water-rock interaction. International Association of Geochemistry and Cosmochemistry and Alberta Research Council, Sub-Group on Water-Rock Interaction, Park City, UT, pp. 669-672.

Schofield, R.K., 1947. A ratio law governing the equilibrium of cations in the soil solution, Proceedings of the Xlth International Congress of Pure and Applied Chemistry, pp. 257-261.

Scott, R.F., 1905. The Voyage of the Discovery. Smith Elder, London.

Seybold, C.A., Balks, M.R., Harms, D.S., 2010. Characterization of active layer water contents in the McMurdo Sound region, Antarctica. Antarctic Science 22, 633-645.

Seyfried, W.E.J., Bischoff, J.L., 1979. Low temperature basalt alteration by seawater: An experimental study at 70°C and 150°C. Geochimica et Cosmochimica Acta 43, 1937-1947.

Shainberg, I., Kemper, W.D., 1966. Hydration stats of adsorbed cations. Soil Science Society of America Proceedings 30, 707-713.

Shaw, J., Healy, T.R., 1980. Morphology of the Onyx River system, McMurdo Sound region, Antarctica. New Zealand Journal of Geology and Geophysics 23, 223-238.

Shouakar-Stash, O., Alexeev, S.V., Frape, S.K., Alexeeva, L.P., Drimmie, R.J., 2007. Geochemistry and stable isotopic signatures, including chlorine and bromine isotopes, of the deep groundwater. Applied Geochemistry 22, 589-605.

Sletten, R.S., Hallet, B., Fletcher, R.C., 2003. Resurfacing time of terrestrial surfaces by the formation and maturation of polygonal patterned ground. Journal of Geophysical Research 108.

Smettan, B.U., Blume, K.H.P., 1987. Salts in sandy desert soils, southwestern Egypt. Catena 14, 333-343.

Smith, R.I.L., 1994. Vascular plants as bioindicators of regional warming in Antarctica. Oecologia 99, 322-328.

Speirs, J.C., Steinhoff, D.F., McGowan, H.A., Bromwich, D.H., Monaghan, A.J., 2010. Foehn winds in the McMurdo Dry Valleys, Antarctica: The origin of extreme warming events. Journal of Climate 23, 3577–3598.

Spencer, R.J., Møller, N., Weare, J.H., 1990. The prediction of mineral solubilities in natural waters: A chemical equilibrium model for the Na-K-Ca-Mg-Cl-$SO_4$-$H_2O$ system at temperatures below 25°C. Geochimica et Cosmochimica Acta 54, 575-590.

Spigel, R.H., Priscu, J.C., 1998. Physical limnology of the McMurdo Dry Valley lakes, in: Priscu, J.C. (Ed.), Ecosystem dynamics in a polar desert: The McMurdo Dry Valleys, Antarctica. AGU, Washington, D. C., pp. 153-188.

Spooner, N.A., 1994. The anomalous fading of infrared-stimulated luminescence from feldspars. Radiation Measurements 23, 625-632.

Staff, S.S., 2010. Keys to Soil Taxonomy, 11th ed. USDA-Natural Resources Conservation Service, Washington, D. C.

Starinsky, A., Katz, A., 2003. The formation of natural cryogenic brines. Geochimica et Cosmochimica Acta 67, 1475-1484.

Steig, E.J., Hart, C., While, J.W.C., Cunningham, W.L., Davis, M.D., Saltzman, E.S., 1998. Changes in climate, ocean and ice sheet conditions in the Ross Embayment at 6 ka. Annals of Glaciology 27, 305-310.

Steig, E.J., Morse, D.L., Waddington, E.D., Stuiver, M., Grootes, P.M., Mayewski, P.A., Twickler, M.S., Whitlow, S.I., 2000. Wisconsinan and Holocene climate history from an ice core at Taylor Dome, western Ross Embayment, Antarctica. Geografiska Annaler: Series A, Physical Geography 82, 213-235.

Steig, E.J., Schneider, D.P., Rutherford, S.D., Mann, M.E., Comiso, J.C., Shindell, D.T., 2009. Warming of the Antarctic ice-sheet surface since the 1957 International Geophysical Year. Nature 475, 459-462.

Stotler, R.L., Frape, S.K., Ruskeeniemi, T., Ahonen, L., Onstott, T.C., Hobbs, M.Y., 2009. Hydrogeochemistry of groundwaters in and below the base of thick permafrost at Lupin, Nunavut, Canada. Journal of Hydrology 373, 80-95.

Stuiver, M., Denton, G.H., Hughes, T.J., Fastook, J.L., 1981. History of the marine ice sheet in West Antarctica during the last glaciation: A working hypothesis, in: Denton, G.H., Hughes, T.J. (Eds.), The Last Great Ice Sheets. John Wiley and Sons, New York, pp. 319-436.

Sugden, D.E., Marchant, D.R., Potter, N., Souches, R.A., Denton, G.H., Swisher, C.C., Tison, J.-L., 2002a. Preservation of Miocene glacier ice in East Antarctica. Nature 376, 412 - 414.

Sugden, D.E., Marchant, D.R., Potter, N.J., Souchez, R.A., Denton, G.H., Swisher, C.C.I., Tison, J.-L., 2002b. Preservation of Miocene glacier ice in East Antarctica. Nature 376, 412-414.

Takahashi, H.A., Wada, H., Nakamura, T., Miura, H., 1999. $^{14}C$ anomaly of freshwater algae in Antarctic coastal ponds and lakes. Polar Geoscience 12, 248-257.

Thiemens, M.H., 2001. The mass-independent ozone isotope effect. Science 293.

Thompsen, K.J., Murray, A.S., Bøtter-Jensen, L., 2007. Determination of burial dose in incompletely bleached fluvial samples using single grains of quart. Radiation Measurements 42, 370-379.

Thrasher, I.M., Mauz, B., Chiverrell, R.C., Lang, A., 2009. Luminescence dating of glaciofluvial deposits: A review. Earth-Science Reviews 97, 133-146.

Toner, J.D., Feathers, J.K., Sletten, R.S., 2012a. Optically stimulated luminescence ages of fluvial terraces in Taylor Valley, Antarctica. In preparation for Earth and Planetary Science Letters.

Toner, J.D., Sletten, R.S., 2012. The formation of Ca-Cl enriched groundwaters in the Dry Valleys of Antarctica by cation exchange reactions: Field measurements and modeling of reactive transport. Submitted to Geochimica et Cosmochimica Acta.

Toner, J.D., Sletten, R.S., Prentice, M.L., 2012b. Soluble salt accumulations in Taylor Valley, Antarctica: Implications for paleolakes and Ross Sea Ice Sheet dynamics. Submitted to the Journal of Geophysical Research.

Toride, N., Inoue, M., Leij, F.J., 2003. Hydrodynamic dispersion in an unsaturated dune sand. Soil Science Society of America Journal 67, 703-712.

Torii, T., Yamagata, N., Ossaka, J., Murata, S., 1977. Salt balance in the Don Juan Basin. Antarctic record 58, 116-130.

Ugolini, F.C., Anderson, D.M., 1973. Ionic migration and weathering in frozen Antarctic soils. Soil Science 115, 461-470.

Ugolini, F.C., Bockheim, J., 2008. Antarctic soils and soil formation in a changing environment: A review. Geoderma 144, 1-8.

Ugolini, F.C., Jackson, M.L., 1982. Weathering and mineral synthesis in Antarctic soils, in: Craddock, C. (Ed.), Third symposium on Antarctic geology and geophysics. International Union of Geological Sciences, Madison, WI, pp. 1101-1108.

Wagenbach, D., Ducroz, F., Mulvaney, R., Keck, L., Minikin, A., Legrand, M., Hall, J., Wolff, E., 1998. Sea-salt aerosol in coastal Antarctic regions. Journal of Geophysical Research 103, 10961-10974.

Wagner, B., Melles, M., Doran, P.T., Kenig, F., S.L., F., Pierau, R., Allan, P., 2006. Glacial and postglacial sedimentation in the Fryxell basin, Taylor Valley, southern Victoria Land, Antarctica. Palaeography, Palaeoclimatology, Palaeoecology 341, 320-337.

Wagner, B., Ortlepp, S., Doran, P.T., Kenig, F., Melles, M., Burkemper, A., 2011. The Holocene environmental history of Lake Hoare, Taylor Valley, Antarctica, reconstructed from sediment cores. Antarctic Science 23, 307-319.

Wallinga, J., 2002. Optically stimulated luminescence dating of fluvial deposits: A review. Boreas 31, 303-322.

Wallinga, J., Murray, A.S., Duller, G.A., T, Törnqvist, T.E., 2001. Testing optically stimulated luminescence dating of sand-sized quartz and feldspar from fuvial deposits. Earth and Planetary Science Letters 193, 617-630.

Wallinga, J., Murray, A.S., Wintle, A.G., 2000. The single-aliquot regenerative-dose (SAR) protocol applied to coarse-grain feldspar. Radiation Measurements 32, 529-533.

Webster, J., Webster, K., Nelson, P., Waterhouse, E., 2003. The behaviour of residual contaminants at a former station site, Antarctica. Environmental Pollution 123, 163-179.

Webster, J.G., Goguel, R.L., 1988. Anions and alkali metals in Lake Vanda, Don Juan Pond and the Onyx River: Further indications of brine origin. Antarctic Journal of the United States 23, 154-156.

Welch, K.A., Lyons, W.B., Whisner, C., Gardner, C.B., Gooseff, M.N., McKnight, D.M., Priscu, J.C., 2010. Spatial variations in the geochemistry of glacial meltwater streams in the Taylor Valley, Antarctica. Antarctic Science 22, 662-672.

Wharton, R.A.J., Parker, B.C., Simmons, G.M., Jr., 1983. Distribution, species, composition, and morphology of algal mats in Antarctic Dry Valley lakes. Phycologia 22, 355-365.

Whittaker, T.E., Hall, B.L., Hendy, C.H., Spaulding, S.A., 2008. Holocene depositional environments and surface-level changes at Lake Fryxell, Antarctica. Holocene 18, 775-786.

Wilch, T.I., Denton, G.H., Lux, D.R., McIntosh, W.C., 1993. Limited Pliocene glacier extent and surface uplift in middle Taylor Valley, Antarctica. Geografiska Annaler. Series A, Physical Geography 75, 331–351.

Wilson, A.T., 1964. Evidence from chemical diffusion of a climatic change in the McMurdo Dry Valleys 1,200 years ago. Nature 201, 176-177.

Wilson, A.T., 1979. Geochemical problems of the Antarctic dry areas. Nature 280, 205-208.

Wintle, A.G., 1973. Anomalous fading of thermo-luminescence in mineral samples. Nature 245, 143 - 144.

Wintle, A.G., Murray, A.S., 2006. A review of quartz optically stimulated luminescence characteristics and their relevance in single-aliquot regeneration dating protocols. Radiation Measurements 41, 369-391.

Witherow, R.A., Lyons, W.B., Bertler, N.A.N., Welch, K.A., Mayewski, P.A., Sneed, S.B., Nylen, T., Handley, M.J., Fountain, A., 2006. The aeolian flux of calcium, chloride, and nitrate to the McMurdo Dry Valleys landscape: Evidence from snow pit analysis. Antarctic Science 18, 497-505.

Wynn-Williams, D.D., Cabrol, N.A., Grin, E.A., Haberle, R.M., Stoker, C.R., 2001. Brines in seepage channels as eluants for subsurface relict biomolecules on Mars? Astrobiology 1, 165-184.

# Appendix A

## Complete Dataset for 2006-2007 Soil Pits

Table A.1. Soluble salt data from the 1:25 soil-water extractions. Also included is the gravimetric water content ($H_2O$) measured by oven drying, the pH measured in 1:2 soil-water solutions, and the <2 mm fraction.

| # | Pit | Latitude | Longitude | Elevation | Horizon | Thickness | $H_2O$ | <2 mm | >2 mm | pH | Ca | Mg | Na | K | Cl | $SO_4$ | $NO_3$ | $HCO_3$ | F | B | Ba | Sr | Charge Balance |
|---|---|---|---|---|---|---|---|---|---|---|---|---|---|---|---|---|---|---|---|---|---|---|---|
| | | | | m | | cm | ——%Wt.—— | | | | ——————————mmol $kg^{-1}$—————————— | | | | | | | | | ——µmol $kg^{-1}$—— | | | % |
| 1 | S004 | -77.62353 | 163.10605 | 22 | DP | 1.5 | | 14 | 86 | 9.7 | 11.5 | 1.6 | 5.7 | 2.1 | 2.4 | 0.3 | 0.0 | 27.9 | 0.4 | 85.3 | 0.4 | 20.0 | 4.1 |
| 4 | S004 | -77.62353 | 163.10605 | 22 | C1 | 4 | | 73 | 27 | 9.9 | 8.6 | 1.7 | 6.8 | 3.1 | 0.7 | 0.3 | 0.0 | 28.0 | 0.4 | 70.8 | 0.5 | 17.1 | 1.4 |
| 7 | S004 | -77.62353 | 163.10605 | 22 | C2 | 15 | | 91 | 9 | 10.0 | 6.2 | 1.6 | 10.3 | 2.1 | 3.9 | 0.5 | 0.0 | 23.6 | 0.3 | 58.7 | 0.6 | 15.1 | 1.4 |
| 10 | S004 | -77.62353 | 163.10605 | 22 | ICS | 1 | | 100 | | 9.2 | 6.3 | 2.2 | 25.3 | 3.1 | 0.6 | 0.3 | 0.0 | 39.1 | 0.4 | 58.0 | 0.4 | 21.1 | 5.5 |
| 12 | S004 | -77.62353 | 163.10605 | 22 | throat | | | 45 | 55 | 9.7 | 6.7 | 1.6 | 3.2 | 2.0 | 0.6 | 0.2 | 0.0 | 21.8 | 0.3 | 30.7 | 0.9 | 15.8 | 3.2 |
| 15 | S004 | -77.62353 | 163.10605 | 22 | wedge | | | 96 | 4 | 10.2 | 3.2 | 1.5 | 17.3 | 2.5 | 3.7 | 0.3 | 0.0 | 23.8 | 0.4 | 63.7 | 0.8 | 11.7 | 1.4 |
| 17 | S005 | -77.63484 | 163.07652 | 111 | DP | 1 | | 27 | 73 | 9.5 | 11.0 | 2.0 | 15.5 | 4.8 | 4.5 | 2.4 | 0.0 | 33.2 | 0.3 | 99.1 | 0.3 | 18.8 | 4.0 |
| 20 | S005 | -77.63484 | 163.07652 | 111 | C1 | 7 | | 95 | 5 | 9.8 | 6.4 | 4.4 | 56.3 | 10.2 | 19.4 | 2.9 | 0.5 | 48.5 | 0.9 | 392.5 | 0.7 | 14.9 | 8.0 |
| 23 | S005 | -77.63484 | 163.07652 | 111 | C2 | 14 | | 67 | 33 | 9.9 | 7.5 | 2.7 | 5.8 | 2.7 | 0.8 | 0.2 | 0.0 | 27.4 | 0.3 | 36.2 | 0.6 | 19.1 | 0.2 |
| 26 | S005 | -77.63484 | 163.07652 | 111 | C3 | 7 | | 95 | 5 | 9.7 | 3.7 | 2.1 | 4.7 | 2.3 | 0.8 | 0.1 | 0.0 | 18.2 | 0.3 | 42.4 | 0.8 | 11.7 | 2.5 |
| 34 | S002 | -77.62904 | 163.09771 | 46 | salt #1 | ? | | 41 | 59 | 9.9 | 4.8 | 1.9 | 8.5 | 3.8 | 1.5 | 0.5 | 0.0 | 23.0 | 0.4 | 106.0 | 0.6 | 11.5 | 0.1 |
| 38 | S002 | -77.62904 | 163.09771 | 46 | salt #2 | 13.4 | | 91 | 9 | 10.0 | 4.1 | 1.0 | 49.2 | 10.1 | 15.1 | 0.9 | 0.0 | 49.1 | 0.5 | 142.1 | 0.0 | 5.2 | 2.1 |
| 41 | S012 | -77.62341 | 163.11014 | 19 | salt #1 | 16.7 | | 68 | 32 | 9.2 | 4.8 | 1.3 | 4.8 | 1.4 | 3.5 | 0.7 | 0.0 | 15.0 | 0.3 | 31.4 | 0.7 | 14.6 | 4.8 |
| 44 | S012 | -77.62341 | 163.11014 | 19 | salt #2 | 14.7 | | 77 | 23 | 9.3 | 5.1 | 1.3 | 4.8 | 1.3 | 2.9 | 0.6 | 0.0 | 17.6 | 0.3 | 19.6 | 0.6 | 15.2 | 7.2 |
| 47 | S012 | -77.62341 | 163.11014 | 19 | salt #3 | 15.6 | | 82 | 18 | 9.2 | 4.0 | 1.2 | 4.1 | 1.2 | 2.8 | 0.2 | 0.0 | 13.8 | 0.3 | 29.2 | 0.5 | 12.9 | 5.6 |
| 50 | S004 | -77.62353 | 163.10605 | 22 | salt #1 | 13.8 | | 75 | 25 | 10.2 | 5.2 | 1.7 | 39.0 | 2.6 | 6.5 | 6.5 | 0.0 | 33.4 | 0.8 | 548.4 | 1.0 | 12.7 | 1.8 |
| 53 | S004 | -77.62353 | 163.10605 | 22 | salt #2 | 15.2 | | 78 | 22 | 9.2 | 7.7 | 2.4 | 14.0 | 2.5 | 6.1 | 2.4 | 0.0 | 25.4 | 0.4 | 97.6 | 1.1 | 21.9 | 0.1 |
| 56 | S004 | -77.62353 | 163.10605 | 22 | salt #3 | 11.2 | | 62 | 38 | 10.3 | 6.7 | 1.6 | 17.0 | 2.8 | 2.5 | 0.6 | 0.0 | 30.1 | 0.5 | 301.9 | 0.0 | 15.1 | 2.9 |
| 59 | S008 | -77.62638 | 163.11592 | 41 | salt #1 | 14 | | 88 | 12 | 10.2 | 6.0 | 1.5 | 12.6 | 3.4 | 2.6 | 0.7 | 0.0 | 27.2 | 0.5 | 27.2 | 1.0 | 14.3 | 0.8 |
| 62 | S008 | -77.62638 | 163.11592 | 41 | salt #2 | 12.5 | | 77 | 23 | 10.3 | 8.1 | 1.4 | 16.4 | 3.6 | 3.1 | 1.1 | 0.0 | 33.1 | 0.6 | 82.0 | 1.1 | 14.6 | 0.0 |
| 65 | S008 | -77.62638 | 163.11592 | 41 | salt #3 | 13.2 | | 87 | 13 | 10.1 | 6.9 | 1.9 | 12.6 | 3.5 | 1.7 | 0.5 | 0.0 | 28.0 | 0.4 | 54.3 | 0.7 | 17.5 | 4.0 |
| 68 | S013 | -77.63206 | 163.11177 | 60 | salt #1 | 13.3 | | 83 | 17 | 10.2 | 6.0 | 1.8 | 10.8 | 3.2 | 0.9 | 0.5 | 0.0 | 27.0 | 0.5 | 21.1 | 1.5 | 10.9 | 0.6 |
| 71 | S013 | -77.63206 | 163.11177 | 60 | salt #2 | 11.6 | | 71 | 29 | 10.2 | 4.9 | 1.4 | 19.7 | 4.6 | 4.2 | 0.8 | 0.0 | 29.9 | 0.6 | 82.9 | 1.3 | 8.9 | 0.8 |
| 74 | S013 | -77.63206 | 163.11177 | 60 | salt #3 | 12.4 | | 89 | 11 | 9.7 | 4.8 | 1.6 | 12.7 | 3.7 | 1.2 | 0.5 | 0.0 | 26.5 | 0.5 | 43.9 | 1.2 | 9.8 | 0.1 |
| 77 | S011 | -77.59063 | 163.47832 | | DP | | | 50 | 50 | 10.1 | 4.2 | 1.6 | 13.9 | 2.8 | 0.9 | 0.3 | 0.0 | 24.5 | 0.3 | 41.8 | 0.7 | 9.4 | 3.4 |
| 80 | S011 | -77.59063 | 163.47832 | | C1 | | | 100 | | 9.8 | 3.5 | 1.5 | 9.2 | 2.8 | 0.4 | 0.2 | 0.0 | 20.4 | 0.3 | 35.7 | 0.3 | 7.1 | 1.4 |
| 84 | S009 | -77.59098 | 163.48609 | 98 | DP | 1.5 | | 46 | 54 | 10.0 | 2.9 | 1.5 | 17.2 | 3.0 | 0.5 | 0.2 | 0.0 | 28.0 | 0.4 | 86.2 | 0.0 | 5.6 | 0.7 |
| 87 | S009 | -77.59098 | 163.48609 | 98 | C1 | 6 | | 90 | 10 | | 0.4 | 1.1 | 43.5 | 2.8 | 7.2 | 0.5 | 0.0 | 34.8 | 0.7 | 88.7 | 1.6 | 3.2 | 5.7 |
| 90 | S009 | -77.59098 | 163.48609 | 98 | C2 | 15 | | 98 | 2 | 9.4 | 3.8 | 2.6 | 9.4 | 3.3 | 1.3 | 0.2 | 0.0 | 22.2 | 0.3 | 33.8 | 0.5 | 7.0 | 2.6 |
| 92 | S009 | -77.59098 | 163.48609 | 98 | ICS | 1 | | 99 | 1 | 9.6 | 3.1 | 1.9 | 13.4 | 2.8 | 1.2 | 0.4 | 0.0 | 23.1 | 0.3 | 52.6 | 0.0 | 6.3 | 1.6 |
| 94 | S010 | -77.58923 | 163.49406 | 72 | DP | 2 | | 38 | 62 | 10.0 | 4.4 | 1.9 | 18.9 | 3.4 | 0.6 | 0.2 | 0.0 | 30.3 | 0.4 | 61.0 | 0.6 | 9.2 | 4.7 |
| 97 | S010 | -77.58923 | 163.49406 | 72 | C1 | 2 | | 93 | 7 | 10.3 | 1.6 | 0.6 | 34.7 | 3.0 | 2.7 | 0.5 | 0.0 | 36.2 | 0.6 | 100.2 | 0.0 | 4.1 | 1.9 |
| 100 | S010 | -77.58923 | 163.49406 | 72 | C2 | 19 | | 96 | 4 | 9.9 | 3.6 | 1.4 | 14.5 | 2.7 | 1.4 | 0.2 | 0.0 | 21.1 | 0.3 | 15.7 | 1.1 | 9.7 | 8.1 |
| 105 | S014 | -77.50472 | 163.69283 | 390 | DP | 3 | | 10 | 90 | 9.8 | 3.4 | 2.1 | 68.1 | 6.2 | 25.1 | 1.9 | 0.0 | 41.3 | 0.6 | 287.4 | 1.6 | 5.6 | 9.3 |
| 108 | S014 | -77.50472 | 163.69283 | 390 | C1 | 4 | | 50 | 50 | 9.9 | 4.3 | 3.0 | 69.8 | 6.9 | 18.5 | 1.5 | 0.0 | 48.1 | 1.0 | 266.0 | 1.8 | 9.6 | 12.7 |
| 112 | S014 | -77.50472 | 163.69283 | 390 | C2 | 37 | | 31 | 69 | 9.7 | 3.7 | 1.7 | 14.0 | 2.6 | 0.6 | 0.2 | 0.0 | 23.0 | 0.3 | 35.9 | 1.4 | 12.8 | 6.0 |
| 126 | S015 | -77.51319 | 163.70152 | 325 | DP | 1.5 | | 39 | 61 | 10.3 | 6.3 | 2.3 | 26.2 | 3.3 | 1.0 | 0.4 | 0.0 | 35.6 | 0.5 | 218.5 | 1.0 | 12.7 | 10.7 |
| 129 | S015 | -77.51319 | 163.70152 | 325 | C1 | 4 | | 91 | 9 | 10.3 | 3.5 | 2.3 | 31.9 | 3.4 | 0.6 | 0.2 | 0.0 | 33.2 | 0.6 | 206.7 | 1.4 | 8.0 | 14.8 |
| 132 | S015 | -77.51319 | 163.70152 | 325 | C2 | 21 | | 91 | 9 | 10.0 | 2.5 | 1.6 | 22.0 | 2.8 | 0.3 | 0.1 | 0.0 | 27.5 | 0.4 | 76.8 | 1.5 | 6.8 | 7.4 |
| 135 | S015 | -77.51319 | 163.70152 | 325 | ICS | 1 | | 94 | 6 | 9.4 | 5.4 | 4.0 | 14.2 | 3.3 | 0.8 | 0.2 | 0.0 | 30.6 | 0.3 | 59.4 | 1.1 | 10.0 | 6.1 |

Table A.1 continued.

| # | Pit | Latitude | Longitude | Elevation | Horizon | Thickness | $H_2O$ | <2 mm | >2 mm | pH | Ca | Mg | Na | K | Cl | $SO_4$ | $NO_3$ | $HCO_3$ | F | B | Ba | Sr | Charge Balance |
|---|---|---|---|---|---|---|---|---|---|---|---|---|---|---|---|---|---|---|---|---|---|---|---|
| | | | | m | | cm | ———%Wt.——— | | | | ——————————mmol $kg^{-1}$—————————— | | | | | | | | | ——µmol $kg^{-1}$—— | | | % |
| 139 | S016 | -77.65640 | 162.97444 | 384 | DP | 1.5 | | 11 | 89 | 8.5 | 92.4 | 4.8 | 27.9 | 7.1 | 20.2 | 76.6 | 0.0 | 28.8 | 0.6 | 121.7 | 0.8 | 710.3 | 6.1 |
| 143 | S016 | -77.65640 | 162.97444 | 384 | C1 | 3 | | 64 | 36 | 8.6 | 76.2 | 5.9 | 30.6 | 5.4 | 27.2 | 56.6 | 0.0 | 28.1 | 1.6 | 66.3 | 4.5 | 2269.9 | 8.1 |
| 147 | S016 | -77.65640 | 162.97444 | 384 | C2 | 18 | | 53 | 47 | 9.1 | 26.9 | 2.6 | 15.5 | 3.7 | 9.5 | 15.1 | 0.0 | 30.0 | 0.9 | 127.9 | 2.7 | 347.8 | 5.0 |
| 151 | S016 | -77.65640 | 162.97444 | 384 | ICS | 2 | | 99 | 1 | 9.5 | 13.3 | 2.9 | 5.2 | 3.3 | 4.8 | 0.6 | 0.0 | 45.8 | 0.4 | 0.0 | 0.2 | 102.2 | 12.4 |
| 155 | S017 | -77.65030 | 162.97164 | 307 | DP | 1.5 | | 17 | 83 | 9.3 | 10.9 | 2.9 | 83.9 | 8.2 | 57.7 | 9.0 | 0.8 | 38.8 | 0.6 | 232.8 | 0.8 | 20.5 | 1.7 |
| 159 | S017 | -77.65030 | 162.97164 | 307 | C1 | 10 | | 67 | 33 | 9.8 | 4.2 | 2.4 | 47.8 | 7.3 | 21.3 | 2.1 | 0.5 | 38.4 | 0.6 | 106.8 | 2.0 | 7.3 | 2.5 |
| 163 | S017 | -77.65030 | 162.97164 | 307 | C2 | 18 | | 50 | 50 | 9.8 | 1.4 | 1.2 | 7.6 | 2.7 | 1.0 | 0.5 | 0.0 | 15.6 | 0.4 | 12.1 | 0.0 | 5.6 | 7.1 |
| 167 | S017 | -77.65030 | 162.97164 | 307 | ICS | 1 | | 56 | 44 | 9.4 | 9.7 | 2.0 | 2.1 | 2.2 | 0.9 | 0.4 | 0.0 | 22.1 | 0.3 | 0.0 | 1.0 | 33.0 | 6.7 |
| 170 | S018 | -77.64499 | 162.98599 | 221 | DP | 1.5 | | 17 | 83 | 8.9 | 15.0 | 3.5 | 47.4 | 5.4 | 42.6 | 6.8 | 0.0 | 27.3 | 0.4 | 31.5 | 0.6 | 42.0 | 3.3 |
| 174 | S018 | -77.64499 | 162.98599 | 221 | C1 | 4 | | 69 | 31 | 9.1 | 11.9 | 14.9 | 72.3 | 8.7 | 60.7 | 3.7 | 0.7 | 36.9 | 0.8 | 96.0 | 0.3 | 37.8 | 11.6 |
| 178 | S018 | -77.64499 | 162.98599 | 221 | C2 | 22 | | 49 | 51 | 9.1 | 2.0 | 0.8 | 2.1 | 1.6 | 0.9 | 0.0 | 0.0 | 8.1 | 0.3 | 0.0 | 0.0 | 6.3 | 0.2 |
| 182 | S018 | -77.64499 | 162.98599 | 221 | C3 | 7 | | 66 | 34 | 9.1 | 2.8 | 0.9 | 2.0 | 1.6 | 0.3 | 0.5 | 0.0 | 8.9 | 0.4 | 1.7 | 0.0 | 8.4 | 2.1 |
| 185 | S018 | -77.64499 | 162.98599 | 221 | salt can | 8 | | 50 | 50 | 10.0 | 9.9 | 4.7 | 30.6 | 5.6 | 11.7 | 1.2 | 0.0 | 34.5 | 0.6 | 55.8 | 1.0 | 24.5 | 14.0 |
| 189 | S019 | -77.64245 | 162.98834 | 181 | DP | 2 | | 8 | 92 | 9.9 | 9.6 | 2.1 | 18.6 | 3.6 | 8.2 | 1.1 | 0.0 | 24.1 | 0.4 | 25.6 | 0.7 | 18.8 | 13.3 |
| 193 | S019 | -77.64245 | 162.98834 | 181 | C1 | 3 | | 63 | 37 | 10.0 | 9.3 | 3.6 | 22.6 | 4.7 | 7.5 | 1.0 | 0.0 | 29.1 | 0.7 | 41.3 | 0.8 | 21.5 | 15.0 |
| 197 | S019 | -77.64245 | 162.98834 | 181 | C2 | 23 | | 57 | 43 | 9.7 | 1.4 | 1.0 | 6.9 | 3.0 | 0.8 | 0.4 | 0.0 | 11.2 | 0.3 | 0.0 | 0.0 | 4.9 | 5.1 |
| 201 | S019 | -77.64245 | 162.98834 | 181 | C3 | 8 | | 64 | 36 | 9.3 | 4.1 | 1.1 | 2.6 | 2.4 | 0.8 | 0.4 | 0.0 | 11.6 | 0.3 | 0.0 | 0.0 | 12.2 | 6.8 |
| 205 | S019 | -77.64245 | 162.98834 | 181 | salt can | 7.5 | | 67 | 33 | 9.9 | 5.7 | 3.7 | 9.1 | 3.2 | 1.9 | 0.5 | 0.0 | 19.5 | 0.5 | 4.9 | 1.0 | 20.1 | 15.1 |
| 238 | S021 | -77.71740 | 162.23349 | 277 | DP | 5 | | 17 | 83 | 8.9 | 6.4 | 1.4 | 4.4 | 1.6 | 3.4 | 3.6 | 0.0 | 7.9 | 0.4 | 0.0 | 0.0 | 10.2 | 6.9 |
| 241 | S021 | -77.71740 | 162.23349 | 277 | C1 | 5 | | 69 | 31 | 8.6 | 85.4 | 5.9 | 21.5 | 2.9 | 20.1 | 60.8 | 0.7 | 15.8 | 0.5 | 0.0 | 0.6 | 68.8 | 13.2 |
| 244 | S021 | -77.71740 | 162.23349 | 277 | C2 | 33 | | 70 | 30 | 8.5 | 26.1 | 13.7 | 22.8 | 3.6 | 43.5 | 15.9 | 2.2 | 8.1 | 0.4 | 78.3 | 0.6 | 73.3 | 10.4 |
| 247 | S022 | -77.71892 | 162.23645 | 206 | DP | 2 | | 20 | 80 | 8.3 | 6.5 | 1.2 | 2.9 | 1.6 | 1.8 | 3.5 | 0.0 | 6.3 | 0.3 | 0.0 | 0.0 | 10.0 | 12.9 |
| 250 | S022 | -77.71892 | 162.23645 | 206 | C1 | 3 | | 59 | 41 | 8.1 | 190.1 | 2.5 | 33.0 | 5.0 | 14.4 | 107.2 | 0.5 | 32.5 | 0.6 | 155.7 | 1.2 | 231.8 | 23.5 |
| 253 | S022 | -77.71892 | 162.23645 | 206 | C2 | 15 | | 52 | 48 | 8.3 | 16.8 | 6.4 | 35.4 | 3.7 | 31.5 | 15.5 | 1.3 | 9.1 | 0.5 | 89.3 | 0.0 | 32.7 | 7.6 |
| 256 | S022 | -77.71892 | 162.23645 | 206 | C3 | 30 | | 75 | 25 | 8.3 | 7.1 | 6.8 | 33.7 | 2.9 | 37.6 | 5.4 | 1.5 | 6.8 | 0.4 | 18.8 | 0.0 | 22.2 | 6.0 |
| 259 | S023 | -77.72023 | 162.23914 | 149 | DP | 3 | | 15 | 85 | 8.9 | 2.0 | 0.8 | 2.0 | 1.3 | 1.4 | 1.1 | 0.0 | 5.0 | 0.3 | 0.0 | 0.0 | 3.4 | 0.1 |
| 262 | S023 | -77.72023 | 162.23914 | 149 | C1 | 2 | | 67 | 33 | 8.4 | 37.0 | 1.3 | 2.2 | 2.0 | 1.1 | 26.6 | 0.0 | 11.8 | 0.4 | 21.8 | 0.3 | 25.0 | 9.6 |
| 265 | S023 | -77.72023 | 162.23914 | 149 | C2 | 25 | | 65 | 35 | 8.4 | 35.5 | 7.7 | 32.6 | 3.1 | 38.8 | 24.2 | 1.5 | 8.5 | 0.4 | 79.1 | 0.5 | 67.8 | 11.2 |
| 268 | S023 | -77.72023 | 162.23914 | 149 | ICS | 1 | | 75 | 25 | 8.5 | 12.7 | 7.4 | 21.0 | 2.5 | 28.6 | 9.2 | 1.6 | 7.0 | 0.4 | 71.4 | 0.2 | 34.8 | 6.4 |
| 272 | S024 | -77.64067 | 162.97821 | 175 | DP | 1 | | 8 | 92 | 9.5 | 10.7 | 1.9 | 13.9 | 3.1 | 5.5 | 2.0 | 0.5 | 21.6 | 0.5 | 31.8 | 0.7 | 19.6 | 13.8 |
| 275 | S024 | -77.64067 | 162.97821 | 175 | C1 | 8 | | 54 | 46 | 9.6 | 9.6 | 2.9 | 32.6 | 6.2 | 12.2 | 1.8 | 0.0 | 28.0 | 0.8 | 67.1 | 2.3 | 28.9 | 17.7 |
| 278 | S024 | -77.64067 | 162.97821 | 175 | C2 | 26 | | 34 | 66 | 9.3 | 10.4 | 4.1 | 6.1 | 3.5 | 3.4 | 0.5 | 0.0 | 23.8 | 0.5 | 0.0 | 0.0 | 38.6 | 14.6 |
| 281 | S024 | -77.64067 | 162.97821 | 175 | ICS | 1 | | 34 | 66 | 9.4 | 11.3 | 2.2 | 3.5 | 3.0 | 0.5 | 0.2 | 0.0 | 28.5 | 0.3 | 31.8 | 0.8 | 51.9 | 6.3 |
| 284 | S025 | -77.63718 | 162.98909 | 143 | DP | 1 | | 20 | 80 | 9.9 | 12.6 | 1.1 | 5.4 | 2.7 | 1.2 | 0.6 | 0.0 | 23.9 | 0.4 | 9.0 | 0.0 | 101.3 | 14.2 |
| 287 | S025 | -77.63718 | 162.98909 | 143 | C1 | 11 | | 83 | 17 | 9.3 | 8.5 | 4.1 | 51.8 | 8.2 | 28.7 | 4.9 | 1.5 | 29.8 | 1.0 | 170.7 | 0.0 | 126.5 | 9.1 |
| 290 | S025 | -77.63718 | 162.98909 | 143 | C2 | 18 | | 88 | 12 | 9.9 | 12.2 | 1.5 | 4.6 | 1.9 | 1.9 | 0.4 | 0.0 | 21.8 | 0.4 | 0.0 | 0.0 | 58.2 | 15.1 |
| 293 | S026 | -77.62464 | 163.19630 | 73 | DP | 1 | | 15 | 85 | 9.5 | 10.9 | 1.9 | 6.4 | 2.3 | 1.0 | 0.4 | 0.0 | 28.1 | 0.3 | 45.0 | 1.1 | 19.2 | 6.6 |
| 296 | S026 | -77.62464 | 163.19630 | 73 | C1 | 8 | | 80 | 20 | 10.2 | 7.6 | 2.5 | 9.8 | 2.9 | 0.7 | 0.2 | 0.0 | 26.1 | 0.3 | 41.5 | 1.5 | 14.2 | 8.5 |
| 299 | S026 | -77.62464 | 163.19630 | 73 | C2 | 21 | | 42 | 58 | 9.8 | 9.2 | 3.0 | 9.2 | 1.2 | 4.6 | 0.3 | 0.0 | 26.5 | 0.3 | 43.0 | 0.7 | 25.2 | 4.3 |
| 302 | S026 | -77.62464 | 163.19630 | 73 | ICS | 1 | | 53 | 47 | 9.3 | 9.2 | 1.8 | 3.3 | 1.4 | 0.6 | 0.2 | 0.0 | 24.0 | 0.3 | 19.8 | 0.8 | 16.8 | 3.2 |

Table A.1 continued.

| # | Pit | Latitude | Longitude | Elevation | Horizon | Thickness | $H_2O$ | <2 mm | >2 mm | pH | Ca | Mg | Na | K | Cl | $SO_4$ | $NO_3$ | $HCO_3$ | F | B | Ba | Sr | Charge Balance |
|---|---|---|---|---|---|---|---|---|---|---|---|---|---|---|---|---|---|---|---|---|---|---|---|
| | | | | m | | cm | ———%Wt.——— | | | | ——————————mmol $kg^{-1}$—————————— | | | | | | | | | ——µmol $kg^{-1}$—— | | | % |
| 306 | S008 | -77.62638 | 163.11592 | 41 | topset | | | 88 | 12 | 9.8 | 7.2 | 1.4 | 3.7 | 1.6 | 1.0 | 0.5 | 0.0 | 15.3 | 0.3 | 0.0 | 0.4 | 18.1 | 12.4 |
| 309 | S008 | -77.62638 | 163.11592 | 41 | foreset | | | 100 | | 9.8 | 7.5 | 1.7 | 5.0 | 1.5 | 1.6 | 0.4 | 0.0 | 16.8 | 0.4 | 0.0 | 0.1 | 23.1 | 11.7 |
| 312 | S001 | -77.62528 | 163.09498 | 45 | DP | 5 | | 16 | 84 | 9.0 | 10.4 | 2.7 | 19.8 | 5.2 | 2.6 | 3.1 | 0.0 | 33.2 | 0.5 | 81.2 | 1.1 | 15.7 | 9.3 |
| 316 | S001 | -77.62528 | 163.09498 | 45 | C1 | 4 | | 83 | 17 | 8.2 | 9.1 | 10.4 | 44.1 | 7.9 | 54.9 | 3.8 | 2.0 | 17.9 | 1.2 | 79.5 | 1.8 | 56.7 | 4.3 |
| 319 | S001 | -77.62528 | 163.09498 | 45 | C2 | 30 | | 74 | 26 | 8.9 | 8.1 | 2.6 | 13.7 | 4.9 | 10.4 | 0.2 | 0.0 | 25.1 | 0.3 | 10.8 | 1.3 | 41.2 | 4.8 |
| 322 | S001 | -77.62528 | 163.09498 | 45 | ICS | 1 | | 64 | 36 | 8.7 | 11.2 | 5.4 | 22.6 | 6.4 | 22.1 | 1.4 | 0.7 | 28.8 | 0.5 | 61.1 | 0.9 | 53.3 | 6.2 |
| 328 | S027 | -77.63657 | 163.12134 | 121 | DP | 1.5 | | 33 | 67 | 9.0 | 9.6 | 3.5 | 32.6 | 4.8 | 19.2 | 5.2 | 0.8 | 28.9 | 0.3 | 144.0 | 0.9 | 15.0 | 3.3 |
| 332 | S027 | -77.63657 | 163.12134 | 121 | C1 | 7 | 0.83 | 74 | 26 | 9.0 | 5.6 | 8.4 | 53.3 | 6.1 | 49.3 | 2.8 | 2.3 | 29.1 | 0.4 | 142.1 | 0.9 | 16.0 | 0.5 |
| 335 | S027 | -77.63657 | 163.12134 | 121 | C2T | 12 | 0.84 | 87 | 13 | 8.8 | 3.6 | 5.9 | 36.5 | 3.6 | 32.9 | 0.8 | 1.3 | 20.6 | 0.2 | 67.8 | 0.7 | 16.7 | 1.9 |
| 338 | S027 | -77.63657 | 163.12134 | 121 | C2B | 12 | | 89 | 11 | 8.9 | 4.2 | 4.1 | 16.1 | 2.3 | 13.0 | 0.2 | 0.4 | 20.6 | 0.2 | 36.4 | 0.5 | 16.3 | 0.8 |
| 341 | S027 | -77.63657 | 163.12134 | 121 | ICS | 2 | 16.57 | 100 | | 9.3 | 2.7 | 2.0 | 5.6 | 1.3 | 2.7 | 0.2 | 0.2 | 14.2 | 0.2 | 31.0 | 0.3 | 7.4 | 3.8 |
| 342 | S028 | -77.63615 | 163.12773 | 120 | DP | 2 | | 19 | 81 | 9.8 | 7.3 | 2.5 | 8.0 | 2.3 | 0.4 | 0.3 | 0.0 | 26.8 | 0.3 | 59.3 | 1.1 | 11.2 | 3.3 |
| 345 | S028 | -77.63615 | 163.12773 | 120 | C1 | 3 | 0.52 | 89 | 11 | 10.2 | 2.0 | 1.7 | 30.1 | 3.0 | 1.3 | 0.3 | 0.2 | 32.3 | 0.6 | 186.8 | 1.5 | 4.9 | 7.1 |
| 348 | S028 | -77.63615 | 163.12773 | 120 | C2T | 14 | 0.74 | 85 | 15 | 10.2 | 1.2 | 1.2 | 22.0 | 1.7 | 2.9 | 0.5 | 0.2 | 23.4 | 0.3 | 88.7 | 0.6 | 4.0 | 1.1 |
| 351 | S028 | -77.63615 | 163.12773 | 120 | C2B | 9 | | 85 | 15 | 9.8 | 3.8 | 2.8 | 9.9 | 1.7 | 2.6 | 0.6 | 0.3 | 20.6 | 0.2 | 21.4 | 0.6 | 10.0 | 0.1 |
| 354 | S028 | -77.63615 | 163.12773 | 120 | ICS | 2 | 11.17 | 84 | 16 | 9.4 | 3.6 | 2.5 | 5.2 | 1.4 | 1.5 | 0.2 | 0.2 | 17.4 | 0.2 | 17.2 | 0.3 | 8.4 | 3.0 |
| 357 | S029 | -77.63527 | 163.12137 | 98 | DP | 1.5 | | 30 | 70 | 9.7 | 9.8 | 2.3 | 3.8 | 2.7 | 0.4 | 0.2 | 0.0 | 28.0 | 0.2 | 7.9 | 1.1 | 23.1 | 3.0 |
| 361 | S029 | -77.63527 | 163.12137 | 98 | C1 | 1.5 | 0.30 | 91 | 9 | 9.8 | 6.8 | 2.3 | 4.6 | 3.0 | 0.4 | 0.1 | 0.0 | 24.1 | 0.2 | 81.1 | 0.9 | 18.4 | 1.7 |
| 364 | S029 | -77.63527 | 163.12137 | 98 | C2 | 10 | 0.37 | 93 | 7 | 10.0 | 4.2 | 2.4 | 6.0 | 2.1 | 0.5 | 0.2 | 0.0 | 19.6 | 0.2 | 67.7 | 0.0 | 12.7 | 1.4 |
| 367 | S029 | -77.63527 | 163.12137 | 98 | C3 | 15 | 0.49 | 84 | 16 | 9.9 | 2.5 | 1.4 | 5.2 | 1.2 | 0.5 | 0.1 | 0.0 | 14.4 | 0.2 | 46.2 | 0.0 | 6.3 | 3.6 |
| 370 | S029 | -77.63527 | 163.12137 | 98 | ICS | 2 | 11.63 | 77 | 23 | 9.4 | 3.9 | 2.0 | 4.5 | 2.3 | 0.5 | 0.1 | 0.0 | 15.4 | 0.2 | 12.5 | 0.6 | 9.2 | 6.1 |
| 372 | S030 | -77.63424 | 163.11624 | 87 | DP | 2.5 | | 24 | 76 | 9.7 | 10.6 | 1.6 | 3.7 | 2.0 | 0.4 | 0.2 | 0.0 | 28.0 | 0.3 | 17.0 | 0.0 | 16.7 | 1.8 |
| 376 | S030 | -77.63424 | 163.11624 | 87 | C1 | 2 | 0.29 | 80 | 20 | 9.8 | 8.8 | 1.6 | 5.1 | 2.3 | 0.4 | 0.2 | 0.0 | 25.6 | 0.3 | 12.6 | 0.0 | 14.0 | 2.4 |
| 380 | S030 | -77.63424 | 163.11624 | 87 | C2 | 14.5 | 0.33 | 61 | 39 | | 7.0 | 2.1 | 4.0 | 1.8 | 0.8 | 0.2 | 0.0 | 22.8 | 0.2 | 9.2 | 0.0 | 17.0 | 0.7 |
| 384 | S030 | -77.63424 | 163.11624 | 87 | C3 | 9 | 0.48 | 94 | 6 | | 6.9 | 2.1 | 3.5 | 1.5 | 0.9 | 0.1 | 0.0 | 21.8 | 0.2 | 0.0 | 0.0 | 17.7 | 0.6 |
| 387 | S030 | -77.63424 | 163.11624 | 87 | ICS | 2 | 5.87 | 84 | 16 | 9.7 | 5.9 | 1.5 | 2.1 | 1.3 | 0.5 | 0.2 | 0.0 | 18.1 | 0.2 | 0.0 | 0.0 | 15.2 | 2.3 |
| 390 | S031 | -77.63308 | 163.11885 | 84 | DP | 1.5 | | 29 | 71 | 9.3 | 8.7 | 2.2 | 3.2 | 2.4 | 0.4 | 0.2 | 0.0 | 24.5 | 0.3 | 0.0 | 0.0 | 17.2 | 3.9 |
| 394 | S031 | -77.63308 | 163.11885 | 84 | C1 | 5 | 0.59 | 89 | 11 | 10.0 | 5.8 | 2.0 | 14.4 | 3.5 | 0.9 | 0.3 | 0.0 | 28.5 | 0.4 | 56.3 | 0.0 | 13.4 | 4.8 |
| 397 | S031 | -77.63308 | 163.11885 | 84 | C2T | 10 | 0.79 | 88 | 12 | 9.9 | 3.8 | 2.7 | 14.8 | 2.1 | 2.0 | 0.7 | 0.0 | 24.8 | 0.4 | 118.1 | 0.0 | 7.8 | 2.3 |
| 400 | S031 | -77.63308 | 163.11885 | 84 | C2B | 12 | | 91 | 9 | 9.5 | 3.9 | 3.2 | 15.0 | 2.3 | 3.6 | 0.3 | 0.3 | 24.8 | 0.2 | 24.9 | 0.0 | 10.2 | 2.9 |
| 403 | S031 | -77.63308 | 163.11885 | 84 | ICS | 2 | 9.91 | 99 | 1 | 9.7 | 6.4 | 1.3 | 5.3 | 1.8 | 0.6 | 0.2 | 0.0 | 22.9 | 0.2 | 66.5 | 0.0 | 11.5 | 3.3 |
| 404 | S032 | -77.62285 | 163.10808 | 20 | DP | 1.5 | | 40 | 60 | 9.6 | 10.5 | 1.8 | 2.5 | 1.9 | 0.4 | 0.2 | 0.0 | 28.0 | 0.2 | 37.2 | 0.0 | 18.7 | 0.4 |
| 407 | S032 | -77.62285 | 163.10808 | 20 | C1 | 1 | 0.26 | 92 | 8 | 9.7 | 11.0 | 1.7 | 3.1 | 2.0 | 0.3 | 0.2 | 0.0 | 29.8 | 0.3 | 39.8 | 0.0 | 18.1 | 0.6 |
| 409 | S032 | -77.62285 | 163.10808 | 20 | C2 | 13.5 | 0.39 | 75 | 25 | 9.7 | 6.6 | 1.5 | 6.2 | 2.1 | 0.9 | 0.2 | 0.0 | 24.8 | 0.3 | 40.7 | 0.0 | 13.9 | 3.6 |
| 412 | S032 | -77.62285 | 163.10808 | 20 | C3 | 12 | 0.42 | 86 | 14 | 9.8 | 5.5 | 1.6 | 5.1 | 0.8 | 1.1 | 0.2 | 0.0 | 20.6 | 0.2 | 28.2 | 0.0 | 15.8 | 4.9 |
| 415 | S032 | -77.62285 | 163.10808 | 20 | ICS | 4.5 | 6.59 | 92 | 8 | | 6.3 | 1.8 | 3.3 | 1.3 | 0.9 | 0.2 | 0.0 | 21.6 | 0.2 | 21.2 | 0.0 | 14.7 | 4.9 |
| 417 | S033 | -77.62582 | 163.11623 | 36 | DP | 1.5 | | 19 | 81 | | 11.7 | 1.5 | 2.0 | 1.7 | 0.4 | 0.3 | 0.0 | 28.4 | 0.3 | 15.1 | 0.0 | 19.5 | 0.8 |
| 421 | S033 | -77.62582 | 163.11623 | 36 | C1 | 2 | 0.24 | 85 | 15 | 9.9 | 9.9 | 1.5 | 4.2 | 2.2 | 0.4 | 0.2 | 0.0 | 27.9 | 0.3 | 27.2 | 0.0 | 17.7 | 0.1 |
| 424 | S033 | -77.62582 | 163.11623 | 36 | C2T | 14 | 0.37 | 77 | 23 | 9.8 | 6.6 | 1.8 | 4.1 | 1.9 | 0.4 | 0.2 | 0.0 | 22.8 | 0.3 | 10.8 | 0.0 | 15.7 | 2.7 |
| 427 | S033 | -77.62582 | 163.11623 | 36 | C2B | 8.5 | | 86 | 14 | 9.7 | 5.9 | 2.5 | 5.6 | 1.6 | 1.3 | 0.2 | 0.0 | 22.4 | 0.2 | 12.5 | 0.0 | 13.3 | 0.8 |

Table A.1 continued.

| # | Pit | Latitude | Longitude | Elevation | Horizon | Thickness | $H_2O$ | <2 mm | >2 mm | pH | Ca | Mg | Na | K | Cl | $SO_4$ | $NO_3$ | $HCO_3$ | F | B | Ba | Sr | Charge Balance |
|---|---|---|---|---|---|---|---|---|---|---|---|---|---|---|---|---|---|---|---|---|---|---|---|
| | | | | m | | cm | ———%Wt.——— | | | | ——————————mmol $kg^{-1}$—————————— | | | | | | | | | ——µmol $kg^{-1}$—— | | | % |
| 430 | S033 | -77.62582 | 163.11623 | 36 | ICS | 3 | 7.87 | 75 | 25 | 9.6 | 7.4 | 1.5 | 3.6 | 1.7 | 0.7 | 0.2 | 0.2 | 23.5 | 0.2 | 4.2 | 0.0 | 17.1 | 3.6 |
| 433 | S034 | -77.63083 | 163.11212 | 65 | DP | 1.5 | | 47 | 53 | 9.6 | 11.2 | 2.4 | 4.9 | 3.0 | 0.3 | 0.1 | 0.0 | 31.3 | 0.4 | 18.8 | 0.0 | 20.2 | 4.1 |
| 437 | S034 | -77.63083 | 163.11212 | 65 | C1 | 9 | 0.84 | 91 | 9 | 9.9 | 3.6 | 2.7 | 14.5 | 4.1 | 0.4 | 0.1 | 0.0 | 26.8 | 0.4 | 39.4 | 0.6 | 9.7 | 5.6 |
| 440 | S034 | -77.63083 | 163.11212 | 65 | C2T | 7.5 | 0.48 | 93 | 7 | 9.9 | 3.3 | 1.6 | 10.1 | 1.4 | 4.0 | 0.3 | 0.0 | 18.4 | 0.3 | 29.7 | 0.0 | 8.7 | 4.3 |
| 442 | S034 | -77.63083 | 163.11212 | 65 | C2B | 6.5 | | 92 | 8 | 9.4 | 5.2 | 2.0 | 4.6 | 1.3 | 2.8 | 0.2 | 0.0 | 19.5 | 0.2 | 14.0 | 0.0 | 14.9 | 6.2 |
| 445 | S034 | -77.63083 | 163.11212 | 65 | ICS | 2 | 14.11 | 84 | 16 | 9.6 | 8.2 | 1.4 | 3.5 | 1.0 | 0.8 | 0.1 | 0.0 | 23.1 | 0.2 | 7.3 | 0.0 | 18.2 | 1.4 |
| 448 | S035 | -77.65659 | 163.01300 | 362 | DP | 2 | | 16 | 84 | | 9.7 | 3.4 | 29.8 | 6.0 | 11.8 | 3.0 | 0.1 | 40.0 | 0.5 | 216.9 | 1.5 | 47.3 | 3.1 |
| 452 | S035 | -77.65659 | 163.01300 | 362 | C1 | 8.5 | 1.46 | 83 | 17 | 9.7 | 3.9 | 2.9 | 28.1 | 9.9 | 4.7 | 0.3 | 0.0 | 39.4 | 0.4 | 3.3 | 3.2 | 20.2 | 6.6 |
| 455 | S035 | -77.65659 | 163.01300 | 362 | C2T | 10 | 4.77 | 93 | 7 | 9.5 | 9.1 | 3.3 | 10.5 | 8.3 | 0.4 | 0.2 | 0.0 | 39.6 | 0.3 | 0.0 | 2.0 | 81.0 | 3.3 |
| 457 | S035 | -77.65659 | 163.01300 | 362 | C2B | 10 | 6.43 | 86 | 14 | 9.1 | 12.7 | 3.6 | 6.9 | 8.0 | 0.6 | 0.2 | 0.0 | 42.2 | 0.4 | 0.0 | 1.7 | 97.5 | 4.3 |
| 460 | S036 | -77.65448 | 163.04523 | 329 | DP | 2 | | 19 | 81 | 10.0 | 9.9 | 2.1 | 7.6 | 2.7 | 1.0 | 0.5 | 0.0 | 32.4 | 0.3 | 20.4 | 1.5 | 19.5 | 0.6 |
| 464 | S036 | -77.65448 | 163.04523 | 329 | C1 | 3.5 | 0.40 | 77 | 23 | 10.0 | 7.9 | 4.9 | 22.6 | 6.0 | 2.0 | 0.7 | 0.0 | 41.7 | 0.5 | 69.3 | 2.4 | 17.2 | 8.6 |
| 467 | S036 | -77.65448 | 163.04523 | 329 | C2 | 6.5 | 0.88 | 75 | 25 | 10.2 | 2.7 | 2.3 | 17.2 | 6.3 | 0.5 | 0.2 | 0.1 | 30.7 | 0.4 | 22.8 | 1.5 | 5.5 | 2.0 |
| 470 | S036 | -77.65448 | 163.04523 | 329 | C3T | 7.5 | 2.86 | 49 | 51 | | 5.3 | 1.6 | 7.9 | 4.4 | 0.5 | 0.2 | 0.0 | 26.1 | 0.3 | 0.0 | 0.9 | 11.6 | 2.3 |
| 473 | S036 | -77.65448 | 163.04523 | 329 | C3B | 7.5 | 4.68 | 82 | 18 | | 7.4 | 2.5 | 5.7 | 4.8 | 0.5 | 0.2 | 0.1 | 28.0 | 0.3 | 0.0 | 2.8 | 25.8 | 1.8 |
| 476 | S037 | -77.64534 | 163.08777 | 215 | DP | 1.5 | | 34 | 66 | | 5.5 | 2.2 | 17.5 | 3.3 | 0.7 | 0.3 | 0.0 | 32.0 | 0.3 | 105.7 | 1.2 | 13.9 | 3.5 |
| 480 | S037 | -77.64534 | 163.08777 | 215 | C1 | 5.5 | 1.22 | 93 | 7 | 10.5 | 3.0 | 2.7 | 34.7 | 5.8 | 1.0 | 0.3 | 0.0 | 40.9 | 0.4 | 101.3 | 3.4 | 14.2 | 9.3 |
| 482 | S037 | -77.64534 | 163.08777 | 215 | C2 | 1.5 | | 89 | 11 | | 2.1 | 2.1 | 20.4 | 5.4 | 0.4 | 0.2 | 0.0 | 27.8 | 0.3 | 23.0 | 3.4 | 10.0 | 8.7 |
| 485 | S037 | -77.64534 | 163.08777 | 215 | C3T | 6 | 4.70 | 84 | 16 | | 2.7 | 1.4 | 6.0 | 3.9 | 0.4 | 0.2 | 0.1 | 16.4 | 0.3 | 20.2 | 1.4 | 9.0 | 1.5 |
| 487 | S037 | -77.64534 | 163.08777 | 215 | C3B | 12 | 14.77 | 91 | 9 | | 4.2 | 1.6 | 5.4 | 3.9 | 0.4 | 0.0 | 0.0 | 19.0 | 0.2 | 10.2 | 1.5 | 11.3 | 3.2 |
| 489 | S038 | -77.63985 | 163.09696 | 170 | DP | 1.5 | | 24 | 76 | | 7.7 | 2.8 | 12.4 | 3.6 | 0.5 | 0.3 | 0.0 | 31.1 | 0.3 | 79.0 | 0.8 | 13.0 | 6.5 |
| 493 | S038 | -77.63985 | 163.09696 | 170 | C1 | 8.5 | 0.80 | 98 | 2 | | 4.2 | 4.7 | 43.2 | 5.9 | 2.5 | 0.5 | 0.0 | 45.3 | 0.8 | 313.7 | 1.9 | 7.7 | 14.8 |
| 495 | S038 | -77.63985 | 163.09696 | 170 | C2 | 4.5 | 1.21 | 97 | 3 | | 1.7 | 1.5 | 18.3 | 2.9 | 1.8 | 0.6 | 0.1 | 23.6 | 0.3 | 18.5 | 0.5 | 5.5 | 0.9 |
| 497 | S038 | -77.63985 | 163.09696 | 170 | C3 | 9.5 | 5.33 | 100 | | | 0.4 | 1.4 | 11.1 | 1.7 | 0.4 | 0.2 | 0.0 | 12.8 | 0.5 | 5.3 | 1.1 | 3.6 | 7.1 |
| 498 | S038 | -77.63985 | 163.09696 | 170 | C4 | 8.5 | 5.30 | 87 | 13 | 9.5 | 0.2 | 0.8 | 8.4 | 1.5 | 0.4 | 0.2 | 0.0 | 12.2 | 0.3 | 4.7 | 0.3 | 1.8 | 5.2 |
| 501 | S039 | -77.63443 | 163.09683 | 110 | DP | 1.5 | | 14 | 86 | 9.9 | 9.9 | 1.8 | 6.1 | 2.5 | 0.8 | 0.5 | 0.1 | 30.8 | 0.4 | 30.6 | 0.0 | 15.8 | 1.5 |
| 505 | S039 | -77.63443 | 163.09683 | 110 | C1 | 9.5 | 0.39 | 77 | 23 | | 7.4 | 3.3 | 7.4 | 3.4 | 0.8 | 0.3 | 0.1 | 28.8 | 0.3 | 19.7 | 0.5 | 17.9 | 2.7 |
| 508 | S039 | -77.63443 | 163.09683 | 110 | C2 | 15 | 0.71 | 92 | 8 | | 5.7 | 3.0 | 4.9 | 2.0 | 0.5 | 0.2 | 0.1 | 23.9 | 0.3 | 40.4 | 0.2 | 19.0 | 1.9 |
| 510 | S039 | -77.63443 | 163.09683 | 110 | C3 | 11.5 | 7.56 | 60 | 40 | | 4.9 | 3.8 | 8.8 | 3.9 | 0.5 | 0.2 | 0.2 | 27.0 | 0.3 | 16.5 | 2.2 | 21.5 | 2.4 |
| 513 | S039 | -77.63443 | 163.09683 | 110 | C4 | 2 | 13.68 | 86 | 14 | | 8.7 | 3.5 | 6.9 | 4.2 | 0.6 | 0.2 | 0.1 | 31.2 | 0.3 | 0.0 | 0.7 | 32.8 | 4.0 |
| 516 | S040 | -77.63304 | 163.11241 | 78 | DP | 1 | | 22 | 78 | | 14.6 | 1.7 | 4.1 | 2.5 | 0.7 | 0.5 | 0.0 | 33.5 | 0.4 | 7.7 | 0.0 | 20.4 | 4.8 |
| 519 | S040 | -77.63304 | 163.11241 | 78 | C1 | 4 | 0.37 | 93 | 7 | 9.7 | 10.1 | 1.9 | 5.8 | 3.7 | 0.4 | 0.5 | 0.0 | 28.8 | 0.4 | 0.0 | 0.0 | 13.8 | 4.8 |
| 521 | S040 | -77.63304 | 163.11241 | 78 | C2 | 4.5 | 0.49 | 61 | 39 | 10.1 | 7.4 | 1.8 | 12.5 | 4.4 | 0.8 | 0.5 | 0.2 | 28.8 | 0.4 | 0.0 | 0.0 | 11.2 | 6.4 |
| 524 | S040 | -77.63304 | 163.11241 | 78 | C3 | 10.5 | 0.78 | 64 | 36 | 9.7 | 5.8 | 2.6 | 19.3 | 3.7 | 6.9 | 1.8 | 0.3 | 26.7 | 0.4 | 0.1 | 0.0 | 12.7 | 2.2 |
| 527 | S040 | -77.63304 | 163.11241 | 78 | C4 | 10.5 | 0.78 | 74 | 26 | | 3.2 | 3.1 | 25.1 | 2.9 | 10.3 | 0.7 | 0.1 | 27.3 | 0.3 | 131.9 | 1.1 | 11.2 | 1.5 |
| 530 | S040 | -77.63304 | 163.11241 | 78 | ICS | 1 | 13.33 | 90 | 10 | | 6.1 | 2.8 | 6.1 | 2.1 | 0.5 | 0.2 | 0.0 | 24.8 | 0.2 | 41.8 | 1.0 | 17.5 | 0.0 |
| 532 | S041 | -77.63131 | 163.10977 | 64 | DP | 1.5 | | 20 | 80 | | 10.6 | 1.9 | 3.1 | 2.0 | 0.5 | 0.2 | 0.0 | 27.4 | 0.3 | 0.0 | 0.0 | 19.1 | 2.3 |
| 536 | S041 | -77.63131 | 163.10977 | 64 | C1 | 1 | 0.28 | 88 | 12 | 9.6 | 11.0 | 2.1 | 3.6 | 2.6 | 0.3 | 0.1 | 0.0 | 29.2 | 0.3 | 0.0 | 0.0 | 18.5 | 3.7 |
| 539 | S041 | -77.63131 | 163.10977 | 64 | C2T | 13 | 0.52 | 81 | 19 | | 8.0 | 2.9 | 8.1 | 2.8 | 0.4 | 0.1 | 0.0 | 28.4 | 0.4 | 5.6 | 0.0 | 17.4 | 5.2 |
| 543 | S041 | -77.63131 | 163.10977 | 64 | C2B | 13 | | 85 | 15 | 9.7 | 6.3 | 2.3 | 6.2 | 1.4 | 1.6 | 0.2 | 0.0 | 22.5 | 0.2 | 0.0 | 0.0 | 14.5 | 0.2 |

Table A.1 continued.

| # | Pit | Latitude | Longitude | Elevation | Horizon | Thickness | $H_2O$ | <2 mm | >2 mm | pH | Ca | Mg | Na | K | Cl | $SO_4$ | $NO_3$ | $HCO_3$ | F | B | Ba | Sr | Charge Balance |
|---|---|---|---|---|---|---|---|---|---|---|---|---|---|---|---|---|---|---|---|---|---|---|---|
| | | | | m | | cm | ———%Wt.——— | | | | ——————————mmol $kg^{-1}$—————————— | | | | | | | | | ——µmol $kg^{-1}$—— | | | % |
| 546 | S041 | -77.63131 | 163.10977 | 64 | ICS | 2 | 12.92 | 76 | 24 | 9.6 | 7.9 | 2.6 | 4.3 | 1.7 | 0.7 | 0.1 | 0.0 | 24.6 | 0.2 | 0.0 | 0.0 | 15.3 | 1.9 |
| 549 | S042 | -77.62658 | 163.11252 | 38 | DP | 1.5 | | 31 | 69 | 9.7 | 9.0 | 1.7 | 3.3 | 1.9 | 0.6 | 0.3 | 0.0 | 24.9 | 0.3 | 39.1 | 0.9 | 20.3 | 0.3 |
| 552 | S042 | -77.62658 | 163.11252 | 38 | C1 | 1 | | 83 | 17 | | 7.0 | 1.5 | 5.8 | 2.0 | 1.4 | 0.5 | 0.0 | 23.3 | 0.3 | 42.0 | 1.0 | 16.1 | 1.9 |
| 555 | S042 | -77.62658 | 163.11252 | 38 | C2T | 10 | 0.36 | 88 | 12 | 9.9 | 5.7 | 2.1 | 7.1 | 1.3 | 1.3 | 0.3 | 0.0 | 22.4 | 0.3 | 54.1 | 1.0 | 16.9 | 1.0 |
| 557 | S042 | -77.62658 | 163.11252 | 38 | C2B | 13.5 | 0.55 | 86 | 14 | | 6.2 | 2.7 | 7.2 | 1.4 | 1.9 | 0.3 | 0.0 | 23.4 | 0.3 | 33.6 | 1.0 | 16.6 | 0.5 |
| 560 | S042 | -77.62658 | 163.11252 | 38 | ICS | 2 | 10.17 | 93 | 7 | | 6.5 | 1.5 | 3.6 | 1.3 | 0.9 | 0.2 | 0.0 | 19.7 | 0.2 | 25.7 | 0.9 | 16.1 | 0.7 |
| 563 | S043 | -77.73785 | 162.32706 | 378 | DP | 3 | | 10 | 90 | | 9.5 | 2.3 | 3.2 | 2.1 | 1.1 | 1.4 | 0.1 | 23.5 | 0.4 | 17.5 | 2.0 | 16.2 | 1.7 |
| 567 | S043 | -77.73785 | 162.32706 | 378 | C1 | 11 | | 38 | 62 | | 5.1 | 3.2 | 2.8 | 2.9 | 0.6 | 0.3 | 0.0 | 17.9 | 0.4 | 0.0 | 3.4 | 10.5 | 6.6 |
| 571 | S043 | -77.73785 | 162.32706 | 378 | C2 | 7 | 4.05 | 44 | 56 | | 4.7 | 4.0 | 3.7 | 4.6 | 0.4 | 0.3 | 0.0 | 20.6 | 0.5 | 8.2 | 3.2 | 10.0 | 7.3 |
| 576 | S044 | -77.73195 | 162.31169 | 261 | DP | 2 | | 20 | 80 | | 8.1 | 2.3 | 1.8 | 2.0 | 0.7 | 0.8 | 0.1 | 19.5 | 0.3 | 4.0 | 2.6 | 15.7 | 4.8 |
| 580 | S044 | -77.73195 | 162.31169 | 261 | C1 | 3 | 0.23 | 60 | 40 | 8.7 | 13.9 | 2.5 | 2.2 | 2.6 | 0.5 | 3.4 | 0.1 | 26.4 | 0.5 | 3.4 | 2.4 | 17.3 | 4.7 |
| 583 | S044 | -77.73195 | 162.31169 | 261 | C2 | 23 | 0.35 | 62 | 38 | | 29.3 | 3.4 | 29.4 | 2.4 | 26.1 | 27.7 | 1.1 | 11.5 | 0.4 | 127.6 | 0.4 | 93.2 | 1.4 |
| 586 | S044 | -77.73195 | 162.31169 | 261 | C3 | 34 | 0.35 | 94 | 6 | | 5.3 | 2.4 | 15.2 | 2.1 | 12.9 | 2.9 | 0.7 | 13.4 | 0.2 | 48.7 | 0.0 | 11.2 | 0.1 |
| 588 | S045 | -77.72746 | 162.31517 | 149 | DP | 1.5 | | 44 | 56 | 8.7 | 13.4 | 1.1 | 2.4 | 1.5 | 1.4 | 3.0 | 0.3 | 23.9 | 0.3 | 137.9 | 0.0 | 25.0 | 1.7 |
| 591 | S045 | -77.72746 | 162.31517 | 149 | C1 | 8 | | 75 | 25 | 8.2 | 50.9 | 2.5 | 6.1 | 4.4 | 1.0 | 46.5 | 0.0 | 24.5 | 0.6 | 181.1 | 0.0 | 55.7 | 0.7 |
| 594 | S045 | -77.72746 | 162.31517 | 149 | C2 | 29 | | 60 | 40 | 8.6 | 40.7 | 19.5 | 59.6 | 8.2 | 73.3 | 44.7 | 2.0 | 21.0 | 0.6 | 677.3 | 0.0 | 248.3 | 0.5 |
| 597 | S045 | -77.72746 | 162.31517 | 149 | C3 | 9 | 1.44 | 58 | 42 | 8.7 | 8.8 | 17.5 | 49.1 | 5.9 | 69.3 | 3.6 | 1.6 | 27.7 | 0.2 | 112.8 | 0.0 | 27.2 | 0.7 |
| 600 | S046 | -77.72657 | 162.31038 | 116 | DP | 1.5 | | 34 | 66 | 8.5 | 30.2 | 3.2 | 14.3 | 3.1 | 12.9 | 21.8 | 0.4 | 21.6 | 0.4 | 143.2 | 0.0 | 57.5 | 3.3 |
| 603 | S046 | -77.72657 | 162.31038 | 116 | C1 | 2.5 | 1.05 | 75 | 25 | 8.4 | 155.5 | 27.3 | 85.2 | 6.8 | 116.9 | 153.1 | 2.1 | 20.3 | 0.8 | 636.6 | 1.3 | 855.6 | 1.3 |
| 606 | S046 | -77.72657 | 162.31038 | 116 | C2 | 29.5 | 1.34 | 73 | 27 | 8.2 | 54.4 | 75.7 | 526.9 | 14.5 | 688.2 | 43.3 | 6.2 | 24.5 | 0.5 | 433.9 | 1.6 | 306.5 | 0.3 |
| 609 | S046 | -77.72657 | 162.31038 | 116 | C3 | 18 | 0.49 | 54 | 46 | 8.8 | 11.7 | 20.5 | 17.9 | 3.9 | 55.7 | 0.6 | 1.8 | 25.4 | 0.2 | 75.7 | 0.0 | 74.1 | 1.1 |
| 612 | S047 | -77.72533 | 162.30296 | 86 | DP | 1 | | 45 | 55 | 8.5 | 27.7 | 1.9 | 14.7 | 2.5 | 9.3 | 21.0 | 0.3 | 21.4 | 0.4 | 125.6 | 0.0 | 39.5 | 2.0 |
| 615 | S047 | -77.72533 | 162.30296 | 86 | C1 | 4 | 1.42 | 84 | 16 | 8.4 | 168.1 | 14.0 | 104.9 | 8.9 | 97.9 | 169.6 | 1.0 | 23.2 | 1.1 | 642.5 | 0.9 | 848.5 | 1.7 |
| 618 | S047 | -77.72533 | 162.30296 | 86 | C2T | 26 | 1.94 | 90 | 10 | 8.2 | 42.2 | 48.5 | 150.2 | 10.4 | 232.4 | 34.8 | 3.1 | 23.0 | 0.7 | 490.1 | 0.0 | 159.6 | 2.0 |
| 620 | S047 | -77.72533 | 162.30296 | 86 | C2B | 30 | | 81 | 19 | 8.3 | 20.4 | 50.1 | 260.1 | 13.2 | 360.4 | 13.9 | 2.8 | 28.5 | 0.6 | 285.8 | 0.5 | 85.8 | 0.7 |
| 622 | S047 | -77.72533 | 162.30296 | 86 | C3 | 5 | 1.84 | 78 | 22 | 8.4 | 11.7 | 32.8 | 77.4 | 9.0 | 133.3 | 3.4 | 2.1 | 27.4 | 0.6 | 293.0 | 0.0 | 31.2 | 1.5 |
| 626 | S048 | -77.63248 | 163.18210 | 123 | DP | 1.5 | | 12 | 88 | | 6.1 | 1.7 | 5.8 | 2.3 | 0.5 | 0.2 | 0.0 | 23.8 | 0.3 | 0.0 | 1.0 | 11.6 | 3.0 |
| 630 | S048 | -77.63248 | 163.18210 | 123 | C1 | 5.5 | | 59 | 41 | | 4.3 | 2.4 | 31.0 | 4.4 | 2.0 | 0.5 | 0.0 | 40.5 | 0.5 | 71.4 | 1.9 | 10.2 | 5.3 |
| 633 | S048 | -77.63248 | 163.18210 | 123 | C2T | 7.5 | 0.86 | 89 | 11 | 10.1 | 0.7 | 1.4 | 32.1 | 2.2 | 6.4 | 0.7 | 0.3 | 25.5 | 0.7 | 0.1 | 0.0 | 2.8 | 5.8 |
| 636 | S048 | -77.63248 | 163.18210 | 123 | C2B | 12.5 | | 88 | 12 | | 1.6 | 1.4 | 15.5 | 2.0 | 4.9 | 0.5 | 0.3 | 19.4 | 0.3 | 79.8 | 0.0 | 3.2 | 4.8 |
| 639 | S048 | -77.63248 | 163.18210 | 123 | ICS | 2 | 14.61 | 87 | 13 | 9.2 | 2.8 | 1.4 | 3.3 | 1.9 | 0.5 | 0.2 | 0.0 | 14.4 | 0.2 | 47.3 | 0.0 | 4.5 | 6.3 |
| 642 | S049 | -77.62691 | 163.18273 | 77 | DP | 1.5 | | 14 | 86 | 9.3 | 7.1 | 2.4 | 6.3 | 2.6 | 1.3 | 0.5 | 0.2 | 24.7 | 0.3 | 42.4 | 0.0 | 12.6 | 0.8 |
| 646 | S049 | -77.62691 | 163.18273 | 77 | C1 | 6.5 | 0.54 | 96 | 4 | | 4.3 | 2.4 | 18.8 | 3.9 | 2.9 | 0.5 | 0.2 | 29.3 | 0.4 | 61.0 | 0.0 | 8.9 | 3.4 |
| 648 | S049 | -77.62691 | 163.18273 | 77 | C2T | 6.5 | 0.76 | 89 | 11 | | 1.1 | 1.6 | 37.2 | 2.9 | 16.1 | 3.9 | 0.6 | 20.0 | 0.6 | 223.2 | 0.0 | 0.9 | 0.4 |
| 651 | S049 | -77.62691 | 163.18273 | 77 | C2B | 12.5 | | 94 | 6 | 9.2 | 2.2 | 2.4 | 17.4 | 2.3 | 10.3 | 0.9 | 0.4 | 18.3 | 0.3 | 20.3 | 0.0 | 5.6 | 3.4 |
| 653 | S049 | -77.62691 | 163.18273 | 77 | ICS | 2.5 | 18.82 | 88 | 12 | 9.5 | 4.1 | 2.1 | 10.7 | 3.0 | 1.8 | 0.2 | 0.3 | 24.1 | 0.3 | 22.3 | 0.0 | 8.6 | 1.3 |
| 655 | S050 | -77.64835 | 163.11734 | 202 | DP | 1.5 | | 20 | 80 | 9.5 | 10.4 | 1.3 | 1.3 | 1.2 | 0.5 | 0.2 | 0.0 | 24.8 | 0.2 | 5.7 | 0.0 | 21.6 | 0.0 |
| 659 | S050 | -77.64835 | 163.11734 | 202 | C1 | 20 | 0.30 | 81 | 19 | 9.5 | 9.1 | 1.5 | 1.3 | 1.0 | 0.5 | 0.2 | 0.0 | 22.9 | 0.2 | 5.0 | 0.0 | 26.3 | 1.1 |
| 662 | S050 | -77.64835 | 163.11734 | 202 | C2 | 14 | 1.34 | 93 | 7 | 9.5 | 7.7 | 1.0 | 1.2 | 0.8 | 0.4 | 0.2 | 0.0 | 20.5 | 0.2 | 0.0 | 0.0 | 16.4 | 4.6 |
| 664 | S050 | -77.64835 | 163.11734 | 202 | ICS | 1 | 9.49 | 79 | 21 | 9.6 | 7.4 | 0.9 | 1.1 | 0.7 | 1.5 | 3.4 | 0.0 | 19.3 | 0.4 | 0.0 | 0.0 | 14.9 | 20.5 |

Table A.1 continued.

| # | Pit | Latitude | Longitude | Elevation | Horizon | Thickness | $H_2O$ | <2 mm | >2 mm | pH | Ca | Mg | Na | K | Cl | $SO_4$ | $NO_3$ | $HCO_3$ | F | B | Ba | Sr | Charge Balance |
|---|---|---|---|---|---|---|---|---|---|---|---|---|---|---|---|---|---|---|---|---|---|---|---|
| | | | | m | | cm | ———%Wt.——— | | | | ——————————mmol $kg^{-1}$—————————— | | | | | | | | | ——µmol $kg^{-1}$—— | | | % |
| 666 | S051 | -77.65063 | 163.11203 | 218 | DP | 1.5 | | 38 | 62 | | 9.8 | 1.4 | 2.8 | 1.6 | 1.8 | 0.9 | 0.0 | 25.3 | 0.5 | 3.7 | 0.0 | 20.3 | 4.6 |
| 669 | S051 | -77.65063 | 163.11203 | 218 | C1T | 18 | 0.40 | 61 | 39 | 9.6 | 7.9 | 2.5 | 3.0 | 1.1 | 0.9 | 0.3 | 0.0 | 22.1 | 0.2 | 39.5 | 0.0 | 17.1 | 2.6 |
| 672 | S051 | -77.65063 | 163.11203 | 218 | C1B | 15 | | 60 | 40 | 9.5 | 10.7 | 2.0 | 3.9 | 2.1 | 0.4 | 0.2 | 0.0 | 27.9 | 0.2 | 8.4 | 0.0 | 21.0 | 4.4 |
| 675 | S052 | -77.63565 | 163.07908 | 112 | DP | 2 | | 23 | 77 | 9.7 | 6.5 | 2.2 | 6.0 | 2.2 | 0.4 | 0.2 | 0.0 | 23.7 | 0.2 | 0.0 | 0.0 | 11.1 | 2.0 |
| 679 | S052 | -77.63565 | 163.07908 | 112 | C1 | 13.5 | 0.55 | 99 | 1 | 10.0 | 2.3 | 1.5 | 15.4 | 1.8 | 1.7 | 0.4 | 0.0 | 20.7 | 0.3 | 6.3 | 0.0 | 4.8 | 3.0 |
| 681 | S052 | -77.63565 | 163.07908 | 112 | C2 | 6.5 | 4.06 | 99 | 1 | 9.6 | 4.3 | 1.8 | 4.6 | 2.0 | 0.3 | 0.1 | 0.0 | 17.9 | 0.2 | 0.0 | 0.0 | 7.3 | 0.2 |
| 682 | S052 | -77.63565 | 163.07908 | 112 | ICS | 2 | 18.95 | 99 | 1 | 9.4 | 5.2 | 2.3 | 3.9 | 2.0 | 0.7 | 0.1 | 0.0 | 21.2 | 0.2 | 0.0 | 0.0 | 8.2 | 3.4 |
| 683 | S053 | -77.65202 | 163.06115 | 289 | DP | 1.5 | | 20 | 80 | | 9.4 | 1.5 | 6.1 | 2.2 | 1.4 | 0.5 | 0.2 | 28.1 | 0.3 | 12.0 | 0.0 | 15.3 | 1.6 |
| 687 | S053 | -77.65202 | 163.06115 | 289 | C1 | 7 | 0.61 | 46 | 54 | | 8.1 | 2.5 | 12.6 | 3.2 | 1.9 | 0.6 | 0.1 | 32.6 | 0.4 | 24.2 | 0.1 | 14.6 | 1.2 |
| 690 | S053 | -77.65202 | 163.06115 | 289 | C2 | 8 | 0.49 | 53 | 47 | | 5.8 | 2.9 | 5.8 | 2.6 | 0.5 | 0.2 | 0.1 | 25.3 | 0.2 | 1.5 | 0.0 | 13.7 | 1.7 |
| 693 | S053 | -77.65202 | 163.06115 | 289 | C3T | 8 | 3.60 | 45 | 55 | 9.7 | 4.8 | 2.8 | 4.9 | 2.5 | 0.4 | 0.2 | 0.1 | 23.0 | 0.2 | 0.0 | 0.1 | 11.2 | 3.5 |
| 696 | S053 | -77.65202 | 163.06115 | 289 | C3M | 15 | | 47 | 53 | 9.3 | 2.8 | 1.3 | 1.2 | 1.2 | 0.5 | 0.2 | 0.1 | 12.9 | 0.2 | 0.0 | 0.0 | 8.1 | 13.7 |
| 699 | S053 | -77.65202 | 163.06115 | 289 | C3B | 5 | 2.88 | 34 | 66 | 9.3 | 1.8 | 1.0 | 1.1 | 1.1 | 0.5 | 0.2 | 0.1 | 8.9 | 0.2 | 0.0 | 0.0 | 5.3 | 12.4 |
| 702 | S055 | -77.64738 | 163.06119 | 243 | DP | 2 | | 46 | 54 | 10.2 | 7.1 | 2.0 | 24.9 | 3.7 | 3.8 | 3.6 | 0.2 | 33.6 | 0.4 | 54.1 | 0.0 | 14.3 | 1.9 |
| 706 | S055 | -77.64738 | 163.06119 | 243 | C1 | 7 | 0.52 | 83 | 17 | 10.2 | 3.6 | 1.8 | 18.5 | 3.5 | 3.7 | 0.7 | 0.1 | 27.5 | 0.3 | 0.0 | 0.2 | 8.7 | 0.4 |
| 709 | S055 | -77.64738 | 163.06119 | 243 | C2 | 4 | | 83 | 17 | | 3.4 | 1.5 | 7.6 | 2.7 | 0.4 | 0.2 | 0.1 | 20.5 | 0.2 | 0.0 | 0.0 | 10.4 | 3.9 |
| 712 | S055 | -77.64738 | 163.06119 | 243 | C3T | 11 | 2.85 | 70 | 30 | 9.5 | 1.8 | 1.7 | 5.6 | 2.9 | 0.4 | 0.1 | 0.0 | 14.9 | 0.3 | 74.9 | 1.2 | 12.4 | 1.0 |
| 715 | S055 | -77.64738 | 163.06119 | 243 | C3B | 11 | 2.98 | 74 | 26 | | 11.2 | 1.9 | 1.7 | 2.2 | 0.4 | 0.2 | 0.0 | 28.7 | 0.2 | 46.8 | 0.2 | 24.5 | 1.0 |
| 718 | S056 | -77.63325 | 163.08997 | 100 | C1 | 3 | | 100 | | | 21.6 | 43.2 | 72.9 | 7.4 | 144.7 | 6.5 | 3.6 | 29.0 | 0.3 | 89.0 | 0.0 | 83.4 | 4.8 |
| 719 | S056 | -77.63325 | 163.08997 | 100 | C2 | 14 | 6.98 | 100 | | 7.9 | 14.7 | 32.0 | 123.7 | 10.8 | 188.0 | 3.0 | 4.4 | 32.9 | 0.7 | 205.5 | 0.0 | 52.4 | 0.9 |
| 720 | S057 | -77.63319 | 163.04278 | 101 | DP | 1.5 | | 17 | 83 | | 7.9 | 2.3 | 7.9 | 2.7 | 4.1 | 0.8 | 0.3 | 25.0 | 0.2 | 50.9 | 0.1 | 17.1 | 0.5 |
| 724 | S057 | -77.63319 | 163.04278 | 101 | C1 | 24 | 2.47 | 96 | 4 | | 35.3 | 23.0 | 64.3 | 9.3 | 74.9 | 33.1 | 2.6 | 32.0 | 0.7 | 286.5 | 0.0 | 84.2 | 3.8 |
| 726 | S057 | -77.63319 | 163.04278 | 101 | C2 | 18 | 3.72 | 94 | 6 | | 9.9 | 14.5 | 47.2 | 10.2 | 58.3 | 0.6 | 1.6 | 31.6 | 0.3 | 5.5 | 1.4 | 56.8 | 6.6 |
| 729 | S057 | -77.63319 | 163.04278 | 101 | ICS | 6 | 26.42 | 85 | 15 | | 3.8 | 2.3 | 3.3 | 3.2 | 0.8 | 0.4 | 0.0 | 18.8 | 0.2 | 3.0 | 0.0 | 21.3 | 4.9 |
| 732 | S058 | -77.63034 | 163.09073 | 65 | DP | 1.5 | | 17 | 83 | | 19.3 | 2.4 | 8.6 | 3.7 | 0.9 | 10.5 | 0.3 | 28.3 | 0.3 | 37.5 | 0.5 | 30.1 | 4.6 |
| 736 | S058 | -77.63034 | 163.09073 | 65 | C1 | 1.5 | 1.80 | 69 | 31 | | 98.0 | 6.4 | 48.7 | 11.4 | 12.1 | 95.4 | 0.4 | 33.6 | 0.9 | 543.7 | 0.0 | 126.4 | 6.1 |
| 739 | S058 | -77.63034 | 163.09073 | 65 | C2 | 5.5 | | 51 | 49 | | 11.2 | 5.4 | 82.4 | 11.5 | 21.3 | 24.1 | 0.9 | 42.0 | 1.1 | 694.7 | 0.0 | 21.7 | 5.6 |
| 742 | S058 | -77.63034 | 163.09073 | 65 | C3 | 13 | 3.97 | 70 | 30 | | 6.8 | 4.5 | 21.5 | 3.5 | 10.8 | 0.4 | 0.5 | 32.2 | 0.4 | 36.4 | 0.1 | 17.7 | 3.3 |
| 745 | S058 | -77.63034 | 163.09073 | 65 | C4 | 8 | | 76 | 24 | | 5.1 | 3.5 | 38.9 | 7.4 | 14.0 | 0.2 | 0.5 | 43.4 | 0.3 | 5.7 | 0.1 | 17.3 | 3.9 |
| 748 | S058 | -77.63034 | 163.09073 | 65 | ICS | 4 | 11.77 | 74 | 26 | | 0.1 | 0.2 | 28.3 | 4.8 | 1.0 | 0.2 | 0.0 | 32.3 | 0.5 | 59.0 | 0.0 | 0.0 | 0.8 |
| 749 | S059 | -77.64540 | 163.04013 | 227 | DP | 2 | | 38 | 62 | 9.4 | 10.5 | 1.8 | 1.7 | 1.9 | 0.4 | 0.2 | 0.0 | 24.3 | 0.2 | 0.0 | 0.0 | 16.2 | 5.2 |
| 753 | S059 | -77.64540 | 163.04013 | 227 | C1 | 7.5 | | 91 | 9 | 9.7 | 9.6 | 2.3 | 3.6 | 2.7 | 0.6 | 0.2 | 0.0 | 28.2 | 0.2 | 0.0 | 0.0 | 17.1 | 1.0 |
| 756 | S059 | -77.64540 | 163.04013 | 227 | C2 | 8.5 | 0.43 | 95 | 5 | 9.9 | 2.8 | 1.8 | 5.7 | 1.8 | 0.7 | 0.2 | 0.0 | 15.9 | 0.2 | 0.0 | 0.0 | 7.5 | 1.3 |
| 758 | S059 | -77.64540 | 163.04013 | 227 | C3 | 11 | 1.99 | 78 | 22 | 9.8 | 4.8 | 2.0 | 4.2 | 1.5 | 0.3 | 0.1 | 0.0 | 19.4 | 0.2 | 0.0 | 0.0 | 12.3 | 2.1 |
| 761 | S059 | -77.64540 | 163.04013 | 227 | ICS | 2 | 9.19 | 86 | 14 | 9.4 | 6.7 | 2.1 | 3.2 | 1.6 | 0.7 | 0.2 | 0.0 | 20.6 | 0.2 | 0.0 | 0.0 | 13.9 | 1.0 |
| 762 | S060 | -77.64540 | 163.04013 | 227 | DP | 2 | | 18 | 82 | 9.8 | 5.1 | 0.8 | 0.9 | 0.7 | 0.4 | 0.1 | 0.0 | 16.4 | 0.1 | 0.0 | 0.0 | 9.0 | 12.2 |
| 766 | S060 | -77.64540 | 163.04013 | 227 | C1 | 10.5 | | 93 | 7 | 10.0 | 3.6 | 2.0 | 8.2 | 3.0 | 0.6 | 0.3 | 0.0 | 21.7 | 0.2 | 75.4 | 0.0 | 8.0 | 1.4 |
| 769 | S060 | -77.64540 | 163.04013 | 227 | C2 | 3.5 | | 89 | 11 | 9.6 | 4.0 | 1.9 | 4.9 | 2.2 | 0.6 | 0.3 | 0.0 | 19.3 | 0.2 | 35.0 | 0.0 | 12.8 | 3.8 |
| 771 | S060 | -77.64540 | 163.04013 | 227 | C3T | 9 | | 71 | 29 | 9.6 | 5.7 | 1.6 | 3.0 | 1.5 | 0.5 | 0.2 | 0.0 | 19.7 | 0.2 | 20.9 | 0.0 | 18.1 | 4.0 |
| 774 | S060 | -77.64540 | 163.04013 | 227 | C3B | 8.5 | | 91 | 9 | 9.5 | 7.5 | 1.7 | 2.7 | 1.7 | 0.4 | 0.2 | 0.0 | 23.3 | 0.2 | 27.1 | 0.0 | 15.7 | 3.4 |

Table A.1 continued.

| # | Pit | Latitude | Longitude | Elevation | Horizon | Thickness | $H_2O$ | <2 mm | >2 mm | pH | Ca | Mg | Na | K | Cl | $SO_4$ | $NO_3$ | $HCO_3$ | F | B | Ba | Sr | Charge Balance |
|---|---|---|---|---|---|---|---|---|---|---|---|---|---|---|---|---|---|---|---|---|---|---|---|
| | | | | m | | cm | ———%Wt.——— | | | | ——————————mmol $kg^{-1}$—————————— | | | | | | | | | ——µmol $kg^{-1}$—— | | | % |
| 776 | S062 | -77.63620 | 162.99936 | 115 | DP | 2 | | 14 | 86 | 9.4 | 9.8 | 1.7 | 3.1 | 2.2 | 0.6 | 0.5 | 0.0 | 25.5 | 0.4 | 16.9 | 0.0 | 20.9 | 1.5 |
| 780 | S062 | -77.63620 | 162.99936 | 115 | C1 | 3.5 | | 88 | 12 | 9.7 | 8.3 | 1.9 | 5.9 | 3.2 | 0.8 | 0.6 | 0.0 | 27.2 | 0.3 | 31.2 | 0.0 | 22.1 | 0.1 |
| 783 | S062 | -77.63620 | 162.99936 | 115 | C2 | 5 | | 85 | 15 | 9.7 | 6.5 | 2.8 | 5.1 | 4.2 | 0.6 | 0.3 | 0.0 | 25.5 | 0.3 | 9.9 | 0.0 | 24.0 | 1.6 |
| 786 | S062 | -77.63620 | 162.99936 | 115 | C3 | 12 | 0.52 | 89 | 11 | 9.7 | 5.6 | 2.3 | 5.3 | 2.4 | 1.8 | 0.2 | 0.0 | 22.0 | 0.2 | 13.0 | 0.0 | 16.9 | 1.9 |
| 789 | S062 | -77.63620 | 162.99936 | 115 | ICS | 4 | 9.60 | 88 | 12 | 9.6 | 6.4 | 1.4 | 2.3 | 1.3 | 0.8 | 0.2 | 0.0 | 19.2 | 0.2 | 0.0 | 0.0 | 24.8 | 3.4 |
| 791 | S063 | -77.61203 | 163.53866 | 347 | DP | 2 | | 21 | 79 | 10.0 | 7.2 | 2.3 | 19.3 | 3.0 | 1.3 | 1.1 | 0.0 | 31.6 | 0.4 | 72.7 | 0.1 | 11.1 | 7.7 |
| 795 | S063 | -77.61203 | 163.53866 | 347 | C1 | 9 | 0.59 | 89 | 11 | 10.4 | 3.6 | 2.3 | 36.4 | 3.7 | 5.0 | 1.4 | 0.0 | 35.0 | 0.6 | 60.6 | 1.0 | 6.2 | 9.0 |
| 797 | S063 | -77.61203 | 163.53866 | 347 | C2 | 12 | 5.35 | 89 | 11 | | 6.3 | 1.3 | 15.6 | 2.9 | 0.5 | 0.3 | 0.0 | 31.0 | 0.3 | 0.0 | 0.0 | 16.6 | 2.5 |
| 800 | S063 | -77.61203 | 163.53866 | 347 | C3 | 5 | 2.34 | 93 | 7 | | 9.7 | 0.7 | 2.4 | 1.2 | 1.1 | 0.2 | 0.3 | 21.3 | 0.7 | 36.2 | 0.0 | 23.8 | 1.4 |
| 802 | S064 | -77.60043 | 163.50843 | 160 | DP | 1.5 | | 21 | 79 | | 5.9 | 1.4 | 20.1 | 2.7 | 1.0 | 0.4 | 0.3 | 27.1 | 0.4 | 102.2 | 0.0 | 7.7 | 11.8 |
| 806 | S064 | -77.60043 | 163.50843 | 160 | C1 | 9 | 0.95 | 72 | 28 | 10.4 | 2.0 | 0.6 | 73.6 | 4.2 | 6.0 | 0.8 | 0.3 | 49.0 | 0.8 | 317.4 | 0.0 | 1.4 | 18.2 |
| 808 | S064 | -77.60043 | 163.50843 | 160 | C2 | 12 | 1.51 | 97 | 3 | 9.6 | 0.4 | 1.2 | 28.7 | 2.2 | 8.7 | 0.5 | 0.3 | 20.0 | 0.4 | 0.0 | 0.4 | 2.1 | 5.6 |
| 810 | S064 | -77.60043 | 163.50843 | 160 | C3 | 12.5 | 4.19 | 90 | 10 | 9.1 | 1.1 | 0.5 | 7.9 | 2.6 | 0.8 | 0.1 | 0.0 | 12.2 | 0.3 | 76.5 | 0.0 | 1.0 | 1.3 |
| 812 | S065 | -77.59134 | 163.49743 | 78 | DP | 1.5 | | 27 | 73 | 9.7 | 5.7 | 2.8 | 10.0 | 3.0 | 0.7 | 0.3 | 0.0 | 23.6 | 0.3 | 0.0 | 0.0 | 12.2 | 8.6 |
| 815 | S065 | -77.59134 | 163.49743 | 78 | C1 | 8 | 0.64 | 72 | 28 | 10.3 | 2.1 | 2.6 | 39.5 | 5.0 | 2.6 | 0.5 | 0.3 | 44.3 | 0.8 | 92.1 | 0.4 | 6.0 | 4.7 |
| 818 | S065 | -77.59134 | 163.49743 | 78 | C2 | 11.5 | 0.71 | 65 | 35 | 9.3 | 1.3 | 1.0 | 9.4 | 2.4 | 2.0 | 0.2 | 0.0 | 18.3 | 0.2 | 0.0 | 0.0 | 5.1 | 12.4 |
| 821 | S065 | -77.59134 | 163.49743 | 78 | C3 | 7 | 3.45 | 85 | 15 | 9.2 | 1.7 | 1.3 | 4.9 | 2.3 | 0.5 | 0.0 | 0.0 | 11.3 | 0.2 | 0.0 | 0.2 | 5.7 | 4.7 |
| 824 | S065 | -77.59134 | 163.49743 | 78 | ICS | 1.5 | 15.64 | 87 | 13 | 9.4 | 5.3 | 1.7 | 4.2 | 2.3 | 0.6 | 0.2 | 0.0 | 17.3 | 0.2 | 0.0 | 0.0 | 9.3 | 5.7 |
| 826 | S066 | -77.58944 | 163.49459 | 70 | DP | 1.5 | | 25 | 75 | 9.6 | 3.9 | 2.2 | 10.0 | 2.6 | 0.8 | 0.3 | 0.0 | 20.6 | 0.3 | 0.0 | 0.0 | 7.5 | 6.1 |
| 830 | S066 | -77.58944 | 163.49459 | 70 | C1 | 8 | 0.58 | 88 | 12 | 10.5 | 1.0 | 0.4 | 33.9 | 2.3 | 2.4 | 0.5 | 0.0 | 31.4 | 0.7 | 258.0 | 0.0 | 0.1 | 4.8 |
| 832 | S066 | -77.58944 | 163.49459 | 70 | C2 | 15 | 0.78 | 96 | 4 | 9.9 | 1.4 | 1.1 | 19.2 | 1.8 | 3.1 | 0.3 | 0.0 | 20.9 | 0.3 | 0.0 | 0.5 | 3.6 | 2.1 |
| 834 | S066 | -77.58944 | 163.49459 | 70 | ICS | 2 | 14.26 | 95 | 5 | 9.6 | 4.3 | 0.8 | 6.6 | 1.9 | 0.6 | 0.2 | 0.0 | 18.5 | 0.2 | 0.0 | 0.0 | 7.2 | 2.4 |
| 836 | S067 | -77.58163 | 163.49048 | 33 | DP | 1.5 | | 27 | 73 | 10.0 | 3.7 | 1.3 | 16.7 | 2.9 | 1.0 | 0.3 | 0.0 | 25.8 | 0.3 | 80.8 | 0.0 | 5.0 | 3.8 |
| 840 | S067 | -77.58163 | 163.49048 | 33 | C1 | 17 | 0.83 | 90 | 10 | 10.2 | 0.3 | 0.9 | 22.6 | 1.9 | 2.8 | 0.3 | 0.0 | 20.2 | 0.4 | 9.0 | 0.0 | 0.7 | 5.6 |
| 842 | S067 | -77.58163 | 163.49048 | 33 | C2 | 7.5 | 1.35 | 96 | 4 | 9.7 | 1.1 | 0.5 | 7.8 | 1.2 | 0.7 | 0.2 | 0.0 | 13.1 | 0.2 | 0.0 | 0.0 | 1.9 | 8.0 |
| 844 | S068 | -77.58607 | 163.50060 | 63 | DP | 2 | | 18 | 82 | 9.8 | 1.2 | 1.4 | 16.8 | 2.6 | 0.6 | 0.2 | 0.0 | 20.6 | 0.3 | 0.0 | 0.0 | 2.4 | 6.1 |
| 848 | S068 | -77.58607 | 163.50060 | 63 | C1 | 4.5 | 1.16 | 92 | 8 | 10.1 | 2.7 | 3.0 | 34.7 | 5.5 | 1.5 | 0.5 | 0.0 | 41.8 | 0.7 | 109.6 | 0.0 | 7.4 | 7.0 |
| 851 | S068 | -77.58607 | 163.50060 | 63 | C2 | 10 | 2.40 | 92 | 8 | 9.5 | 1.0 | 1.9 | 25.1 | 3.4 | 7.9 | 0.4 | 0.0 | 19.9 | 0.4 | 0.0 | 0.3 | 4.8 | 8.3 |
| 853 | S068 | -77.58607 | 163.50060 | 63 | C3 | 9 | 3.41 | 54 | 46 | 9.3 | 0.8 | 0.8 | 7.3 | 2.1 | 0.9 | 0.1 | 0.0 | 10.0 | 0.3 | 0.0 | 0.0 | 1.5 | 4.7 |
| 857 | S069 | -77.60729 | 163.50866 | 241 | DP | 1.5 | | 19 | 81 | | 5.8 | 1.4 | 18.0 | 2.5 | 1.1 | 0.4 | 0.0 | 25.2 | 0.4 | 121.5 | 0.0 | 7.8 | 12.0 |
| 861 | S069 | -77.60729 | 163.50866 | 241 | C1 | 6 | 1.17 | 62 | 38 | 9.9 | 5.3 | 2.8 | 27.1 | 3.4 | 4.0 | 0.5 | 0.0 | 31.5 | 0.5 | 115.5 | 0.0 | 9.0 | 11.8 |
| 865 | S069 | -77.60729 | 163.50866 | 241 | C2 | 9 | 4.71 | 61 | 39 | | 0.5 | 0.4 | 13.7 | 2.1 | 0.6 | 0.2 | 0.0 | 18.0 | 0.3 | 104.5 | 0.0 | 0.0 | 3.8 |
| 868 | S069 | -77.60729 | 163.50866 | 241 | C3 | 2 | 5.64 | 66 | 34 | | 0.5 | 0.6 | 12.4 | 2.4 | 0.8 | 0.2 | 0.0 | 16.7 | 0.4 | 75.3 | 0.0 | 0.4 | 3.2 |
| 871 | S070 | -77.60425 | 163.49029 | 207 | DP | 2 | | 35 | 65 | 10.0 | 4.4 | 1.6 | 32.6 | 4.1 | 7.6 | 1.3 | 0.0 | 27.6 | 0.4 | 153.2 | 0.0 | 7.8 | 12.1 |
| 875 | S070 | -77.60425 | 163.49029 | 207 | C1 | 3 | 1.04 | 79 | 21 | 10.2 | 4.5 | 1.4 | 22.9 | 2.9 | 2.7 | 0.3 | 0.0 | 28.8 | 0.4 | 96.4 | 0.0 | 7.7 | 7.3 |
| 878 | S070 | -77.60425 | 163.49029 | 207 | C2 | 7 | 3.57 | 81 | 19 | 9.9 | 3.1 | 0.8 | 11.1 | 2.9 | 0.5 | 0.2 | 0.0 | 19.4 | 0.2 | 64.2 | 0.0 | 4.6 | 2.9 |
| 881 | S070 | -77.60425 | 163.49029 | 207 | C3 | 10 | 9.13 | 83 | 17 | | 0.5 | 0.2 | 9.2 | 1.9 | 0.6 | 0.2 | 0.0 | 11.8 | 0.3 | 56.9 | 0.0 | 0.1 | 1.8 |
| 883 | S071 | -77.60458 | 163.50340 | 194 | DP | 1 | | 24 | 76 | 10.0 | 7.3 | 1.6 | 10.3 | 2.3 | 0.7 | 0.4 | 0.0 | 24.6 | 0.3 | 69.3 | 0.0 | 11.4 | 7.2 |
| 886 | S071 | -77.60458 | 163.50340 | 194 | C1 | 5 | 0.50 | 86 | 14 | 10.5 | 3.4 | 0.9 | 27.6 | 2.4 | 1.3 | 0.9 | 0.0 | 27.8 | 0.5 | 171.2 | 0.0 | 5.5 | 10.3 |
| 889 | S071 | -77.60458 | 163.50340 | 194 | C2T | 10 | 0.54 | 81 | 19 | 10.4 | 1.3 | 0.3 | 25.3 | 1.6 | 2.9 | 0.5 | 0.0 | 23.7 | 0.4 | 79.7 | 0.0 | 0.9 | 3.9 |

Table A.1 continued.

| # | Pit | Latitude | Longitude | Elevation | Horizon | Thickness | $H_2O$ | <2 mm | >2 mm | pH | Ca | Mg | Na | K | Cl | $SO_4$ | $NO_3$ | $HCO_3$ | F | B | Ba | Sr | Charge Balance |
|---|---|---|---|---|---|---|---|---|---|---|---|---|---|---|---|---|---|---|---|---|---|---|---|
| | | | | m | | cm | ———%Wt.——— | | | | ——————————mmol $kg^{-1}$—————————— | | | | | | | | | ——µmol $kg^{-1}$—— | | | % |
| 892 | S071 | -77.60458 | 163.50340 | 194 | C2B | 10 | 0.64 | 88 | 12 | 9.6 | 4.2 | 0.8 | 7.1 | 1.7 | 1.7 | 0.2 | 0.0 | 16.9 | 0.2 | 35.4 | 0.0 | 7.4 | 1.1 |
| 894 | S071 | -77.60458 | 163.50340 | 194 | C3 | 3 | 13.52 | 89 | 11 | 9.6 | 5.4 | 1.3 | 5.6 | 2.1 | 0.5 | 0.2 | 0.0 | 19.8 | 0.2 | 37.7 | 0.0 | 7.7 | 0.3 |
| 897 | CR03 | -77.58222 | 163.43451 | 120 | DP | 1.5 | | 23 | 77 | 9.8 | 3.7 | 1.6 | 31.0 | 3.5 | 5.3 | 0.5 | 0.5 | 35.6 | 0.5 | 171.5 | 0.0 | 4.4 | 2.5 |
| 901 | CR03 | -77.58222 | 163.43451 | 120 | C1 | 10 | 6.64 | 75 | 25 | 9.4 | 0.9 | 1.6 | 188.8 | 7.2 | 81.4 | 11.0 | 3.0 | 66.7 | 1.8 | 2527.4 | 0.0 | 0.9 | 7.0 |
| 904 | CR03 | -77.58222 | 163.43451 | 120 | C2 | 15 | 7.20 | 59 | 41 | 9.5 | 0.0 | 0.0 | 92.8 | 4.4 | 36.4 | 0.5 | 0.9 | 46.4 | 0.7 | 154.8 | 0.0 | 0.0 | 6.4 |
| 907 | CR03 | -77.58222 | 163.43451 | 120 | C3 | 2 | 51.38 | 68 | 32 | 9.6 | 0.0 | 0.0 | 23.3 | 1.1 | 1.8 | 0.2 | 0.4 | 17.7 | 1.3 | 109.4 | 0.0 | 0.0 | 6.2 |
| 909 | CR04 | -77.58157 | 163.42870 | 123 | C1 | 6 | | 97 | 3 | 8.2 | 35.4 | 69.5 | 291.9 | 12.0 | 367.2 | 54.1 | 10.3 | 28.2 | 0.8 | 1937.6 | 0.0 | 207.8 | 0.1 |
| 911 | CR04 | -77.58157 | 163.42870 | 123 | C2 | 14 | | 89 | 11 | 8.3 | 3.9 | 12.5 | 158.8 | 9.4 | 149.2 | 5.5 | 3.9 | 31.9 | 0.4 | 156.2 | 0.0 | 12.2 | 1.1 |
| 913 | CR04 | -77.58157 | 163.42870 | 123 | ICS | 2 | 35.77 | 98 | 2 | 9.6 | 0.2 | 0.2 | 22.9 | 1.9 | 3.1 | 1.0 | 0.4 | 20.3 | 0.5 | 184.6 | 0.0 | 0.0 | 1.0 |
| 922 | JT01 | -77.65691 | 163.13810 | 265 | | 10 | | 49 | 51 | | 6.2 | 2.7 | 3.2 | 2.4 | 1.0 | 0.8 | 0.0 | 23.7 | 0.0 | 64.8 | 3.5 | 23.7 | 5.8 |
| 923 | JT02 | -77.65601 | 163.14231 | 244 | | 10 | | 50 | 50 | | 7.1 | 5.0 | 11.6 | 3.7 | 2.4 | 2.0 | 0.0 | 34.4 | 0.0 | 132.7 | 3.3 | 23.7 | 1.8 |
| 924 | JT03 | -77.65325 | 163.14455 | 223 | | 10 | | 47 | 53 | | 9.2 | 4.3 | 13.8 | 3.2 | 4.9 | 3.1 | 0.0 | 34.9 | 0.0 | 62.3 | 1.7 | 23.3 | 2.4 |
| 925 | JT04 | -77.65105 | 163.14776 | 201 | | 10 | | 62 | 38 | | 5.2 | 1.8 | 15.8 | 3.6 | 4.0 | 1.1 | 0.0 | 29.9 | 0.0 | 59.1 | 1.5 | 20.9 | 4.1 |
| 926 | JT05 | -77.64958 | 163.14940 | 184 | | 10 | | 61 | 39 | | 5.5 | 4.9 | 23.6 | 8.4 | 1.8 | 0.7 | 0.0 | 46.2 | 0.0 | 93.6 | 3.7 | 22.0 | 3.1 |
| 927 | JT06 | -77.64541 | 163.15260 | 169 | | 10 | | 62 | 38 | | 0.8 | 1.0 | 25.2 | 3.3 | 1.2 | 0.6 | 0.0 | 32.5 | 0.0 | 67.7 | 1.5 | 3.8 | 3.6 |
| 928 | JT07 | -77.64187 | 163.15324 | 149 | | 10 | | 95 | 5 | | 4.6 | 2.7 | 25.8 | 4.6 | 1.2 | 0.6 | 0.0 | 43.5 | 0.0 | 97.5 | 1.4 | 15.1 | 1.0 |
| 929 | JT08 | -77.64003 | 163.14676 | 142 | | 10 | | 66 | 34 | | 7.3 | 3.7 | 19.3 | 3.9 | 5.0 | 2.0 | 0.0 | 36.2 | 0.0 | 228.2 | 1.7 | 28.9 | 0.0 |
| 930 | JT09 | -77.63897 | 163.14389 | 135 | | 10 | | 86 | 14 | | 0.5 | 1.4 | 37.4 | 3.4 | 2.6 | 0.7 | 0.0 | 36.0 | 0.0 | 70.8 | 3.2 | 4.4 | 5.5 |
| 931 | JT10 | -77.63714 | 163.13711 | 121 | | 10 | | 93 | 7 | | 5.4 | 4.8 | 24.0 | 6.2 | 0.7 | 0.6 | 0.0 | 45.0 | 0.0 | 131.7 | 2.8 | 16.7 | 3.8 |
| 932 | JT11 | -77.63638 | 163.12969 | 114 | | 10 | | 63 | 37 | | 6.1 | 18.8 | 175.0 | 11.1 | 132.9 | 8.6 | 0.0 | 55.1 | 0.0 | 676.4 | 6.9 | 22.3 | 7.0 |
| 933 | JT12 | -77.63564 | 163.13008 | 105 | | 10 | | 92 | 8 | | 2.5 | 4.2 | 136.7 | 9.2 | 36.1 | 3.6 | 0.0 | 84.7 | 0.0 | 613.2 | 5.1 | 13.7 | 10.9 |
| 934 | JT13 | -77.63487 | 163.12869 | 102 | | 10 | | 90 | 10 | | 10.0 | 5.5 | 39.3 | 4.6 | 7.0 | 2.3 | 0.0 | 58.6 | 0.0 | 154.9 | 2.4 | 34.4 | 3.2 |
| 935 | JT14 | -77.63417 | 163.12749 | 91 | | 10 | | 76 | 24 | | 45.2 | 12.8 | 27.3 | 3.5 | 35.3 | 42.6 | 0.0 | 31.1 | 0.0 | 96.4 | 0.7 | 80.3 | 1.6 |
| 936 | JT15 | -77.63344 | 163.12683 | 88 | | 10 | | 93 | 7 | | 87.9 | 13.5 | 75.4 | 12.8 | 38.7 | 103.7 | 0.0 | 31.0 | 0.0 | 228.6 | 0.7 | 161.0 | 2.4 |
| 937 | JT16 | -77.63208 | 163.12410 | 75 | | 10 | | 80 | 20 | | 5.4 | 3.3 | 11.7 | 3.5 | 1.1 | 1.0 | 0.0 | 32.9 | 0.0 | 70.1 | 1.8 | 12.9 | 5.0 |
| 938 | JT17 | -77.63021 | 163.11876 | 63 | | 10 | | 75 | 25 | | 4.7 | 2.5 | 26.2 | 4.2 | 3.3 | 1.6 | 0.0 | 36.3 | 0.0 | 82.3 | 2.7 | 8.8 | 2.3 |
| 939 | JT18 | -77.62878 | 163.11708 | 59 | | 10 | | 100 | | | 4.5 | 2.0 | 14.4 | 4.3 | 0.6 | 0.6 | 0.0 | 29.8 | 0.0 | 53.5 | 2.4 | 12.1 | 0.1 |
| 940 | JT19 | -77.62775 | 163.11744 | 46 | | 10 | | 77 | 23 | | 5.9 | 3.1 | 32.3 | 4.1 | 9.7 | 1.9 | 0.0 | 35.8 | 0.0 | 212.7 | 2.4 | 17.1 | 5.0 |
| 941 | JT20 | -77.62655 | 163.11816 | 29 | | 10 | | 80 | 20 | | 3.4 | 2.3 | 10.9 | 3.9 | 0.6 | 0.5 | 0.0 | 25.1 | 0.0 | 40.6 | 2.1 | 11.9 | 0.6 |
| 942 | JT21 | -77.62529 | 163.11721 | 22 | | 10 | | 93 | 7 | | 0.3 | 1.4 | 22.8 | 1.8 | 0.9 | 0.5 | 0.0 | 25.3 | 0.0 | 204.3 | 2.7 | 2.4 | 1.5 |
| 943 | JT22 | -77.62417 | 163.11613 | 22 | | 10 | | 51 | 49 | | 31.2 | 17.0 | 88.7 | 15.8 | 87.3 | 35.5 | 0.0 | 45.3 | 0.0 | 662.0 | 1.5 | 121.1 | 0.6 |

Table A.2. Ion concentrations measured in 1:10 soil-water extractions for select samples.

| # | Pit | Ca | Mg | Na | K | Cl | $SO_4$ | $NO_3$ | $HCO_3$ | F |
|---|---|---|---|---|---|---|---|---|---|---|
| | | mmol $kg^{-1}$ | | | | | | | | |
| 1 | S004 | 0.79 | 0.32 | 4.21 | 0.77 | 2.19 | 0.29 | 0.00 | | 0.15 |
| 4 | S004 | 0.53 | 0.33 | 4.27 | 1.08 | 0.54 | 0.18 | 0.00 | | 0.16 |
| 7 | S004 | 0.20 | 0.22 | 7.66 | 0.78 | 3.82 | 0.39 | 0.00 | | 0.13 |
| 10 | S004 | 0.25 | 0.18 | 9.81 | 0.66 | 0.53 | 0.16 | 0.00 | | 0.28 |
| 12 | S004 | 0.83 | 0.48 | 2.49 | 0.82 | 0.54 | 0.17 | 0.00 | | 0.10 |
| 15 | S004 | 0.11 | 0.43 | 10.82 | 0.83 | 3.54 | 0.28 | 0.00 | | 0.18 |
| 17 | S005 | 0.94 | 0.49 | 11.66 | 1.80 | 4.49 | 2.23 | 0.18 | | 0.16 |
| 20 | S005 | 0.33 | 0.68 | 40.25 | 2.90 | 19.01 | 2.05 | 0.00 | | 0.40 |
| 23 | S005 | 0.36 | 0.42 | 3.66 | 0.99 | 0.69 | 0.09 | 0.00 | | 0.11 |
| 26 | S005 | 0.23 | 0.38 | 3.06 | 0.76 | 0.67 | 0.08 | 0.00 | | 0.10 |
| 87 | S009 | 0.11 | 0.40 | 22.86 | 1.17 | 7.57 | 0.42 | 0.00 | | 0.33 |
| 126 | S015 | 0.11 | 0.26 | 14.13 | 0.93 | 0.51 | 0.15 | 0.00 | | 0.35 |
| 129 | S015 | 0.17 | 0.37 | 17.76 | 0.97 | 0.53 | 0.16 | 0.00 | | 0.36 |
| 132 | S015 | 0.01 | 0.12 | 5.77 | 0.38 | 0.18 | 0.08 | 0.00 | | 0.19 |
| 135 | S015 | 0.11 | 0.22 | 4.70 | 0.58 | 0.71 | 0.13 | 0.00 | | 0.13 |
| 139 | S016 | 68.51 | 3.95 | 25.12 | 4.82 | 19.35 | 39.03 | 0.59 | | 0.18 |
| 143 | S016 | 68.02 | 5.06 | 27.82 | 3.80 | 25.84 | 41.66 | 0.76 | 2.71 | 0.46 |
| 147 | S016 | 11.73 | 1.74 | 13.59 | 2.09 | 8.85 | 12.45 | 0.00 | | 0.47 |
| 151 | S016 | 1.02 | 0.91 | 3.73 | 1.35 | 3.96 | 0.20 | 0.09 | | 0.10 |
| 155 | S017 | 1.36 | 0.70 | 78.78 | 3.96 | 59.00 | 8.65 | 0.40 | | 0.26 |
| 159 | S017 | 0.32 | 0.67 | 37.28 | 2.30 | 21.26 | 2.15 | 0.17 | | 0.31 |
| 163 | S017 | 0.09 | 0.31 | 3.82 | 0.77 | 0.38 | 0.08 | 0.00 | | 0.11 |
| 167 | S017 | 1.10 | 0.56 | 1.53 | 0.80 | 0.35 | 0.11 | 0.19 | | 0.12 |
| 170 | S018 | 4.29 | 1.63 | 46.21 | 3.03 | 38.55 | 5.89 | 0.19 | 3.88 | 0.10 |
| 174 | S018 | 1.76 | 6.70 | 67.26 | 4.29 | 52.87 | 3.36 | 0.51 | | 0.26 |
| 178 | S018 | 0.30 | 0.30 | 1.67 | 0.58 | 0.50 | 0.10 | 0.00 | | 0.08 |
| 182 | S018 | 0.38 | 0.32 | 1.23 | 0.51 | 0.21 | 0.07 | 0.00 | 2.31 | 0.08 |
| 185 | S018 | 0.49 | 0.85 | 21.11 | 1.81 | 9.37 | 0.93 | 0.00 | | 0.39 |
| 189 | S019 | 0.59 | 0.41 | 13.86 | 1.33 | 7.30 | 0.92 | 0.00 | | 0.18 |
| 193 | S019 | 0.51 | 0.70 | 14.95 | 1.27 | 6.74 | 0.66 | 0.00 | | 0.24 |
| 197 | S019 | 0.03 | 0.18 | 3.63 | 0.63 | 0.20 | 0.07 | 0.00 | | 0.10 |
| 201 | S019 | 0.47 | 0.28 | 1.84 | 0.89 | 0.26 | 0.08 | 0.00 | | 0.10 |
| 205 | S019 | 0.45 | 0.72 | 5.85 | 1.33 | 1.55 | 0.20 | 0.00 | | 0.18 |

Table A.3. Total salt contents for all soil pits in this study.

| Pit | Ca | Mg | Na | K | Cl | $SO_4$ | $NO_3$ | $HCO_3$ | F | B | Ba | Sr | Total |
|---|---|---|---|---|---|---|---|---|---|---|---|---|---|
| | ——————————————mol $m^{-2}$—————————————— | | | | | | | | | ——umol $m^{-2}$—— | | | eq $m^{-2}$ |
| S001 | 3.97 | 1.69 | 8.41 | 2.5 | 7.37 | 0.37 | 0.12 | 11.71 | 0.2 | 10.91 | 0.63 | 20.02 | 30.71 |
| S002 | 0.8 | 0.2 | 9.68 | 1.99 | 2.98 | 0.19 | 0 | 9.66 | 0.1 | 27.96 | 0 | 1.03 | 17.15 |
| S004 | 1.94 | 0.49 | 3.02 | 0.69 | 0.91 | 0.13 | 0 | 7.35 | 0.1 | 17.81 | 0.15 | 4.61 | 9.87 |
| S005 | 2.4 | 1.17 | 7.49 | 1.8 | 2.29 | 0.36 | 0.05 | 11.86 | 0.18 | 52.46 | 0.27 | 6.15 | 19.73 |
| S009 | 0.99 | 0.73 | 6.41 | 1.08 | 0.95 | 0.09 | 0 | 8.89 | 0.15 | 17.52 | 0.25 | 2.07 | 12.24 |
| S010 | 1.17 | 0.45 | 5.53 | 0.91 | 0.48 | 0.08 | 0 | 7.65 | 0.11 | 8.51 | 0.34 | 3.06 | 10.45 |
| S014 | 1.12 | 0.55 | 6.8 | 0.98 | 1.07 | 0.12 | 0 | 8.02 | 0.11 | 21.72 | 0.44 | 3.65 | 12.57 |
| S015 | 1.14 | 0.73 | 9.18 | 1.17 | 0.17 | 0.07 | 0 | 11.32 | 0.16 | 39.37 | 0.57 | 2.89 | 14.58 |
| S016 | 8.48 | 0.79 | 4.23 | 1.02 | 2.96 | 5.14 | 0 | 8.11 | 0.25 | 26.62 | 0.68 | 150.58 | 37.6 |
| S017 | 0.93 | 0.55 | 7.66 | 1.44 | 3.11 | 0.4 | 0.06 | 7.89 | 0.15 | 16.48 | 0.25 | 2.36 | 16.19 |
| S018 | 2.11 | 1.36 | 6.88 | 1.39 | 4.37 | 0.36 | 0.04 | 7.16 | 0.2 | 9.45 | 0.1 | 6.09 | 20.61 |
| S019 | 1.61 | 0.82 | 3.64 | 1.43 | 0.74 | 0.23 | 0 | 6.74 | 0.18 | 1.99 | 0.12 | 4.98 | 11.35 |
| S021 | 16.12 | 6.02 | 10.76 | 1.67 | 19.16 | 10.35 | 0.96 | 4.46 | 0.21 | 32.11 | 0.28 | 34.52 | 97.83 |
| S022 | 11.68 | 3.74 | 19.71 | 1.88 | 20.01 | 8.06 | 0.8 | 5.19 | 0.24 | 26.09 | 0.04 | 21.43 | 89.7 |
| S023 | 11.52 | 2.4 | 9.94 | 1.02 | 11.84 | 7.89 | 0.45 | 2.93 | 0.14 | 24.75 | 0.17 | 21.08 | 67.08 |
| S024 | 2.86 | 1.03 | 3.94 | 1.22 | 1.68 | 0.25 | 0 | 7.09 | 0.15 | 5.91 | 0.2 | 10.11 | 15.3 |
| S025 | 4.51 | 1.01 | 9.12 | 1.76 | 4.88 | 0.87 | 0.24 | 10.3 | 0.26 | 26.05 | 0 | 34.84 | 29.13 |
| S026 | 2.61 | 0.84 | 2.79 | 0.55 | 0.92 | 0.08 | 0 | 7.97 | 0.1 | 12.64 | 0.31 | 6.35 | 11.46 |
| S027 | 2.03 | 2.58 | 14.36 | 1.66 | 12.61 | 0.48 | 0.51 | 10.47 | 0.12 | 33.22 | 0.31 | 7.53 | 49.79 |
| S028 | 0.97 | 0.74 | 7.1 | 0.73 | 1 | 0.19 | 0.09 | 9.34 | 0.13 | 29.32 | 0.29 | 2.6 | 22.08 |
| S029 | 1.5 | 0.78 | 2.24 | 0.72 | 0.19 | 0.06 | 0 | 7.16 | 0.09 | 21.99 | 0.05 | 4.1 | 14.99 |
| S030 | 2.62 | 0.73 | 1.37 | 0.63 | 0.29 | 0.07 | 0 | 8.25 | 0.09 | 2.09 | 0 | 6.2 | 17.39 |
| S031 | 1.93 | 1.16 | 6 | 1.03 | 1.01 | 0.19 | 0.05 | 10.94 | 0.14 | 27.52 | 0 | 4.42 | 25.6 |
| S032 | 2.81 | 0.71 | 2.24 | 0.66 | 0.43 | 0.08 | 0 | 10.08 | 0.1 | 14.42 | 0 | 6.61 | 20.63 |
| S033 | 2.58 | 0.73 | 1.71 | 0.67 | 0.27 | 0.08 | 0.01 | 8.82 | 0.09 | 4.54 | 0 | 5.8 | 18.24 |
| S034 | 1.72 | 0.8 | 3.65 | 0.89 | 0.79 | 0.07 | 0 | 8.55 | 0.11 | 10.34 | 0.08 | 4.47 | 19.07 |
| S035 | 3.68 | 1.37 | 6.07 | 3.57 | 0.79 | 0.13 | 0 | 16.8 | 0.15 | 2.08 | 0.93 | 28.61 | 37.6 |
| S036 | 1.83 | 0.82 | 3.73 | 1.66 | 0.23 | 0.09 | 0.02 | 9.61 | 0.11 | 5.32 | 0.61 | 4.95 | 20.72 |
| S037 | 1.32 | 0.69 | 4.92 | 1.63 | 0.2 | 0.05 | 0.01 | 9 | 0.11 | 13.4 | 0.74 | 4.27 | 19.87 |
| S038 | 0.81 | 1.03 | 9.65 | 1.43 | 0.57 | 0.15 | 0.01 | 11.16 | 0.23 | 44.19 | 0.48 | 2.25 | 26.81 |
| S039 | 3.11 | 1.67 | 3.38 | 1.51 | 0.28 | 0.13 | 0.08 | 13.41 | 0.16 | 13.71 | 0.42 | 10.22 | 28.48 |
| S040 | 2.29 | 0.99 | 6.85 | 1.33 | 2.32 | 0.37 | 0.06 | 10.67 | 0.15 | 18.5 | 0.16 | 4.82 | 28.52 |
| S041 | 3.01 | 1.04 | 2.77 | 0.85 | 0.4 | 0.05 | 0 | 10.43 | 0.13 | 1 | 0 | 6.54 | 22.65 |
| S042 | 2.39 | 0.9 | 2.63 | 0.54 | 0.6 | 0.12 | 0 | 8.85 | 0.12 | 15.92 | 0.39 | 6.51 | 19.44 |
| S044 | 10.98 | 2.22 | 15.6 | 1.84 | 13.48 | 8.89 | 0.65 | 10.9 | 0.22 | 58.65 | 0.22 | 31.09 | 86.66 |
| S045 | 19.57 | 8.32 | 24.85 | 3.71 | 30.78 | 19.75 | 0.8 | 12.41 | 0.3 | 251.92 | 0 | 89.52 | 167.85 |
| S046 | 28.11 | 33.32 | 205.04 | 6.45 | 273.96 | 21.67 | 2.75 | 14.88 | 0.24 | 200.14 | 0.64 | 157.99 | 669.27 |
| S047 | 34.74 | 41.85 | 174.43 | 10.43 | 249.88 | 28.75 | 2.52 | 23.7 | 0.61 | 359.03 | 0.27 | 145.27 | 671.63 |
| S048 | 0.74 | 0.61 | 8.28 | 0.93 | 1.71 | 0.2 | 0.07 | 9.24 | 0.17 | 20.04 | 0.12 | 1.7 | 23.33 |
| S049 | 1.12 | 0.94 | 9.02 | 1.21 | 3.8 | 0.59 | 0.17 | 9.17 | 0.16 | 31.83 | 0 | 2.38 | 28.65 |
| S050 | 4.28 | 0.64 | 0.64 | 0.46 | 0.24 | 0.14 | 0 | 10.98 | 0.1 | 1.4 | 0 | 10.97 | 22.43 |
| S051 | 3.55 | 0.88 | 1.32 | 0.61 | 0.28 | 0.11 | 0 | 9.54 | 0.08 | 9.54 | 0 | 7.3 | 20.83 |
| S052 | 1.14 | 0.59 | 3.84 | 0.67 | 0.41 | 0.1 | 0 | 7 | 0.1 | 1.31 | 0 | 2.1 | 15.57 |
| S053 | 1.88 | 0.83 | 1.9 | 0.83 | 0.3 | 0.11 | 0.05 | 8.19 | 0.1 | 1.77 | 0.01 | 4.33 | 16.89 |
| S055 | 2.52 | 0.8 | 3.69 | 1.26 | 0.56 | 0.2 | 0.02 | 10.55 | 0.12 | 17.91 | 0.22 | 6.86 | 23.12 |
| S056 | 4.19 | 2.69 | 8.95 | 30.23 | 47.52 | 0.96 | 1.13 | 8.48 | 0.16 | 48.74 | 0 | 15.24 | 118.25 |
| S057 | 15.87 | 12.46 | 36.41 | 6.42 | 43.03 | 12.25 | 1.37 | 21.87 | 0.34 | 106.23 | 0.39 | 47.83 | 190.27 |
| S058 | 4.19 | 1.54 | 14.48 | 2.46 | 4.67 | 3.24 | 0.19 | 14.53 | 0.2 | 57.79 | 0.03 | 8.4 | 54.28 |
| S059 | 2.47 | 0.87 | 1.86 | 0.83 | 0.22 | 0.07 | 0 | 8.97 | 0.09 | 0 | 0 | 5.29 | 18.7 |
| S060 | 2.39 | 0.82 | 2.2 | 0.97 | 0.23 | 0.11 | 0 | 9.63 | 0.1 | 19.24 | 0 | 5.97 | 19.67 |
| S062 | 2.28 | 0.79 | 1.74 | 0.97 | 0.44 | 0.1 | 0 | 8.27 | 0.09 | 4.66 | 0 | 7.32 | 17.76 |
| S063 | 2.37 | 0.61 | 7.81 | 1.12 | 0.84 | 0.25 | 0.02 | 11.83 | 0.18 | 11.28 | 0.12 | 5.57 | 28.08 |
| S064 | 0.56 | 0.39 | 15.22 | 1.38 | 2.41 | 0.21 | 0.08 | 11.65 | 0.22 | 50.86 | 0 | 0.77 | 33.05 |
| S065 | 0.72 | 0.58 | 5.95 | 1.13 | 0.61 | 0.08 | 0.03 | 8.68 | 0.14 | 9.33 | 0.05 | 2.18 | 19.15 |
| S066 | 0.6 | 0.33 | 8.53 | 0.76 | 1 | 0.14 | 0 | 9.06 | 0.16 | 29.59 | 0.03 | 1.1 | 21.48 |
| S067 | 0.23 | 0.3 | 6.62 | 0.64 | 0.78 | 0.11 | 0 | 6.71 | 0.14 | 2.95 | 0 | 0.43 | 16.02 |
| S068 | 0.41 | 0.57 | 6.84 | 1.09 | 1.36 | 0.11 | 0 | 6.83 | 0.14 | 7.28 | 0.04 | 1.36 | 18.3 |
| S069 | 0.47 | 0.26 | 3.67 | 0.53 | 0.36 | 0.06 | 0 | 4.55 | 0.07 | 21.14 | 0 | 0.68 | 10.69 |
| S070 | 0.61 | 0.19 | 3.74 | 0.71 | 0.35 | 0.07 | 0 | 5.07 | 0.08 | 20.18 | 0 | 0.88 | 11.62 |
| S071 | 1.3 | 0.28 | 6.73 | 0.74 | 0.76 | 0.17 | 0 | 8.63 | 0.13 | 30.1 | 0 | 1.98 | 20.36 |
| CR03 | 0.14 | 1.72 | 0.22 | 40.76 | 16.71 | 1.52 | 0.55 | 17.09 | 0.38 | 357.86 | 0 | 0.15 | 80.6 |
| CR04 | 4.04 | 3.08 | 8.89 | 59.63 | 63.96 | 6.1 | 1.75 | 9.68 | 0.17 | 214.46 | 0 | 21.47 | 176.16 |

Table A.3 continued.

| Pit | Ca | Mg | Na | K | Cl | $SO_4$ | $NO_3$ | $HCO_3$ | F | B | Ba | Sr | Total |
|---|---|---|---|---|---|---|---|---|---|---|---|---|---|
| | mol $m^{-2}$ | | | | | | | | | umol $m^{-2}$ | | | eq $m^{-2}$ |
| Jt01 | 0.6 | 0.26 | 0.31 | 0.23 | 0.09 | 0.08 | 0 | 2.3 | 0 | 6.29 | 0.34 | 2.3 | 4.81 |
| Jt02 | 0.69 | 0.49 | 1.13 | 0.36 | 0.24 | 0.2 | 0 | 3.37 | 0 | 12.98 | 0.32 | 2.31 | 7.86 |
| Jt03 | 0.86 | 0.4 | 1.3 | 0.3 | 0.46 | 0.3 | 0 | 3.28 | 0 | 5.87 | 0.16 | 2.19 | 8.46 |
| Jt04 | 0.59 | 0.21 | 1.81 | 0.42 | 0.46 | 0.13 | 0 | 3.43 | 0 | 6.77 | 0.18 | 2.39 | 7.98 |
| Jt05 | 0.62 | 0.55 | 2.67 | 0.95 | 0.2 | 0.08 | 0 | 5.24 | 0 | 10.61 | 0.42 | 2.49 | 11.57 |
| Jt06 | 0.1 | 0.12 | 2.88 | 0.38 | 0.13 | 0.06 | 0 | 3.71 | 0 | 7.73 | 0.17 | 0.43 | 7.65 |
| Jt07 | 0.7 | 0.4 | 3.88 | 0.7 | 0.18 | 0.1 | 0 | 6.55 | 0 | 14.68 | 0.21 | 2.27 | 13.7 |
| Jt08 | 0.87 | 0.45 | 2.3 | 0.46 | 0.59 | 0.23 | 0 | 4.33 | 0 | 27.27 | 0.2 | 3.45 | 10.78 |
| Jt09 | 0.08 | 0.2 | 5.31 | 0.49 | 0.36 | 0.11 | 0 | 5.1 | 0 | 10.04 | 0.46 | 0.62 | 12.02 |
| Jt10 | 0.81 | 0.7 | 3.56 | 0.92 | 0.1 | 0.1 | 0 | 6.67 | 0 | 19.51 | 0.42 | 2.47 | 14.47 |
| Jt11 | 0.7 | 2.18 | 20.26 | 1.29 | 15.4 | 0.99 | 0 | 6.38 | 0 | 78.34 | 0.8 | 2.58 | 51.08 |
| Jt12 | 0.37 | 0.62 | 20.13 | 1.35 | 5.31 | 0.53 | 0 | 12.48 | 0 | 90.29 | 0.75 | 2.02 | 42.3 |
| Jt13 | 1.46 | 0.8 | 5.73 | 0.67 | 1.02 | 0.33 | 0 | 8.55 | 0 | 22.6 | 0.36 | 5.03 | 21.16 |
| Jt14 | 5.93 | 1.67 | 3.58 | 0.46 | 4.63 | 5.58 | 0 | 4.07 | 0 | 12.63 | 0.09 | 10.52 | 39.12 |
| Jt15 | 13.03 | 2 | 11.17 | 1.89 | 5.73 | 15.37 | 0 | 4.6 | 0 | 33.88 | 0.11 | 23.86 | 84.21 |
| Jt16 | 0.73 | 0.44 | 1.6 | 0.48 | 0.15 | 0.13 | 0 | 4.48 | 0 | 9.53 | 0.25 | 1.76 | 9.32 |
| Jt17 | 0.61 | 0.33 | 3.42 | 0.55 | 0.43 | 0.21 | 0 | 4.74 | 0 | 10.75 | 0.35 | 1.15 | 11.43 |
| Jt18 | 0.69 | 0.31 | 2.23 | 0.67 | 0.1 | 0.09 | 0 | 4.61 | 0 | 8.29 | 0.37 | 1.87 | 9.79 |
| Jt19 | 0.78 | 0.41 | 4.28 | 0.54 | 1.29 | 0.25 | 0 | 4.74 | 0 | 28.18 | 0.32 | 2.26 | 13.75 |
| Jt20 | 0.46 | 0.32 | 1.48 | 0.53 | 0.08 | 0.06 | 0 | 3.4 | 0 | 5.51 | 0.29 | 1.62 | 7.17 |
| Jt21 | 0.04 | 0.21 | 3.39 | 0.27 | 0.13 | 0.07 | 0 | 3.76 | 0 | 30.41 | 0.41 | 0.36 | 8.22 |
| Jt22 | 3.13 | 1.71 | 8.88 | 1.59 | 8.75 | 3.55 | 0 | 4.54 | 0 | 66.32 | 0.15 | 12.13 | 40.53 |

## Appendix B

## Total Salt Contents Calculated from Other Author's Datasets

Table B.1. Total salt contents calculated from the data of Bockheim (2003), available at available at http://nsidc.org/data/ggd221.html.

| Pit | Ca | Mg | Na | K | Cl | $SO_4$ | $NO_3$ |
|---|---|---|---|---|---|---|---|
| | | | | eq $m^{-2}$ | | | |
| 75-1 | 2.6 | 2.5 | 1268.1 | 0.3 | 12.1 | 1236.3 | – |
| 75-3 | 15.9 | 2.4 | 76.0 | 2.3 | 59.3 | 27.7 | – |
| 75-5 | 1.4 | 1.8 | 470.4 | 0.1 | 4.0 | 451.1 | – |
| 75-6 | 1.7 | 1.2 | 355.8 | 0.1 | 2.9 | 344.0 | – |
| 75-7 | 2.6 | 1.7 | 898.9 | 0.3 | 7.8 | 804.5 | – |
| 75-8 | 2.4 | 2.1 | 472.2 | 0.1 | 4.0 | – | – |
| 75-9 | 0.3 | 0.3 | 2.8 | 0.2 | 1.8 | 1.1 | – |
| 75-10 | 1.2 | 1.3 | 444.1 | 0.1 | 4.0 | 430.5 | – |
| 75-11 | 0.7 | 0.8 | 308.8 | 0.1 | 2.8 | 313.9 | – |
| 75-12 | 18.7 | 2.4 | 5.0 | 0.8 | 5.8 | 16.1 | – |
| 75-13 | 0.3 | 0.2 | 2.8 | 0.0 | 0.0 | 2.9 | – |
| 75-14 | 0.1 | 0.1 | 4.5 | | 3.5 | 0.8 | – |
| 75-15 | 2.8 | 3.6 | 1025.2 | 0.3 | 9.3 | 991.0 | – |
| 76-2 | 59.6 | 4.7 | 104.4 | 2.4 | 58.8 | 48.0 | – |
| 76-9 | 19.6 | 36.4 | 66.7 | 7.4 | 82.4 | 34.0 | – |
| 76-11 | 68.9 | 30.7 | 356.4 | 7.1 | 495.5 | 42.6 | 2.9 |
| 76-15 | 2.3 | 0.7 | 3.5 | 0.9 | 0.4 | 0.3 | 0.0 |
| 76-20 | 16.3 | 15.0 | 67.7 | 3.9 | 135.9 | 0.9 | 0.8 |
| 76-21 | 71.9 | 49.6 | 410.8 | 15.9 | 563.8 | 31.7 | 2.7 |
| 76-23 | 35.6 | 17.3 | 70.5 | 10.6 | 140.5 | 2.2 | 1.1 |
| 76-24 | 194.0 | 51.7 | 192.8 | 10.7 | 366.7 | 61.4 | 2.2 |
| 76-25 | 114.1 | 43.0 | 180.2 | 11.9 | 268.7 | 34.5 | – |
| 76-27 | 28.8 | 260.9 | 2810.6 | 46.6 | 572.7 | 43.8 | – |
| 76-52 | 11.8 | 66.0 | 347.6 | 13.6 | 136.9 | 87.1 | – |
| 76-53 | 36.2 | 103.2 | 526.2 | 16.5 | 444.1 | 93.4 | – |
| 76-54 | 38.4 | 243.5 | 1454.8 | 20.3 | 1556.8 | 53.4 | – |
| 76-55 | 35.6 | 174.9 | 378.0 | 13.2 | 344.1 | 93.0 | – |
| 76-56 | 28.8 | 146.6 | 704.4 | 20.4 | 431.8 | 448.0 | – |
| 76-57 | 21.6 | 82.2 | 564.0 | 11.7 | 399.8 | 74.7 | – |
| 76-58 | 71.7 | 90.2 | 387.8 | 11.7 | 389.5 | 123.4 | – |
| 76-61 | 20.5 | 10.3 | 72.1 | 4.2 | 22.9 | 1.3 | – |
| 76-62 | 21.5 | 19.4 | 70.1 | 5.1 | 66.8 | 2.1 | – |
| 76-63 | 4.2 | 3.5 | 23.0 | 1.2 | 7.1 | 1.2 | – |
| 76-64 | 8.5 | 7.5 | 47.9 | 3.1 | 6.5 | 6.6 | – |
| 76-65 | 9.8 | 7.0 | 30.9 | 3.4 | 2.7 | 0.5 | – |
| 76-66 | 13.8 | 6.7 | 32.5 | 3.1 | 7.5 | 1.4 | – |
| 77-47 | 32.0 | 42.6 | 61.9 | 4.7 | 92.7 | 21.7 | 26.9 |
| 77-48 | 3.7 | 3.9 | 6.6 | 0.8 | 8.9 | 4.4 | 1.7 |
| 77-50 | 24.6 | 68.0 | 77.5 | 7.1 | 142.6 | 9.6 | 25.0 |
| 77-52 | 39.9 | 63.2 | 57.2 | 4.5 | 131.9 | 3.2 | 29.6 |
| 78-7 | 1.3 | 0.1 | 14.8 | 0.9 | 9.0 | 4.8 | 0.1 |
| 78-8 | 0.7 | 0.3 | 0.8 | 0.2 | 0.4 | 0.4 | 0.1 |
| 79-5 | 13.2 | 3.1 | 19.6 | 0.5 | 19.6 | 15.3 | 1.4 |
| 81-2 | 20.5 | 25.3 | 531.0 | 3.3 | 503.5 | 24.5 | 0.4 |
| 81-4 | 12.7 | 18.5 | 509.0 | 9.1 | 517.7 | 22.6 | 4.9 |
| 81-6 | 33.1 | 26.0 | 289.1 | 5.0 | 271.3 | 33.4 | 1.6 |
| 81-9 | 87.5 | 24.1 | 611.9 | 6.5 | 704.8 | 96.2 | 3.5 |
| 81-10 | 59.8 | 73.4 | 527.3 | 10.2 | 659.3 | 68.7 | 14.9 |
| 81-12 | 18.9 | 8.0 | 25.2 | 1.0 | 28.7 | 20.5 | 2.2 |
| 81-13 | 14.5 | 5.9 | 18.4 | 0.9 | 23.5 | 15.4 | 1.7 |
| 81-14 | 62.3 | 17.8 | 897.1 | 5.0 | 928.1 | 73.9 | 5.9 |
| 83-1 | 10.4 | 1.4 | 140.0 | 1.6 | 7.1 | 147.0 | 0.6 |
| 83-7 | 39.7 | 12.0 | 206.1 | 4.7 | 213.3 | 39.1 | 1.4 |
| 83-9 | 14.7 | 47.4 | 60.5 | 9.5 | 111.2 | 20.8 | 1.9 |
| 83-10 | 41.2 | 88.9 | 320.9 | 16.5 | 382.8 | 67.4 | 4.8 |
| 83-13 | 18.4 | 27.8 | 105.2 | 4.2 | 117.6 | 16.4 | 1.9 |

Table B.2. Total salt contents calculated from the data of Gibb et al. (2002), available at http://soils.landcareresearch.co.nz/contents/index.aspx.

| Pit | Ca | Mg | Na | K | Cl | $SO_4$ | $NO_3$ |
|---|---|---|---|---|---|---|---|
| | | | | eq $m^{-2}$ | | | |
| 333 | 42.6 | 49.3 | 91.5 | 4.3 | 100.8 | 45.3 | 8.0 |
| 332 | 119.6 | 32.9 | 90.1 | 3.5 | 80.3 | 183.5 | 13.8 |
| 331 | 28.9 | 16.6 | 52.4 | 1.5 | 39.1 | 57.8 | 6.1 |
| 330 | 2.4 | 1.3 | 2.2 | 0.3 | 0.4 | 1.3 | 0.2 |
| 329 | 0.1 | 0.7 | 1.7 | 0.1 | 0.3 | 0.5 | 0.1 |
| 328 | 186.3 | 5.8 | 93.1 | 7.3 | 46.1 | 43.1 | 17.9 |
| 327 | 276.6 | 90.0 | 138.3 | 68.2 | 184.0 | 101.6 | 15.5 |
| 326 | 860.6 | 69.6 | 430.3 | 154.0 | 500.2 | 86.9 | 84.7 |
| 324 | 419.4 | 169.8 | 209.7 | 83.2 | 247.6 | 112.4 | 57.3 |
| 314 | 136.8 | 48.2 | 68.4 | 69.1 | 135.3 | 56.4 | 1.6 |
| 306 | 1228.8 | 63.3 | 614.4 | 268.9 | 438.7 | 76.4 | 3.3 |
| 305 | 85.5 | 72.4 | 42.7 | 75.3 | 803.2 | 45.9 | 0.2 |

## Appendix C

## Data from the borehole soil.

Table C.1. Soluble ion data, measured in 1:10 soil-water extractions from the upper 30 cm of the borehole soil.

| Depth | Ca | Mg | Na | K | $HCO_3$ | $SO_4$ | $NO_3$ | Cl | F | Sr | B |
|---|---|---|---|---|---|---|---|---|---|---|---|
| cm | ——— | | | mmol $kg^{-1}$ | ——— | | | | ——µmol $kg^{-1}$ | | —— |
| 0-5 | 0.35 | 0.24 | 5.09 | 0.82 | 4.24 | 0.31 | 0.09 | 0.83 | 287.32 | 1.06 | 40.32 |
| 5-7 | 0.23 | 0.25 | 4.61 | 0.78 | 4.18 | 0.13 | 0.02 | 0.42 | 235.63 | 0.84 | 23.69 |
| 7-10 | 0.25 | 0.26 | 6.05 | 0.68 | 3.74 | 0.21 | 0.00 | 1.28 | 261.45 | 0.96 | 44.89 |
| 10-12 | 0.14 | 0.36 | 6.19 | 0.55 | 3.84 | 0.17 | 0.07 | 1.13 | 281.17 | 0.95 | 56.07 |
| 12-17 | 0.16 | 0.23 | 7.63 | 0.52 | 3.73 | 0.43 | 0.07 | 2.81 | 174.56 | 0.80 | 24.45 |
| 17-22 | 0.11 | 0.09 | 5.89 | 0.31 | 2.71 | 0.35 | 0.08 | 3.09 | 199.26 | 0.43 | 12.01 |
| 22-30 | 0.15 | 0.23 | 4.04 | 0.37 | 2.38 | 0.05 | 0.05 | 1.89 | 118.42 | 1.09 | 3.17 |

Table C.2. Ion concentrations measured in the ice-cemented borehole sediment after thawing.

| Depth | Ca | Mg | Na | K | $HCO_3$ | $SO_4$ | $NO_3$ | Cl | F | Sr | B | Mn | Br |
|---|---|---|---|---|---|---|---|---|---|---|---|---|---|
| cm | mM | mM | mM | mM | mM | mM | mM | mM | µM | µM | µM | µM | µM |
| 30-40 | 0.43 | 0.40 | 6.18 | 0.35 | 1.58 | 0.94 | 0.18 | 4.53 | 41.68 | 2.38 | 9.46 | 0.080 | 1.75 |
| 40-50 | 2.19 | 2.60 | 13.82 | 0.76 | 1.10 | 2.63 | 0.45 | 18.35 | 51.11 | 12.24 | 15.08 | 0.375 | 4.00 |
| 50-60 | 3.35 | 3.90 | 15.26 | 0.84 | 0.86 | 3.50 | 0.53 | 22.67 | 63.16 | 16.45 | 7.97 | 1.042 | 5.26 |
| 60-70 | 2.28 | 2.50 | 11.07 | 0.77 | 0.70 | 1.57 | 0.33 | 17.79 | 42.32 | 10.04 | 4.70 | 0.713 | 4.88 |
| 70-80 | 3.04 | 3.11 | 11.26 | 0.82 | 0.65 | 0.84 | 0.38 | 22.42 | 35.63 | 11.91 | 4.58 | 1.361 | 5.51 |
| 80-90 | 3.66 | 3.62 | 11.07 | 0.88 | 0.69 | 0.78 | 0.38 | 24.01 | 31.68 | 13.18 | 4.06 | 1.840 | 6.26 |
| 90-100 | 4.72 | 3.98 | 10.76 | 0.94 | 0.45 | 0.71 | 0.29 | 26.17 | 30.32 | 15.90 | 3.40 | 2.236 | 8.01 |
| 100-110 | 5.31 | 4.02 | 9.20 | 0.84 | 0.31 | 0.56 | 0.31 | 26.80 | 36.95 | 16.14 | 1.95 | 2.073 | 8.26 |
| 110-120 | 6.18 | 4.47 | 9.38 | 0.94 | 0.50 | 0.48 | 0.28 | 29.50 | 36.95 | 19.36 | 3.05 | 3.231 | 9.26 |
| 120-130 | 6.78 | 4.30 | 9.63 | 1.04 | 0.34 | 0.55 | 0.19 | 31.05 | 31.47 | 20.95 | 1.93 | 3.407 | 11.14 |
| 130-140 | 9.98 | 6.13 | 10.85 | 1.23 | 0.54 | 0.50 | 0.19 | 43.80 | 28.74 | 31.40 | 1.98 | 5.919 | 14.89 |
| 140-150 | 10.98 | 6.69 | 10.72 | 1.20 | 0.60 | 0.62 | 0.18 | 46.61 | 26.21 | 32.05 | 1.84 | 7.568 | 16.77 |
| 150-160 | 12.32 | 6.68 | 10.90 | 1.20 | 0.29 | 0.48 | 0.09 | 50.11 | 34.21 | 34.24 | 1.47 | 6.626 | 19.77 |
| 160-170 | 10.60 | 5.74 | 9.90 | 0.96 | 0.22 | 0.30 | 0.05 | 43.44 | 50.16 | 29.26 | 1.09 | 5.365 | 19.02 |
| 170-180 | 5.64 | 3.08 | 8.67 | 0.86 | 0.33 | 0.28 | 0.04 | 27.01 | 77.53 | 17.14 | 1.10 | 2.964 | 15.14 |
| 180-190 | 2.56 | 2.30 | 11.81 | 0.80 | 0.75 | 0.34 | 0.04 | 21.87 | 229.47 | 9.49 | 1.45 | 2.050 | 16.14 |
| 190-200 | 1.21 | 2.21 | 18.86 | 0.87 | 0.50 | 0.49 | 0.04 | 26.07 | 346.84 | 5.18 | 2.08 | 1.276 | 33.79 |
| 200-210 | 0.91 | 2.17 | 33.44 | 1.55 | 1.28 | 0.82 | 0.08 | 40.56 | 369.47 | 5.11 | 4.02 | 0.941 | 68.33 |

Table C.3. Stable water isotopes in the borehole ice-cement.

| Depth | δD | $\delta^{18}O$ | $d_{excess}$ |
|---|---|---|---|
| cm | ‰ | ‰ | ‰ |
| 30-40 | -145.4 | -10.8 | -58.9 |
| 40-50 | -148.4 | -12.0 | -52.1 |
| 50-60 | -157.5 | -13.9 | -46.2 |
| 60-70 | -169.5 | -16.6 | -36.5 |
| 70-80 | -188.6 | -19.7 | -30.8 |
| 80-90 | -199.9 | -21.8 | -25.6 |
| 90-100 | -208.2 | -23.4 | -21.1 |
| 100-110 | -215.4 | -24.9 | -16.6 |
| 110-120 | -218.9 | -25.4 | -15.6 |
| 120-130 | -220.9 | -26.0 | -13.2 |
| 130-140 | -223.4 | -26.7 | -10.0 |
| 140-150 | -224.7 | -27.1 | -7.7 |
| 150-160 | -227.2 | -27.3 | -8.7 |
| 160-170 | -228.5 | -27.8 | -6.1 |
| 170-180 | -230.0 | -27.8 | -7.8 |
| 180-190 | -232.3 | -28.2 | -7.0 |
| 190-200 | -235.7 | -29.0 | -3.3 |
| 200-210 | -238.6 | -29.3 | -4.4 |

Table C.4. Exchangeable cations and CEC, calculated as the equivalent sum of exchangeable cations, in the borehole ice-cement.

| Depth cm | Ca | Mg | Na | K | CEC |
|---|---|---|---|---|---|
| | meq $kg^{-1}$ | | | | |
| 0-5 | 9.3 | 4.8 | 9.1 | 6.5 | 29.6 |
| 5-7 | 4.3 | 4.6 | 8.8 | 5.9 | 23.5 |
| 7-10 | 2.1 | 4.8 | 11.4 | 4.3 | 22.7 |
| 10-12 | 1.6 | 7.2 | 14.9 | 5.8 | 29.6 |
| 12-17 | 0.1 | 6.3 | 12.5 | 4.0 | 22.9 |
| 17-22 | 2.5 | 7.6 | 13.2 | 3.8 | 27.1 |
| 22-30 | 14.0 | 9.1 | 8.1 | 5.3 | 36.5 |
| 30-40 | 8.2 | 4.6 | 5.9 | 3.5 | 22.2 |
| 40-50 | 7.5 | 4.5 | 5.4 | 2.9 | 20.4 |
| 50-60 | 7.8 | 4.3 | 4.2 | 2.9 | 19.2 |
| 60-70 | 7.4 | 4.5 | 4.1 | 3.1 | 19.0 |
| 70-80 | 8.1 | 4.8 | 3.8 | 3.1 | 19.8 |
| 80-90 | 9.0 | 4.8 | 3.7 | 3.2 | 20.8 |
| 90-100 | 10.0 | 5.1 | 4.1 | 3.8 | 23.0 |
| 100-110 | 9.9 | 4.9 | 3.9 | 3.4 | 22.0 |
| 110-120 | 10.1 | 4.3 | 3.4 | 3.3 | 21.0 |
| 120-130 | 9.4 | 3.8 | 3.3 | 3.2 | 19.7 |
| 130-140 | 10.6 | 4.3 | 4.1 | 4.1 | 23.0 |
| 140-150 | 13.1 | 5.2 | 4.1 | 4.5 | 26.9 |
| 150-160 | 18.3 | 6.6 | 5.3 | 5.7 | 36.0 |
| 160-170 | 19.5 | 7.3 | 5.8 | 6.1 | 38.7 |
| 170-180 | 17.7 | 6.6 | 5.1 | 5.8 | 35.2 |
| 180-190 | 14.4 | 7.8 | 6.6 | 6.9 | 35.7 |
| 190-200 | 13.2 | 11.0 | 11.0 | 7.4 | 42.6 |
| 200-210 | 12.5 | 16.3 | 20.6 | 12.3 | 61.6 |

Table C.5. Particle size characteristics of the borehole with the particle size classes defined as: clay (<0.004 mm), silt (0.004 – 0.0625 mm), very fine sand (0.0625 – 0.125 mm), fine sand (0.125 – 0.25 mm), medium sand (0.25 – 0.5 mm), coarse sand (0.5 – 1 mm), and very coarse sand (1 – 2 mm). Also included is skewness (S), kurtosis (K), and specific surface area (SSA).

| Depth cm | Clay % | Silt % | V. Fine Sand % | Fine Sand % | Medium Sand % | Coarse Sand % | V. Coarse Sand % | S | K | SSA $m^2 g^{-1}$ |
|---|---|---|---|---|---|---|---|---|---|---|
| 0-5 | 1.5 | 3.0 | 1.7 | 15.9 | 33.1 | 31.2 | 13.4 | 1.15 | 0.97 | 0.034 |
| 5-7 | 1.2 | 1.3 | 0.6 | 9.1 | 32.5 | 46.6 | 8.6 | 0.80 | 0.73 | 0.030 |
| 7-10 | 0.3 | 0.8 | 0.6 | 6.2 | 16.9 | 43.5 | 31.7 | 0.40 | -0.52 | 0.010 |
| 10-12 | 0.5 | 0.9 | 1.9 | 21.7 | 37.3 | 29.7 | 8.0 | 1.35 | 1.73 | 0.017 |
| 12-17 | 0.3 | 0.7 | 1.2 | 13.9 | 28.9 | 33.9 | 21.0 | 0.90 | -0.01 | 0.012 |
| 17-22 | 0.4 | 0.8 | 1.8 | 18.8 | 33.5 | 30.3 | 14.3 | 1.24 | 1.00 | 0.014 |
| 22-30 | 0.4 | 1.0 | 1.7 | 15.9 | 31.5 | 32.7 | 16.8 | 1.14 | 0.65 | 0.014 |
| 30-40 | 0.7 | 2.3 | 1.6 | 10.9 | 30.9 | 41.7 | 11.7 | 0.65 | -0.13 | 0.018 |
| 40-50 | 0.9 | 2.9 | 1.7 | 9.7 | 28.2 | 39.8 | 16.7 | 0.52 | -0.51 | 0.021 |
| 50-60 | 1.1 | 3.6 | 1.9 | 8.7 | 25.2 | 42.4 | 16.8 | 0.47 | -0.48 | 0.026 |
| 60-70 | 1.6 | 5.5 | 2.7 | 11.6 | 31.4 | 34.0 | 12.9 | 1.13 | 1.08 | 0.037 |
| 70-80 | 1.5 | 5.2 | 2.6 | 13.2 | 30.6 | 33.5 | 13.1 | 1.08 | 0.86 | 0.036 |
| 80-90 | 1.3 | 4.4 | 2.3 | 11.4 | 26.8 | 36.0 | 17.5 | 0.88 | 0.23 | 0.031 |
| 90-100 | 1.7 | 5.6 | 2.9 | 13.1 | 30.5 | 33.4 | 12.5 | 1.11 | 1.01 | 0.038 |
| 100-110 | 1.5 | 5.0 | 2.7 | 13.5 | 29.6 | 33.2 | 14.3 | 1.06 | 0.72 | 0.035 |
| 110-120 | 1.4 | 4.7 | 2.5 | 13.1 | 29.8 | 33.7 | 14.5 | 1.03 | 0.65 | 0.034 |
| 120-130 | 1.5 | 5.1 | 2.5 | 10.5 | 24.9 | 33.8 | 21.4 | 0.77 | -0.16 | 0.035 |
| 130-140 | 1.6 | 5.5 | 2.7 | 10.2 | 24.5 | 36.9 | 18.2 | 0.80 | 0.10 | 0.036 |
| 140-150 | 1.7 | 6.0 | 3.3 | 13.3 | 25.1 | 32.9 | 17.2 | 0.93 | 0.24 | 0.039 |
| 150-160 | 1.8 | 6.4 | 4.0 | 15.2 | 20.4 | 29.5 | 22.2 | 0.77 | -0.34 | 0.040 |
| 160-170 | 2.5 | 8.5 | 5.3 | 21.9 | 24.6 | 24.8 | 11.9 | 1.16 | 0.74 | 0.054 |
| 170-180 | 3.2 | 10.6 | 6.1 | 26.4 | 27.4 | 16.6 | 8.9 | 1.70 | 2.64 | 0.068 |
| 180-190 | 4.0 | 13.0 | 7.1 | 29.6 | 30.2 | 12.4 | 2.9 | 1.63 | 3.00 | 0.083 |
| 190-200 | 3.8 | 12.9 | 5.8 | 23.8 | 31.1 | 17.8 | 4.1 | 1.41 | 2.10 | 0.079 |
| 200-210 | 5.4 | 17.4 | 6.2 | 22.3 | 28.1 | 16.4 | 3.3 | 1.31 | 1.51 | 0.105 |

## Appendix D

**Histogram plots of single-grain luminescence age distributions.**

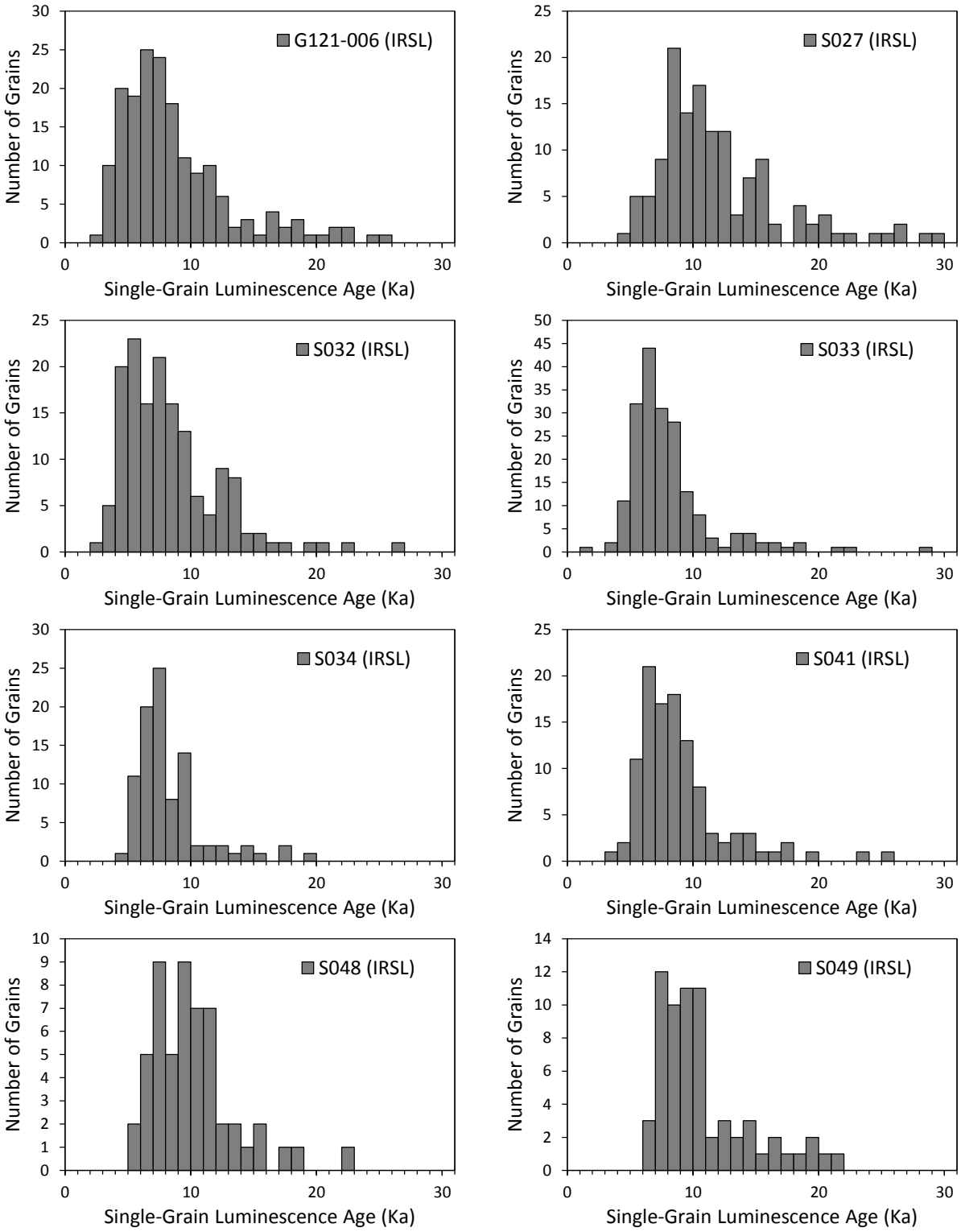
G121-006 (IRSL)
S027 (IRSL)
S032 (IRSL)
S033 (IRSL)
S034 (IRSL)
S041 (IRSL)
S048 (IRSL)
S049 (IRSL)
Number of Grains
Single-Grain Luminescence Age (Ka)

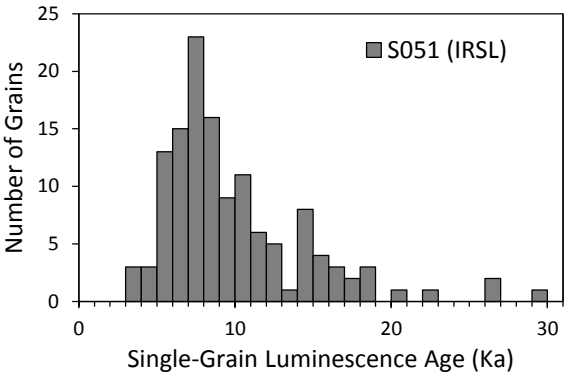
S051 (IRSL)
Number of Grains
Single-Grain Luminescence Age (Ka)
0
5
10
15
20
25
0
10
20
30

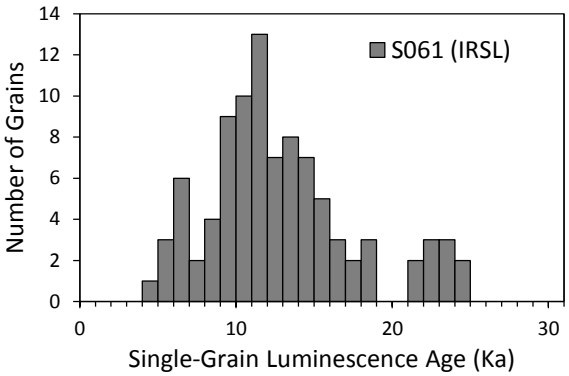
S061 (IRSL)
Number of Grains
Single-Grain Luminescence Age (Ka)
0
2
4
6
8
10
12
14
0
10
20
30

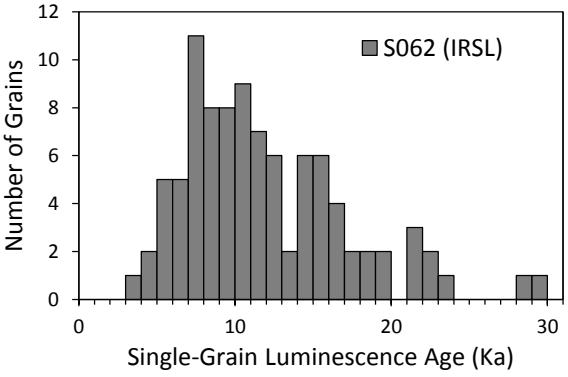
S062 (IRSL)
Number of Grains
Single-Grain Luminescence Age (Ka)
0
2
4
6
8
10
12
0
10
20
30

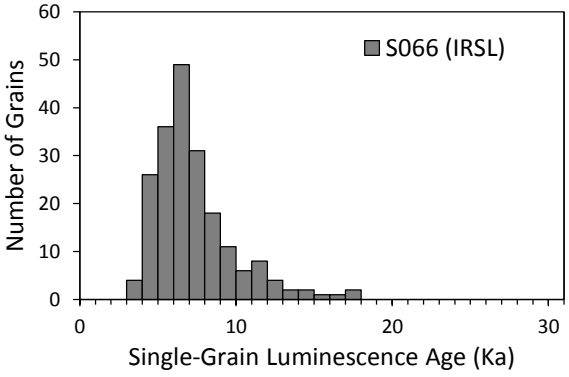
S066 (IRSL)
Number of Grains
Single-Grain Luminescence Age (Ka)
0
10
20
30
40
50
60
0
10
20
30

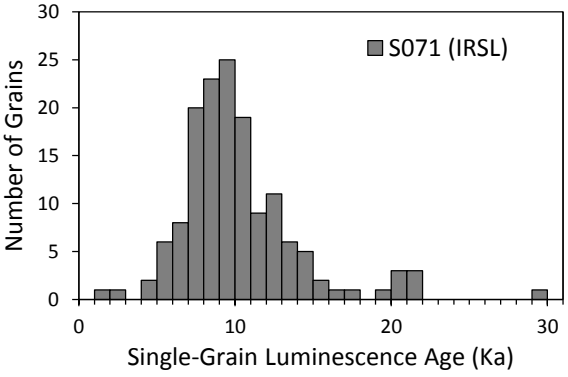
S071 (IRSL)
Number of Grains
Single-Grain Luminescence Age (Ka)
0
5
10
15
20
25
30
0
10
20
30

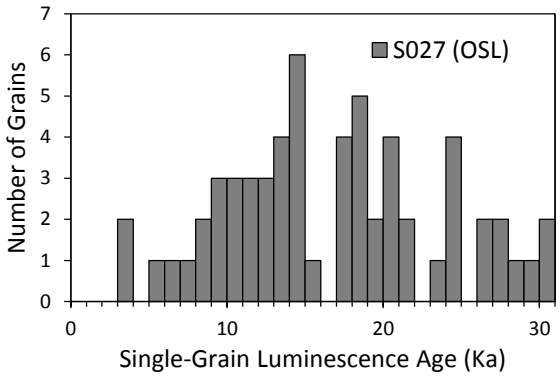
S027 (OSL)
Number of Grains
Single-Grain Luminescence Age (Ka)

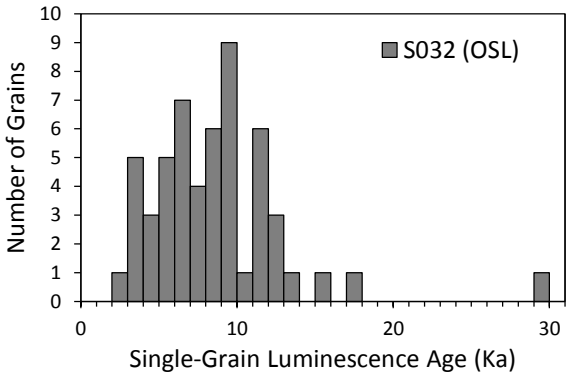
S032 (OSL)
Number of Grains
Single-Grain Luminescence Age (Ka)

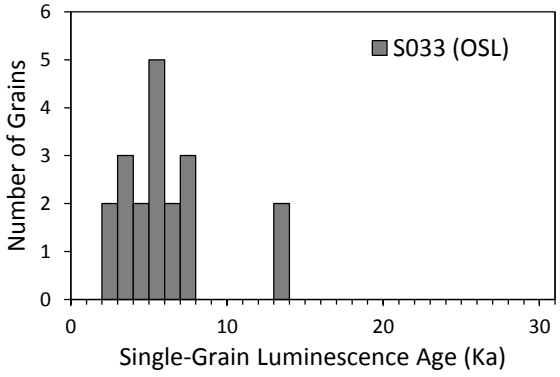
S033 (OSL)
Number of Grains
Single-Grain Luminescence Age (Ka)

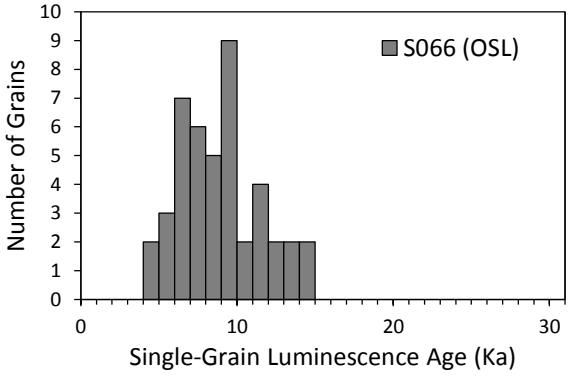
S066 (OSL)
Number of Grains
Single-Grain Luminescence Age (Ka)

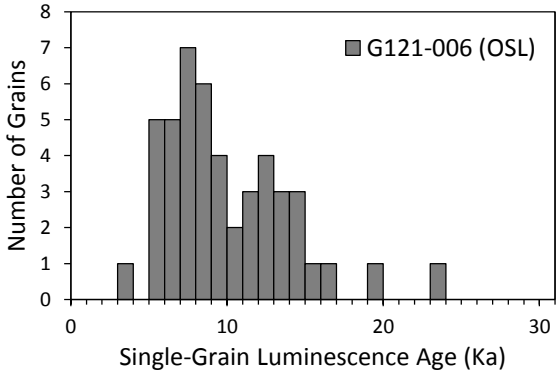
G121-006 (OSL)
Number of Grains
Single-Grain Luminescence Age (Ka)

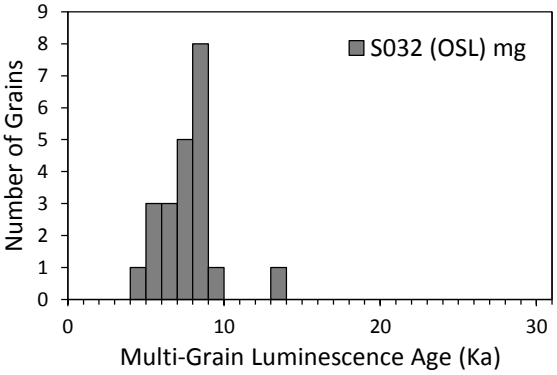
S032 (OSL) mg
Number of Grains
Multi-Grain Luminescence Age (Ka)

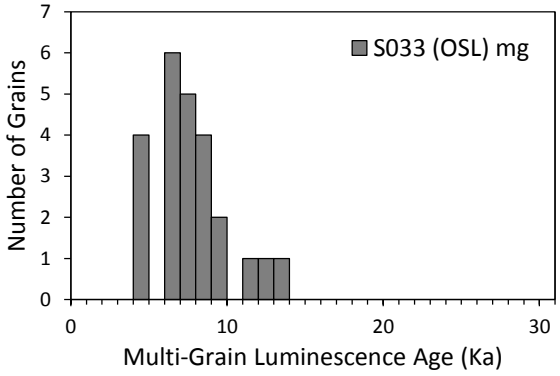
S033 (OSL) mg
Number of Grains
Multi-Grain Luminescence Age (Ka)

## Appendix E

## Changes Made to the PHREEQC Code

To use PHREEQC for low-temperature modeling two small changes were made in the PHREEQC code. Source files for PHREEQC were obtained from http://wwwbrr.cr.usgs.gov/projects/GWC_coupled/phreeqc/ and the program was built with a C compiler. To incorporate the FREZCHEM temperature dependence of the Debye-Hückel ($A_\phi$) into PHREEQC changes were made to the pitzer.c file in the PTEMP subroutine, which calculates the temperature dependence of pitzer parameters. The specific changes are in red.

```
 PTEMP(LDBLE TK)
/* ---------------------------------------------------------------------- */
{
/*
C
C     SUBROUTINE TO CALUCLATE TEMPERATURE DEPENDENCE OF PITZER PARAMETER
C
*/
LDBLE DC0;
int i;
LDBLE TR = 298.15;

if (fabs(TK - OTEMP) < 0.001e0)
                        return OK;
OTEMP = TK;
/*
C     Set DW0
*/
DW(TK);
for (i = 0; i < count_pitz_param; i++)
{
calc_pitz_param(pitz_params[i], TK, TR);
}
DC0 = DC(TK);

A0 = 86.6836498e0 + (TK)*0.084879594e0 - (0.0000888785e0)*pow(TK,(LDBLE) 2.0e0) + (4.88096e-
8)*pow(TK,(LDBLE) 3.0e0) - (1327.31477e0/(TK)) - 17.6460172e0*log(TK);

/*
C     if (fabs(TK - TR) < 0.001e0)
C     {A0 = 0.392e0;
C     }
C     else
C     {
C     DC0 = DC(TK);
C     A0 = 1.400684e6 * sqrt(DW0 / (pow((DC0 * TK), (LDBLE) 3.0e0)));
C     /*A0=1.400684D6*(DW0/(DC0*TK)**3.0D0)**0.5D0 */
C     }
*/

return OK;
}
```

To address the error in the density finding routine the DFIND subroutine in dw.c was altered. These changes are in red.

```
DFIND(LDBLE * DOUT, LDBLE P, LDBLE D, LDBLE T)

/* ------------------------------------------------------------------------ */
/*
C
C    ROUTINE TO FIND DENSITY CORRESPONDING TO INPUT PRESSURE P(MPA), AN
C    TEMPERATURE T(K), USING INITIAL GUESS DENSITY D(G/CM3). THE OUTPUT
C    DENSITY IS IN G/CM3.
C
C    FROM L. HAAR, J. S. GALLAGHER, AND G. S. KELL, (1984)
C
*/
{
int L;
LDBLE DD, RT, PP_dfind, DPD, DPDX, DP, X;
/*      LDBLE DD, RT, PP, DPD, DPDX, DP, X; */

DD = D;
RT = GASCON * T;
if (DD <= 0.e0)
DD = 1.e-8;
if (DD > 1.9e0)
DD = 1.9e0;
L = 0;
for (L = 1; L <= 30; L++)
{
if (DD <= 0.e0)
DD = 1.e-8;
if (DD > 1.9e0)
DD = 1.9e0;
QQ(T, DD);
PP_dfind = RT * DD * BASE(DD) + Q0;
DPD = RT * (Z + Y * DZ) + Q5;
/*
C
C  THE FOLLOWING 3 LINES CHECK FOR NEGATIVE DP/DRHO, AND IF SO ASSUME
C    GUESS TO BE IN 2-PHASE REGION, AND CORRECT GUESS ACCORDINGLY.
C
*/
if (DPD <= 0.e0)
{
if (D >= .2967e0)
DD = DD * 1.02e0;
if (D < .2967e0)
DD = DD * .98e0;
if (L <= 10)
continue;
}
else
{
/* 13 */
DPDX = DPD * 1.1e0;
if (DPDX < 0.1e0)
DPDX = 0.1e0;
```

```
DP = fabs(1.e0 - PP_dfind / P);
if (DP < 1.e-8)
break;
if (D > .3e0 && DP < 1.e-7)
break;
if (D > .7e0 && DP < 1.e-6)
break;
X = (P - PP_dfind) / DPDX;
if (fabs(X) > .1e0)
X = X * .1e0 / fabs(X);
DD = DD + X;
if (DD < 0.e0)
DD = 1.e-8;
}
}
if (L > 30)
/*     error_msg("In subroutine DFIND", STOP);     */
DD = 1;
/*   20 CONTINUE */
*DOUT = DD;
return OK;
}
```

**Appendix F**
**Soil Descriptions and Photographs for the 2006-2007 Soil Pits**

Soil: S001, Elevation: 45 m, Depth to ICS: 34 cm
Latitude: -77.62528, Longitude: 163.09498
Date Excavated: 12/19/2006

| Horizon | Depth (cm) | Description |
|---|---|---|
| DP | 1.5 – 0 | calcium carbonate coatings stage 1, ventifacts stage 1 to none, rough, young |
| C1 | 0 – 4 | silty gravelly sand, aeolian, beds, weak structure, calcium carbonate coatings stage 2, cemented sands on clast bottoms |
| C2 | 4 –19 | variegated sandy gravel, calcium carbonate coatings stage 2, very weak structure |
| ICS | 19+ | over ice (may be same as C2) |

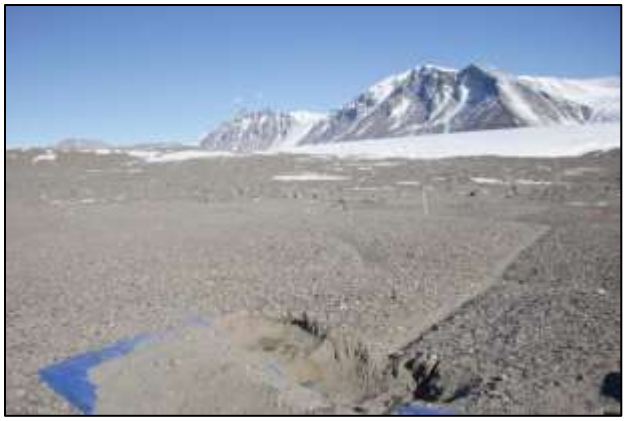


Soil: S004, Elevation: 22 m, Depth to ICS: 34 cm
Latitude: -77.62353, Longitude: 163.10605
Date Excavated: 11/26/2006

| Horizon | Depth (cm) | Description |
|---|---|---|
| DP | 1.5 – 0 | gravely desert pavement displaying grounded rocks, some ventifacts, with coarse sand infill, no varnish apparent |
| C1 | 0 – 4 | unstratified, possibly inflated |
| C2 | 4 –19 | variable textured sand, fine to coarse, looks aeolian, some stranded rocks, NP, NS, very weak cementation up to 10 cm probably due to salts, possible water |
| ICS | 19+ | ice-cemented material, basically silt, SS, SP, next horizon is up thrust near crack due to the sand wedge |



Soil: S005, Elevation: 111 m, Depth to ICS: 28 cm
Latitude: -77.63484, Longitude: 163.07652
Date Excavated: 11/25/2006

| Horizon | Depth (cm) | Description |
|---|---|---|
| DP | 1 – 0 | mixed lithology, ventifacts are moderately well developed |
| C1 | 0 – 7 | well sorted sands, very lightly cemented, displaying some horizontal banding suggesting aeolian deposition |
| C2 | 7 –21 | gravely sand, looks like surface rock are aeolian, loose, variegated |
| C3 | 21 – 28 | less well sorted sand, loose, variegated, no calcium carbonate coatings |

Soil: S008, Elevation: 41 m, Depth to ICS: 30 cm
Latitude: -77.62638, Longitude: 163.11592
Date Excavated: 12/19/2006

Note: This soil was sampled with an auger drill to a depth of 210 cm. Following this, the pit was excavated to approximately 60 cm depth to visualize the stratigraphy of the terrace. The white string in this photo is level, and is at 30 cm depth. Above 30 cm depth the soil is dry and loose, with cross-bedded stratigraphy. Below 30 cm depth the soil is ice-cemented, showing foreset stratigraphy dipping towards Lake Fryxell.

Soil: S010, Elevation: 72 m, Depth to ICS: 21 cm
Latitude: -77.58923, Longitude: 163.49406
Date Excavated: 11/30/2006

| Horizon | Depth (cm) | Description |
|---|---|---|
| DP | 2 – 0 | moderately formed ventifacts, calcium carbonate coatings stage 1 |
| C1 | 0 – 2 | loose sand, variegated |
| C2 | 2 –21 | lightly stratified aeolian sediment, the top 2 cm has some salt cementation, sand with some gravel |

Soil: S014, Elevation: 390 m, Depth to ICS: not found
Latitude: -77.50472, Longitude: 163.69283
Date Excavated: 12/08/2006

| Horizon | Depth (cm) | Description |
|---|---|---|
| DP | 3 – 0 | |
| C1 | 0 – 4 | |
| C2 | 4 –41 | |

Soil: S015, Elevation: 325 m, Depth to ICS: 25 cm
Latitude: -77.51319, Longitude: 163.70152
Date Excavated: 12/09/2006

| Horizon | Depth (cm) | Description |
|---|---|---|
| DP | 1.5 – 0 | gravelly, angular, no calcium carbonate coatings, rudimentary ventifacts |
| C1 | 0 – 4 | very lightly cemented, mostly sand, fine to medium, with some coarse gravel |
| C2 | 4 –25 | unstratified aeolian sands, with a few stranded small rocks, damp |
| ICS | 25+ | uplifted wedge or maybe original aeolian, appears the same as C2, but can see discontinuity |

Soil: S016, Elevation: 384 m, Depth to ICS: 21 cm
Latitude: -77.65640, Longitude: 162.97444
Date Excavated: 12/11/2006

| Horizon | Depth (cm) | Description |
|---|---|---|
| DP | 1.5 – 0 | well formed, ventifacted, 100% cover, probably stage 3, calcium carbonate coatings stage 2 |
| C1 | 0 – 3 | silty gravelly sand, very lightly cemented, calcium carbonate coatings |
| C2 | 3 –21 | sandy gravel, contains salt pendants, ventifacted rocks, appears to be inflated |
| ICS | 21+ | sand with some gravel, ICS, maybe original till |

Note: This soil contained massive salt accumulations, shown in the bottom-left photo above.


Soil: S017, Elevation: 307 m, Depth to ICS: 18 cm
Latitude: -77.65030, Longitude: 162.97164
Date Excavated: 12/11/2006

| Horizon | Depth (cm) | Description |
|---|---|---|
| DP | 1.5 – 0 | ventifacts stage 2, calcium carbonate coatings stage 2 |
| C1 | 0 – 10 | gravelly silty sand, salt cemented, firm structure, breaks apart |
| C2 | 10 –28 | loose, moist, sand with gravel, compacted |
| ICS | 28+ | |



Soil: S018, Elevation: 221 m, Depth to ICS: 33 cm
Latitude: -77.64499, Longitude: 162.98599
Date Excavated: 12/12/2006

| Horizon | Depth (cm) | Description |
|---|---|---|
| DP | 1.5 – 0 | mixed size, some rocks with ventifacts stage 2, calcium carbonate coatings stage 2 |
| C1 | 0 – 4 | salt crusted, silty gravelly sand, aeolian, appears to be inflational soil, calcium carbonate coatings stage 2 |
| C2 | 4 –26 | gravely sand with coarse sand, loose, variegated, calcium carbonate stage 1, damp, some rocks near top are ventifacted, top may be aeolian |
| C3 | 26 –33 | sandy soil with a few cobbles, loose, damp, variegated |

Soil: S019, Elevation: 181 m, Depth to ICS: 34 cm
Latitude: -77.64245, Longitude: 162.98834
Date Excavated: 12/12/2006

| Horizon | Depth (cm) | Description |
|---|---|---|
| DP | 2 – 0 | ventifacts stage 2, calcium carbonate coatings stage 1 |
| C1 | 0 – 3 | salt crusted, weak structure, very lightly cemented, calcium carbonate coatings stage 2, gravel with some ventifacts |
| C2 | 3 –26 | gravelly sand, moist, calcium carbonate coatings stage 1 with cemented sand on clast bottoms |
| C3 | 26 –34 | less gravel, more sand, few ventifacts, calcium carbonate coatings stage 1, moist |

Soil: S021, Elevation: 277 m, Depth to ICS: not found
Latitude: -77.7174, Longitude: 162.23349
Date Excavated: 12/15/2006

| Horizon | Depth (cm) | Description |
|---|---|---|
| DP | 5 – 0 | ventifacts stage 1, cobbles, gravelly, with coarse sand dolerite, granite, sandstone volcanics |
| C1 | 0 – 5 | gravelly sand, slightly more silt, very weak cementation, calcium carbonate coatings stage 1 |
| C2 | 5 –38 | gravelly sand, maybe slight salt cementation, calcium carbonate coatings stage 1 |

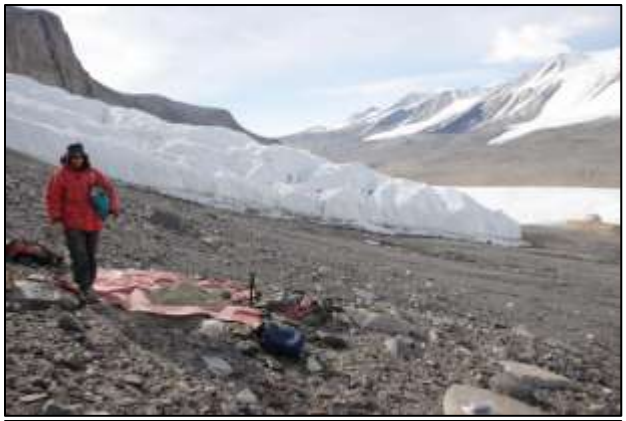

Soil: S022, Elevation: 206 m, Depth to ICS: not found
Latitude: -77.71892, Longitude: 162.23645
Date Excavated: 12/15/2006

| Horizon | Depth (cm) | Description |
|---|---|---|
| DP | 2 – 0 | ventifacts stage 1, calcium carbonate coatings stage 1 |
| C1 | 0 – 3 | band of oxidation, calcium carbonate coatings stage 1, silt caps |
| C2 | 3 –18 | gravelly sand, lightly cemented, variegated, silt caps |
| C3 | 18 – 48+ | loose gravelly sand |


Soil: S023, Elevation: 149 m, Depth to ICS: not found
Latitude: -77.72023, Longitude: 162.23914
Date Excavated: 12/15/2006

| Horizon | Depth (cm) | Description |
|---|---|---|
| DP | 3 – 0 | ventifacts not on pavement, similar to above, possibly more volcanics |
| C1 | 0 – 2 | calcium carbonate coatings stage 1 |
| C2 | 2 –27 | calcium carbonate coatings stage 1 |
| ICS | 27+ | |

Soil: S024, Elevation: 175 m, Depth to ICS: 34 cm
Latitude: -77.64067, Longitude: 162.97821
Date Excavated: 12/16/2006

| Horizon | Depth (cm) | Description |
|---|---|---|
| DP | 1 – 0 | ventifact stage 2, calcium carbonate coatings stage 2, granite, dolomites, sandstone materials with a rough, but fairly well developed DP |
| C1 | 0 – 8 | slightly salt cemented horizon, calcium carbonate coatings stage 1 |
| C2 | 8 –34 | gravelly sand, loose, variegated, calcium carbonate coatings stage 2 |
| ICS | 34+ | |

Soil: S025, Elevation: 143 m, Depth to ICS: 29 cm
Latitude: -77.63718, Longitude: 162.98909
Date Excavated: 12/16/2006

| Horizon | Depth (cm) | Description |
|---|---|---|
| DP | 1 – 0 | ventifacts stage 1, calcium carbonate coatings stage 1 |
| C1 | 0 – 11 | cemented slightly with salts, calcium carbonate coatings stage 2 |
| C2 | 11 –29 | loose, very little salt, gravelly sand |

Soil: S026, Elevation: 73 m, Depth to ICS: 29 cm
Latitude: -77.62464, Longitude: 163.1963
Date Excavated: 12/17/2006

| Horizon | Depth (cm) | Description |
|---|---|---|
| DP | 1 – 0 | calcium carbonate coatings stage 1, ventifacts stage 1, sub-rounded gravel |
| C1 | 0 – 8 | stratified aeolian sands/gravel, gravelly sand, very weak structure, calcium carbonate coatings stage 1, variegated |
| C2 | 8 –29 | gravelly sand, probably wind and from original strata |
| ICS | 29+ | flat beds |



Soil: S027, Elevation: 121 m, Depth to ICS: 31 cm
Latitude: -77.63657, Longitude: 163.12134
Date Excavated: 11/15/2007

| Horizon | Depth (cm) | Description |
|---|---|---|
| DP | 1.5 – 0 | angular stones up to 3 cm, calcium carbonate coatings stage 1, ventifacts stage 1, Munsell Color: Dry - 10YR 8/1, Wet - 10YR 4/1 |
| C1 | 0 – 7 | weakly salt cemented coarse sand with clasts up to 2 cm, Munsell Color: Dry - 10YR 8/1, Wet - 10YR 4/1 |
| 1C2 | 7 – 19 | slightly cohesive structure, stratified, cross bedded, sandy-pebbly material with some angular gravel, no ventifacts, no calcium carbonate coatings, variegated |
| 2C2 | 19 – 31 | slightly cohesive structure, stratified, cross bedded, sandy-pebbly material with some angular gravel, no ventifacts, no calcium carbonate coatings, variegated |
| ICS | 31+ | similar to C2, variegated |

Note: Pit is adjacent to terrace front on a flat surface. Kenyte is present in the DP. Sample for luminescence dating collected.

Soil: S028, Elevation: 120 m, Depth to ICS: 26 cm
Latitude: -77.63615, Longitude: 163.12773
Date Excavated: 11/15/2007

| Horizon | Depth (cm) | Description |
|---|---|---|
| DP | 2 – 0 | angular stones up to 3 cm , calcium carbonate coatings state 1, ventifacts stage 1, kenyte present, Munsell Color: Dry - 10YR 8/2, Wet - 10YR 5/2 |
| C1 | 0 – 3 | moderately cemented medium sand containing larger stones, ventifacts stage 1, Munsell Color: Dry - 10YR 8/1, Wet - 10YR 5/3 |
| 1C2 | 3 – 17 | cross bedded layers of sand and pebbles, variegated |
| 2C2 | 17 – 26 | cross bedded layers of sand and pebbles, variegated |
| ICS | 26+ | variegated |

Note: pit is located halfway between terrace front and till. Across Delta Stream from S027. Sample for luminescence dating collected.

Soil: S029, Elevation: 98 m, Depth to ICS: 26.5 cm
Latitude: -77.63527, Longitude: 163.12137
Date Excavated: 11/16/2007

| Horizon | Depth (cm) | Description |
|---|---|---|
| DP | 1.5 – 0 | ventifacts stage 1, calcium carbonate coatings stage 1, made of angular stones up to 5 cm, variegated |
| C1 | 0 – 1.5 | very weakly cemented pebbly sand with larger clasts up to 2 cm (salt cemented sand on bottom), Munsell Color: Dry - 10YR 8/1, Wet - 10YR 5/1 |
| C2 | 1.5 – 11.5 | more strongly cemented than C1, coarse pebbly sand, no ventifacts, no calcium carbonate coatings, cross bedded layers of sand and pebbles, variegated |
| C3 | 11.5 – 26.5 | same as C2 but more weakly cemented, variegated |
| ICS | 26.5+ | variegated |

Note: Sample for luminescence dating collected.

Soil: S030, Elevation: 87 m, Depth to ICS: 25.5 cm
Latitude: -77.63424, Longitude: 163.11624
Date Excavated: 11/16/2007

| Horizon | Depth (cm) | Description |
|---|---|---|
| DP | 2.5 – 0 | ventifacts stage 1, calcium carbonate coatings stage 1, composed of many large stones up to 7 cm, very angular, Munsell Color: Dry - 10YR 8/1, Wet - 10YR 5/2 |
| C1 | 0 – 2 | very weakly salt cemented, pebbly sand, Munsell Color: Dry - 10YR 8/1, Wet - 10YR 5/2 |
| C2 | 2 – 16.5 | gravelly sand with stones up to 3 cm, very loose, stones have sand cemented onto bottom, no calcium carbonate coatings and no ventifacts, variegated |
| C3 | 16.5 – 25.5 | cohesive, pebbly sand, some stratification observed, variegated |
| ICS | 25.5+ | variegated |

Note: Sample for luminescence dating collected.

Soil: S031, Elevation: 84 m, Depth to ICS: 27 cm
Latitude: -77.63308, Longitude: 163.11885
Date Excavated: 11/16/2007

| Horizon | Depth (cm) | Description |
|---|---|---|
| DP | 1.5 – 0 | ventifacts stage 2, calcium carbonate coatings stage 1, angular stones, some up to 5 cm, closely interlocking stones in pavement, Munsell Color: Dry - 10YR 8/1, Wet - 10YR 5/2 |
| C1 | 0 – 5 | weakly cemented pebbly sand with clasts up to 2 cm, Munsell Color: Dry - 10YR 8/1, Wet - 10YR 5/2 |
| 1C2 | 5 – 15 | some stratification evident, even more weakly cemented but has some cohesiveness, pebbly sand with clasts up to 2 cm, variegated |
| 2C2 | 15 – 27 | some stratification evident, even more weakly cemented but has some cohesiveness, pebbly sand with clasts up to 2 cm, variegated |
| ICS | 27+ | variegated |

Note: Sample for luminescence dating collected.

Soil: S032, Elevation: 20 m, Depth to ICS: 26.5 cm
Latitude: -77.62285, Longitude: 163.10808
Date Excavated: 11/17/2007

| Horizon | Depth (cm) | Description |
|---|---|---|
| DP | 1.5 – 0 | trace calcium carbonate coatings, ventifacts stage 1, stones are angular up to 4 cm, kenyte present, Munsell Color: Dry - 10YR 8/1, Wet - 10YR 5/2 |
| C1 | 0 – 1 | very loose coarse pebbly sand, Munsell Color: Dry - 10YR 8/1, Wet - 10YR 5/2 |
| C2 | 1 – 14.5 | very weakly cemented pebbly sand with abundant clasts up to 3 cm, stratified alternating layers of sand and pebbles, cross bedded, variegated |
| C3 | 14.5 – 26.5 | same as C2 but even less cementation, variegated |
| ICS | 26.5 – 31 | variegated |

Note: Located adjacent to Lake Fryxell near the edge of a delta slope, just about 10 m right of last year's GPR line (still visible). Sample for luminescence dating collected.

Soil: S033, Elevation: 36 m, Depth to ICS: 24.5 cm
Latitude: -77.62582, Longitude: 163.11623
Date Excavated: 11/17/2007

| Horizon | Depth (cm) | Description |
|---|---|---|
| DP | 1.5 – 0 | ventifacts stage 1, calcium carbonate coatings stage 1, angular stones up to 6 cm, kenyte present, Munsell Color: Dry - 10YR 8/1, Wet - 10YR 5/2 |
| C1 | 0 – 2 | very loose pebbly sand, Munsell Color: Dry - 10YR 8/1, Wet - 10YR 5/2 |
| 1C2 | 2 – 16 | stratified pebbly sand with numerous clasts up to 3 cm, stratified, dipping 30 degrees downstream, variegated |
| 2C2 | 16 – 24.5 | same as 1C2, variegated |
| ICS | 24.5 – 27.5 | variegated |

Note: Sample for luminescence dating collected.

Soil: S034, Elevation: 66 m, Depth to ICS: 23 cm
Latitude: -77.63083, Longitude: 163.11212
Date Excavated: 11/17/2007

| Horizon | Depth (cm) | Description |
|---|---|---|
| DP | 1.5 – 0 | ventifacts stage 1, calcium carbonate coatings stage 1, angular stones, some up to 7 cm, Munsell Color: Dry - 10YR 8/1, Wet - 10YR 5/2 |
| C1 | 0 – 9 | moderately salt cemented coarse sand with larger clasts up to 3 cm, some clasts are ventifacts stage 1, no calcium carbonate coatings, stratified, beds dip 30 degrees downstream and 10 degrees away from the stream, Munsell Color: Dry - 10YR 8/1, Wet - 10YR 5/2 |
| 1C2 | 9 – 16.5 | same as C1 but very weakly cemented, variegated |
| 2C2 | 16.5 – 23 | same as 1C2, variegated |
| ICS | 23 – 25 | variegated |

Note: Sample for luminescence dating collected.

Soil: S035, Elevation: 362 m, Depth to ICS: 8.5 cm
Latitude: -77.65659, Longitude: 163.013
Date Excavated: 11/18/2007

| Horizon | Depth (cm) | Description |
|---|---|---|
| DP | 2 – 0 | ventifacts stage 2, calcium carbonate coatings stage 1-2, stones are angular up to 30 cm maximum with stones of 10 cm common, Munsell Color: Dry - 10YR 8/1, Wet - 10YR 5/2 |
| C1 | 0 – 8.5 | moderately cemented silty sand with a few pebble clasts, Munsell Color: Dry - 10YR 7/2, Wet - 10YR 4/2 |
| 1C2 | 8.5 – 18.5 | ice-cemented, pebbly fine sand with some clasts up to 3 cm, Munsell Color: Dry - 10YR 7/2, Wet - 10YR 4/2 |
| 2C2 | 18.5 – 28.5 | same as 1C2, Munsell Color: Dry - 10YR 7/2, Wet - 10YR 4/2 |

Note: Surface is ventifacts stage 2, below pit 16 at 380 m, appears to be younger, less ventifacted than pit 16. Pit is located on what appears to be a moraine crest; polygons are about 10 – 15 cm across. Surface consists of some boulders up to 1.5 m across. Granite, gneiss, dike rocks.

Soil: S036, Elevation: 329 m, Depth to ICS: 10 cm
Latitude: -77.65448, Longitude: 163.04523
Date Excavated: 11/18/2007

| Horizon | Depth (cm) | Description |
|---|---|---|
| DP | 1.5 – 0 | ventifacts stage 2, calcium carbonate coatings stage 2, composed of stones up to 10 cm, no kenyte found, dike rocks, metamorphic rocks present, variegated |
| C1 | 0 – 2 | weakly-moderately cemented, pebbly silty sand with some clasts up to 3 cm, Munsell Color: Dry - 10YR 7/3, Wet - 10YR 4/3 |
| C2 | 2 – 3.5 | weakly cemented, gravelly sand, not ice-cemented, Munsell Color: Dry - 10YR 7/3, Wet - 10YR 4/3 |
| 1C3 | 3.5 – 10 | same as C2 but ice-cemented, Munsell Color: Dry - 10YR 8/2, Wet - 10YR 4/2 |
| 2C3 | 10 – 17.5 | same as C2 but ice-cemented, Munsell Color: Dry - 10YR 8/2, Wet - 10YR 4/3 |

Note: Polygons are 15 m, located on what appears to be a moraine, rounded and flattened at the top. Surface is ventifacts stage 2. Significant weathering of boulders is observed (bread rock).

Soil: S037, Elevation: 215 m, Depth to ICS: 16 cm
Latitude: -77.64534, Longitude: 163.08777
Date Excavated: 11/19/2007

| Horizon | Depth (cm) | Description |
|---|---|---|
| DP | 1.5 – 0 | ventifacts stage 1-2, calcium carbonate coatings stage 2, mostly angular stones about 3 cm, variegated |
| C1 | 0 – 2 | weakly cemented coarse sandy loam with some pebbles, varies from 45-6 cm, clear undulating boundary, Munsell Color: Dry - 10YR 8/2, Wet - 10YR 4/3 |
| C2 | 2 – 16 | not ice-cemented, not salt cemented, loose, varies from 1-2 cm, Munsell Color: Dry - 10YR 8/2, Wet - 10YR 4/2 |
| 1C3 | 16 – 24.5 | coarse sand, ice-cemented, ice content increases with depth, Munsell Color: Dry - 10YR 8/2, Wet - 10YR 4/2 |
| 2C3 | 24.5 – 27.5 | even higher ice content, gravelly coarse sand, Munsell Color: Dry - 10YR 8/2, Wet - 10YR 4/2 |

Note: Located on the flat top of a moraine system, surface is ventifacts stage 1-2 with embedded boulders up to 1 m in size and abundant smaller cobbles.

Soil: S038, Elevation: 170 m, Depth to ICS: 13 cm
Latitude: -77.63985, Longitude: 163.09696
Date Excavated: 11/20/2007

| Horizon | Depth (cm) | Description |
|---|---|---|
| DP | 1.5 – 0 | ventifacts stage 1-2, calcium carbonate coatings stage 2, kenyte present, Munsell Color: Dry - 10YR 8/1, Wet - 10YR 4/1 |
| C1 | 0 – 8.5 | weakly cemented horizon of medium to fine sand, shows horizontal stratification, probably due to aeolian input, 2.5 Munsell Color: Dry - 10YR 7/3, Wet - 10YR 4/4 |
| C2 | 8.5 – 13 | loose fine-medium sand, varies from 4.5 - 5 cm, variegated |
| C3 | 13 – 22.5 | appears to be the same as C2 but is ice-cemented, variegated |
| C4 | 22.5 – 31 | gravelly sand, more ice-cemented than C5, variegated |

Note: Pit lies on the crest of a large moraine system; kenyte is abundant along with black volcanic. Surface is composed of boulders up to 1 m in size. An aluminum rod and cairn mark the location. Polygons are from 14 – 20 m in size with troughs about 30 cm deep.

Soil: S039, Elevation: 110 m, Depth to ICS: 24.5 cm
Latitude: -77.63443, Longitude: 163.09683
Date Excavated: 11/20/2007

| Horizon | Depth (cm) | Description |
|---|---|---|
| DP | 1.5 – 0 | ventifacts stage 1-2, calcium carbonate coatings stage 4, Munsell Color: Dry - 10YR 8/1, Wet - variegated |
| C1 | 0 – 9.5 | fine-medium sand with some pebbles, moderately salt cemented, bedding observed, probably due to aeolian input, Munsell Color: Dry - 10YR 8/2, Wet - 10YR 4/3 |
| C2 | 9.5 – 24.5 | very weakly cemented, medium to coarse sand with some gravel, variegated |
| C3 | 24.5 – 36 | ice-cemented gravelly sand, Munsell Color: Dry - 10YR 8/1, Wet - 10YR 4/2 |
| C4 | 36 – 38 | less gravelly than C3, more strongly ice-cemented, Munsell Color: Dry - 10YR 8/2, Wet - 10YR 4/3 |

Note: Pit is located on a highpoint within a moraine complex. Kenyte found. Composed of boulders up to 1 m in diameter, but pit lies in area free of large boulders. Ventifact stage 1 or 2. Polygons are 10 – 15 m and sand wedges are about 20 – 30 cm deep.


Soil: S040, Elevation: 78 m, Depth to ICS: 29.5 cm
Latitude: -77.63304, Longitude: 163.11241
Date Excavated: 11/21/2007

| Horizon | Depth (cm) | Description |
|---|---|---|
| DP | 1 – 0 | calcium carbonate coatings stage 1-2, ventifacts stage 3, Munsell Color: Dry - 10YR 8/2, Wet - 10YR 4/3 |
| C1 | 0 – 4 | weakly cemented fine-medium sand with some pebbles, Munsell Color: Dry - 10YR 8/2, Wet - 10YR 4/3 |
| C2 | 4 – 8.5 | weakly cemented gravelly sand, variegated |
| C3 | 8.5 – 19 | same as C2 but loose and more coarse, variegated |
| C4 | 19 – 29.5 | same as C2 but weakly ice-cemented and contains some interlayers of silty sand, variegated |
| ICS | 29.5 – 30.5 | variegated |

Note: Sample for luminescence dating collected.



Soil: S041, Elevation: 64 m, Depth to ICS: 27 cm
Latitude: -77.63131, Longitude: 163.10977
Date Excavated: 11/21/2007

| Horizon | Depth (cm) | Description |
|---|---|---|
| DP | 1.5 – 0 | calcium carbonate coatings stage 1, ventifacts stage 1, angular stones up to 5 cm, variegated |
| C1 | 0 – 1 | loose, fine to medium sand, Munsell Color: Dry - 10YR 8/1, Wet - 10YR 4/2 |
| 1C2 | 1 – 14 | alternating bands of fine silty sand and gravelly sand, very weakly cemented, loose, Munsell Color: Dry - 10YR 8/1, Wet - 10YR 4/2 |
| 2C2 | 14 – 27 | same as 1C2, variegated |
| ICS | 27 – 29 | variegated |

Note: Sample for luminescence dating collected.


Soil: S042, Elevation: 38 m, Depth to ICS: 24.5 cm
Latitude: -77.62658, Longitude: 163.11252
Date Excavated: 11/21/2007

| Horizon | Depth (cm) | Description |
|---|---|---|
| DP | 1.5 – 0 | calcium carbonate coatings stage 1, ventifacts stage 1, angular stones up to 5 cm, variegated |
| C1 | 0 – 1 | very loose layer beneath the DP, fine-medium sand, variegated |
| 1C2 | 1 – 11 | very loose gravelly sand, some stratification can be seen dipping away from the stream at about 10 degrees, variegated |
| 2C2 | 11 – 24.5 | same as 1C2, variegated |
| ICS | 24.5 – 26.5 | variegated |

Note: Sample for luminescence dating collected.

Soil: S044, Elevation: 261 m, Depth to ICS: not found
Latitude: -77.73195, Longitude: 162.31169
Date Excavated: 11/23/2007

| Horizon | Depth (cm) | Description |
|---|---|---|
| DP | 2 – 0 | calcium carbonate coatings stage 1, ventifacts stage 2, dolerite and granite present, Munsell Color: Dry - 10YR 8/2, Wet - 10YR 4/2 |
| C1 | 0 – 3 | gravelly sand with silt working its way in, lightly salt cemented, Munsell Color: Dry - 10YR 8/3, Wet - 10YR 5/3 |
| C2 | 3 – 26 | gravelly coarse sand, weakly cemented, some stratification, Munsell Color: Dry - 10YR 7/1, Wet - variegated |
| C3 | 26 – 60 | sand, Munsell Color: Dry - 10YR 8/1, Wet - variegated |

Note: Pit lies on the crest of a moraine overlooking Lake Bonney. Boulders are very well ventifacted, dolerites and granites, rudimentary wedges present.



Soil: S045, Elevation: 149 m, Depth to ICS: not found
Latitude: -77.72746, Longitude: 162.31517
Date Excavated: 11/23/2007

| Horizon | Depth (cm) | Description |
|---|---|---|
| DP | 1.5 – 0 | Munsell Color: Dry - 10YR 8/1, Wet - 10YR 4/1 |
| C1 | 0 – 8 | cemented, shows layering, pebbly silt with some rocks, Munsell Color: Dry - 10YR 7/3, Wet - 10YR 5/3 |
| C2 | 8 – 37 | gravelly pebbly silt, very weakly cemented, Munsell Color: Dry - 10YR 7/2, Wet - 10YR 5/2 |
| C3 | 37 – 46 | gravelly silt, very compacted, difficult to dig, may be cemented with salts, Munsell Color: Dry - 10YR 7/2, Wet - 10YR 5/2 |

Note: Pit lies on top of a mound, probably bedrock controlled. Surrounding boulders are very well ventifacted. This soils is extremely silts and may be inflated or a silty till.

Soil: S046, Elevation: 116 m, Depth to ICS: not found
Latitude: -77.72657, Longitude: 162.31038
Date Excavated: 11/23/2007

| Horizon | Depth (cm) | Description |
|---|---|---|
| DP | 1.5 – 0 | Munsell Color: Dry - 10YR 7/2, Wet - 10YR 5/2 |
| C1 | 0 – 2.5 | very weakly cemented, gravelly silt, Munsell Color: Dry - 10YR 7/3, Wet - 10YR 5/3 |
| C2 | 2.5 – 32 | very angular gravelly silt, weakly cemented, may be inflated, some ventifacted rocks present, Munsell Color: Dry - 10YR 7/3, Wet - 10YR 5/3 |
| C3 | 32 – 50 | gravelly sandy silt, has more gravel and pebbles than C2, no ventifacted rocks present, Munsell Color: Dry - 10YR 7/2, Wet - 10YR 5/3 |

Note: Located at a prominent shoreline as seen on a satellite photo; large, well ventifacted boulders present.

Soil: S047, Elevation: 86 m, Depth to ICS: not found
Latitude: -77.72533, Longitude: 162.30296
Date Excavated: 11/23/2007

| Horizon | Depth (cm) | Description |
|---|---|---|
| DP | 1 – 0 | Munsell Color: Dry - 10YR 7/2, Wet - 10YR 4/2 |
| C1 | 0 – 4 | some horizontal stratification, probably aeolian, Munsell Color: Dry - 10YR 7/3, Wet - 10YR 5/4 |
| 1C2 | 4 – 30 | gravelly silt with matrix supported clasts, there is a 2 cm sandy band at 30 cm, silt polygons at 15 cm diameter, abundant carbonate chips (shells?), Munsell Color: Dry - 10YR 7/3, Wet - 10YR 5/3 |
| 2C2 | 30 – 60 | same as 1C2, Munsell Color: Dry - 10YR 7/3, Wet - 10YR 5/4 |
| C3 | 60 – 65 | indurated, compacted, possibly compacted by Taylor glacier, Munsell Color: Dry - 10YR 7/3, Wet - 10YR 5/4 |

Soil: S048, Elevation: 123 m, Depth to ICS: 25.5 cm
Latitude: -77.63248, Longitude: 163.1821
Date Excavated: 11/24/2007

| Horizon | Depth (cm) | Description |
|---|---|---|
| DP | 1.5 – 0 | ventifacts stage 1, calcium carbonate coatings stage 2, variegated |
| C1 | 0 – 5.5 | varies from 5 - 6 cm, gravelly fine-medium sand, weakly cemented, ventifacts present, Munsell Color: Dry - 10YR 8/2, Wet - 10YR 5/2 |
| 1C2 | 5.5 – 13 | layers of stratified fine sand and pebbly sand, some ventifacted stones present, cross bedded, variegated |
| 2C2 | 13 – 25.5 | same as 1C2, variegated |
| ICS | 25.5 – 27.5 | variegated |

Note: The pit lies 4 m from the terrace front and 30 cm from Crescent Stream. This terrace is cut in two by the stream and the corresponding terrace is visible across the stream. Wind ripples are evident on the DP surface. Sample for luminescence dating collected.

Soil: S049, Elevation: 77 m, Depth to ICS: 25.5 cm
Latitude: -77.62691, Longitude: 163.18273
Date Excavated: 11/24/2007

| Horizon | Depth (cm) | Description |
|---|---|---|
| DP | 1.5 – 0 | calcium carbonate coatings stage 1, ventifacts stage 1, angular stones up to 5 cm, variegated |
| C1 | 0 – 6.5 | weakly salt cemented layers of silty sand and coarse or pebbly sand, cross bedded, Munsell Color: Dry - 10YR 8/2, Wet - 10YR 5/2 |
| 1C2 | 6.5 – 13 | same as C1 but loose, variegated |
| 2C2 | 13 – 25.5 | same as C1 but loose, variegated |
| ICS | 25.5 – 28 | variegated |

Note: Sample for luminescence dating collected.

Soil: S050, Elevation: 202 m, Depth to ICS: 34 cm
Latitude: -77.64835, Longitude: 163.11734
Date Excavated: 11/25/2007

| Horizon | Depth (cm) | Description |
|---|---|---|
| DP | 1.5 – 0 | trace calcium carbonate coatings, ventifacts stage 3, variegated |
| C1 | 0 – 20 | very loose coarse sand with some gravel, foreset beds are evident sloping downstream at 30 degrees (aeolian?) , variegated |
| C2 | 20 – 34 | lightly ice-cemented material similar to C2, variegated |
| ICS | 34 – 35 | variegated |

Note: Sample for luminescence dating collected.

Soil: S051, Elevation: 218 m, Depth to ICS: 33 cm
Latitude: -77.65063, Longitude: 163.11203
Date Excavated: 11/25/2007

| Horizon | Depth (cm) | Description |
|---|---|---|
| DP | 1.5 – 0 | trace calcium carbonate coatings, ventifacts stage 2, variegated |
| 1C1 | 0 – 18 | coarse gravelly sand with foreset beds inclining 30 degrees downstream. inclined beds exhibit wavy patters and cut across horizontal stratification on the upstream side of the pit (aeolian?) , variegated |
| 2C1 | 18 – 33 | same as 1C1, variegated |

Note: Sample for luminescence dating collected.

Soil: S052, Elevation: 112 m, Depth to ICS: 20 cm
Latitude: -77.63565, Longitude: 163.07908
Date Excavated: 11/25/2007

| Horizon | Depth (cm) | Description |
|---|---|---|
| DP | 2 – 0 | stones up to 8 cm, trace calcium carbonate coatings, ventifacts stage 3, variegated |
| C1 | 0 – 13.5 | fine to medium sand with silt interbeds, stratified foreset beds inclining at 30 degrees, some layers of coarse sand, inclined beds are weak (aeolian?), algae found, unknown if it was a bed of algae, variegated |
| C2 | 13.5 – 20 | same as C1 but lightly ice-cemented, variegated |
| ICS | 20 – 22 | variegated |

Note: Sample for luminescence dating collected.



Soil: S053, Elevation: 289 m, Depth to ICS: 15 cm
Latitude: -77.65202, Longitude: 163.06115
Date Excavated: 11/26/2007

| Horizon | Depth (cm) | Description |
|---|---|---|
| DP | 1.5 – 0 | calcium carbonate coatings stage 2, ventifacts stage 4, variegated |
| C1 | 0 – 7 | gravelly sand with some silt, cemented weakly, Munsell Color: Dry - 10YR 8/2, Wet - 10YR 4/2 |
| C2 | 7 – 15 | gravelly sand, no fines, little structure, weakly stratified, no ice-cement, Munsell Color: Dry - 10YR 8/2, Wet - 10YR 4/2 |
| 1C3 | 15 – 23 | same as C2, ice-cemented, increasing ice with depth, Munsell Color: Dry - 10YR 8/2, Wet - 10YR 4/2 |
| 2C3 | 23 – 38 | same as C2, ice-cemented, increasing ice with depth, variegated |
| 3C3 | 38 – 43 | same as C2, ice-cemented, increasing ice with depth, variegated |

Note: This pit lies next to a large ice-cored moraine (the ”lima bean”) on a small line of moraines. There are a few boulders up to 2 m, with smaller cobbles. Sand wedges on the moraines system are deep and the moraine may be ice-core. Black volcanics are abundant, kenyte found.

Soil: S055, Elevation: 243 m, Depth to ICS: 11 cm
Latitude: -77.64738, Longitude: 163.06119
Date Excavated: 11/26/2007

| Horizon | Depth (cm) | Description |
|---|---|---|
| DP | 2 – 0 | calcium carbonate coatings stage 2, ventifacts stage 3, Munsell Color: Dry - 10YR 8/2, Wet - 10YR 4/2 |
| C1 | 0 – 7 | gravelly sand, weakly cemented, coarse-angular gravelly sand, Munsell Color: Dry - 10YR 8/2, Wet - 10YR 4/2 |
| C2 | 7 – 11 | dry loose sand, variegated, Munsell Color: Dry - 10YR 8/2, Wet - 10YR 4/2 |
| 1C3 | 11 – 22 | gravelly medium sand, ice-cement content increases with depth, Munsell Color: Dry - 10YR 8/2, Wet - 10YR 4/2 |
| 2C3 | 22 – 33 | same as 1C3, Munsell Color: Dry - 10YR 8/2, Wet - 10YR 4/2 |

Soil: S056, Elevation: 100 m, Depth to ICS: 17 cm
Latitude: -77.63325, Longitude: 163.08997
Date Excavated: 11/27/2007

| Horizon | Depth (cm) | Description |
|---|---|---|
| DP | 1 – 0 | no ventifacts evident |
| C1 | 0 – 3 | medium sand with some pebbles |
| C2 | 3 – 17 | laminated silt and fine sand. Silt layers are about 1 – 2 mm thick. |
| ICS | 17+ | |

Note: This pit lies in a depression south of a large Taylor moraine. Sample for luminescence dating collected.



Soil: S057, Elevation: 101 m, Depth to ICS: 48 cm
Latitude: -77.63319, Longitude: 163.04278
Date Excavated: 11/28/2007

| Horizon | Depth (cm) | Description |
|---|---|---|
| DP | 1.5 – 0 | angular rocks some stage 1-2 ventifacts, calcium carbonate coatings stage 1, granites turning into grus, Munsell Color: Dry - 10YR 8/1, Wet - 10YR 4/2 |
| C1 | 0 – 24 | weak horizontal bedding, maybe due to inflation, silty-gravelly (we also saw a lot of silt in Bonney Basin), Munsell Color: Dry - 10YR 8/2, Wet - 10YR 5/3 |
| C2 | 24 – 42 | similar to C1, Munsell Color: Dry - 10YR 8/2, Wet - 10YR 5/3 |
| C3 | 42 – 48 | sandy, maybe original till, there is a fairly large aeolian horizon here and salts may reflect position in a basin rather than old age, Munsell Color: Dry - 10YR 8/2, Wet - 10YR 5/3 |

Note: This soil appears to be a Taylor moraine overriding Ross Sea till. Beacon sandstone, dolerite, granite, basement rocks…no kenyte found.



Soil: S058, Elevation: 65 m, Depth to ICS: 30 cm
Latitude: -77.63034, Longitude: 163.09073
Date Excavated: 11/28/2007

| Horizon | Depth (cm) | Description |
|---|---|---|
| DP | 1.5 – 0 | calcium carbonate coatings stage 1, ventifacts stage 1-3, Munsell Color: Dry - 10YR 8/1, Wet - 10YR 4/2 |
| C1 | 0 – 1.5 | probably aeolian, weakly cemented, Munsell Color: Dry - 10YR 8/3, Wet - 10YR 5/3 |
| C2 | 1.5 – 7 | silty gravel, horizontal banding, some flakes (shells?) are found here, Munsell Color: Dry - 10YR 8/3, Wet - 10YR 5/3 |
| C3 | 7 – 20 | sandy gravel, no silt, lots of carbonate fragments, may be shells, Munsell Color: Dry - 10YR 8/2, Wet - 10YR 4/2 |
| C4 | 20 – 28 | silty sand, Munsell Color: Dry - 10YR 8/2, Wet - 10YR 5/2 |
| ICS | 28 – 32 | ice-cemented soil, ice-cement starts at 30 cm, Munsell Color: Dry - 10YR 8/2, Wet - 10YR 4/2 |

Note: This soil apears to be on a Ross Sea moraine, but no kenyte was found. Also, no marble or sandstone is present. Pit lies on top of the moraine adjacent and below a large Taylor moraine.

Soil: S059, Elevation: 227 m, Depth to ICS: 16 cm
Latitude: -77.6454, Longitude: 163.04013
Date Excavated: 11/28/2007

| Horizon | Depth (cm) | Description |
|---|---|---|
| DP | 2 – 0 | calcium carbonate coatings stage 2, ventifacts stage 1-4, Munsell Color: Dry - 10YR 8/1, Wet - 10YR 4/1 |
| C1 | 0 – 7.5 | weakly salt cemented layers of silty sand and coarse sand with gravel, Munsell Color: Dry - 10YR 8/1, Wet - 10YR 4/1 |
| C2 | 7.5 – 16 | same as C1 but loose, variegated |
| C3 | 16 – 27 | ice-cemented, variegated |
| ICS | 27 – 29 | hard ice-cement, variegated |

Note: Sample for luminescence dating collected.

Soil: S060, Elevation: 227 m, Depth to ICS: 23 cm
Latitude: -77.6454, Longitude: 163.04013
Date Excavated: 11/28/2007

| Horizon | Depth (cm) | Description |
|---|---|---|
| DP | 2 – 0 | calcium carbonate coatings stage 1-2, ventifacts stage 3, variegated |
| C1 | 0 – 10.5 | moderately salt cemented, laminated fine sand/silt interlayered with medium-fine sand, Munsell Color: Dry - 10YR 8/1, Wet - 10YR 5/2 |
| 1C2 | 10.5 – 14 | gravelly sand, weakly cemented, coarse-angular gravelly sand, variegated |
| 2C2 | 14 – 23 | same as 1C2, variegated |
| ICS | 23 – 31.5 | ice-cemented, Munsell Color: Dry - 10YR 8/1, Wet - 10YR 5/2 |

Note: This pit is on the same terraces as S059, 10 m up-slope. Sample for luminescence dating collected.


Soil: S062, Elevation: 115 m, Depth to ICS: 20.5 cm
Latitude: -77.6362, Longitude: 162.99936
Date Excavated: 11/28/2007

| Horizon | Depth (cm) | Description |
|---|---|---|
| DP | 2 – 0 | calcium carbonate coatings stage 2, ventifacts stage 2, Munsell Color: Dry - 10YR 8/1, Wet - 10YR 5/2 |
| C1 | 0 – 3.5 | weakly cemented unstratified fine-medium sand with pebbles, Munsell Color: Dry - 10YR 8/1, Wet - 10YR 5/2 |
| C2 | 3.5 – 8.5 | weakly cemented cross bedded layers of silt and sand with some gravel, Munsell Color: Dry - 10YR 8/1, Wet - 10YR 5/3 |
| C3 | 8.5 – 20.5 | same as C2 but loose, variegated |
| ICS | 20.5 – 24.5 | Munsell Color: Dry - 10YR 8/1, Wet - variegated |

Note: Sample for luminescence dating collected.

Soil: S063, Elevation: 347 m, Depth to ICS: 11 cm
Latitude: -77.61203, Longitude: 163.53866
Date Excavated: 12/02/2007

| Horizon | Depth (cm) | Description |
|---|---|---|
| DP | 2 – 0 | ventifacts stage 2+, granites and sill rock, calcium carbonate coatings stage 2, some salt pendants found, Munsell Color: Dry - 10YR 8/2, Wet - 10YR 5/3 |
| C1 | 0 – 9 | medium to coarse sand, lightly cemented, Munsell Color: Dry - 10YR 8/2, Wet - 10YR 5/3 |
| C2 | 9 – 21 | ICS is at 11 cm, higher water content than below, Munsell Color: Dry - 10YR 8/2, Wet - 10YR 5/3 |
| C3 | 21 – 26 | variegated |

Note: This pit lies on what appears to be old ice-core moraine. Very lumpy terrain with wide-deep sand wedge cracks and many snow patches. The DP is well oxidized and black volcanics are abundant. Sand wedges are 1 – 1.5 m deep and polygons are about 10 – 15 m across.

**No Images Available**

Soil: S064, Elevation: 160 m, Depth to ICS: 9 cm
Latitude: -77.60043, Longitude: 163.50843
Date Excavated: 12/03/2007

| Horizon | Depth (cm) | Description |
|---|---|---|
| DP | 1.5 – 0 | calcium carbonate coatings stage 1, ventifacts stage 1, granites and some black volcanics, Munsell Color: Dry - 10YR 8/1, Wet - 10YR 5/2 |
| C1 | 0 – 9 | fine-medium gravelly-pebbly sand, moderately cemented, Munsell Color: Dry - 10YR 7/2, Wet - 10YR 4/2 |
| C2 | 9 – 21 | same as C1 only weakly cemented, Munsell Color: Dry - 10YR 7/1, Wet - 10YR 4/1 |
| C3 | 21 – 33.5 | same as C1 only weakly ice-cemented, variegated |

**No Images Available**

Soil: S065, Elevation: 78 m, Depth to ICS: 7 cm
Latitude: - 77.59134, Longitude: 163.49743
Date Excavated: 12/04/2007

| Horizon | Depth (cm) | Description |
|---|---|---|
| DP | 1.5 – 0 | trace calcium carbonate coatings, ventifacts stage 2, Munsell Color: Dry - 10YR 7/2, Wet - 10YR 4/2 |
| C1 | 0 – 8 | varies from 5 - 8 cm, moderately cemented, shows weak stratification, medium-find grained pebbly sand with some gravel, Munsell Color: Dry - 10YR 7/2, Wet - 10YR 4/2 |
| C2 | 8 – 19.5 | fine-medium gravelly sand, Munsell Color: Dry - 10YR 8/1, Wet - variegated |
| C3 | 19.5 – 26.5 | same as C2, moist, variegated |
| ICS | 26.5 – 28 | hard ICS, variegated |

Note: Sample for luminescence dating collected.

Soil: S066, Elevation: 70 m, Depth to ICS: 23 cm
Latitude: -77.58944, Longitude: 163.49459
Date Excavated: 12/04/2007

| Horizon | Depth (cm) | Description |
|---|---|---|
| DP | 1.5 – 0 | calcium carbonate coatings stage 1-2, ventifacts stage 3, variegated |
| C1 | 0 – 8 | fine sand with visible laminations, weakly cemented, Munsell Color: Dry - 10YR 8/1, Wet - 10YR 4/1 |
| C2 | 8 – 23 | fine sand interlayered with pebbly sand, cross bedding, variegated |
| ICS | 23 – 25 | variegated |

Note: Sample for luminescence dating collected.

**No Images Available**

Soil: S067, Elevation: 33 m, Depth to ICS: 17 cm
Latitude: - 77.58163, Longitude: 163.49048
Date Excavated: 12/04/2007

| Horizon | Depth (cm) | Description |
|---|---|---|
| DP | 1.5 – 0 | ventifacts stage 1, calcium carbonate coatings stage 2, variegated |
| C1 | 0 – 17 | cross bedded fine sand and pebbly sand, Munsell Color: Dry - 10YR 8/1, Wet - 10YR 4/1 |
| C2 | 17 – 24.5 | same as C1 but lightly ice-cemented, variegated |

Note: Sample for luminescence dating collected.

**No Images Available**

Soil: S068, Elevation: 63 m, Depth to ICS: 23.5 cm
Latitude: - 77.58607, Longitude: 163.5006
Date Excavated: 12/05/2007

| Horizon | Depth (cm) | Description |
|---|---|---|
| DP | 2 – 0 | calcium carbonate coatings stage 1, ventifacts stage 2, Munsell Color: Dry - 10YR 8/1, Wet - 10YR 4/1 |
| C1 | 0 – 4.5 | weakly cemented fine-medium sand with pebbles, some laminations present, Munsell Color: Dry - 10YR 7/3, Wet - 10YR 4/3 |
| C2 | 4.5 – 14.5 | fine-medium pebbly, gravelly sand, very weakly cemented, Munsell Color: Dry - 10YR 8/1, Wet - 10YR 4/1 |
| C3 | 14.5 – 23.5 | very loose, variegated coarse sand, variegated |

Note: Sample for luminescence dating collected.

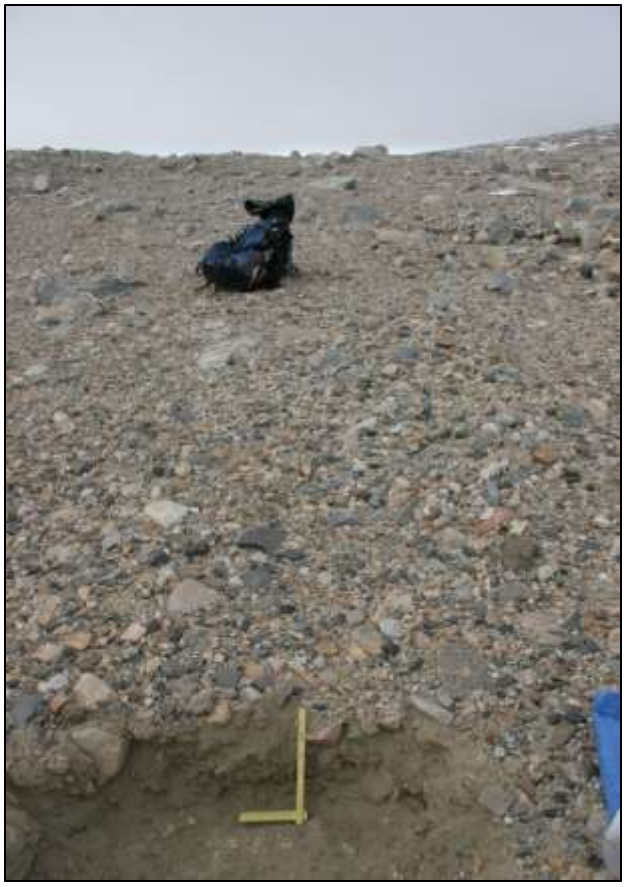

Soil: S069, Elevation: 241 m, Depth to ICS: 15 cm
Latitude: -77.60729, Longitude: 163.50866
Date Excavated: 12/05/2007

| Horizon | Depth (cm) | Description |
|---|---|---|
| DP | 1.5 – 0 | calcium carbonate coatings stage 1, ventifacts stage 2, Munsell Color: Dry - 10YR 7/3, Wet - 10YR 4/3 |
| C1 | 0 – 6 | gravelly sand, calcium carbonate coatings stage 2, appears to be inflated, weakly cemented, ventifacts present, Munsell Color: Dry - 10YR 7/3, Wet - 10YR 4/3 |
| C2 | 6 – 15 | very gravelly sand, probably inflated, weak stratification, calcium carbonate coatings stage 1-2, ventifacts present, Munsell Color: Dry - 10YR 7/2, Wet - 10YR 4/3 |
| C3 | 15 – 17 | cobbles, gravelly sand, may be original material, strongly ice-cemented, stones are more angular than C1 or C2, Munsell Color: Dry - 10YR 7/2, Wet - 10YR 4/2 |

Note: This pit lies near the top of a very large moraine. The surface is bouldery, with many cobbles of granite, volcanics, and kenyte. The pit is in a flat part of the moraine, absent of large boulders.



Soil: S070, Elevation: 207 m, Depth to ICS: 7 cm
Latitude: -77.60425, Longitude: 163.49029
Date Excavated: 12/05/2007

| Horizon | Depth (cm) | Description |
|---|---|---|
| DP | 2 – 0 | pebbles in between stones, vents stage 1, calcium carbonate coatings stage 1, Munsell Color: Dry - 10YR 7/3, Wet - 10YR 4/2 |
| C1 | 0 – 3 | loose, medium-fine sand, Munsell Color: Dry - 10YR 7/3, Wet - 10YR 4/2 |
| C2 | 3 – 10 | medium sand, damp, non-cemented, Munsell Color: Dry - 10YR 7/3, Wet - 10YR 4/2 |
| C3 | 10 – 20 | calcium carbonate coatings stage 2, gravelly pebbly sand, very hard ice-cement, ICS starts at this horizon, Munsell Color: Dry - 10YR 7/2, Wet - 10YR 4/3 |

Notes: Pit lies on a large rib of moraine descending from S069. DP has granite, volcanics, and kenyte. Surface consists of boulders and cobbles and is often irregular. Sand wedges are weakly developed, about 15 – 20 cm deep and about 30 m in diameter. This moraine and the large moraine on S069 enclose a large basin though which flows Wales Stream.

Soil: S071, Elevation: 194 m, Depth to ICS: 25 cm
Latitude: -77.60458, Longitude: 163.5034
Date Excavated: 12/06/2007

| Horizon | Depth (cm) | Description |
|---|---|---|
| DP | 1 – 0 | gravel, ventifacts stage 1-2, some salt crusts, trace calcium carbonate coatings, Munsell Color: Dry - 10YR 8/2, Wet - 10YR 4/1 |
| C1 | 0 – 5 | weakly cemented, weakly stratified, appears to be aeolian, Munsell Color: Dry - 10YR 8/2, Wet - 10YR 5/3 |
| 1C2 | 5 – 15 | original stratified sand, pebbles and gravel, compacted, stands up well, coarse sand to fine sand layers, cross bedded, variegated |
| 2C2 | 15 – 25 | same as 1C2, variegated |
| ICS | 25 – 28 | variegated |

Notes: This pit lies on the lower of a series of two fluvial terraces. Sample for luminescence dating collected.

Soil: CR01, Elevation: 140 m, Depth to ICS: 40 cm
Latitude: -77.58468, Longitude: 163.44975
Date Excavated: 12/07/2007

| Horizon | Depth (cm) | Description |
|---|---|---|
| DP | 2 – 0 | ventifacts stage 1, calcium carbonate coatings stage 1 |
| C1 | 0 – 9 | weakly cemented silt, some stratification |
| C2 | 9 – 17 | fine gravelly silt showing some stratification |
| C3 | 17 – 40 | massive ice with suspended stones |
| C4 | 40 – 50+ | similar to C3 |

Soil: CR03, Elevation: 120 m, Depth to ICS: 25 cm
Latitude: -77.58222, Longitude: 163.43451
Date Excavated: 12/07/2007

| Horizon | Depth (cm) | Description |
|---|---|---|
| DP | 1.5 – 0 | ventifacts stage 1, calcium carbonate coatings stage 1, Munsell Color: Dry - 10YR 8/1, Wet - variegated |
| C1 | 0 – 10 | 25% clasts, varies from a fine sand to a silty horizon, weakly cemented, Munsell Color: Dry - 10YR 6/3, Wet - 10YR 3/3 |
| C2 | 10 – 25 | gravelly to silty sand, stratified, seems to have aeolian influences, Munsell Color: Dry - 10YR 6/2, Wet - 10YR 4/3 |
| C3 | 25+ | ice lenses found at 35 cm, Munsell Color: Dry - 10YR 6/2, Wet - 10YR 3/2 |

Soil: CR04, Elevation: 123 m, Depth to ICS: 20 cm
Latitude: -77.58157, Longitude: 163.4287
Date Excavated: 12/07/2007

| Horizon | Depth (cm) | Description |
|---|---|---|
| DP | 1.5 – 0 | ventifacts stage 1, trace calcium carbonate coatings |
| C1 | 0 – 6 | silt rich horizon, very weakly cemented, Munsell Color: Dry - 10YR 6/3, Wet - 10YR 3/3 |
| C2 | 6 – 20 | fine to medium sand, may be aeolian, Munsell Color: Dry - 10YR 6/2, Wet - 10YR 3/3 |
| ICS | 20+ | fine to medium sand, ice lenses present, Munsell Color: Dry - 10YR 8/1, Wet - 10YR 4/1 |

Soil: CR05, Elevation: 116 m, Depth to ICS: 11 cm
Latitude: - 77.57127, Longitude: 163.42657
Date Excavated: 12/07/2007

| Horizon | Depth (cm) | Description |
|---|---|---|
| DP | 2 – 0 | ventifacts stage 1, calcium carbonate coatings stage 1 |
| C1 | 0 – 11 | silty horizon |
| C2 | 11 – 23+ | dense, cemented sand, may be original till, with overlying aeolian material, few matrix supported clasts |

# Vita

Jonathan Toner was born in Levittown, Pennsylvannia, on October 10th, 1982. He grew up in Levittown and attdended Neshaminy High School, graduating in 2002. After high school, he attended The College of New Jersey on a full four-year scholarship and graduated in 2006 with a B.Sc. in Physics. Jonathan entered graduate school at the University of Washington in Autumn Quarter 2006 studying Geophysics, but soon changed his focus to Geochemistry. Most people assume that he entered higher education for noble academic reasons…suckers. After the completion of his Ph.D., Jonathan will enter the great unknown and experience much angst. To put off reality, he will spend three months bicycling around Europe with his wife, Lisa, in search of good cheese, wine, and free camping nirvana. Upon returning, his job prospects include: contracting the terrible disease *academia vulgaris* and being quarantined to a postdoc, becoming one with the corporate BORG, or earning minimum wage by wearing a purple dinosaur suit for kiddie birthday parties. Possibly, he may work at McDonald's, using his advanced degree to expertly add salt to orders of fries. "You want to supersize that?" ;)